Microorganisms and electron acceptors affecting methane oxidation in freshwater and marine systems

Sigrid van Grinsven

Sigrid van Grinsven
Microorganisms and electron acceptors affecting methane oxidation in freshwater and marine systems

ISBN 978-94-6332-631-5
Layout Loes Kema

This thesis is printed on 100% recycled paper by GVO drukkers & vormgevers, Ede.

Microorganisms and electron acceptors affecting methane oxidation in freshwater and marine systems

Micro-organismen en elektronenacceptoren betrokken bij methaanoxidatie in zoet- en zoutwater systemen
(met een samenvatting in het Nederlands)

Proefschrift

ter verkrijging van de graad van doctor aan de Universiteit Utrecht
op gezag van de rector magnificus, prof.dr. H.R.B.M. Kummeling,
ingevolge het besluit van het college voor promoties
in het openbaar te verdedigen op woensdag 1 juli 2020 des middags te 12.45 uur

door

Sigrid van Grinsven

geboren op 10 mei 1991
te Zevenaar

Promotoren:

Prof. dr. J. S. Sinninghe Damsté

Prof. dr. S. Schouten

Copromotor:

Dr. L. Villanueva

Contents

Chapter 1	Introduction	7
Chapter 2	Are elusive anaerobic pathways key methane sinks in eutrophic lakes and reservoirs?	23
Chapter 3	Methane oxidation in anoxic lake water stimulated by nitrate and sulfate addition	47
Chapter 4	Impact of electron acceptor availability on methane-influenced microorganisms in an enrichment culture obtained from a stratified lake	87
Chapter 5	Nitrate enables the transfer of methane-derived carbon from the methanotroph *Methylobacter* sp. to the methylotroph *Methylotenera* sp. in eutrophic lake water	117
Chapter 6	Assessing the effect of humic substances and Fe(III) as potential electron acceptors for anaerobic methane oxidation in a marine anoxic system	143
Summary/Samenvatting		167
Synthesis		175
Acknowledgements/Dankwoord		179
About the author		183

Chapter 1. Introduction

Aquatic methane production and consumption

Methane (CH_4) is one of the greenhouse gasses causing global warming. Although atmospheric methane concentrations and emissions are lower than those of carbon dioxide (CO_2), its high warming potential (about 30x that of CO_2) makes it an important contributor to the greenhouse effect, accounting for 20% of the greenhouse gas induced warming since the pre-industrial era (Kirschke *et al.*, 2013). Sources of methane to the atmosphere are ubiquitous, both natural and anthropogenic, and include emissions from fossil fuel burning, agriculture, landfills, soils and aquatic systems such as lakes and seas. This thesis focuses on methane cycling in freshwater and marine aquatic systems, which are known to accommodate both methane production (methanogenesis) and consumption (methanotrophy). A comprehensive overview of the methane cycling processes in aquatic systems is shown in Fig. 1. Seas and lakes are a relatively minor source of methane to the atmosphere when considering the high methane production rates found in these systems (Reeburgh, 2007). It is estimated that 80-90% of the methane that is produced in lake sediments is consumed by methane oxidation before it can reach the atmosphere (Utsumi *et al.*, 1998; Bastviken *et al.*, 2002; Kankaala *et al.*, 2007). Methane oxidation is therefore a key process in limiting aquatic methane emissions. In general, key players in aerobic (oxygen dependent) methane oxidation are methane oxidizing bacteria (MOB), whereas anaerobic (independent of oxygen) methane oxidation is generally carried out by anaerobic methane oxidizing archaea (ANME), plus some very specific types of MOB. The aim of this thesis is to study how different electron acceptors affect methane oxidation rates and the microorganisms that are involved and affected by methane oxidation.

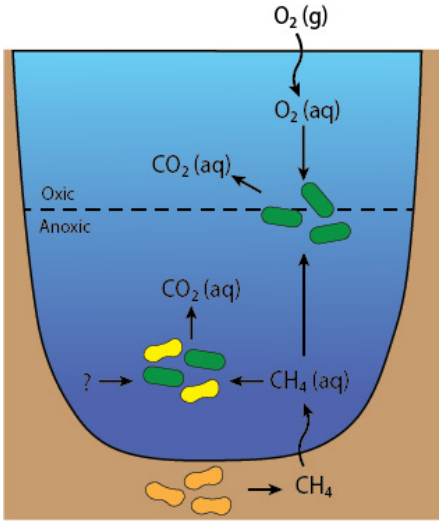

Fig. 1. Simplified, not to scale representation of the aquatic microbial methane cycle in a stratified lake or sea. The orange cells represent methanogenic archaea, which produce methane in the anoxic sediments. This methane may diffuse into the water column, where it can be consumed by methane oxidizing archaea (in yellow) or methane oxidizing bacteria (in green) at different locations in the water column. In some aquatic systems, methane production in the anoxic and oxic water column is observed. The electron acceptor involved in anaerobic methane oxidation in the anoxic water column often remains unknown. The dissolved methane that is not consumed in the anoxic water column can be used by aerobic methane oxidizing bacteria living at the oxycline, where they can profit from both methane and (low concentrations of) oxygen. The methane that is oxidized by the methanotrophs is converted to carbon dioxide (CO_2). Methane that is not consumed in the water column may reach the upper water layer and be emitted to the atmosphere.

Electron acceptors involved in methane oxidation

Microbial methane consumption is a redox reaction with methane as electron donor. Aerobic methanotrophy, with oxygen as electron acceptor, was already discovered in 1906 (Söhngen, 1906), while anaerobic methanotrophy was discovered much later, in the late 1970's (Barnes and Goldberg, 1976; Reeburgh, 1976, 1980; Panganiban *et al.*, 1979; Zehnder and Brock, 1980). An overview of the known terminal electron acceptors involved in methane oxidation is provided in Fig. 2, and each of these is discussed individually below.

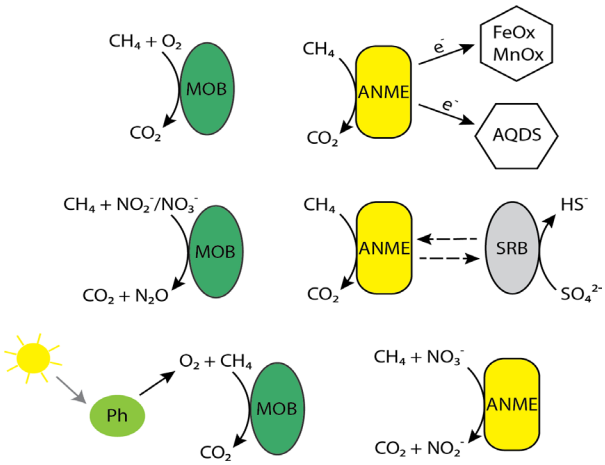

Fig. 2. Electron acceptors potentially involved in methane oxidation, with or without a microbial partner. MOB = Methane oxidizing bacteria; ANME = Anaerobic methane oxidizing archaea; SRB = Sulfate reducing bacteria; Ph = Phototroph; AQDS = Anthraquinone-2,6-disulfonate; FeOx & MnOx: Iron oxides and manganese oxides.

Oxygen is generally the preferential electron acceptor for methane oxidation performed by methane oxidizing bacteria (MOB), due to its high energy yield (standard Gibbs free energy ΔG –858 kJ mol^{-1} CH_4). Aerobic methane oxidation occurs predominantly at the oxic-anoxic interface of stratified water columns and sediments, where methane oxidizing organisms can benefit from both the methane input from the anoxic zone and the oxygen input of the oxic zone (Harrits and Hanson, 1980). Aerobic methane oxidation has also been observed in anoxic lake waters, where aerobic methane oxidation could occur via a symbiosis between methane oxidizers and phototrophs, in which the oxygen produced by photosynthesis is further used by aerobic methanotrophs (Oswald *et al.*, 2015). Methane oxidizing archaea (ANME) are strict anaerobes who cannot survive in oxic environments and are therefore incapable of using oxygen as an electron acceptor.

Sulfate-dependent anaerobic oxidation of methane (AOM) is the most common form of aquatic AOM, mostly taking place in marine sediments (Alperin and Reeburgh, 1985; Reeburgh, 2007; Knittel and Boetius, 2009). Although less common, freshwater sulfate-dependent AOM also occurs (Grossman *et al.*, 2002; Eller *et al.*, 2005; Zigah *et al.*, 2015). Sulfate-dependent AOM has a relatively low energy yield ($\Delta G°$ –33 kJ mol^{-1} CH_4; Segarra *et al.*, 2013) and is, therefore, mostly found to occur in places where no alternative electron acceptors are available.
Nitrite- and nitrate-dependent methane oxidation is predominantly observed in freshwater systems, which can experience high nitrate inputs due to eutrophication and terrestrial runoff

(Raghoebarsing *et al.*, 2006; Deutzmann and Schink, 2011; Luesken *et al.*, 2011; Deutzmann *et al.*, 2014) although organisms related to nitrite-dependent AOM have also been suggested to occur in marine environments (He *et al.*, 2015). The energy yield of nitrate and nitrite dependent methane oxidation is relatively high ($\Delta G°$ –801 and –1007 kJ mol^{-1} CH_4, respectively, Segarra *et al.*, 2013).

Methane oxidation coupled to the reduction of iron oxides and manganese oxides has been detected in marine sediments (Beal *et al.*, 2009; Egger *et al.*, 2014) and has also been suggested to take place in freshwater systems (Crowe *et al.*, 2011). Water column concentrations of these compounds are generally low. Under anoxic conditions, iron and manganese oxides can react rapidly with reduced compounds such as sulfide, further decreasing the concentration (Canfield, 1989). Therefore, only sediments that are relatively young or environments that receive a regular input of metal oxides generally contain concentrations high enough to enable metal-dependent methane oxidation. Besides their direct role as electron acceptors, iron oxides are also known to stimulate sulfate-driven methane oxidation in marine systems (Sivan et al. 2014).

Lastly, organic molecules have also been found to play a role as electron acceptors in anoxic environments (Lovley et al., 1996). Methanogens, which are closely related to methanotrophic archaea, were shown to reduce both the artificial 9,10-anthraquinone-2,6-disulfonate (AQDS) and soil organic matter (Bond and Lovley, 2002). Although the role of organic molecules in AOM has not yet been confirmed, they have been suggested to drive AOM in various environments (Smemo and Yavitt, 2011; Blodau and Deppe, 2012; Segarra *et al.*, 2015).

Electron acceptor availability

Water column stratification is one of the main factors determining electron acceptor availability. In a well-mixed water column, water masses, particulate and dissolved matter and gasses can move freely through the water column, resulting in homogeneous temperature, nutrient, oxygen and other gas concentration profiles, as is illustrated in Fig. 3. Stratified systems, by contrast, consist of two or more layers separated by a steep gradient in temperature or dissolved substances, which limits vertical transport of water, particles and gasses (Fig. 3). The diffusion of atmospheric gasses such as oxygen is limited to the upper water layer, whilst gasses that diffuse from the sediment, such as methane, get trapped in the bottom water layer. The bottom water layer can become oxygen depleted, creating an oxygen gradient within the water column with distinct niches for aerobic and anaerobic microorganisms, including methane producers and oxidizers.

Stratification can occur seasonally, as is observed in many lakes, or be permanent, like in the Black Sea. The microbial community within the anoxic zone of the Black Sea is highly adapted to the permanently anoxic conditions (Deuser, 1971). In seasonally stratified systems, however, microorganisms that are able to adapt to the changing conditions may have a competitive advantage, e.g. facultative anaerobes and fast-growing microorganisms.

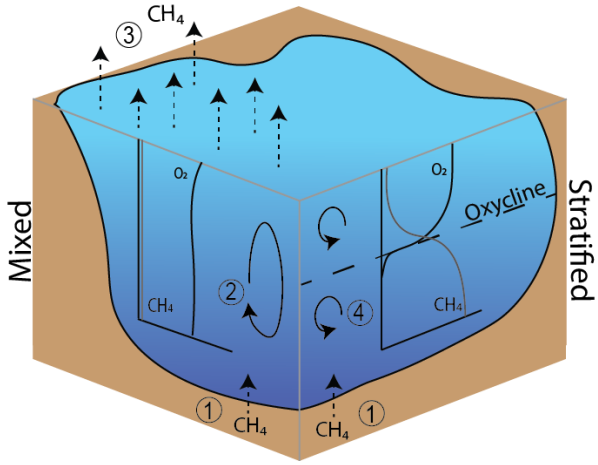

Fig. 3. Simplified representation of a seasonally stratified aquatic system. In the mixed situation (left side), the water column is homogeneous and well-mixed. The oxic-anoxic interface is located in the sediment. In the stratified situation (right side), two or more water masses exist, separated by an area that is characterized by a steep oxygen gradient, called the oxycline, which forms the oxic-anoxic interface. Methane is produced by methanogenic microorganisms (i.e. archaea) in the anoxic sediments (1), where it may partly already be oxidized. The remaining methane diffuses into the water column, both in the mixed and stratified situation. In the stratified situation, methane may also be produced in the anoxic water column. In the mixed situation, the dissolved, diffused methane that escaped sedimentary methane oxidation can be transported through the whole water column (2), and will reach the surface waters, from where it can be emitted to the atmosphere (3). Water column methane oxidation in the oxic, mixed situation is generally considered to be inhibited by high oxygen concentrations. In the stratified water column, the oxycline acts as a barrier for the dissolved methane, limiting diffusion and trapping methane in the bottom water layer, resulting in an increase in methane concentration over time (4). Methane may be oxidized in the anoxic water column or at the oxycline, or can be released when mixing of the water layers occurs, ending stratification.

Microorganisms involved in methane consumption

Methane oxidizing bacteria

Methane oxidizing organisms were first detected in 1906 by N.L. Söhngen (Söhngen, 1906). In 1970, Whittenbury, Phillips, and Wilkinson classified over 100 species of methane oxidizing bacteria, laying the basis for the current classification system (Whittenbury *et al.*, 1970), which was later revised by Bowman *et al.* (1994). Methane oxidizing bacteria are found within the Alpha- and Gammaproteobacteria and the Verrucomicrobia and they are divided into type I, type II and type X methanotrophs, although several studies have suggested a sharp separation between these groups is arbitrary and groups should not be distinguished (Op den Camp *et al.*, 2009; Knief, 2015).

Several studies suggested aquatic methane oxidation is limited or inhibited by high concentrations of oxygen. Indeed, some methanotrophs have been shown to oxidize more methane under low-oxygen conditions compared to high oxygen environments (Rudd and Hamilton, 1975; Blees *et al.*, 2014). Methanotrophic bacteria have been detected in anoxic lake waters (Biderre-Petit *et al.*, 2011; Blees *et al.*, 2014; Zigah *et al.*, 2015), although the mechanisms they deploy to cope with the oxygen limitation often remain unclear. Specific types of MOB

have been discovered to be capable of oxidizing methane under anoxic conditions, such as *Methylomonas denitrificans*, which is a facultative anaerobe capable of methane oxidation coupled to the reduction of both nitrate and oxygen (Kits *et al.*, 2015). NC10 bacteria, among which 'Candidatus *Methylomirabilis oxyfera*', were found to perform nitrite-dependent methane oxidation (Raghoebarsing *et al.*, 2006; Ettwig *et al.*, 2008) via an 'intra-aerobic' pathway, in which oxygen is produced from nitrite, and used for 'aerobic' methane oxidation (Ettwig *et al.*, 2010).

Methane oxidizing archaea and partners

Although anaerobic methane oxidation was discovered in the 1970s, the involved microorganisms were only identified 20 years later (Hinrichs *et al.*, 1999; Boetius *et al.*, 2000; Pancost *et al.*, 2000). ANME, anaerobic methane oxidizing archaea, are strict anaerobes, belonging to the Euryarchaeota. The genus is divided into three phylogenetic clusters: ANME-1, ANME-2 and ANME-3, with several subgroups (Hinrichs *et al.*, 1999; Orphan *et al.*, 2001; Knittel *et al.*, 2005; Niemann *et al.*, 2006). The different clusters are all related to different methanogenic archaea. The anaerobic methane oxidation pathway of ANME follows a reversed methanogenesis pathway (Hinrichs *et al.*, 1999; Hallam *et al.*, 2004) and is therefore completely different from the methane oxidation pathway found in methane oxidizing bacteria.

Consortia of ANME and sulfate reducing bacteria (SRB) are commonly observed in marine sediments. ANME-1 and ANME-2 are known to form consortia with *Desulfosarcina* and *Desulfococcus*, whereas ANME-3 generally forms consortia with *Desulfobulbus* (Boetius *et al.*, 2000; Orphan *et al.*, 2002; Niemann *et al.*, 2006). All three ANME-clades can also exist without SRB-partners (Beal *et al.*, 2009; Knittel and Boetius, 2009). Candidatus '*Methanoperedens nitroreducens*', belonging to clade ANME-2D, is able to perform nitrate-dependent methane oxidation (Haroon *et al.*, 2013), together with a bacterial partner that oxidizes the produced nitrite. Methane oxidation rates in sediments have been seen to increase 3.5 to 5 times by the addition of iron and manganese oxides, suggesting ANME are capable of using metal oxides as electron acceptors (Beal et al. 2009), which was also suggested by studies in freshwater and marine sediments (Sivan *et al.*, 2011; Egger *et al.*, 2014).

Effect of methane oxidation on the aquatic carbon cycle

Methanotrophs are the only microorganisms that can directly consume and assimilate carbon from methane. Other aquatic microorganisms may, however, use methane-derived carbon indirectly. Part of the methane-derived carbon that is processed by methane oxidizing bacteria is released as CO_2, while 20-55% of the CH_4 derived carbon is assimilated into MOB-biomass (Roslev *et al.*, 1997; Roslev and Iversen, 1999; Murase and Frenzel, 2007). Reaction intermediates, such as methanol, formaldehyde and formate, may be excreted by the methanotrophs and used by other community members (Cébron *et al.*, 2007; Martineau *et al.*, 2010; He *et al.*, 2012; Beck *et al.*, 2013), although it is unclear to which extend and in which situations this occurs, as it seems energetically unfavorable for the MOB. Acetate and lactate can be formed and excreted when MOB perform fermentation-based methanotrophy, which has been observed under oxygen-depleted conditions (Kalyuzhnaya *et al.*, 2013). In addition,

protozoal grazers consume assimilated methane-derived carbon in the form of methanotroph biomass (Murase and Frenzel, 2007; Jones and Grey, 2011). Overall, methane oxidizing bacteria can play an important role in distributing methane-derived carbon to non-methanotrophic microorganisms, as well as to higher trophic levels (i.e. protists and fish; Murase and Frenzel, 2007, Jones and Grey, 2011 and Sanseverino *et al.*, 2012).
In contrast to MOB, methane-derived carbon incorporation into ANME biomass is very low (0.25-1.3%, Wegener *et al.*, 2008) and the majority of the methane-derived carbon is released as CO_2, which can be used by autotrophic organisms of the microbial community. No release of reaction intermediates or other methane-derived carbon products is recognized in ANME.

Methods to study methane oxidation and microbial players

Determination of methane oxidation rates
Methane oxidation rates can be measured by several different methods, varying in accuracy, reliability, costs and complexity. The simplest is based on measurements of the methane concentration in incubation vials over time. A linear regression model is applied to calculate the methane oxidation rate from the methane concentration decline over time. This method, which only requires a system to measure the methane concentration in a gas sample, such as a gas chromatograph (GC), works especially well at high methane oxidation rates, as the difference between the timepoints is more likely to be statistically significant. A disadvantage of this method is that only net methane consumption can be determined, while methane oxidation and methane production may both affect the methane decrease over time. The consumption rate may thus be an underestimation of the methane oxidation rate. In order to separate the rates of the two processes, the methane oxidation inhibitors difluoromethane, acetylene or ethylene can be added to a subset of the incubation vials to be able to determine the gross methane oxidation rate (Miller *et al.*, 1998; Chan and Parkin, 2000). Methanogenesis inhibitors such as bromoethanesulfonate are known to often also inhibit methane consumption, specifically in ANME, and are therefore less suitable (Nauhaus *et al.*, 2005).
Another method to measure gross methane oxidation is by using ^{13}C-labeled methane (Groot *et al.*, 2003). ^{13}C-methane is added to incubation vials, after which the gas composition in the vials is analyzed on a GC system equipped with a mass spectrometer. By measuring $^{13}CO_2$ and ^{13}C incorporation in biomass, methane oxidation rates can be determined. The amount of ^{13}C-methane that needs to be added is, however, relatively high and therefore disturbs the natural conditions in environmental samples. Methods that require only very small amounts of methane to be added involve the use of the radioisotopes $^{14}C\text{-}CH_4$ or $^{3}H\text{-}CH_4$ (Rudd *et al.*, 1974; Valentine *et al.*, 2001; Pack *et al.*, 2011; Mau *et al.*, 2013). A radioisotope laboratory and training are however required to use these methods.
To determine the methane oxidation rates in the actual water column, rather than via incubation experiments, methods based on the natural ^{13}C-depletion of methane can be used (Barker and Fritz, 1981; Whiticar, 1999). These methods are based on the natural discrimination against ^{13}C, compared to ^{12}C, during microbial methanogenesis and methanotrophy, and require a trace gas isotope ratio mass spectrometer to determine the ^{13}C-depletion in δ units (‰) relative to the PDB standard. To calculate a methane oxidation rate from the $\delta^{13}C\text{-}CH_4$ values, the in situ fractionation factor needs to be determined (Coleman *et al.*, 1981), and

the methane oxidation rate must be calculated (Happell *et al.*, 1994; Tyler *et al.*, 1997; Liptay *et al.*, 1998). The formulas that are used for this calculation are dependent on whether the researcher classifies their system as a closed or open system, and determines largely what the outcome in terms of methane oxidation rates will be. Bastviken et al. (2002) compared the use of different formulas, and concluded that large under- or overestimations can be expected dependent on the chosen formula.

Diversity and abundance of the microbial community

The diversity and abundance of the microbial community, as a whole, and specifically of methanotrophs, can be determined by different methods based on gene determination or microscopic visualization. Methods based on targeting the 16S rRNA gene allow the detection of specific microbial groups either by using specific primers or by novel next generation amplicon sequencing approaches (Caporaso *et al.*, 2012; Liu *et al.*, 2012). DNA stable isotope probing (DNA-SIP) can be used to determine both the activity and the taxonomic information of the microbial population involved in the consumption of a labelled substrate, for the case of methanotrophs being isotopically labelled methane ($^{13}CH_4$). Both the lighter (^{12}C-containing) and the heavier (^{13}C-labelled) DNA fractions obtained from a DNA-SIP experiment can be further analyzed by 16S rRNA gene amplicon sequencing as described above and as previously applied in other studies (Radajewski *et al.*, 2000; Hutchens *et al.*, 2004) to determine the diversity of the entire microbial community.

The methanotrophic community can also be identified by targeting the particulate methane monoxygenase (*pmoA*, for MOB) or Methyl Coenzyme M Reductase A (*mcrA*, for ANME) genes, which can be used as phylogenetic markers (as seen for the 16S rRNA gene), but also as functional gene probes that can be targeted for gene expression and activity determination (McDonald and Murrell, 1997; Hallam *et al.*, 2003). Besides, the quantification of specific 16S rRNA, *pmoA* and *mcrA* genes by quantitative PCR can be used as method to estimate the abundance of genes attributed to target species and therefore as a proxy of their cell abundance (Kolb *et al.*, 2003; Nunoura *et al.*, 2008).

In addition to this targeted gene approach, whole genome analysis can provide information about the entire gene potential of a specific microorganism, including both the taxonomic information as well as its potential metabolic pathways (Tringe and Rubin, 2005). This method can be applied to isolated microorganisms or to a complex environmental community, the latter by a metagenomic sequencing approach. Metagenomic approaches are a powerful method to link microbial community diversity, activity and their potential role in biogeochemical cycles (Tyson *et al.*, 2004). However, it is also subjected to challenges regarding the integration of the genomic data by bioinformatic approaches and the prediction of genes and pathways based on previous studies (Pop and Salzberg, 2008).

Likewise, microscopic visualization methods targeting specific 16S rRNA gene sequences by fluorescent in situ hybridization (FISH), using fluorescently labelled DNA-specific oligonucleotide probes (Bauman *et al.*, 1980), allows the quantification of target cells, visualization of cell consortia and cell locations. For example, previous studies have used this approach to study both aerobic and anaerobic methanotrophs (Boetius *et al.*, 2000; Eller *et al.*, 2001; Wendeberg *et al.*, 2012). The FISH method has been further adapted and optimized over time, for example by the addition of horseradish peroxidase labeled probes and tyramide signal amplification in the CARD-FISH method (Pernthaler *et al.*, 2002). CARD-FISH is

routinely combined with nanoscale secondary ion mass spectrometry (NanoSIMS) to both taxonomically identify the targeted cells and determine their metabolic activities.

Scope of this thesis

Although the importance of methane oxidation in limiting methane emissions is well recognized, knowledge on the effect of 'unconventional' electron acceptors (other than oxygen or sulfate) is lacking. These alternative electron acceptors (for example nitrate, metal oxides or humic substances) could greatly expand the environmental niches where methane oxidation could take place and could alter methanotroph-partner interactions. Therefore, the aim of this thesis is not only to investigate the methane oxidizers and their preferential electron acceptor niches, but also their interactions with other microbes and the effects of electron acceptor availability on the wider microbial community.

In Chapter two, methane oxidation rate measurements were combined with a modeling approach to explore the electron acceptors potentially involved in methane oxidation in hypereutrophic Lacamas Lake (US). The modeling exercise showed that the in situ concentrations of commonly known electron acceptors were insufficient to support the observed methane oxidation rates, leading to the conclusion that an unknown electron acceptor, redox cycle or methane oxidation pathway must have been responsible, at least partly, for methane oxidation in the lake water column.

In Chapter three, the effect of different electron acceptors on water column methane oxidation was tested by incubation experiments. Lacamas Lake was used as a model system. Water column incubations with material from the anoxic, stratified water column showed an increase in methane oxidation and methanotroph abundance after the addition of either sulfate or nitrate, whilst humic substances and oxygen decreased methane oxidation rates. The preference of the dominant methanotroph for oxic or anoxic conditions was tested in incubation experiments with oxic water column material, of which a subset was made anoxic. An increase in both the methane oxidation rate and in methanotroph abundance was observed under anoxic conditions. The methanotroph that was dominating all incubation experiments, a *Methylobacter* species, was further explored using a metagenomic analysis, which revealed that the *Methylobacter* sp. lacked a complete denitrification pathway, despite the enhanced methane oxidation rates in the nitrate-amended experiments.

Chapter four describes an enrichment culture that was obtained with water column suspended matter of Lacamas Lake and that was used to study the methanotrophs and wider community in more detail. The enrichment culture was dominated by the same *Methylobacter* species that was present in the environmental samples, but, in contrast to the lake water column incubations, experiments with the enrichment culture showed no methane oxidation under anoxic conditions in the laboratory experiments. The addition of nitrate to oxic incubations experiments did result in enhanced methane oxidation rates compared to oxic experiments with ammonium. When comparing the effect of different oxygen concentrations (trace, micro-oxic and oxygen saturation) on the methane oxidation rates, it was shown that saturated

oxygen conditions yielded the highest methane oxidation rates. Besides the *Methylobacter* species, a *Methylotenera* species, capable of methanol oxidation but not methanotrophy, also became highly abundant in the enrichment culture. *Methylotenera* sp. genome analysis revealed the presence of a denitrification pathway in this organism, which could be related to the enhanced methane oxidation rate that was observed in the presence of nitrate.

In Chapter five, the co-occurrence and potential syntrophy between the methanotroph *Methylobacter* sp. and non-methanotrophic methylotroph *Methylotenera* sp. was further investigated. Methane-derived carbon transfer in the enrichment culture was followed using ^{13}C-labeled methane. DNA-SIP showed an incorporation of ^{13}C-carbon into both microbes that was strongly enhanced in the presence of nitrate, suggesting a coupling between nitrate availability and methane-derived carbon transport from *Methylobacter* sp. to *Methylotenera* sp. NanoSIMS analysis confirmed the ^{13}C-label incorporation, and showed no cell-to-cell contact between the two species was required for the transfer of methane-derived carbon between the species.

In Chapter six, the effect of different electron acceptors (sulfate, Fe^{3+} and AQDS) on anaerobic methane oxidation was tested using suspended particulate matter (SPM) collected from the permanently anoxic basin of the Black Sea. SPM collected from 1,000 m depth contained ANME-1b and was further used to perform incubation experiments with ^{13}C-labeled methane. Methane oxidation was enhanced in incubation experiments with molybdate and with the humic-acid analogue AQDS (in the presence of molybdate) compared to incubations with only sulfate and with Fe^{3+}. Microbial community analysis showed an increase in abundance of certain sulfur-cycling organisms in the incubations with active methane oxidation, possibly suggesting a role of these organisms in methane oxidation performed by ANME-1b.

In summary, the results described in this thesis show that several novel pathways of anaerobic methanotrophy seem to exists in known methanotrophs. Nitrate, a nutrient well-available in eutrophic lakes, stimulates both methanotrophy and methane-derived carbon transport though the freshwater microbial community. In the marine Black Sea environment, humic substances could possibly stimulate anaerobic methane oxidation by ANME-1b. Our results also show, however, that the translation between laboratory and field studies is challenging, and combining both field and culture-based studies is essential. More research is, therefore, required to determine the implications of these findings in natural environments.

References

Alperin, M.J. and Reeburgh, W.S. (1985) Inhibition experiments on aerobic methane oxidation. *Appl. Environ. Microbiol.* **50**: 940–945.

Barker, J.F. and Fritz, P. (1981) Carbon isotope fractionation during microbial methane oxidation. *Nature* **293**: 289–291.

Barnes, R.O. and Goldberg, E.D. (1976) Methane production and consumption in anoxic marine sediments. *Geology* **4.5**: 297–300.

Bastviken, D., Ejlertsson, J., and Tranvik, L. (2002) Measurement of methane oxidation in lakes: A comparison of methods. *Environ. Sci. Technol.* **36**: 3354–3361.

Bauman, J.G.J., Wiegant, J., Borst, P., and van Duijn, P. (1980) A new method for fluorescence microscopical localization of specific DNA sequences by in situ hybridization of fluorochrome-labelled RNA. *Exp. Cell Res.* **128**: 485–490.

Beal, E.J., House, C.H., and Orphan, V.J. (2009) Manganese- and iron-dependent marine methane oxidation. *Science* **325**: 184–187.

Biderre-Petit, C., Jézéquel, D., Dugat-Bony, E., Lopes, F., Kuever, J., Borrel, G., et al. (2011) Identification of microbial communities involved in the methane cycle of a freshwater meromictic lake. *FEMS Microbiol. Ecol.* **77**: 533–545.

Blees, J., Niemann, H., Wenk, C.B., Zopfi, J., Schubert, C.J., Kirf, M.K., et al. (2014) Micro-aerobic bacterial methane oxidation in the chemocline and anoxic water column of deep south-Alpine Lake Lugano (Switzerland). *Limnol. Oceanogr.* **59**: 311–324.

Blodau, C. and Deppe, M. (2012) Humic acid addition lowers methane release in peats of the Mer Bleue bog, Canada. *Soil Biol. Biochem.* **52**: 96–98.

Boetius, A., Ravenschlag, K., Schubert, C.J., Rickert, D., Widdel, F., Gieseke, A., et al. (2000) A marine microbial consortium apparently mediating anaerobic oxidation of methane. *Nature* **407**: 623–626.

Bond, D.R. and Lovley, D.R. (2002) Reduction of Fe(III) oxide by methanogens in the presence and absence of extracellular quinones. *Environ. Microbiol.* **4.2**: 115–124.

Bowman, J.P., Sly, L.I., Nichols, P.D., and Hayward, A.C. (1994) Revised taxonomy of the methanotrophs: Description of Methylobacter gen. nov., Emendation of Methylococcus, validation of Methylosinus and Methylocystis species, and a proposal that the family Methylococcaceae includes only the group I methanotrophs. *Int. J. Syst. Bacteriol.* **44**: 375–375.

Canfield, D.E. (1989) Reactive iron in marine sediments. *Geochim. Cosmochim. Acta* **53**: 619–632.

Caporaso, J.G., Lauber, C.L., Walters, W.A., Berg-Lyons, D., Huntley, J., Fierer, N., et al. (2012) Ultra-high-throughput microbial community analysis on the Illumina HiSeq and MiSeq platforms. *ISME J.* **6**: 1621–1624.

Chan, a. S.K. and Parkin, T.B. (2000) Evaluation of potential inhibitors of methanogenesis and methane oxidation in a landfill cover soil. *Soil Biol. Biochem.* **32**: 1581–1590.

Coleman, D.D., Risatti, J.B., and Schoell, M. (1981) Fractionation of carbon and hydrogen isotopes by methane-oxidizing bacteria. *Geochim. Cosmochim. Acta* **45**: 1033–1037.

Crowe, S.A., Katsev, S., Leslie, K., Sturm, A., Magen, C., Nomosatryo, S., et al. (2011) The methane cycle in ferruginous Lake Matano. *Geobiology* **9**: 61–78.

Deuser, W.G. (1971) Organic-carbon budget of the Black Sea. *Deep. Res. Oceanogr. Abstr.* **18**: 995–1004.

Deutzmann, J.S. and Schink, B. (2011) Anaerobic Oxidation of Methane in Sediments of Lake Constance, an Oligotrophic Freshwater Lake. *Appl. Environ. Microbiol.* **77**: 4429–4436.

Deutzmann, J.S., Stief, P., Brandes, J., and Schink, B. (2014) Anaerobic methane oxidation coupled to denitrification is the dominant methane sink in a deep lake. *Proc. Natl. Acad. Sci. U. S. A.* **111**: 18273–18278.

Egger, M., Rasigraf, O., Sapart, C.J., Jilbert, T., Jetten, M.S.M., Röckmann, T., et al. (2014) Iron-mediated anaerobic oxidation of methane in brackish coastal sediments. *Environ. Sci. Technol.* **49**: 277–283.

Eller, G., Känel, L., Krüger, M., Ka, L., and Kru, M. (2005) Cooccurrence of Aerobic and Anaerobic Methane Oxidation in the Water Column of Lake Plußsee. *Appl. Environ. Microbiol.* **71**: 8925–8928.

Eller, G., Stubner, S., and Frenzel, P. (2001) Group-specific 16S rRNA targeted probes for the detection of type I and type II methanotrophs by fluorescence in situ hybridisation. *FEMS Microbiol. Lett.* **198**: 91–97.

Ettwig, K.F., Butler, M.K., Le Paslier, D., Pelletier, E., Mangenot, S., Kuypers, M.M.M., et al. (2010) Nitrite-driven anaerobic methane oxidation by oxygenic bacteria. *Nature* **464**: 543–548.

Ettwig, K.F., Shima, S., Van De Pas-Schoonen, K.T., Kahnt, J., Medema, M.H., Op Den Camp, H.J.M., et al. (2008) Denitrifying bacteria anaerobically oxidize methane in the absence of Archaea. *Environ. Microbiol.* **10**: 3164–3173.

Groot, T.T., Van Bodegom, P.M., Harren, F.J.M., and Meijer, H.A.J. (2003) Quantification of methane oxidation in the rice rhizosphere using 13C-labelled methane. *Biogeochemistry* **64**: 355–372.

Grossman, E.L., Cifuentes, L.A., and Cozzarelli, I.M. (2002) Anaerobic methane oxidation in a landfill-leachate plume. *Environ. Sci. Technol.* **36.11**: 2436–2442.

Hallam, S.J., Girguis, P.R., Preston, C.M., Richardson, P.M., and DeLong, E.F. (2003) Identification of methyl coenzyme M reductase A (mcrA) genes associated with methane-oxidizing archaea. *Appl. Environ. Microbiol.* **69**: 5483–5491.

Hallam, S.J., Putnam, N., Preston, C.M., Detter, J.C., Rokhsar, D., Richardson, P.M., and DeLong, E.F. (2004) Reverse methanogenesis: testing the hypothesis with environmental genomics. *Science.* **305**: 1457–1462.

Happell, J.D., Chanton, J.P., and Showers, W.S. (1994) The influence of methane oxidation on the stable isotopic composition of methane emitted from Florida swamp forests. *Geochim. Cosmochim. Acta* **58**: 4377–4388.

Haroon, M.F., Hu, S., Shi, Y., Imelfort, M., Keller, J., Hugenholtz, P., et al. (2013) Anaerobic oxidation of methane coupled to nitrate reduction in a novel archaeal lineage. *Nature* **500**: 567–70.

Harrits, S.M. and Hanson, R.S. (1980) Stratification of aerobic methane-oxidizing organisms in Lake Mendota, Madison, Wisconsin. *Limnol. Oceanogr.* **25**: 412–421.

He, Z., Geng, S., Cai, C., Liu, S., Liu, Y., Pan, Y., et al. (2015) Anaerobic oxidation of methane coupled to nitrite reduction by halophilic marine NC10 bacteria. *Appl. Environ. Microbiol.* **81**: 5538–5545.

Hinrichs, K.U., Hayes, J.M., Sylva, S.P., Brewert, P.G., and DeLong, E.F. (1999) Methane-consuming archaebacteria in marine sediments. *Nature* **398**: 802–805.

Hutchens, E., Radajewski, S., Dumont, M.G., McDonald, I.R., and Murrell, J.C. (2004) Analysis of methanotrophic bacteria in Movile Cave by stable isotope probing. *Environ. Microbiol.* **6**: 111–120.

Jones, R.I. and Grey, J. (2011) Biogenic methane in freshwater food webs. *Freshw. Biol.* **56**: 213–229.

Kalyuzhnaya, M.G., Yang, S., Rozova, O.N., Smalley, N.E., Clubb, J., Lamb, A., et al. (2013) Highly efficient methane biocatalysis revealed in a methanotrophic bacterium. *Nat. Commun.* **4**: 1–7.

Kankaala, P., Taipale, S., Nykänen, H., and Jones, R.I. (2007) Oxidation, efflux, and isotopic fractionation of methane during autumnal turnover in a polyhumic, boreal lake. *J. Geophys. Res. Biogeosciences* **112**: 1–7.

Kirschke, S., Bousquet, P., Ciais, P., Saunois, M., Canadell, J.G., Dlugokencky, E.J., et al. (2013) Three decades of global methane sources and sinks. *Nat. Geosci.* **6**: 813–823.

Kits, K.D., Klotz, M.G., and Stein, L.Y. (2015) Methane oxidation coupled to nitrate reduction under hypoxia by the Gammaproteobacterium Methylomonas denitrificans , sp . nov . type strain FJG1. *Environ. Microbiol.* **17**: 3219–3232.

Knief, C. (2015) Diversity and habitat preferences of cultivated and uncultivated aerobic methanotrophic bacteria evaluated based on pmoA as molecular marker. *Front. Microbiol.* **6**: 1346.

Knittel, K. and Boetius, A. (2009) Anaerobic Oxidation of Methane: Progress with an Unknown Process. *Annu. Rev. Microbiol.* **63**: 311–334.

Knittel, K., Lösekann, T., Boetius, A., Kort, R., and Amann, R. (2005) Diversity and distribution of methanotrophic archaea at cold seeps. *Appl. Environ. Microbiol.* **71**: 467–479.

Kolb, S., Knief, C., Stubner, S., and Conrad, R. (2003) Quantitative detection of methanotrophs in soil by novel pmoA-targeted real-time PCR Assays. *Appl. Environ. Microbiol.* **69**: 2423–2429.

Liptay, K., Chanton, J., Czepiel, P., and Mosher, B. (1998) Use of stable isotopes to determine methane oxidation in landfill cover soils. *J. Geophys. Res. Atmos.* **103**: 8243–8250.

Liu, L., Li, Y., Li, S., Hu, N., He, Y., Pong, R., et al. (2012) Comparison of next-generation sequencing systems. *J. Biomed. Biotechnol.*

Luesken, F.A., Zhu, B., van Alen, T.A., Butler, M.K., Diaz, M.R., Song, B., et al. (2011) pmoA primers for detection of anaerobic methanotrophs. *Appl. Environ. Microbiol.* **77**: 3877–3880.

Mau, S., Blees, J., Helmke, E., Niemann, H., and Damm, E. (2013) Vertical distribution of methane oxidation and methanotrophic response to elevated methane concentrations in stratified waters of the Arctic fjord Storfjorden (Svalbard, Norway). *Biogeosciences* **10**: 6267–6268.

McDonald, I.R. and Murrell, J.C. (1997) The particulate methane monooxygenase gene pmoA and its use as a functional gene probe for methanotrophs. *FEMS Microbiol. Lett.* **156**: 205–210.

Miller, L.G., Sasson, C., and Oremland, R.S. (1998) Difluoromethane, a new and improved inhibitor of methanotrophy. *Appl. Environ. Microbiol.* **64**: 4357–4362.

Murase, J. and Frenzel, P. (2007) A methane-driven microbial food web in a wetland rice soil. *Environ. Microbiol.* **9**: 3025–3034.

Nauhaus, K., Treude, T., Boetius, A., and Krüger, M. (2005) Environmental regulation of the anaerobic oxidation of methane: a comparison of ANME-I and ANME-II communities. *Environ. Microbiol.* **7**: 98–106.

Niemann, H., Lösekann, T., De Beer, D., Elvert, M., Nadalig, T., Knittel, K., et al. (2006) Novel microbial communities of the Haakon Mosby mud volcano and their role as a methane sink. *Nature* **443**: 854–858.

Nunoura, T., Oida, H., Miyazaki, J., Miyashita, A., Imachi, H., and Takai, K. (2008) Quantification of mcrA by fluorescent PCR in methanogenic and methanotrophic microbial communities. *FEMS Microbiol. Ecol.* **64**: 240–247.

Op den Camp, H.J.M., Islam, T., Stott, M.B., Harhangi, H.R., Hynes, A., Schouten, S., et al. (2009) Environmental, genomic and taxonomic perspectives on methanotrophic Verrucomicrobia. *Environ. Microbiol. Rep.* **1.5**: 293–306.

Orphan, V.J., Hinrichs, K., Iii, W.U., Paull, C.K., Taylor, L.T., Sylva, S.P., et al. (2001) Comparative Analysis of Methane-Oxidizing Archaea and Sulfate-Reducing Bacteria in Anoxic Marine Sediment. **67**: 1922–1934.

Orphan, V.J., House, C.H., Hinrichs, K., Mckeegan, K.D., and Delong, E.F. (2002) Multiple archaeal groups mediate methane oxidation in anoxic cold seep sediments. *Proc. Natl. Acad. Sci.* **99**: 7663–7668.

Oswald, K., Milucka, J., Brand, A., Littmann, S., Wehrli, B., Kuypers, M.M.M., and Schubert, C.J. (2015) Light-dependent aerobic methane oxidation reduces methane emissions from seasonally stratified lakes. *PLoS One* **10**: e0132574.

Pack, M. a., Heintz, M.B., Reeburgh, W.S., Trumbore, S.E., Valentine, D.L., Xu, X., and Druffel, E.R.M. (2011) A method for measuring methane oxidation rates using low levels of 14C-labeled methane and accelerator mass spectrometry. *Limnol. Oceanogr. Methods* **9**: 245–260.

Pancost, R.D., Damsté, J.S.S., Lint, S. De, Maarel, M.J.E.C. Van Der, Gottschal, J.C., and Party, T.M.S.S. (2000) Biomarker evidence for widespread anaerobic methane oxidation in mediterranean sediments by a consortium of methaogenic archaea and bacteria. *Appl. Environ. Microbiol.* **66**: 1126–1132.

Panganiban, A.T., Patt, T.E., Hart, W., and Hanson, R.S. (1979) Oxidation of methane in the absence of oxygen in lake water samples. *Appl. Environ. Microbiol.* **37**: 303–309.

Pernthaler, A., Pernthaler, J., and Amann, R. (2002) Fluorescence in situ hybridization and catalyzed reporter deposition for the identification of marine bacteria. *Appl. Environ. Microbiol.* **68**: 3094–3101.

Pop, M. and Salzberg, S.L. (2008) Bioinformatics challenges of new sequencing technology. *Trends Genet.* **24**: 142–149.

Radajewski, S., Ineson, P., Parekh, N.R., and Murrell, J.C. (2000) Stable-isotope probing as a tool in microbial ecology. *Nature* **403**: 646–649.

Raghoebarsing, A.A., Pol, A., van de Pas-Schoonen, K.T., Smolders, A.J., Ettwig, K.F., Rijpstra, W.I., et al. (2006) A microbial consortium couples anaerobic methane oxidation to denitrification. *Nature* **440**: 918–921.

Reeburgh, W.S. (1980) Anaerobic methane oxidation: Rate depth distributions in Skan Bay sediments. *Earth Planet. Sci. Lett.* **47**: 345–352.

Reeburgh, W.S. (1976) Methane consumption in Cariaco Trench waters and sediments. *Earth Planet. Sci. Lett.* **28**: 337–344.

Reeburgh, W.S. (2007) Oceanic methane biogeochemistry. *Chem. Rev.* **107**: 486–513.

Roslev, P. and Iversen, N. (1999) Radioactive fingerprinting of microorganisms that oxidize atmospheric methane in different soils. *Appl. Environ. Microbiol.* **65**: 4064–4070.

Roslev, P., Iversen, N., and Henriksen, K. (1997) Oxidation and assimilation of atmospheric methane by soil methane oxidizers. *Appl. Environ. Microbiol.* **63**: 874–880.

Rudd, J.W.M. and Hamilton, R.D. (1975) Factors controlling rates of methane oxidation and the distribution of the methane oxidizers in a small stratified lake. *Arch. Hydrobiol* **75**: 522–538.

Rudd, J.W.M., Hamilton, R.D., and Campbell, N.E.. (1974) Measurement of microbial oxidation of methane in lake water. *Limnol. Oceanogr.* **19**: 519–524.

Sanseverino, A.M., Bastviken, D., Sundh, I., Pickova, J., and Enrich-Prast, A. (2012) Methane carbon supports aquatic food webs to the fish level. *PLoS One* **7**: e42723.

Segarra, K.E.A., Comerford, C., Slaughter, J., and Joye, S.B. (2013) Impact of electron acceptor availability on the anaerobic oxidation of methane in coastal freshwater and brackish wetland sediments. *Geochim. Cosmochim. Acta* **115**: 15–30.

Segarra, Schubotz, F., Samarkin, V., Yoshinaga, M.Y., Hinrichs, K., and Joye, S.B. (2015) High rates of anaerobic methane oxidation in freshwater wetlands reduce potential atmospheric methane emissions. *Nat. Commun.* **6**: 1–8.

Sivan, O., Adler, M., Pearson, A., Gelman, F., Bar-Or, I., John, S.G., and Eckert, W. (2011) Geochemical evidence for iron-mediated anaerobic oxidation of methane. *Limnol. Oceanogr.* **56**: 1536–1544.

Smemo, K.A. and Yavitt, J.B. (2011) Anaerobic oxidation of methane: An underappreciated aspect of methane cycling in peatland ecosystems? *Biogeosciences* **8**: 779–793.

Söhngen, N.L. (1906) Über Bakterien, welche Methan als Kohlenstoffnahrung und Energiequelle gebrauchen. *Cent. Bakt. Parasitenk. II*.

Tringe, S.G. and Rubin, E.M. (2005) Metagenomics: DNA sequencing of environmental samples. *Nat. Rev. Genet.* **6**: 805–814.

Tyler, S.C., Bilek, R.S., Sass, R.L., and Fisher, F.M. (1997) Methane oxidation and pathways of production in a Texas paddy field deduced from measurements of flux, 13C, and D of CH4. *Global Biogeochem. Cycles* **11**: 323–348.

Tyson, G.W., Chapman, J., Hugenholtz, P., Allen, E.E., Ram, R.J., Richardson, P.M., et al. (2004) Community structure and metabolism through reconstruction of microbial genomes from the environment. *Nature* **428**: 37–43.

Utsumi, M., Nojiri, Y., Nakamura, T., Nozawa, T., Otsuki, A., Takamura, N., et al. (1998) Dynamics of dissolved methane and methane oxidation in dimictic Lake Nojiri during winter. *Limnol. Oceanogr.* **43**: 10–17.

Valentine, D.L., Blanton, D.C., Reeburgh, W.S., and Kastner, M. (2001) Water column methane oxidation adjacent to an area of active hydrate dissociation, Eel River Basin. *Geochim. Cosmochim. Acta* **65**: 2633–2640.

Wegener, G., Niemann, H., Elvert, M., Hinrichs, K.U., and Boetius, A. (2008) Assimilation of methane and inorganic carbon by microbial communities mediating the anaerobic oxidation of methane. *Environ. Microbiol.* **10**: 2287–2298.

Wendeberg, A., Zielinski, F.U., Borowski, C., and Dubilier, N. (2012) Expression patterns of mRNAs for methanotrophy and thiotrophy in symbionts of the hydrothermal vent mussel Bathymodiolus puteoserpentis. *ISME J.* **6**: 104–112.

Whiticar, M.J. (1999) Carbon and hydrogen isotope systematics of bacterial formation and oxidation of methane. *Chem. Geol.* **161**: 291–314.

Whittenbury, R., Phillips, K.C., and Wilkinson, J.F. (1970) Enrichment, Isolation and Some Properties of Methane-utilizing Bacteria. *J. Gen. Microbiol.* **61**: 205–218.

Zehnder, A.J.B. and Brock, T.D. (1980) Anaerobic methane oxidation: Occurrence and ecology. *Appl. Environ. Microbiol.* **39**: 194–204.

Zigah, P.K., Oswald, K., Brand, A., Dinkel, C., Wehrli, B., and Schubert, C.J. (2015) Methane oxidation pathways and associated methanotrophic communities in the water column of a tropical lake. *Limnol. Oceanogr.* **60**: 553–572.

Chapter 2. Are elusive anaerobic pathways key methane sinks in eutrophic lakes and reservoirs?

Daniel C. Reed
Bridget R. Deemer
Sigrid van Grinsven
& John A. Harrison

Published in Biogeochemistry, 2017, 134(1-2), 29-39.

Abstract

Collectively, freshwaters constitute a significant source of methane to the atmosphere, and both methane production and methane oxidation can strongly influence net emissions. Anaerobic methane oxidation (AOM) is recognized as a strong regulator of marine methane emissions and appreciation of AOM's importance in freshwater is growing. In spite of renewed interest, recent work and reactive transport modeling results we present in this paper point to unresolved pathways for AOM. Comparison of recent observations from a eutrophic reservoir with predictions of a 1D steady-state model of water-column methane dynamics indicates that high rates of methane oxidation measured via bottle assays cannot be explained with conventional electron acceptors (O_2, NO_2^-, NO_3^-, SO_4^{2-}, Mn^{4+}, and Fe^{3+}). Reactive transport modeling suggests that the observed solute oxidant concentration at the thermocline would have to be around 10 times higher than observed to explain the measured methane consumption. Dissolved organic acids, a major constituent of dissolved organic matter in lake systems, may serve as additional electron acceptors. We evaluate several lines of evidence suggesting organic acids may be involved in AOM. In our case study, we quantify the potential for organic acids to support unexplained AOM and estimate that somewhere between 0.02 and 0.15 mol DOC L^{-1} would be required at the Lacamas thermocline to support the observed rates of oxidation – concentrations much lower than those observed in Lacamas. We point to several observations consistent with organic acid-mediated AOM, both in Lacamas Lake and in other systems. Nevertheless, direct evidence of this pathway is still lacking and testing for this remains an important direction for future work. To this end, we identify several new avenues of research that would help quantify the role of organic acid-mediated AOM relative to other electron acceptors.

Methane oxidation

Methane is a potent greenhouse gas with rapidly increasing atmospheric concentrations (Mhyre et al. 2013). Collectively, lakes and reservoirs contribute upwards of 90 Tg CH_4 yr^{-1} to the atmosphere (Bastviken et al. 2011), more than 10% of all sources in the global CH_4 budget (Ciais et al. 2013). Still, there is considerable uncertainty associated with modeling and upscaling field-scale CH_4 measurements (Wik et al. 2016). One uncertainty arises from the critically important role of methanotrophs (i.e., methane oxidizers) in attenuating atmospheric CH_4 emissions. In a review of 7 lakes, between 50 and 95% of methane produced in lake sediments was found to be oxidized prior to release (Bastviken et al. 2008).

In the ocean, 70-304 Tg of methane (10-55% of the total global atmospheric CH_4 flux) are oxidized each year (Reeburgh 2007, Ciais et al. 2013). Most (>90%) of this oceanic methane consumption occurs in the absence of oxygen via anaerobic oxidation of methane (AOM, Hinrichs and Boetius 2002; Reeburgh 2007). Marine AOM is generally observed in sediments in a region known as the "sulfate-methane transition zone" where anaerobic methanotrophic archaea are thought to work in concert with a sulfate-reducing "partner" (Knittel and Boetius 2009). Given high concentrations of sulfate (SO_4^{2-}) in seawater, sediment-based production of CH_4 rarely outpaces SO_4^{2-} supply from the overlying water column (although exceptions include seeps, vents, and gas-laden tidal flats, Knittel and Boetius 2009). In addition to SO_4^{2-}, recent studies have identified a number of alternative electron acceptors that drive AOM across marine and freshwater ecosystems (nitrate-nitrite-mediated, Ettwig et al. 2010 and Kojima et al. 2014; nitrate, iron, and manganese-mediated, Segarra et al. 2013; iron-mediated, Egger et al. 2015; 9,10-anthraquinone-2,6-disulfonate (AQDS), iron, and humic acid-mediated, Scheller et al. 2016; sulfate, iron, and AQDS driven, Valenzuela et al. 2017; Table 1). These findings have coincided with work highlighting the potential importance of AOM outside of marine sediments. For example, a recent review estimates that AOM reduces atmospheric CH_4 emissions from wetlands by >50% (Segarra et al. 2015).

Here, we define AOM broadly as all methane oxidation pathways that occur in the absence of oxygen. This includes methane oxidation coupled to SO_4^{2-} reduction by anaerobic methanotrophic archaea (ANME), denitrification by oxygenic bacteria (Ettwig et al. 2010), and other electron acceptors such as iron and manganese oxides (by ANME, gammaproteobacteria and other heretofore unidentified microorganisms, Borrel et al. 2011; Scheller et al. 2016; Oswald et al. 2016).

AOM in lakes & reservoirs

Until recently, relatively little work had been done to characterize AOM in freshwater lakes and reservoirs due, in part, to a widely held assumption that AOM was fueled solely by SO_4^{2-} (Borrel et al. 2011). High concentrations of CH_4 are widely observed to accumulate in the anoxic bottom waters of stratified lakes and reservoirs (Bastviken et al. 2008), but CH_4 oxidation is thought to occur predominantly near the oxycline where micro-aerophillic bacteria can use O_2 as a terminal electron acceptor (TEA, Blees et al. 2014). Still, the potential role of AOM in mediating lake and reservoir CH_4 emissions is starting to gain attention. About 10 years after the discovery of marine AOM, the earliest indications of lentic AOM were reported in

bottle incubations from Lake Mendota (Panganiban et al. 1979). Several recent studies have used isotopic, microbiological, and incubation-based evidence as well as reactive transport modeling to document AOM in the anoxic hypolimnion of lakes and reservoirs (Eller et al. 2005; Pimenov et al. 2010; Schubert et al. 2010; Crowe et al. 2011; Lopes et al. 2011; Blees et al. 2014; Kojima et al. 2014; Saxton et al. 2016; Oswald et al. 2016). Methanotrophs are known to preferentially oxidize lighter methane (^{12}C isotope), such that regions of high methane oxidation can result in relatively depleted $\delta\ ^{13}C$ in dissolved inorganic carbon (DIC) and relatively enriched $\delta\ ^{13}C$ in dissolved methane. Several lake and reservoir studies have reported peaks in methane $\delta\ ^{13}C$ (Eller et al. 2005; Schubert et al. 2010; Crowe et al. 2011; Itoh et al. 2015; Oswald et al. 2016) and drops in DIC $\delta\ ^{13}C$ (Crowe et al. 2011) in anoxic regions where microbiological analyses (Eller et al. 2005; Crowe et al. 2011; Kojima et al. 2014; Saxton et al. 2016; Oswald et al. 2016), geochemical evidence (Eller et al. 2005; Saxton et al. 2016) and/or bottle assays (Pimenov et al. 2010; Schubert et al. 2010; Lopes et al. 2011; Saxton et al. 2016; Oswald et al. 2016) suggest the presence of AOM. Together, these studies constitute a growing body of evidence highlighting the potential importance of AOM in eutrophic lakes and reservoirs. In the sections that follow, we draw upon a case study and a synthesis of recent literature to build a case that AOM is important in lakes and reservoirs and that an elusive oxidant may play an important, heretofore underappreciated role in mediating this important biogeochemical process.

Material and methods

Electron Acceptor Concentrations and Oxidation Rate Measurements

To examine the balance between methane oxidation and electron acceptor availability, we measured water column temperatures, methane oxidation rates and electron acceptor concentrations along a vertical profile near the deepest site (16.8 m) in a well-characterized lake: Lacamas Lake. Lacamas Lake is a small, monomictic, eutrophic reservoir located in southwest Washington, U.S.A. Sampling was conducted at 4, 5.5, 7, 9, 11, 13, 15, and 17 m depth during mid-fall when the thermocline had begun to deepen but the reservoir had not yet fully mixed (28 Oct 2014). Temperature and oxygen concentrations were measured with a Hach DS5X Sonde. For analysis of NO_3^-, NO_2^-, and SO_4^{2-}, samples were collected with a Van Dorn, filtered (Whatman GF/F 0.45 µm), and stored frozen in acid-washed 30 mL plastic HDPE Nalgene bottles until analyzed. NO_3^-, NO_2^-, and SO_4^{2-} were analyzed on a Westco discrete nutrient analyzer using standard EPA-approved colorimetric methods (method number 353.2 for NO_2^- and NO_3^-, and 4500 for SO_4^{2-}, National Environmental Methods Index, www.nemi.gov). The detection limits were 0.4 µmol L^{-1} for NO_3^- and NO_2^-, and 7.2 µmol L^{-1} for SO_4^{2-}. We estimated the potential role of Fe and Mn oxides as TEAs for methane oxidation by measuring the rate of accumulation of dissolved Fe and Mn in the hypolimnion during four summer stratified seasons (July through early September 2010-2013) using the hypolimnion accumulation method described in Deemer et al. (2011). For analysis of dissolved Mn and Fe, 5 mL aliquots of filtered water samples were acidified with 0.15 mL of concentrated HNO_3 to achieve 3% v/v HNO_3. Samples were then run on an Agilent 7700 inductively coupled plasma mass spectrometer (ICP-MS). We consider dissolved Mn and Fe as a proxy for reduced Mn and Fe given that oxidized forms of these metals are quite insoluble and our samples were filtered.

Methane oxidation rates were estimated using difluoromethane (DFM, Sigma Aldrich) as an inhibitor of methane oxidation. 0.5 mL DFM was added to half the samples (n=4 for each treatment) at the start of the experiment as in Miller et al. (1998) and Kankaala et al. (2006). All samples were then incubated in the dark for 24 hours in water baths within ±2°C of lake temperature at the time of collection. Incubations were terminated by addition of $ZnCl_2$ and a 10 mL ultra-high purity helium headspace was introduced. The headspace was analyzed by a gas chromatograph equipped with an electron capture detector (Hewlett-Packard 5890 Series II-Plus). Headspace methane concentrations were used to calculate original dissolved gas concentrations using the appropriate solubility tables (Weiss and Price 1980). The air-tightness of vials over the 24-hour incubation period was confirmed using a Membrane-Inlet Mass Spectrometer (Pfeiffer).

Reactive-transport modeling

Observed chemical dynamics were compared with a simple numerical model describing the transport and oxidation of methane in Lacamas Lake: the Methane and Oxygen Dynamics in Eutrophic Lakes Model (MODEL^2 hereafter). MODEL^2 considers transport by turbulent mixing and methane oxidation by both aerobic and anaerobic pathways. Consistent with observations (Iversen et al. 1987; Smemo and Yavitt 2011), reaction kinetics for methane oxidation are assumed to be first order with respect to methane concentration (Fig. 1), and methane oxidation rate (R; mol L^{-1} d^{-1}) was calculated as:

$$R = k[CH_4] \quad (1)$$

where k is the rate constant (d^{-1}) and $[CH_4]$ is methane concentration (mol L^{-1}). Fitting equation 1 to observations using the lm() function in the R base package gives a rate constant of 0.12 d^{-1} (R^2=0.97; Fig. 1), which is similar to previous estimates of aerobic methane oxidation rate constants in lakes (e.g., cf. 0.14 d^{-1}, Lopes et al. 2011). When oxygen is present we assume that methane oxidation progresses aerobically, according to the following reaction:

$$CH_4 + 2O_2 \rightarrow HCO_3^- + H^+ + H_2O$$

Upon depletion of oxygen, modeled methane oxidation is attributed to unspecified anaerobic pathways.

We assume that solute (e.g., methane, oxygen) transport is dominated by turbulent mixing, which is quantified using an eddy diffusion coefficient, K_z, that is proportional to the reciprocal of the buoyancy frequency, N^2 (e.g., Katsev et al. 2010):

$$K_z \propto (N^2)^{-1} \quad (2)$$

The constant of proportionality is chosen to reproduce profiles of methane concentration, oxygen concentration, and measured methane oxidation rates. Resulting eddy diffusion coefficients, K_z, are in the range of 10^{-6}–10^{-5}, which is within the expected range for lakes although at the upper bound for monomictic lakes (e.g., Salas de León et al. 2016). If mixing and, therefore, oxygen supply to the hypolimnion are overestimated in MODEL^2, then MODEL^2-based estimates of anaerobic methane oxidation are too low.

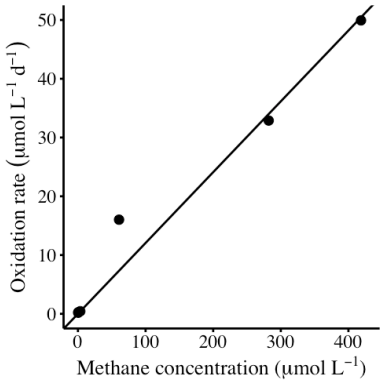

Fig. 1. Methane oxidation rate versus methane concentration. Circles denote observations, while the line shows equation 1 fit to these data ($R^2 = 0.97$).

Within MODEL^2, the lake is divided into vertical layers of 1 cm in thickness between 5 m and 15 m depth. In layer *i* of the model, oxygen and methane dynamics subject to turbulent diffusive mixing and methane oxidation are modeled using the following volumetric diffusion-reaction equation with the transport term (which incorporates K_z) implemented in the ReacTran package (Soetaert & Meysman, 2012):

$$\frac{d[O_2]_i}{dt} = -\frac{\Delta_i\{-E \cdot \Delta[O_2]\}}{V_i} - R\delta_{iO_2} = 0 \quad (3)$$

$$\frac{d[CH4]i}{dt} = -\frac{\Delta_i\{-E \cdot \Delta[CH4]\}}{V_i} - R_i = 0 \quad (4)$$

where Δ_i is the difference across the layer, $[O_2]$ is the oxygen concentration (mol m^{-3}), $[CH_4]$ is the methane concentration (mol m^{-3}), V_i is the volume of the layer ($A_i \times dz_i$ where A_i is the area and dz_i is the thickness of layer *i*, respectively; m^3), E is the bulk dispersion coefficient ($K_z \times A_i / dz_i$; m^3 d^{-1}), R_i is the rate of methane oxidation, and δ_{O_2} is a switch that forces aerobic methane oxidation to zero when oxygen is depleted. Equations 3 & 4 are solved using the steady.1D() function of the rootSolve package using the stode method (Soetaert & Herman, 2009). We define δ_{O_2} as,

$$\delta_{O_2} = \left(\frac{[O_2]}{O_2 + 3 \cdot 10^{-6}}\right) \quad (5)$$

We use this expression rather than a binary switch $\left(\text{e.g., } \delta_{O_2} = \begin{cases} 1, \text{when } O_2 > 0 \\ 0, \text{when } O_2 = 0 \end{cases}\right)$ because sharp boundaries create problems with the numerical solver. $3 \cdot 10^{-6}$ in the denominator is equivalent to a Michaelis-Menten half-saturation coefficient for oxygen of 3 nM, which is the lowest concentration at which microbial growth via aerobic pathways has been observed (Stolper et al., 2010). Data and model code are available for download at https://github.com/DanielReedOcean/MODEL2. [Note to reviewers: these will be made available upon acceptance for publication.]

Model sensitivity

The model contains two parameters estimated from observations: the first order rate constant for methane oxidation, *k*, and the eddy diffusion coefficient, K_z. To examine the influence of these parameters on model behavior, we varied the magnitudes of the parameters and reran

the baseline scenario described above. The mixing coefficient K_z was varied across 6 orders of magnitude encompassing the typical range of values observed in thermally-stratified lakes (Salas de León et al., 2016) and the observed rate constant (Fig. 1) was varied by ± 50%. Changes in the mixing coefficient, K_z, caused all profiles – methane and oxygen concentrations, as well as methane oxidation rate – to deviate from observations, providing confidence in the chosen parameter values (Supplemental Material). While methane and oxygen profiles were largely unaffected by variations in the rate constant, the methane oxidation rate profile departed markedly from observations in the sensitivity analysis (Supplemental Material). A detailed discussion of the sensitivity analysis is included in the Supplemental Material.

Table 1. Potential methane oxidation pathways.

Terminal electron acceptor	Reaction	ΔG° (kJ mol^{-1} CH_4)
Sulfate	$CH_4 + SO_4^{=} \rightarrow HCO_3^- + HS^- + H_2O$	-33[a]
AQDS	$CH_4 + 4AQDS + 3H_2O \rightarrow HCO_3^- + H^+ + 4AQDH_2DS$	-41[b]
Iron oxyhydroxides	$CH_4 + 8Fe(OH)_3 + 15H^+ \rightarrow HCO_3^- + 8Fe^{2+} + 21H^2O$	-571[a]
p-Benzoquinone	$CH_4 + Q + 2H_2O \rightarrow CO_2 + 4QH_2$	-731[c]
Manganese oxides	$CH_4 + 4MnO_2 + 7H^+ \rightarrow HCO_3^- + 4Mn^{2+} + 5H_2O$	-790[a]
Nitrate	$CH_4 + 4NO_3^- \rightarrow CO_2 + 4NO_2 + 2H_2O$	-801[a]
Nitrite	$3CH_4 + 8NO_2^- + 8H^+ \rightarrow 3CO_2 + 4N_2 + 10H_2O$	-1007[a]
Oxygen	$CH_4 + 2O_2 \rightarrow CO_2 + 2H_2O$	-858[d]

[a]Adjusted from Segarra et al. (2013). [b]Adjusted from Scheller et al. (2016). [c]Calculated based on Uchimiya and Stone (2009), see supplemental materials for detailed calculation. [d]Calculated using the CHNOSZ package (Dick 2008).

Results

MODEL[2] faithfully reproduces observed oxygen concentration, methane concentration, and methane oxidation rate profiles (Fig. 2). However comparison of model output and measured oxidation rates reveals that aerobic methane oxidation can account for, at most, just 14% of hypolimnion methane consumption. Other processes may also consume oxygen in the water column (e.g., oxidation of organic matter, Fe^{2+}, Mn^{2+}), so 14% may well be an overestimate. While these results suggest the occurrence of AOM, traditional anaerobic electron acceptors (e.g. NO_3^-, NO_2^-, and SO_4^{2-}, Table 2, Fig. 3) are not present in sufficient concentrations to explain the methane oxidation rates observed at Lacamas Lake. The potential for Mn and Fe oxides to fuel AOM also appears to be small given the relatively low rates of reduced Fe and Mn accumulation we observed in the reservoir hypolimnion across 4 years of data.

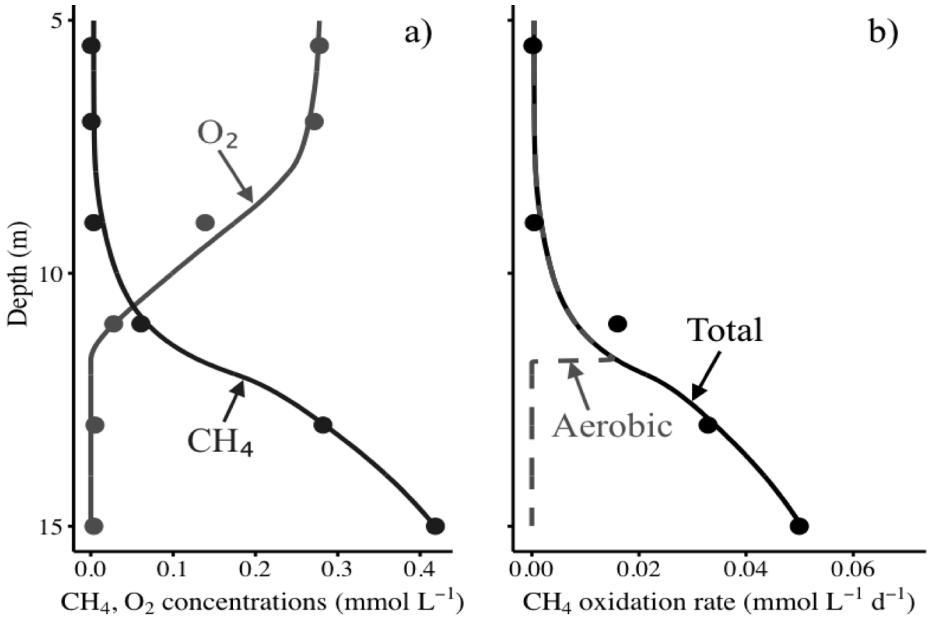

Fig. 2: Profiles of methane, oxygen, and methane oxidation rate in Lacamas Lake for 28 October, 2014. Circles represent observations, while lines represent model output. Panel (A) shows methane and oxygen concentrations over a depth profile; panel (B) shows measured methane oxidation rate (black points), total modeled methane oxidation rates (aerobic plus anaerobic; black line), and modeled aerobic methane oxidation rate (dashed line). Oxygen measurements are accurate to ±0.003 mmol L^{-1} and methane measurements are accurate within 2.2% of actual values based on the coefficient of variation of repeat standards.

Table 2. Concentrations of conventional electron acceptors measured at 4 m depth in Lacamas Lake (representing the boundary conditions for the reactive transport model).

Terminal electron acceptor	Concentration (mmol L^{-1})
Oxygen	0.196
Sulfate	0.090
Nitrate	0.005
Nitrite	0.001

NO_3^-, NO_2^-, and SO_4^{2-} are introduced to the model by recasting the oxygen variable as a generic oxidant for methane, G, that represents the sum of all these species. To account for the different stoichiometries of anaerobic methane oxidation, the concentration of G at the upper bound is specified using the measured electron acceptor concentrations at a depth of 4 m (Table 2) – that is, in well-mixed oxygenated surface waters above the thermocline that are the source of oxidants – using the following equation:

$$G_{4m} = [O_2 + 4NO_3^- + \frac{8}{3} NO_2^- + SO_4^{2-}]_{4m}$$

Together these oxidants explain an additional 6% of observed methane oxidation, leaving 80% of CH_4 oxidation unaccounted for. As manganese and iron oxides occur in the water column as particulates, they are subject to different transport processes (e.g., sinking) and cannot be incorporated within G, which only represents solutes. Nevertheless, estimates of reduced Mn and Fe accumulation in the water column, based on biweekly profiles, show that the contribution of these species to water column methane oxidation is likely to be negligible. Assuming all iron and manganese reduction is coupled to methane oxidation, the maximum rate at which Fe^{2+} and Mn^{2+} accumulate in the hypolimnion (approximately 0.2 kmol Mn d^{-1} and 2.2 kmol Fe d^{-1}) can only explain 1.0 and 5.3% of the observed methane oxidation, respectively (Fig. 3). Our simulations suggest that about 10 times the solute oxidant concentration that is present at the thermocline is required to explain the methane consumption observed (Fig. 3). This raises the question: is there another important yet elusive electron acceptor mediating AOM?

Results from this reactive transport modeling exercise as well as observations reported in previous studies both point to an unresolved pathway for AOM. While a balanced electron budget was constructed for eutrophic, monomictic Lake Rotsee based on estimations of turbulent diffusive transport, ultimately the authors concluded that "the question of which species are involved in methane oxidation could not be solved completely" (Schubert et al. 2010). In meromictic, oligotrophic Lake Gek-Gel, relatively high rates of anaerobic methane oxidation were observed within the sediment, but did not line up with the sulfate reducing zone leaving the dominant electron acceptor unidentified (Pimenov et al. 2010). In meromictic Lake Matano, the authors estimate that Fe and Mn must be recycled several times in the water column (i.e., across the oxycline) to balance the upward flux of CH_4 (Crowe et al. 2011), but whether this mixing is actually occurring is unknown. In eutrophic, meromictic Lake Lugano, bottle assays from the anoxic hypolimnion reveal greater rates of oxidation than can be explained by O_2, SO_4^{2-}, NO_3^-, NO_2^-, and Fe^{3+} concentrations (Blees et al. 2014). While Lake Lugano's methane oxidation budget is dominated by microaerophilic oxidation at the oxic-anoxic interface, the authors could not rule out AOM in deeper waters, asserting that "further investigation is required to ascertain potential anaerobic modes of CH_4 oxidation in Lake Lugano's anoxic hypolimnion" (Blees et al. 2014).

Recent work has linked methane oxidation in anoxic lake waters to instantaneous O_2 production via photosynthetic algae (Milucka et al. 2015), but the methane oxidation incubations we report were conducted in the dark. Additionally, the secchi depths at Lacamas Lake are generally quite shallow (mean summertime depth of 1.4 m, Carlson et al. 1985) such that no photosynthetic active radiation can reach 12-15 m depth (where the highest rates of oxidation were observed). Oxidation and reduction reactions can also sometimes be "cryptic" whereby rapid co-occurring reactions can result in an apparent lack of particular oxidants simply because the oxidant is turning over so quickly (Canfield et al. 2010). Nevertheless, cryptic oxidation reactions still require some source of oxidant (such as sulfide oxidation linked to nitrate/nitrite reduction as in the case of the cryptic N and S cycle in oceanic oxygen minimum zones, Canfield et al. 2010). In the electron budgeting exercises presented here, however, we could not identify a potential oxidant source using traditional electron acceptors.

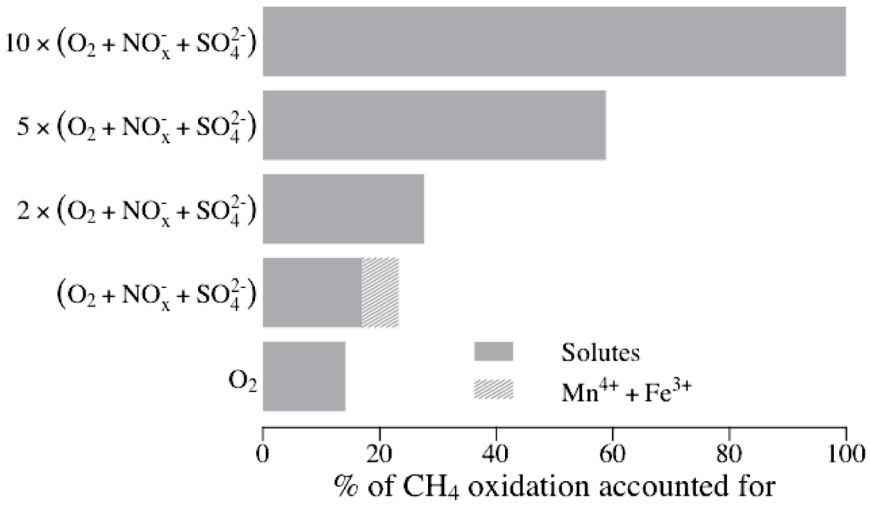

Fig. 3: Fraction of methane oxidation that can be explained when assuming different oxidant concentrations at the thermocline. The bottom gray bar represents a simulation considering observed oxygen concentrations only, while the gray bar immediately above also includes observed NO_2^-, NO_3^-, and SO_4^{2-} concentrations. The top three gray bars represent simulations with multiples of all the observed oxidants. In addition, the maximum fraction of oxidation that can be explained by manganese and iron reduction is depicted by a dashed bar. Mn^{4+} and $Fe^{\#+}$ are not depicted in the scenarios where we multiply solute oxidant concentrations at the upper bound of the model because oxidized Mn and Fe exist in particulate form.

Are organic acids elusive electron acceptors?

While it is well known that organic matter functional groups can accept electrons during fermentation-based molecule dismutation, a growing body of work reports the capacity for organic acids to serve as external TEAs in redox sensitive biogeochemical reactions (Lovley et al. 1996; Fimmen et al. 2007; Martinez et al. 2013). Experimental organic acid additions have been shown to limit freshwater CH_4 emissions in bogs (Blodau and Deppe 2012) and wetlands (Keller et al. 2009). Quinones, often considered a model redox-sensitive organic acid functional group, have recently been reported to serve as important electron acceptors in a variety of settings, such as peat soils (Lipson et al. 2010), freshwater sediments (Kappler et al. 2004), and periodically anoxic environments (Klüpfel et al. 2014). In addition to quinones, two independent studies found that nonquinone organic acid functional groups were responsible for anywhere between 44 and 58% of total electron transfer capacity (as cited in Martinez et al. 2013). Organic acids may thus limit aquatic CH_4 emissions to the atmosphere by extending the redox ladder, limiting the development and persistence of the highly reducing conditions required for methanogenesis (Cervantes et al. 2000).

In addition to extending the redox ladder, organic acids may also function as an intermediary by shuttling electrons across redox gradients in space or time to oxidize reduced species that

are subsequently employed in AOM (Klüpfel et al. 2014). In the context of lakes and reservoirs, organic TEAs may be replenished on seasonal timescales wherein lake turnover drives the oxidation of organic acids both within the hypolimnion and at the sediment water interface, as has been observed in a northern bog undergoing seasonal oxic-anoxic cycles (Heitmann et al. 2007). Furthermore, particle-associated organic TEAs may be supplied to anoxic waters in stratified lakes and reservoirs throughout the year with organic matter sinking across the oxycline. In this way, organic acids could also function to regenerate more common oxidants, such as iron oxyhydroxides and thiosulfate (via oxidation of Fe^{2+} and H_2S, Lovley et al. 1996; Heitmann and Blodau 2006; Saxton et al. 2016). Such indirect oxidation could give rise to complex reaction networks, for example by linking organic acid-rich environments (like sediments or sinking particles) with methane dissolved in the water column through intermediary species (e.g., iron).

Alternatively – or in addition – organic acids may serve as direct electron acceptors in the anaerobic oxidation of methane diffusing from freshwater sediments. Reductive dehalogenation of fluvic acids has recently been posited to fuel AOM in a permanently ice covered lake (Saxton et al. 2016) and AQDS, a model quinone organic acid, was recently shown to serve as an electron acceptor for ANME-mediated methane oxidation in marine sediments (Scheller et al. 2016). Recent work in wetland sediments also provides spectroscopic and incubation-based evidence for organic acid mediated AOM (in both the natural organic matter pool and in response to Pahokee Peat and AQDS amendments, Valenzuela et al. 2017). Quinone-fueled AOM is more thermodynamically-favorable than several common methanotrophic metabolisms that use inorganic electron acceptors (Table 1). This is particularly relevant for organic-rich (i.e., eutrophic) systems, as organic acids have been shown to be a major constituent of DOM in natural waters (>75% of all freshwater DOC on average, Perdue and Ritchie 2003), and quinoid functional groups are ubiquitous (Fimmen et al. 2007). The dearth of inorganic TEAs in the Lacamas water column late in the stratified season, in concert with an abundance of organic material (Deemer et al. 2011), lead us to hypothesize that dissolved organic acids act as important electron acceptors for AOM at this site. Assuming 75% of the DOC in Lacamas was composed of organic acids and assuming the stoichiometry for methane oxidation with the model quinones AQDS and p-benzoquinone (e.g. 75 mols and 8 mols of DOC per 1 mol of CH_4, Table 1), we estimate that somewhere between 0.02 and 0.15 mol DOC L^{-1} would be required at the Lacamas thermocline to support the observed rates of oxidation. This is well within the observed concentrations of DOC in other temperate lake systems and much lower than DOC concentrations measured at the thermocline in Lacamas during the period of our simulation (1.7-4.1 mg C L^{-1}).

Future work: a call to researchers

Despite observations consistent with organic acid-mediated AOM in Lacamas Lake and several other systems, direct evidence of this pathway is lacking (but see Scheller et al. 2016; Valenzuela et al. 2017) and testing for this is an important direction for future work. We have identified several avenues of research that would help the field to advance towards a fuller understanding of AOM more generally and organic acid-mediated AOM in particular.

1. Continued effort should aim to better characterize the capacity for inhibitor and isotope-based tools to uncover AOM dynamics. Currently, specific methane oxidation inhibitors that target AOM pathways have yet to be identified. Future work should aim to identify inhibitors that act solely on AOM pathways so that the magnitude and controls on AOM can be better elucidated. This is not a trivial task given that anaerobic methanotrophic archaea can use a reversed methanogenesis pathway (Borrel et al. 2011) making it likely that many of the enzymes that inhibitors target may be involved in both AOM and methanogenesis (as is the case with bromoethanesulfonate, Nauhaus et al. 2005). Isotope-wise, while methanotrophs generally preferentially oxidize lighter methane, evidence from SO_4^{2-}-mediated AOM in marine sediments suggests that AOM may either enrich or deplete the $^{13}CH_4$ pool depending on the availability of SO_4^{2-} (Yoshinaga et al. 2014) – a pattern that is consistent with observations in an ice covered lake (Saxton et al. 2016). Isotope labeling experiments across a range of electron acceptor availabilities in systems where AOM pathways are known to dominate would provide a useful reference for researchers aiming to use spatial or temporal patterns in isotopic signatures to infer the presence of AOM.
2. Organic acids have been shown to be ecologically relevant in freshwaters (Lennon et al. 2013). Precise characterization of DOM in natural waters (e.g. Kellerman et al. 2015) and continued efforts to identify redox couples (e.g. Fimmen et al. 2007) would help to quantify substrate availability for microbes that employ organic acids as electron acceptors. Such information would give researchers a better idea of how to amend bottle assays to target organic acid mediated AOM (rather than relying on stock DOM that may or may not be representative of natural DOM).
3. The relative role of organic acids as direct electron acceptors (Scheller et al. 2016) versus electron shuttles (Heitmann and Blodau 2006; Martinez et al. 2013; Klüpfel et al. 2014) in supporting AOM should be examined in freshwater ecosystems. This question could be addressed using bottle assays (and appropriate methanogenesis inhibitors if necessary) to incubate water with known AOM with amendments of both organic acids and reduced intermediaries such as H_2S, Mn^{2+} and Fe^{2+}. If organic acids only facilitate AOM in the presence of intermediary amendments, then it may be that their role as electron shuttles is more important than their role as direct electron acceptors.
4. A diverse array of bacteria and archaea are known to be capable of reducing organic acids (Martinez et al. 2013). Scheller and colleagues recently showed that ANME-2 archaea groups were involved in direct organic acid (AQDS)-mediated AOM and that the process was decoupled from a sulfate reducing partner (Scheller et al. 2016). Still, the potential for other archaea and bacteria to couple organic acid reduction to methane oxidation is currently unknown. It is likely that groups other than ANME are able to couple organic acid reduction to AOM given that ANME were barely detected in wetland sediments undergoing organic acid mediated AOM (Valenzuela et al. 2017). Characterizing the microbial communities responsible for AOM linked to organic acids, as well as associated biochemical parameters (e.g., half-saturation coefficients, rate constants), is key to understanding these pathways. State-of-the-art molecular tools (e.g., metagenomics, metatranscriptomics) and single cell isotope probing and imaging techniques (FISH-SIMS, single cell genomics) together with classical incubation and culturing approaches will prove invaluable to this end.

Acknowledgements

The authors thank M. Keith Birchfield for assistance with data organization, field, and lab work. We also appreciate helpful input from Anna Withington and Jason Keller in the early stages of paper development. Finally, we thank Marc Kramer for helpful feedback and comments on a draft version of this manuscript. Financial support for this work was provided by GEF/UNESCO-4500226031, USACE-IWR and NSF DEB1355211 to Harrison.

Supplemental material

Methane oxidation coupled to quinone reduction

Quinone half reaction:*

Reaction	**ΔG° (kJ mol^{-1})**
$Q + e^- \rightarrow Q^-$	-7.526
$Q^- + e^- \rightarrow Q^=$	-2.316
$Q^= + H^+ \rightarrow HQ^-$	-68.60
$HQ^- + H^+ \rightarrow QH_2$	-57.99
$Q + 2e^- + 2H^+ \rightarrow QH_2$	-136.4

Methane half reaction:

Reaction	**ΔG° (kJ mol^{-1})**
$CH_4 + 2H_2O \rightarrow CO_2 + 8H^+ + 8e^-$	-185.28

Overall reaction:

Reaction	**ΔG° (kJ mol^{-1})**
$CH_4 + 4Q + 2H_2O \rightarrow CO_2 + 4QH_2$	-731.01

*Derived from Uchimaya & Stone (2009) based on the comproportionation between p-benzoquinone and hydroquinone. N.B. that the ΔG° value given by Uchimaya & Stone for the reaction, $Q^- + e^- \rightarrow Q^=$, should have the opposite sign as shown above.

Sensitivity analysis

To examine the sensitivity of the model to the two parameters estimated from observation, the mixing coefficient K_z was varied over 6 orders of magnitude and the rate constant was varied by ± 50%. Model output from these simulations are plotted in Fig.s S1 and S2, respectively. Increasing mixing enhances the transport of methane upwards from sediments and, consequently, the total rate of methane oxidation within the hypolimnion increases. Similarly, elevated mixing transports more oxygen downwards and, therefore, aerobic methane oxidation increases as a result. This response is evident from the profile for aerobic methane oxidation rate; the oxygen profile, however, exhibits a more complex response. Initially, as mixing increases the oxygen profile shoals as more methane is mixed upwards, thus consuming oxygen during aerobic methane oxidation. Nevertheless, as the mean mixing coefficient passes 10^{-5} m^2 s^{-1} – the mixing rate in the baseline scenario – oxygen begins to penetrate deeper into the hypolimnion, as the rate of oxygen supply due to mixing surpasses demand by methane oxidation, which tends towards its maximum rate. In short, methane oxidation becomes limited by reaction kinetics rather than substrate supply through physical transport. This behavior is clear when considering the appropriate Damköhler number.

A Damköhler number is constructed to compare the time scales of transport (i.e., diffusive mixing) and reaction (i.e., methane oxidation):

$$Da = \frac{kL^2}{Kz} \tag{S1}$$

where Da is the Damköhler number (unitless), L is the thickness of the hypolimnion (m), and all other symbols retain their previous definitions. When this dimensionless quantity is large (>10), substrates are consumed faster through reaction than they are supplied by transport – that is to say, the system is substrate limited. In contrast, a small Damköhler number (<0.1) is indicative of a transport dominated system. As shown in Fig. S3, when K_z is equal to 10^{-5} m^2 s^{-1} (red circle) the system is on the cusp of being reaction dominated and increasing mixing thus transitions the system towards transport domination. Varying the rate constant has a much less pronounced effect than mixing, as *k* has a much smaller range. Da values remain close to 10 when *k* is varied by ±50% (Fig. S4) and, consequently, there is no clear transition between reaction and transition dominated states like that observed when considering sensitivity to mixing.

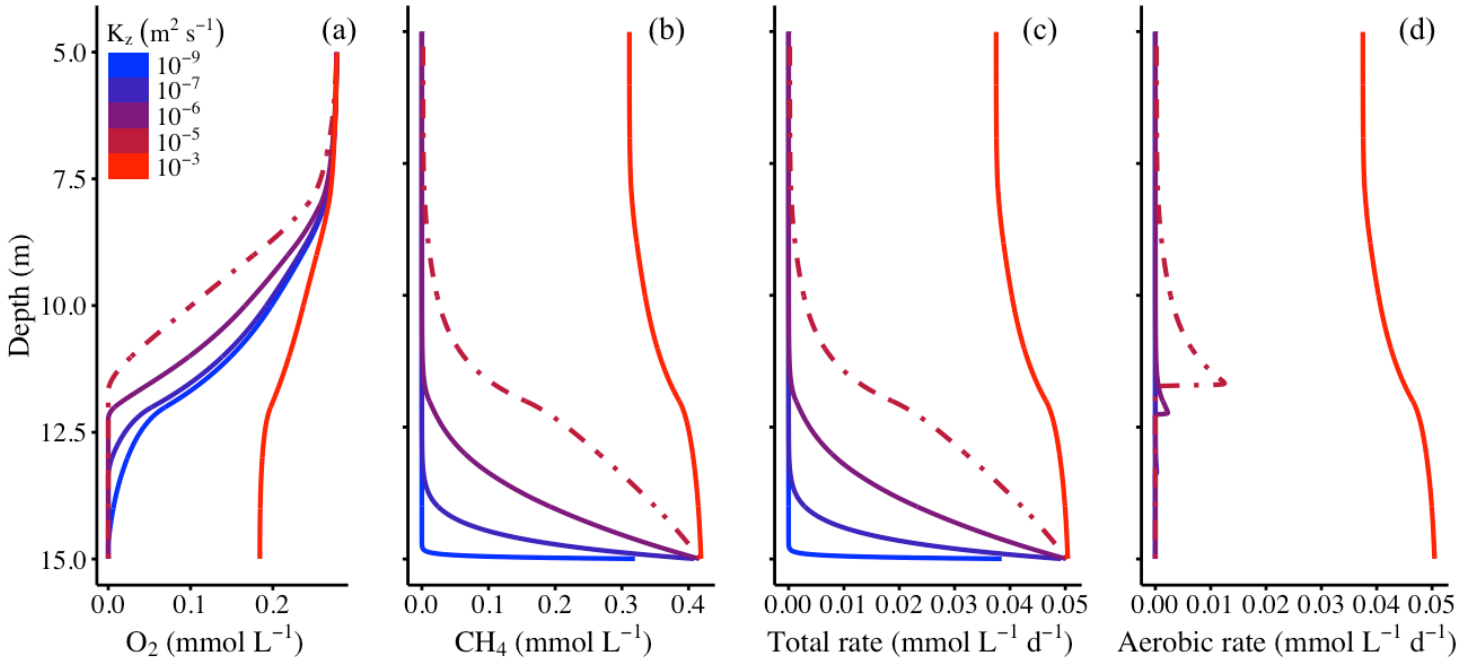

Fig. S1: Sensitivity of model results to mixing coefficients. The shape of the original mixing coefficient (K_z) profile is maintained, but the magnitude is scaled to achieve depth-averaged mixing coefficients of 10^{-9}, 10^{-7}, 10^{-6}, 10^{-5}, and 10^{-3} m^2 s^{-1}. Oxygen and methane profiles are plotted in panel (a) and (b), respectively, while panel (c) shows the total rate of methane oxidation and (d) shows the rate that is attributable to aerobic oxidation. The dash-dot lines in all panels shows the values used by the baseline scenario. Note that as methane oxidation is directly proportional to methane concentration (see equation 1) panels (b) and (c) differ only by a multiplicative factor of 0.12 – the rate constant, *k*.

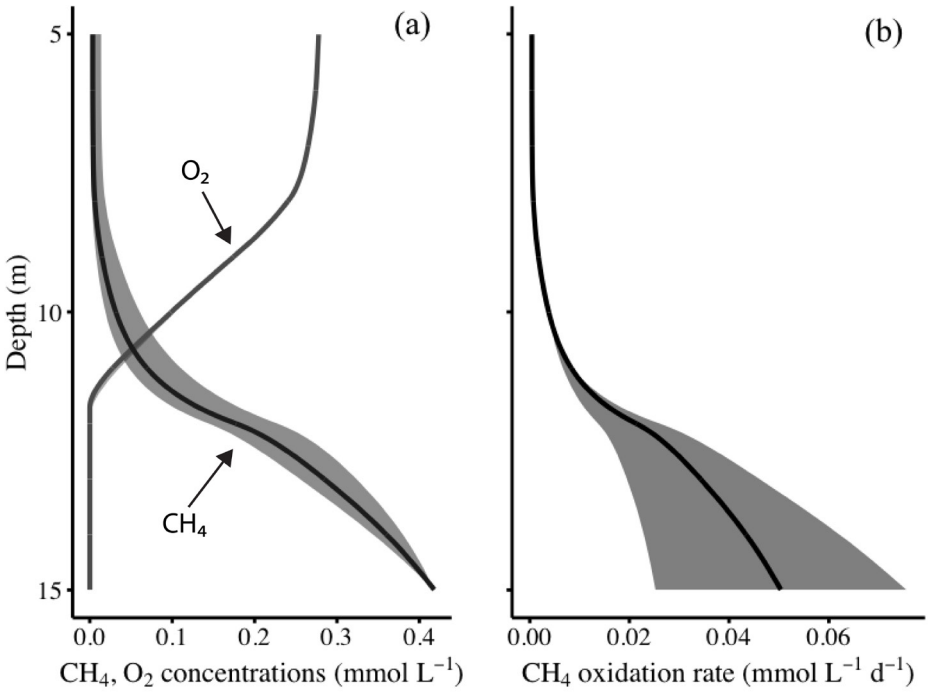

Fig. S2: Sensitivity of model results to the methane oxidation rate constant. The observed rate constant is varied by ± 50%. Oxygen and methane profiles are plotted in panel (a), while panel (b) shows the methane oxidation. The solid lines represent the baseline scenario and the ribbons around these lines show the variations that result from varying the rate constant.

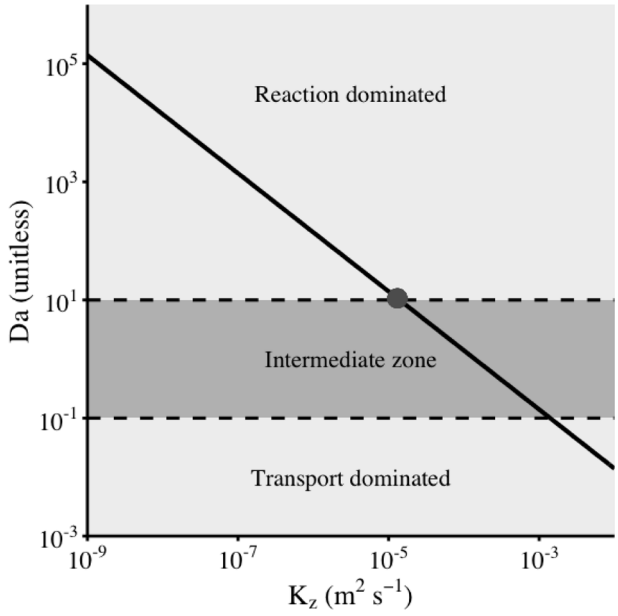

Fig. S3: A comparison of the time scales of solute transport and methane oxidation for a range of mixing coefficients, assuming a hypolimnion depth of 10 m (Fig. 2) and a first order rate constant of 0.12 d^{-1} (Fig. 1). The solid black line shows the Damköhler number (Da) as a function of mixing coefficient (K_z), while the circle denotes conditions in Lacamas Lake at the time of the study. Dashed lines delineate the regions where mixing or oxidation processes dominate.

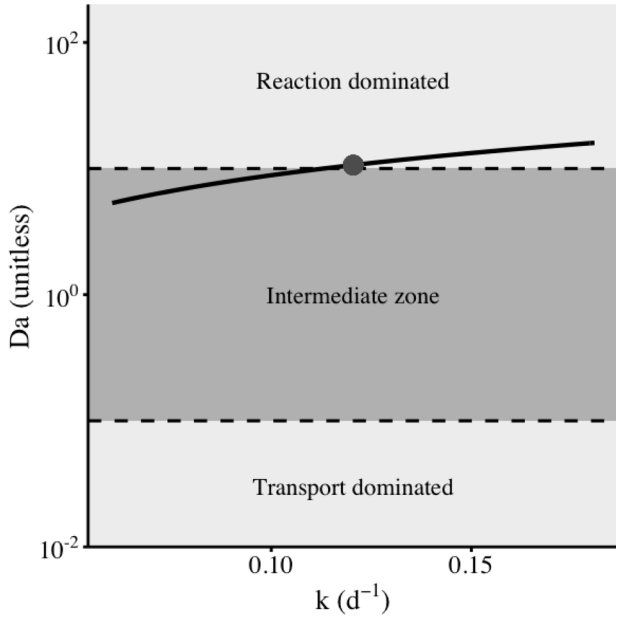

Fig. S4: A comparison of the time scales of solute transport and methane oxidation for a range of methane oxidation rate constants, assuming a hypolimnion depth of 10 m (Fig. 2) and mixing coefficients calculated from the buoyancy frequency profile, as described in the *Reactive-Transport Modelling* section of the main text. The solid black line shows the Damköhler number (Da) as a function of the first order rate constant (k), while the circle denotes conditions in Lacamas Lake at the time of the study. Dashed lines delineate the regions where mixing or oxidation processes dominate.

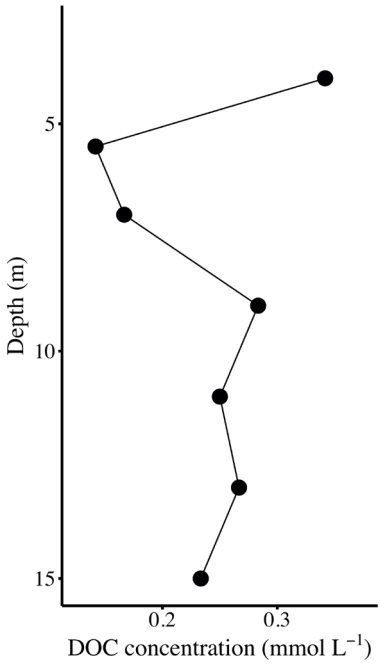

Fig. S5: Dissolved organic carbon (DOC) concentrations from filtered samples collected the same day as methane oxidation assays (28 October 2014). The shape of the profile indicates a source(s) of DOC at depth (e.g., dissolution of sinking and re-suspended particles and/or benthic DOC flux) and a sink at the thermocline, although the magnitudes of these fluxes and processes are presently unknown.

References

Bastviken, D., J. J. Cole, M. L. Pace, and M. C. Van de Bogert. 2008. Fates of methane from different lake habitats: Connecting whole-lake budgets and CH_4 emissions. J. Geophys. Res. **113**. doi:10.1029/2007JG000608

Bastviken, D., L. J. Tranvik, J. A. Downing, P. M. Crill, and A. Enrich-Prast. 2011. Freshwater methane emissions offset the continental carbon sink. Science **331**: 50–50. doi:10.1126/science.1196808

Blees, J., H. Niemann, C. B. Wenk, and others. 2014. Micro-aerobic bacterial methane oxidation in the chemocline and anoxic water column of deep south-Alpine Lake Lugano (Switzerland). Limnol. Oceanogr. **59**: 311–324. doi:10.4319/lo.2014.59.2.0311

Blodau, C., and M. Deppe. 2012. Humic acid addition lowers methane release in peats of the Mer Bleue bog, Canada. Soil Biol. Biochem. **52**: 96–98. doi:10.1016/j.soilbio.2012.04.023

Borrel, G., D. Jézéquel, C. Biderre-Petit, N. Morel-Desrosiers, J.-P. Morel, P. Peyret, G. Fonty, and A.-C. Lehours. 2011. Production and consumption of methane in freshwater lake ecosystems. Res. Microbiol. **162**: 832–847. doi:10.1016/j.resmic.2011.06.004

Canfield, D. E., F. J. Stewart, B. Thamdrup, L. D. Brabandere, T. Dalsgaard, E. F. Delong, N. P. Revsbech, and O. Ulloa. 2010. A cryptic sulfur cycle in oxygen-minimum-zone waters off the Chilean coast. Science **330**: 1375–1378. doi:10.1126/science.1196889

Carlson, K., N. S. Geiger, T. Waltz, M. Grant, J. Luzier, D. Anglin, and G. Hough. 1985. Lacamas-Round Lake Diagnostic and Restoration Analysis. Project D2925. Project D2925 Intergovernmental Resource Center.

Cervantes, F. J., S. van der Velde, G. Lettinga, and J. A. Field. 2000. Competition between methanogenesis and quinone respiration for ecologically important substrates in anaerobic consortia. FEMS Microbiol. Ecol. **34**: 161–171.

Ciais, P., G. Sabine, G. Bala, and others. 2013. Carbon and Other Biogeochemical Cycles, *In* T.F. Stocker, D. Qin, G.-K. Plattner, et al. [eds.], Climate Change 2013: The Physical Science Basis. Contribution of Working Group I to the Fifth Assessment Report of the Intergovernmental Panel on Climate Change. Cambridge University Press.

Crowe, S. A., S. Katsev, K. Leslie, and others. 2011. The methane cycle in ferruginous Lake Matano. Geobiology **9**: 61–78. doi:10.1111/j.1472-4669.2010.00257.x

Deemer, B. R., J. A. Harrison, and E. W. Whitling. 2011. Microbial dinitrogen and nitrous oxide production in a small eutrophic reservoir: An in situ approach to quantifying hypolimnetic process rates. Limnol. Oceanogr. **56**: 1189–1199. doi:10.4319/lo.2011.56.4.1189

Dick, J. M. 2008. Calculation of the relative metastabilities of proteins using the CHNOSZ software package. Geochem. Trans. **9**: 10. doi:10.1186/1467-4866-9-10

Egger, M., O. Rasigraf, C. J. Sapart, and others. 2015. Iron-mediated anaerobic oxidation of methane in brackish coastal sediments. Environ. Sci. Technol. **49**: 277–283. doi:10.1021/es503663z

Eller, G., L. Kanel, and M. Kruger. 2005. Cooccurrence of aerobic and anaerobic methane oxidation in the water column of Lake Plu see. Appl. Environ. Microbiol. **71**: 8925–8928. doi:10.1128/AEM.71.12.8925-8928.2005

Ettwig, K. F., M. K. Butler, D. Le Paslier, and others. 2010. Nitrite-driven anaerobic methane oxidation by oxygenic bacteria. Nature **464**: 543–548. doi:10.1038/nature08883

Fimmen, R. L., R. M. Cory, Y.-P. Chin, T. D. Trouts, and D. M. McKnight. 2007. Probing the oxidation–reduction properties of terrestrially and microbially derived dissolved organic matter. Geochim. Cosmochim. Acta **71**: 3003–3015. doi:10.1016/j.gca.2007.04.009

Heitmann, T., and C. Blodau. 2006. Oxidation and incorporation of hydrogen sulfide by dissolved organic matter. Chem. Geol. **235**: 12–20. doi:10.1016/j.chemgeo.2006.05.011

Hinrichs, K.-U., and A. Boetius. 2002. The Anaerobic Oxidation of Methane: New Insights in Microbial Ecology and Biogeochemistry, p. 457–477. *In* G. Wefer, D. Billett, D. Hebbeln, B.B. Jørgensen, M. Schlüter, and T.C.E. Van Weering [eds.], Ocean Margin Systems. Springer-Verlag.

Itoh, M., Y. Kobayashi, T.-Y. Chen, and others. 2015. Effect of interannual variation in winter vertical mixing on CH_4 dynamics in a subtropical reservoir. J. Geophys. Res. Biogeosciences **120**: 1246–1261. doi:10.1002/2015JG002972

Iversen, N., R. S. Oremland, and M. J. Klug. 1987. Big Soda Lake (Nevada). 3. Pelagic methanogenesis and anaerobic methane oxidation. Limnol Ocean. **32**: 804–8.

Kankaala, P., J. Huotari, E. Peltomaa, T. Saloranta, and A. Ojala. 2006. Methanotrophic activity in relation to methane efflux and total heterotrophic bacterial production in a stratified, humic, boreal lake. Limnol. Oceanogr. **51**: 1195–1204. doi:10.4319/lo.2006.51.2.1195

Kappler, A., M. Benz, B. Schink, and A. Brune. 2004. Electron shuttling via humic acids in microbial iron(III) reduction in a freshwater sediment. FEMS Microbiol. Ecol. **47**: 85–92. doi:10.1016/S0168-6496(03)00245-9

Katsev, S., S. A. Crowe, A. Mucci, B. Sundby, S. Nomosatryo, G. Douglas Haffner, and D. A. Fowle. 2010. Mixing and its effects on biogeochemistry in the persistently stratified, deep, tropical Lake Matano, Indonesia. Limnol. Oceanogr. **55**: 763.

Keller, J. K., P. B. Weisenhorn, and J. P. Megonigal. 2009. Humic acids as electron acceptors in wetland decomposition. Soil Biol. Biochem. **41**: 1518–1522. doi:10.1016/j.soilbio.2009.04.008

Kellerman, A. M., D. N. Kothawala, T. Dittmar, and L. J. Tranvik. 2015. Persistence of dissolved organic matter in lakes related to its molecular characteristics. Nat. Geosci. **8**: 454–457. doi:10.1038/ngeo2440

Klüpfel, L., A. Piepenbrock, A. Kappler, and M. Sander. 2014. Humic substances as fully regenerable electron acceptors in recurrently anoxic environments. Nat. Geosci. **7**: 195–200. doi:10.1038/ngeo2084

Knittel, K., and A. Boetius. 2009. Anaerobic oxidation of methane: progress with an unknown process. Annu. Rev. Microbiol. **63**: 311–334. doi:10.1146/annurev.micro.61.080706.093130

Kojima, H., R. Tokizawa, K. Kogure, Y. Kobayashi, M. Itoh, F.-K. Shiah, N. Okuda, and M. Fukui. 2014. Community structure of planktonic methane-oxidizing bacteria in a subtropical reservoir characterized by dominance of phylotype closely related to nitrite reducer. Sci. Rep. **4**. doi:10.1038/srep05728

Lennon, J. T., S. K. Hamilton, M. E. Muscarella, A. S. Grandy, K. Wickings, and S. E. Jones. 2013. A source of terrestrial organic carbon to investigate the browning of aquatic ecosystems. PLoS ONE **8**: e75771. doi:10.1371/journal.pone.0075771

Lipson, D. A., M. Jha, T. K. Raab, and W. C. Oechel. 2010. Reduction of iron (III) and humic substances plays a major role in anaerobic respiration in an Arctic peat soil. J. Geophys. Res. **115**. doi:10.1029/2009JG001147

Lopes, F., E. Viollier, A. Thiam, and others. 2011. Biogeochemical modelling of anaerobic vs. aerobic methane oxidation in a meromictic crater lake (Lake Pavin, France). Appl. Geochem. **26**: 1919–1932. doi:10.1016/j.apgeochem.2011.06.021

Lovley, D. R., J. D. Coates, E. L. Blunt-Harris, E. J. P. Phillips, and J. C. Woodward. 1996. Humic substances as electron acceptors for microbial respiration. Nature **382**: 445–448.

Martinez, C. M., L. H. Alvarez, L. B. Celis, and F. J. Cervantes. 2013. Humus-reducing microorganisms and their valuable contribution in environmental processes. Appl. Microbiol. Biotechnol. **97**: 10293–10308. doi:10.1007/s00253-013-5350-7

Miller, L. G., C. Sasson, and R. S. Oremland. 1998. Difluoromethane, a new and improved inhibitor of methanotrophy. Appl. Environ. Microbiol. **64**: 4357–4362.

Milucka, J., M. Kirf, L. Lu, A. Krupke, P. Lam, S. Littmann, M. M. Kuypers, and C. J. Schubert. 2015. Methane oxidation coupled to oxygenic photosynthesis in anoxic waters. ISME J. **9**: 1991–2002. doi:10.1038/ismej.2015.12

Nauhaus, K., T. Treude, A. Boetius, and M. Kruger. 2005. Environmental regulation of the anaerobic oxidation of methane: a comparison of ANME-I and ANME-II communities. Environ. Microbiol. **7**: 98–106. doi:10.1111/j.1462-2920.2004.00669.x

Oswald, K., J. Milucka, A. Brand, P. Hach, S. Littmann, B. Wehrli, M. M. M. Kuypers, and C. J. Schubert. 2016. Aerobic gammaproteobacterial methanotrophs mitigate methane emissions from oxic and anoxic lake waters: Methane oxidation in Lake Zug. Limnol. Oceanogr. doi:10.1002/lno.10312

Panganiban, A. T., T. E. Patt, W. Hart, and R. S. Hanson. 1979. Oxidation of methane in the absence of oxygen in lake water samples. Appl. Environ. Microbiol. **37**: 303–309.

Pimenov, N. V., A. Y. Kallistova, I. I. Rusanov, and others. 2010. Methane formation and oxidation in the meromictic oligotrophic Lake Gek-Gel (Azerbaijan). Microbiology **79**: 247–252. doi:10.1134/S0026261710020177

Reeburgh, W. S. 2007. Oceanic methane biogeochemistry. Chem. Rev. **107**: 486–513. doi:10.1021/cr050362v

Salas de León, D. A., J. Alcocer, V. Ardiles Gloria, and B. Quiroz-Martínez. 2016. Estimation of the eddy diffusivity coefficient in a warm monomictic tropical Lake. J. Limnol. **75**. doi:10.4081/jlimnol.2016.1431

Saxton, M. A., V. A. Samarkin, C. A. Schutte, M. W. Bowles, M. T. Madigan, S. B. Cadieux, L. M. Pratt, and S. B. Joye. 2016. Biogeochemical and 16S rRNA gene sequence evidence supports a novel mode of anaerobic methanotrophy in permanently ice-covered Lake Fryxell, Antarctica. Limnol. Oceanogr. **61**: 119–130. doi:10.1002/lno.10320

Scheller, S., H. Yu, G. L. Chadwick, S. E. McGlynn, and V. J. Orphan. 2016. Artificial electron acceptors decouple archaeal methane oxidation from sulfate reduction. Science **351**: 703–707.

Schubert, C. J., F. S. Lucas, E. Durisch-Kaiser, R. Stierli, T. Diem, O. Scheidegger, F. Vazquez, and B. Müller. 2010. Oxidation and emission of methane in a monomictic lake (Rotsee, Switzerland). Aquat. Sci. **72**: 455–466. doi:10.1007/s00027-010-0148-5

Segarra, K. E. A., C. Comerford, J. Slaughter, and S. B. Joye. 2013. Impact of electron acceptor availability on the anaerobic oxidation of methane in coastal freshwater and brackish wetland sediments. Geochim. Cosmochim. Acta **115**: 15–30. doi:10.1016/j.gca.2013.03.029

Segarra, K. E. A., F. Schubotz, V. Samarkin, M. Y. Yoshinaga, K.-U. Hinrichs, and S. B. Joye. 2015. High rates of anaerobic methane oxidation in freshwater wetlands reduce potential atmospheric methane emissions. Nat. Commun. **6**: 7477. doi:10.1038/ncomms8477

Smemo, K. A., and J. B. Yavitt. 2011. Anaerobic oxidation of methane: an underappreciated aspect of methane cycling in peatland ecosystems? Biogeosciences **8**: 779–793. doi:10.5194/bg-8-779-2011

Uchimiya, M., and A. T. Stone. 2009. Reversible redox chemistry of quinones: Impact on biogeochemical cycles. Chemosphere **77**: 451–458. doi:10.1016/j.chemosphere.2009.07.025

Valenzuela, E. I., A. Prieto-Davó, N. E. López-Lozano, and others. 2017. Anaerobic methane oxidation driven by microbial reduction of natural organic matter in a tropical wetland. Appl. Environ. Microbiol. AEM.00645-17. doi:10.1128/AEM.00645-17

Weiss, R. F., and B. A. Price. 1980. Nitrous oxide solubility in water and seawater. Mar. Chem. **8**: 347–359. doi:10.1016/0304-4203(80)90024-9

Wik, M., R. K. Varner, K. W. Anthony, S. MacIntyre, and D. Bastviken. 2016. Climate-sensitive northern lakes and ponds are critical components of methane release. Nat. Geosci. **9**: 99–105. doi:10.1038/ngeo2578

Yoshinaga, M. Y., T. Holler, T. Goldhammer, and others. 2014. Carbon isotope equilibration during sulphate-limited anaerobic oxidation of methane. Nat. Geosci. **7**: 190–194. doi:10.1038/ngeo206

Chapter 3. Methane oxidation in anoxic lake water stimulated by nitrate and sulfate addition

Sigrid van Grinsven
Jaap S. Sinninghe Damsté
Alejandro Abdala Asbun
Julia C. Engelmann
John Harrison
& Laura Villanueva

Published in Environmental Microbiology, 2020, 22(2), 766–782

Abstract

Methanotrophic bacteria play a key role in limiting methane emissions from lakes. It is generally assumed that methanotrophic bacteria are mostly active at the oxic-anoxic transition zone in stratified lakes, where they use oxygen to oxidize methane. Here, we describe a methanotroph of the genera *Methylobacter* that is performing high-rate (up to 72 mM day^{-1}) methane oxidation in the anoxic hypolimnion of the temperate Lacamas Lake (Washington, USA), stimulated by both nitrate and sulfate addition. Oxic and anoxic incubations both showed active methane oxidation by a *Methylobacter* species, with anoxic rates being three-fold higher. In anoxic incubations, *Methylobacter* cell numbers increased almost two orders of magnitude within three days, suggesting that this specific *Methylobacter* species is a facultative anaerobe with a rapid response capability. Genomic analysis revealed adaptations to oxygen-limitation as well as pathways for mixed-acid fermentation and H_2 production. The denitrification pathway was incomplete, lacking the genes *narG*/*napA* and *nosZ*, allowing only for methane oxidation coupled to nitrite-reduction. Our data suggests that *Methylobacter* can be an important driver of the conversion of methane in oxygen-limited lake systems and potentially uses alternative electron acceptors or fermentation to remain active under oxygen-depleted conditions.

Introduction

The concentration of atmospheric methane, a potent greenhouse gas, has increased strongly since the pre-industrial era. Knittel & Boetius (2009) estimated that 10-20% of all reactive organic matter buried in sediments is converted to methane. For the oceans, this is estimated to be 85-300 Tg of methane per year. Freshwater lakes and reservoirs have been a long-overlooked source of methane, but recent research has shown their importance for the global methane budget (Bastviken *et al*, 2011; Deemer *et al.*, 2016). Methane production in shallow lakes may further increase as a result of increasing air and water temperatures due to global warming (Marotta *et al.*, 2014).

Methane emissions are strongly limited by both aerobic and anaerobic methane oxidation. Marine methane oxidation is generally performed by a consortium of anaerobic methane oxidizing archaea (ANME) and sulfate-reducing bacteria, which use the widely abundant sulfate as a terminal electron acceptor (Reeburgh, 2007). Recently, iron and manganese oxides have also been suggested to function as potential electron acceptors for methane oxidation in brackish sediments (Egger *et al.*, 2014; Ettwig *et al.*, 2016). In freshwater systems and wetland soils, microaerobic methane oxidation at oxic-anoxic interfaces is a major pathway for methane removal both in the sediment and in the water column (Rudd *et al.*, 1976). Freshwater anaerobic oxidation of methane (AOM) with sulfate has been suggested to take place in freshwater sediments (Schubert *et al.*, 2011). Both nitrate and nitrite were used as electron acceptors for AOM in methanotrophic cultures originating from freshwater sediments or water (Raghoebarsing *et al.*, 2006; Ettwig *et al.*, 2010; Deutzmann and Schink, 2011; Kits *et al.*, 2015b; Oswald *et al.*, 2017). Iron and manganese have been shown to enhance lacustrine AOM in a Swiss lake; the responsible process could, however, not be determined (Oswald *et al.*, 2016). Dissolved organic matter and humic substances can also function as electron acceptors and may be relevant for methane oxidation in eutrophic systems (Valenzuela *et al.*, 2019). The humic acid analogues quinone and anthraquinone-2,7-disulfonate have been implicated in anaerobic methane oxidation, although a direct coupling between methane oxidation and reduction of organic material has not yet been demonstrated (Reed *et al.*, 2017).

Microaerophilic methane oxidation is performed by type I (gammaproteobacteria) or type II (alphaproteobacteria) methane oxidizing bacteria, commonly called methanotrophs. Recently, specific methanothrophs of the genus *Methylomonas* were discovered to be facultative anaerobes, capable of methane oxidation with nitrate as the terminal electron acceptor (Kits *et al.*, 2015b). Earlier, *Ca*. Methylomirabilis oxyfera, a bacterium of the NC10 division, was found to perform methane oxidation in anoxic environments by using nitrite as an electron acceptor for methane oxidation, via internal oxygen production (Ettwig *et al.*, 2010). Recently, Oswald et al. (2017) discovered that *Crenothrix polyspora* possesses the key methane oxidizing enzyme methane monooxygenase, and that it may be an important methane oxidizer in stratified lakes. They showed *C. polyspora* can grow under both oxygen-rich and oxygen-depleted conditions, and that its genome encodes pathways for respiration of both oxygen and nitrate, suggesting it is a facultative anaerobic methane oxidizer that can couple methane oxidation to nitrate reduction. Although there is a growing recognition that methane oxidation is carried out by a diverse array of organisms utilizing a combination of aerobic and anaerobic metabolic pathways, our knowledge of these organisms, their metabolic strategies, and their ecosystem effects remain poorly understood.

This study is aimed at expanding our knowledge of the potential terminal electron acceptors and the diversity and role of methanotrophs in the anoxic water column of stratified, eutrophic lakes. The anoxic water column can become a methane reservoir during stratified periods, with a potential for anaerobic methane oxidation, potentially supported by nitrate as an electron acceptor for methanotrophs. Our study site is Lacamas Lake, a seasonally stratified reservoir in Washington State, USA with methane concentrations up to 270 mM in the anoxic hypolimnion during summer. We addressed the following research questions: i) to what extent can alternative terminal electron acceptors (i.e. not O_2) stimulate methane oxidation in the anoxic water column, ii) what are the responsible organisms, and iii) how do they achieve methane oxidation and biomass production even in conditions that appear unfavourable. To this end, we explored the effect of enhanced nitrate and sulfate concentrations and oxic-anoxic conditions on methane oxidation rates in 24- and 72-hour incubation experiments. The methanotrophic community was analysed by both 16S rRNA and particulate methane monoxygenase subunit A (*pmo*A) coding gene amplicon sequencing and quantitative PCR. The most abundant methanotroph, a novel *Methylobacter* species, was further investigated using a metagenomic sequencing approach.

Material and methods

Site description

Lacamas lake is a temperate zone lake in Washington, USA (45.62N, 122.43W) with an average and maximum depth of 7.8 and 19.8 m, respectively. In 1938, a dam was built to enlarge and deepen the existing lake to its current size of 1.3 km^2. Lacamas lake is an Environmental Protection Agency 303[d] listed hypereutrophic system. It is monomictic, with thermal stratification established in May and a turnover period from October to December during which the oxycline deepens and weakens gradually.

Sample collection

Samples were taken from one sampling location in the centre of the lake (water depth 17.8 m) on 23-31 August 2016 and 6-10 February 2017. The depth of the oxycline was determined using a Hydrolab DS5X sonde (Hach, Loveland, US) with sensors for conductivity, temperature, dissolved oxygen (Clark cell), and pH. Water samples were taken using a VanDorn sampler or Niskin bottle. For determination of nutrient (NO_3^-, NO_2^1, SO_4^{2-}) concentrations, bulk water samples were subsampled in the field, treated as described in Table S6 and kept on ice until they could be frozen and stored at -20 °C until further analysis using a Technicon TRAACS 800 auto-analyzer. Samples for the measurement of methane oxidation rates were taken directly into double waded 12 ml exetainers (Labco, High Wycombe, UK), or in glass bottles (Neubor, San Vito al Tagliamento Pordenone, Italy), overflowing the vessels with three times the sample volume before filling the vessels without any headspace. Water for DNA sampling was stored in plastic carboys or jugs and kept shielded from temperature fluctuations and light with emergency insulation blankets, to be filtered later in the laboratory. In Table S6, an overview of the sampling depths, sampling purposes and handling is provided.

Determination of methane oxidation rates

In order to determine natural net methane oxidation rates, samples were directly sampled into double waded 12 ml exetainers (Labco, High Wycombe, UK). For each depth, 16 exetainers were filled, of which 4 were treated with approximately 50 ml of saturated zinc chloride solution ($ZnCl_2$), added immediately to terminate any biological activity. Exetainers were kept in coolers at lake temperature until back in the lab, where they were stored in the dark, in water baths within ±2°C of in situ temperature. Approximately 50 ml of saturated $ZnCl_2$ solution was injected into four exetainers, functioning as biological replicates, per time point, at 6, 12 and 24 h after the start of the incubation.

To determine the net methane oxidation rate in summer samples with added electron acceptors, samples were taken in a slightly different way. In the field, samples of 12 m depth were taken into glass bottles (315 ml with rubber stopper), which already contained ~0.005g $NaNO_3$, ~0.1g Na_2SO_4 or ~0.004 g of commercially available humic substances (Sigma Aldrich). Bottles were not overflown but were carefully filled without any headspace. Oxygen addition was tested by leaving a 10 ml air headspace in the bottle, which was shaken to dissolve the oxygen into the water. In the lab, using the method of Holtappels et al. (2011) nutrient samples and 16 exetainers were filled, 2-8 h after sample collection. These were further treated in the same way as the natural methane oxidation rate samples.

During winter sampling, exetainers for natural net methane oxidation rate and methane-added incubations were taken similarly to the summer natural methane oxidation rate samples. Samples for the anoxic incubations were taken in glass bottles (315 ml with rubber stopper), overflowing the vessels with three times the sample volume before filling the vessels without any headspace, bubbled with ultra-high purity helium for 10-15 min to remove oxygen, and transferred to exetainers using the method of Holtappels et al. (2011). We use the term "anoxic" for these experiments, and for experiments with summer hypolimnion water, despite the fact that we cannot be certain that no traces of oxygen were present in the incubation vials. The possible effects of residual oxygen are explored in the discussion. Both the methane-added and anoxic incubations got methane added by injection through the stopper of the exetainers, to a final concentration of 134-260 µM. Control incubations were left unamended and did, therefore, not receive methane, neither were they purged with helium. Four exetainers got approximately 50 ml of saturated $ZnCl_2$ solution injected immediately to determine the t_0 methane concentration. The other exetainers, four biological replicates per treatment, were incubated in the dark in water baths within ±2°C of in situ temperature, and $ZnCl_2$ was added 6, 12 and 24 h after the start of the incubation. $ZnCl_2$-poisoned samples were stored upside down at room temperature until further analysis. To measure the methane concentration in the exetainers, 1 ml high purity nitrogen (N_2) headspace was generated, the exetainers were left to equilibrate for at least 48 h and then measured as technical triplicates on a GC-FID. Net methane oxidation rates were determined using linear regression ($p < 0.05$). The addition experiments had final nitrate concentrations approximately 10 times higher than the natural concentrations of the control experiment, or sulfate concentrations 100 times higher than the natural concentrations of the control experiments (Table S1). The concentrations of oxygen, nitrate and sulfate at the end of the experiments were not determined. In the 7 m depth summer incubations, the methane concentration reached zero before the end of the incubations, and only the time points before methane depletion were used. In the 15 m summer control experiment, the concentration increased initially,

but decreased linearly from 6 until 24 h. Only this last part of the incubation was used for determination of the methane oxidation rate. To calculate the theoretical amount of methane that could be oxidized with the concentration of electron acceptor in the vial, an 8:3 ratio of NO_3:CH_4 and a 1:1 ratio of SO_4:CH_4 was assumed, after Segarra et al. (2013). The simplification was made that no other processes consumed the oxidizing power of the added electron acceptor.
Per cell methane oxidation rates were calculated by dividing the oxidation rate per L by the number of cells per L. The doubling time was calculated with the formula: doubling time = t/(3.3*log(b/B)), with t being the time in h, b being the number of cells at t_{end} and B being the number of cells at t_o.

Microbial community sampling and incubations
For the natural community samples, 3.9 l sample water was filtered over pre-ashed 0.3 mM glass fiber filters (45 mm diameter, Whatman, Maidstone, UK) within 2-4 h after sample collection. Filters were stored at -20°C until DNA extraction. Water for summer microbial community incubations was collected in 3.9 L jugs. If applicable, salts ($NaNO_3$ or Na_2SO_4) were added in the same concentrations as those in the methane oxidation rate incubations. Winter microbial community samples were taken in the above-mentioned glass bottles with rubber stoppers. Anoxic incubations were bubbled with ultrapure helium for 10 min to remove oxygen. The methane-addition and O_2 removal experiments got 0.66 ml of 99.99% pure methane gas added per bottle, in a headspace of 12 ml ultrahigh purity helium, leading to a concentration of 150 – 260 mM methane. To maintain oxic conditions, the oxic winter incubations with and without methane had an air headspace of 12 ml. All microbial community incubations were kept in the dark at ±2°C of in situ temperature and were shaken every 24 h. After 72 h, they were filtered over pre-ashed 0.3 mM glass fiber filters (Whatman, Maidstone, UK) and stored at -20°C.

DNA extraction and 16S rRNA, pmoA gene amplification, analysis and phylogeny
DNA was extracted from 1/32 to 1/8 part of the filters using the PowerSoil DNA extraction kit (Mo Bio Laboratories, Carlsbad, CA, USA). DNA extracts were stored at minus 80°C until further analysis. The 16S rRNA gene amplicon sequencing and analysis was performed with the general 16S rRNA archaeal and bacteria primer pair 515F and 806RB targeting the V4 region (Caporaso *et al.*, 2012) as described in Besseling *et al.* (2018).
A fragment of the *pmo*A gene (approximately 550-583 bp) was targeted for amplicon sequencing by using the forward primer A189 and an equimolar mixture of the reverse primers A682r and Mb661r (Holmes *et al.*, 1995; Costello and Lidstrom, 1999). PCR products were gel purified using the QIAquick Gel-Purification kit (Qiagen), pooled and diluted. Sequencing was performed by the Utrecht Sequencing Facility (Utrecht, the Netherlands), using an Illumina MiSeq sequencing platform. The 16S rRNA gene amplicon sequences were analyzed by the Cascabel pipeline (Asbun *et* al., 2019) including quality assessment by FastQC (Andrews, 2010), assembly of the paired-end reads with Pear (Zhang *et al.*, 2014), library demultiplexing, OTU clustering and representative sequence selection ('longest' method) by diverse Qiime scripts (Caporaso *et al.*, 2010). The OTU clustering algorithm was uclust (Edgar, 2010) with an identity threshold of 97% and assign taxonomy with BLAST (Altschul *et al.*, 1990) by using the Silva 128 release as reference database (http://www. arb-silva.de/; Quast *et al.*, 2013). Representative

methanotrophic sequences were extracted from the dataset and the sequences were added to the reference tree of the release 128 of the Silva NR SSU Ref database (http://www.arb-silva.de/; Quast et al., 2013) using the ARB software package (Ludwig *et al.*, 2004) by means of the ARB Parsimony tool. The 16S rRNA amplicon reads (raw data) have been deposited in the NCBI Sequence Read Archive (SRA) under BioProject number PRJNA524776 (Biosamples SAMN11032793 to SAMN11032810).

The *pmo*A gene amplicon sequences were analysed with the same in-house pipeline mentioned above for the 16S rRNA gene analysis (including clustering of OTUs at 97%) but performing the taxonomy assignation through BLAST against the NCBI database of non-redundant nucleotides (NT). The phylogenetic tree was restricted to the ca. 200 amino acid-fragment covered by the *pmo*A gene amplicon sequencing analysis. Representative *pmo*A gene sequences from the amplicon sequencing analysis as well as the *pmo*A gene sequence(s) extracted from the metagenome assembled genomes (MAGs) were added to the phylogenetic tree of compiled *pmo*A gene coding sequences included in Oswald et al. (2017). The phylogenetic tree included PmoA protein sequences retrieved from the Integrated Microbial Genomes database (IMG-ER; Markowitz et al., 2009) as indicated in Oswald et al., 2017, protein sequences of 'unusual' PmoA of *C. polyspora* (accession ABC59822–ABC59827; Stoecker *et al.*, 2006), partial PmoA of *C. fusca* (accession ABL64049; Vigliotta *et al.*, 2007), as well as the PmoA protein sequences of *Crenothrix* retrieved by Oswald et al. 2017. Alignments were performed in MEGA6 (Tamura *et al.*, 2013) with Muscle (Edgar, 2004). Models of protein evolution were determined in MEGA6. Maximum likelihood phylogenetic trees were determined using PhyML v.3.0 (Guindon *et al.*, 2010). The pmoA reads have been deposited in NCBI, the accession numbers are pending.

Quantitative PCR 16S rRNA gene

16S rRNA gene copies were quantified using quantitative PCR (qPCR) with the same primer pair as used for amplicon sequencing (515F, 806RB). The qPCR reaction mixture (25 ml) contained 1 U of Pico Maxx high fidelity DNA polymerase (Stratagene, Agilent Technologies, Santa Clara, CA) 2.5 µl of 10x Pico Maxx PCR buffer, 2.5 µl 2.5 mM of each dNTP, 0.5 µl BSA (20 mg/ml), 0.02 pmol/µl of primers, 10,000 times diluted SYBR Green® (Invitrogen) (optimized concentration), 0.5 µl of $MgCl_2$ (50 mM) and ultrapure sterile water. The cycling conditions for the qPCR reaction were the following: initial denaturation at 98°C for 30s, 45 cycles of 98°C for 10 s, 56°C for 20 s, followed by a plate read, 72°C for 30 s, 80°C for 25 s. Specificity of the reaction was tested with a gradient melting temperature assay, from 55 to 95°C with a 0.5°C increment for 5 s. The qPCR reactions were performed in triplicate with standard curves from 100 to 107 molecules per microliter. qPCR efficiency for the 16S rRNA quantification was 103.7% with R^2=0.993, and 109.8% with R^2=0.991. For quantification of microbial groups, we made the assumption that all the microorganisms of the microbial community in Lacamas Lake contained a single 16S rRNA copy in their genome. For analysis purposes, only species with a relative abundance > 0.01% were assumed significant.

Metagenome analysis

Sample collection and DNA extraction of the sample used for metagenome sequencing are described above. DNA of the sample of interest was used to prepare a TruSeq DNA nano library which was further sequenced with Illumina MiSeq 2×300 bp generating over 46

million 2×300 bp paired-end reads. Data was analyzed with an in-house pipeline including evaluation of sequence quality with FastQC v.0.11.3 (Andrews, 2010) and removal of the adapters with Trimomatic v.0.35 (Bolger *et al.*, 2014). Reads were assembled into contigs using MetaSPAdes v.3.11.1 (Nurk S, Meleshko D, Korobeynikov A, 2017), and evaluation of the quality of the assembly with Quast v.4.5 (Gurevich *et al.*, 2013). The assembled reads were mapped back against the raw data with BWA-MEM v.0.7.12-r1039) (Gurevich *et al.*, 2013). Contigs were binned into draft genome sequences based on tetra-nucleotide frequencies with MetaBAT v.2.11.1, which was also used for estimation of the contig depth, coverage and statistics with the script jgi_summarize_bam_contig_depths (Kang *et al.*, 2015). Quality of the MAGs was assessed using CheckM v1.0.7 running the lineage-specific workflow (Parks *et al.*, 2015). MAGs were annotated with Prokka v1.12 (Seemann, 2014) and by the Rapid annotation using subsystem technology (RAST) pipeline v2.0 (Aziz *et al.*, 2008). The annotation of key metabolic pathways was refined manually. In order to classify the MAGs according to their relative abundance in the sequenced sample, MetaBAT was run again by using the abundance estimation (total average depth, average abundance or also called average coverage of each contig included in the bin) generated by MetaSPAdes and checked again with CheckM. The phylogenetic placement of the MAGs with higher average abundance was determined by using Phylosift (v. 1.0.1, Darling *et al.* (2014)) extracting 34 marker genes as described in Dombrowski *et al.* (2018) (Table S7). The MAGs were then compared to all publicly available genomes from the same taxonomic group. Additionally, GTDB-Tk (v0.3.2; http://gtdb.ecogenomic.org) and GC coverage plots (gc cov.pl script included in https://www.michaelgerth.net/resources.html) were also used to assign the taxonomic classification of the MAGs (see Table S4, Fig. S6).

The metagenome of the winter water sample incubation under anoxic conditions and supplementation of methane (Lac_W_12m_72h) is available in NCBI under project number PRJNA524776, biosample SAMN11032804. The sequence of the MAGs bin-19, bin-37 and bin-63 are deposited in Integrated Microbial Genomes and Microbiomes (IMG; https://img.jgi.doe.gov/) under submission ID numbers 204587, 204588, and 204589, respectively.

Identification of specific coding genes and phylogenetic analyses

Specific coding genes of the methane metabolism, as well as coding genes involved in the potential aerobic and anaerobic respiration in MAG bin-63 that failed to be annotated by Prokka and RAST were further investigated by performing protein blast searches with curated protein sequence reference datasets.

Results

Physicochemical characteristics

During our late August sampling, the lake was stratified, with an anoxic, methane-rich (38-270 µM CH_4; Fig. 1) hypolimnion. The oxycline was located at 3-5 m. Nitrate concentrations were 10-20 mM at 5-9 m, but < 0.5 mM in the shallow (3 m) and deep (15-17 m) waters, despite the high concentration in the inflowing stream (153 µM; Fig. 1). Sulfate concentrations were around 20 mM in the shallow water and decreased gradually to 9 µM at 17 m, lower than that of the inflowing stream (48 µM; Fig. 1). During winter sampling in February, the water column

was homogeneously oxygenated and the methane concentration was low (0.2-0.8 µM; Fig. 1). Water column nitrate concentrations were 4-300 times higher than in summer (76 mM in surface waters, decreasing to 49 mM above the sediment), while the nitrate concentration in the inlet water had decreased to 60 µM. Sulfate concentrations of the winter water column were 17-18 mM throughout the water column (Fig. 1). Nitrite concentrations were low year-round (0.1-1 mM; Fig. 1).

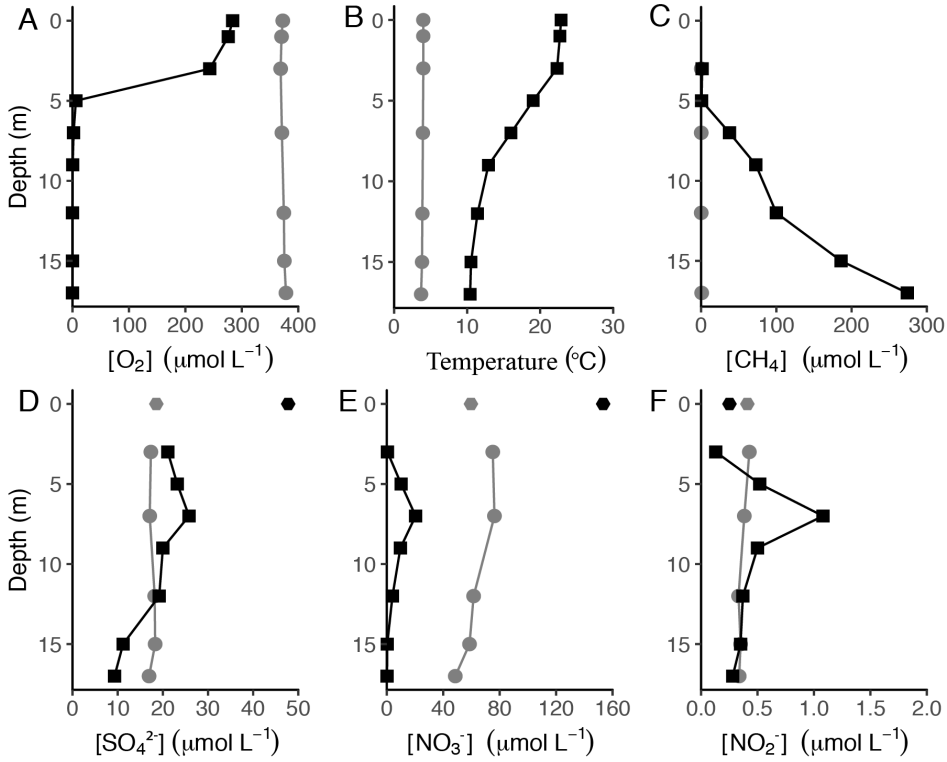

Fig.1. Physicochemical conditions of Lacamas Lake in August 2016 (black squares) and February 2017 (grey circles). A. Dissolved oxygen concentration. B. Temperature (°C). C. dissolved methane concentration. D. Sulfate concentration. E. Nitrate concentration. F. Nitrite concentration. All concentrations are in µmol L^{-1}. The data points at 0 m in panels D, E and F represent the concentrations of sulfate, nitrate and nitrite, respectively, in the inlet stream in summer and winter, sampled 1.5 km upstream of the lake.

Methane oxidation rates

During summer stratification, net methane oxidation was detected throughout the hypolimnion (7-17 m) with rates ranging from 7.3 to 46 mM day^{-1}, peaking at 7 and 15 m (Fig. 2A, Table S1). Incubation experiments revealed that at 7 m >60% of the methane was oxidized within 24 h, whilst at 9-15 m this was only 6–16% (Table S1). No methane oxidation was detected in the oxic zone (3-5 m depth) of the summer water column, despite the natural presence of dissolved methane (2.2–2.7 mM; Table S1). Additions of nitrate (10x natural

concentration, 74-146 mM) and sulfate (100x natural concentration, up to 2.2 mM) increased the methane oxidation rate at all measured depths (5–15 m) except for 7 m, where methane was limiting. Nitrate and sulfate stimulated rates were up to 8 times higher than control rates, up to 72 mM day^{-1} at 12 m with nitrate added, and up to 74 mM day^{-1} at 15 m with sulfate added (Fig. 2A). With the addition of humic substances and oxygen to the anoxic waters at 12 m, methane oxidation completely diminished (Fig. S1).

In winter, methane concentrations in the water column were <1 µM and no methane oxidation was detected (Figs. 1 and 2B). To test the potential for methane oxidation, methane concentrations were increased to 150-260 mM, corresponding to concentrations in the hypolimnion in summer (Table S1), and part of the incubations were performed under anoxic conditions (see Experimental Procedures for details). The potential methane oxidation rate under anoxic conditions was 37 mM day^{-1}, 3 times higher than in oxic methane-amended conditions at 17 m depth (Fig. 2B). At 12 m, methane was oxidized at a rate of 20 µM day^{-1} under anoxic conditions, whilst the methane concentration increased over time in oxic conditions.

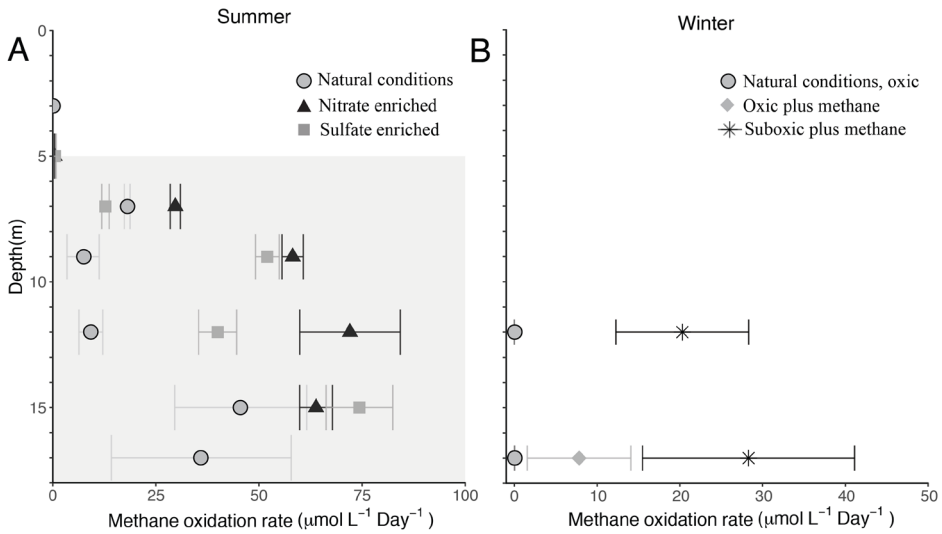

Fig. 2. Methane oxidation rates as determined from incubation experiments in (A) summer electron acceptor experiments and (B) winter methane addition experiments. In panel A the observed methane oxidation rates in natural (unamended) summer conditions (light grey circles), nitrate enriched conditions (black triangles) and sulfate enriched conditions (dark grey squares) are shown. The grey shading indicates the anoxic zone. At 3 and 17 m depth, no enrichment experiments were performed. At 5 m depth, all methane oxidation rates were <0.5 µmol L^{-1} day^{-1}. In panel B, natural (unamended) oxic conditions (dark grey inverted triangles), oxic conditions with methane added (grey diamonds) and anoxic conditions with methane added (black stars) are shown for samples from 12 and 17 m depth. A negative oxidation rate was observed in the oxic + methane experiment at 12 m depth (results not shown). Note the different scale on both axes. Details in Table S1.

Identity and abundance of methanotrophs in the water column

We screened the operational taxonomic units (OTUs) obtained by 16S rRNA gene amplicon sequencing for methanotrophic taxa and applied a minimum threshold of 0.1% of the total reads in a given sample. The detected OTUs include members of the Methylococcales, specifically of *Methylomonas*, *Methylobacter* clade 2 (including the cultivated *Methylobacter tundripaludum* and *M. psychrophilus*, as described in Smith et al., 2018), Crenotrichaceae (*Crenothrix*), and the pLW and CABC2E06 groups (Fig. 3). The eight *Methylobacter* clade 2 OTUs were all closely related (i.e. >96% identical) to that of *M. tundripaludum* (Fig. 3). Total methanotroph abundance as estimated from the 16S rRNA copies was substantially higher in summer than in winter (Fig. 4; Table S2). In summer, methanotrophs were detected at all depths analyzed, except at 3 m (Fig. 4A). Both their diversity and their relative abundance were highest at 79 m (Fig. 4A); methanotrophs represented 5% of all 16S rRNA gene reads at 7 m (Table S2), with the Methylococcales pLW group being the most abundant (3.3%, 1.5×10^7 16S rRNA gene copies L^{-1}). In the deep anoxic water column, at >12 m, sequences affiliated to the *Methylobacter* clade 2 were the most abundant ($0.3–0.5 \times 10^7$ 16S rRNA gene copies L^{-1}; Fig. 4A). No methane oxidizing archaea (ANME) were detected. In the oxygen-rich water column in winter a different picture emerged with only the *Methylobacter* clade 2 present throughout the water column, except at 15 m (Fig. 4B; Table S2).

Functional gene (i.e. *pmo*A) amplicon analysis indicated the presence of four OTUs, of which two dominate (Fig. 4C-D). Their identity was revealed by comparison with available PmoA sequences in databases (Fig. 5). In summer, the upper part of the water column was dominated by the LL-PmoA OTU LL-pmoA-3 (Fig. 4C), which is closely (85 %) related to a PmoA coding sequence from a metagenome from the epilimnion of Lake Mendota, and 77–78% identical to that of *Methylobacter* sp. KS41, derived from a metagenome from an acid forest soil enrichment culture. The deeper part of the summer water column was dominated by OTU LL-pmoA-1 (Fig. 4C), which also dominated the entire water column in winter (Fig. 4D). The most closely related PmoA sequences are those from a metagenome from the hypolimnion of Lake Trout Bog, and from *Methylobacter* sp. KS41. Closely related PmoA sequences of cultured relatives of both OTU LL-pmoA-1 and -3 are those of *M. tundripaludum* strains (Fig. 5), which fall in *Methylobacter* clade 2 (Fig. 3).

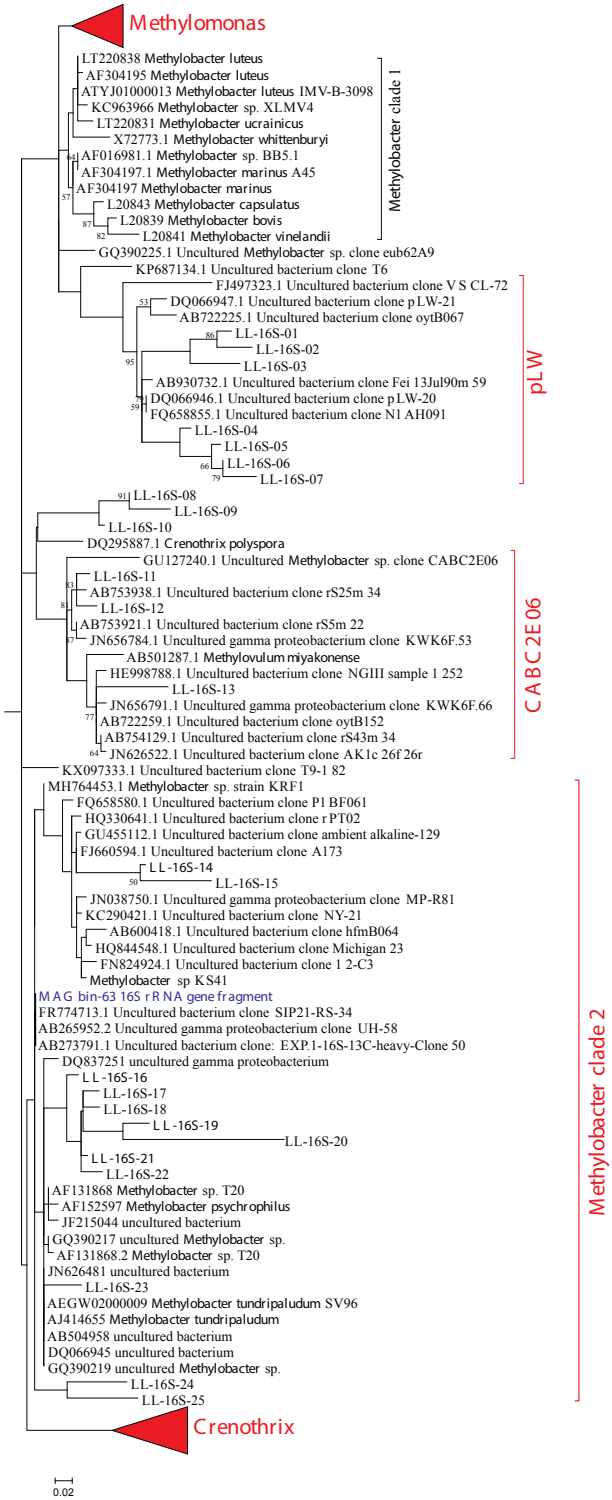

Fig. 3. Phylogenetic 16S rRNA gene tree showing 25 representative sequences of the OTUs of the four methanotrophic groups (in red) detected in Lacamas Lake natural waters and incubation experiments (labeled LL-16S- followed by a number) and their closest relatives. The most abundant OTUs in the incubations are indicated in bold. OTUs falling in the *Methylobacter* clade 1 cluster were not detected. The relative abundance of the LL-16S-OTUs in each sample are shown in Table S8. The phylogenetic analysis was restricted to the sequence fragment (approximately 290 bp) obtained with the 16S rRNA amplicon sequencing analysis. Maximum likelihood estimation was performed using the General Time Reversible model.

Identity and abundance of methanotrophs in incubation experiments

Anoxic water at 12 m was sampled for summer incubation experiments, based on its high methane concentration (100 mM) and its position ca. 6 m below the oxycline and ca. 6 m above the sediment-water interface, which limits potential contamination with sediment or oxycline particles and microbes. Incubations for 72 h with nitrate or sulfate but no added methane were performed to study the effect of electron acceptor availability on the methane oxidation rate and methanotrophic community. The relative abundance of methanotrophs increased from 1.5% of the total 16S rRNA gene reads in the natural water column up to 17.7, 21.1 and 22.4%, for control incubations and incubations supplied with nitrate or sulfate, respectively (Table S2). Sequences affiliated to the *Methylobacter* clade 2 were the most abundant in these incubations (approximately 12% of the total 16S rRNA gene reads), with the OTU sequences LL-16S-16 and LL-16S-19 (Fig. 3) being the most abundant ones (>9.5% each of the total sequences classified as *Methylobacter* clade 2) in the incubations supplemented with nitrate. In the summer incubations, nitrate addition slightly stimulated the abundance of PmoA OTUs LL-pmoA-4 and LL-pmoA-2 (12 and 3.2%, respectively; Fig. S2), which were of minor abundance in the natural water column (1.5 and 1.3%, respectively; Fig. 4C). The addition of sulfate mimicked the conditions in the deeper water column (i.e. >12 m) and led to strong dominance of the sequence of the OTU LL-pmoA-1 (Fig. 4; Fig. S2).

In winter, when the water column was oxic and depleted of methane, the addition of methane to water from 12 m depth resulted in an increase in the relative abundance of *Methylobacter* clade 2 sequences from 0.7 to 7% of the total 16S rRNA gene reads, corresponding to a slight increase in the absolute abundance (Fig. 6). In addition, incubations were performed under artificially induced anoxic, methane-rich (194 mM) conditions, mimicking the bottom waters of the stratified lake during summer. This induced a more than 100-fold increase of the estimated absolute abundance of the *Methylobacter* clade 2 species (Fig. 6), resulting in a major increase in the relative abundance of *Methylobacter* clade 2 from 0.7% of all detected OTUs (control) to 35.4% with OTU LL-16S-16 as the most abundant one (i.e. 49% of the sequences classified as *Methylobacter* clade 2; Fig. 3). This corresponds to a doubling time of 9.7 h and, when assuming all methane oxidation is performed by this group, a rate of 0.05 pmol cell^{-1} day^{-1}. The doubling time of the methanotrophs in the not-amended incubations and the methane amended incubations was lower (i.e. 63.2 and 18.6 h, respectively). In the anoxic incubations, several other methanotrophs were also detected, although in much lower relative abundances than *Methylobacter* clade 2 species (0.1–1%; Fig. 6). Similar results were observed in incubations with water of 17 m depth although the absolute abundances in the incubations were lower (Fig. S3). The *pmo*A gene amplicon analysis showed the LL-pmoA-1 OTU remained dominant in all winter incubations (Fig. S2), as it was in the winter water column (Fig. 4D).

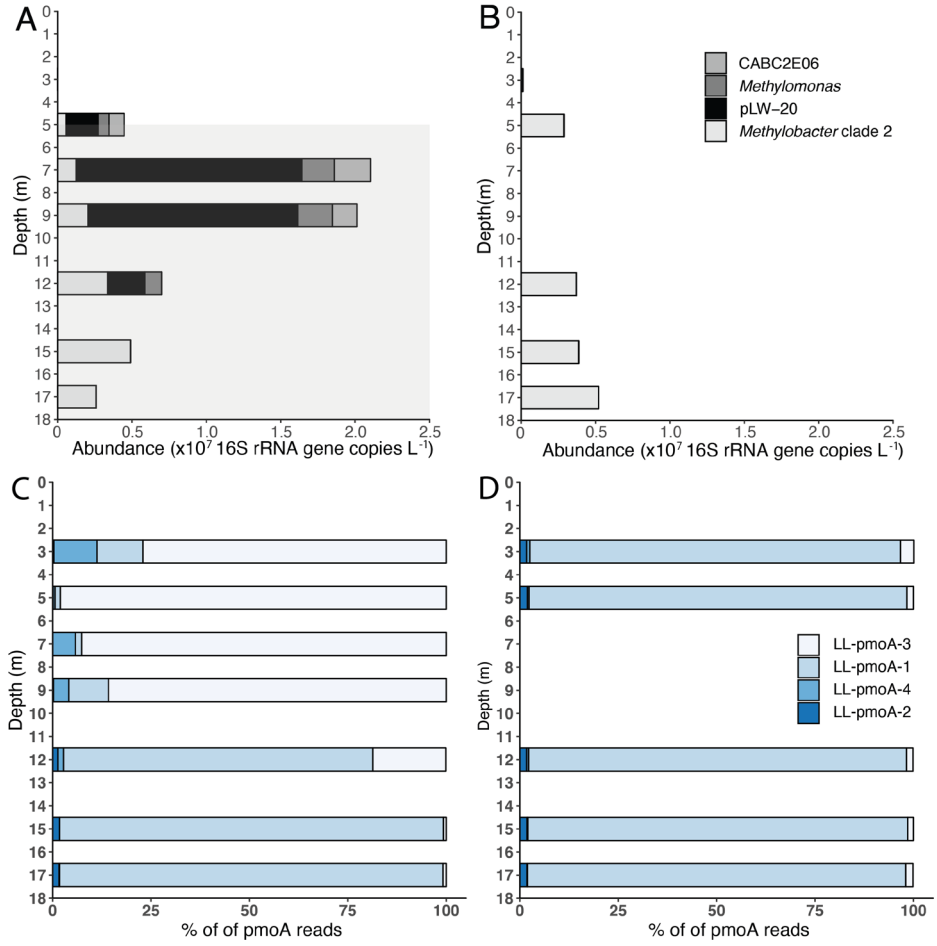

Fig. 4. Abundance and composition of the methanotrophic community in the Lacamas Lake water column in summer and winter. (A) and (B) show the absolute abundance of the most important methanotrophic community members, as detected by 16S rRNA gene amplicon sequencing combined with quantitative PCR analysis using the same primers. (C) and (D) show the relative abundance of the detected PmoA sequences. The taxonomic assignment of the 16S rRNA gene and pmoA OTUs is specified in Fig. 3 and Fig. 5, respectively. The grey area of panel A indicates the anoxic hypolimnion. Details in Table S2 and S3.

Methylobacter species metagenomic analysis

The winter incubation under anoxic conditions and added methane resulted in a methanotrophic enrichment with members of the *Methylobacter* clade 2 representing more than a third (35.4%) of all 16S rRNA gene reads. Sequencing following a metagenomic approach resulted in several metagenome-assembled genomes (MAGs), including three MAGs (i.e. bin-19, -37 and -63) affiliated with the Methylococcales (Table S4; supplementary File S1). MAG bin-63 was of high quality (96.3% completeness, 0.74% contamination, 0%

strain heterogeneity; Table S4) and had the highest average abundance (based on the average coverage of each contig included in the bin; see Experimental Procedures for details) of all MAGs obtained. Phylogeny of 34 concatenated marker genes following the method of Dombrowski et al. (2018) and GTDB-Tk analyses revealed that the three obtained MAGs of methanotrophs were most closely affiliated with *Methylobacter* sp. KS41 of the *Methylobacter* clade 2 (Fig. S5). The affiliation of the MAGs was further supported by GC coverage plots indicating that the MAG bin-63 was affiliated to the family Methylomonadaceae (Fig. S6). Furthermore, a phylogenetic analysis of the 16S rRNA gene of the MAG bin-63, restricted to the 305 bp 16S rRNA gene fragment used for the amplicon sequencing analysis, revealed that it was closely related (average 98%) to the 16S rRNA gene sequences of the *Methylobacter* clade 2 (Fig. 3). Surprisingly, this 16S rRNA gene fragment was not completely identical to the most abundant OTUs (e.g. OTU sequence LL-16S-16) of both the anoxic methane-supplemented winter and nitrate-supplemented summer incubations (Fig. 3). This may be due to miss-assembly typically encountered in the SSU rRNA gene (Miller, 2013; Yuan *et al.*, 2015) or to potential sequencing mistakes in the amplicon sequencing assay.

The PmoA protein sequence of the MAG bin-63 was 95.5% identical to the PmoA protein sequence of *Methylobacter* sp. KS41 of the *Methylobacter* clade 2 (see Fig. 3) but the phylogeny is not well supported (58% bootstrap support) similarly to what was observed previously by Nguyen *et al.* (2018). OTU LL-pmoA-1 is not identical to the *pmo*A gene coding sequence retrieved from the MAG bin-63, but as this OTU represented 97% of the total *pmo*A gene sequences in the sample from which the metagenome was obtained, it is likely that both the pmoA of MAG bin-63 and the OTU LL-pmoA-1 are the same. MAG bin-63 was by far the most abundant bin retrieved from the enrichment and is therefore unlikely related to a species that represented less than 3% of the *pmoA* gene sequences.

Based on the highest average abundance (Table S4) of the MAG bin-63, its closest homology to the representative 16S rRNA gene sequences affiliated with the *Methylobacter* clade 2 in that given sample (Fig. 3), and the phylogenetic placement of the MAGs reported in this study, we conclude that the MAG bin-63 is very likely affiliated to the *Methylobacter* clade 2 and representative for the *Methylobacter* species that in summer predominantly resides in the anoxic hypolimnion of Lacamas Lake and in winter is present throughout the oxic water column albeit in lower abundances.

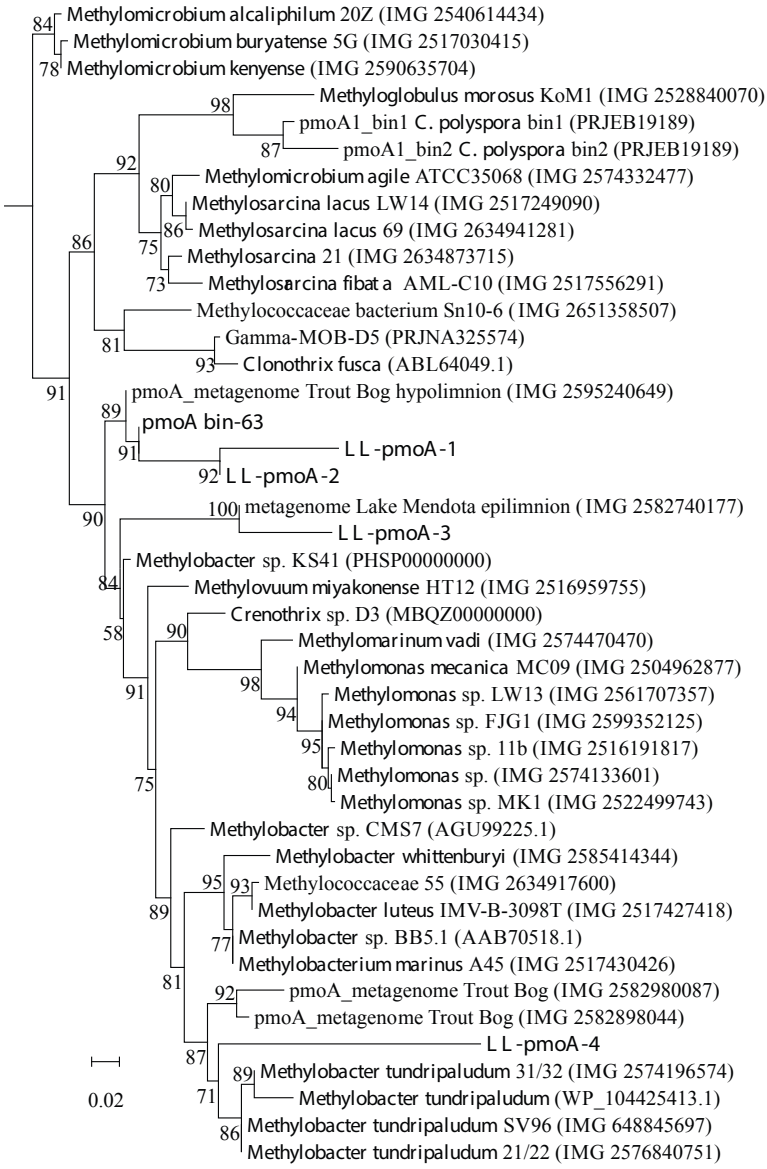

Fig. 5. Maximum likelihood phylogenetic tree of PmoA protein sequences (200 amino fragment) obtained with the *pmoA* amplicon sequencing assay (see Experimental Procedures for details). The main OTU sequences of Lacamas Lake (LL-pmoA) as well as the MAG bin-63 sequence are indicated in bold. Model of protein evolution was LG plus gamma distribution and invariant site, LG+G+I. The scale bar represents number of substitutions per site. Branch support was calculated with the approximate likelihood ratio test (aLRT) and values (%) are indicated on the branches. IMG gene ID number or NCBI accession number are indicated between parentheses.

Genome-inferred metabolism of the Methylobacter MAG bin-63

Due to its high quality and highest average abundance compared to the other MAGs, we will focus here on the description of the metabolic potential of MAG bin-63. All genes encoding for particulate methane monooxygenase (pMMO) are present and organized in the *pmo*CAB operon (see supplementary File S1), uniquely found in type Ia methanotrophs (Trotsenko and Murrell, 2008; Villada *et al*., 2019). The sequence-divergent particulate monooxygenase (Pxm; Tavormina *et al.* (2011), Knief (2015)) is absent based on a blast search with the PxmA sequence of *M. tundripaludum*. Homologues of the soluble methane monooxygenase (sMMO) are also absent based on a blast search with the *mmo*X gene of *Crenothrix polyspora*. The gene coding for methanol dehydrogenase is present (Fig. 7).

Genes for a complete RuMP pathway for C-1 assimilation from formaldehyde is present, as well as those for the oxidative TCA cycle, while the serine cycle is incomplete (Fig. 7). Genes involved in H_4folate (*mtd*A-*fch*), membrane-associated quinoprotein formaldehyde dehydrogenase (*ald*), and formate oxidation (*fds*) are identified (Fig. 7; Supplementary File S1). Genes for the H_4MTP-linked C-1 transfer are present with the exception of the methylene-tetrahydromethanopterine dehydrogenase (*mtd*B, see Fig. 7). MAG bin-63 has the genetic potential to perform mixed-acid fermentation from pyruvate to succinate, and from pyruvate to acetate via acetyl-CoA (Fig. S4). Genes for the formation of lactate from pyruvate are lacking, as well as a complete pathway from pyruvate to acetate via acetylphosphate (Fig. S4).

The MAG also includes the genes of the bidirectional NAD-reducing hydrogenase Hox system that could either produce hydrogen or use H_2 as electron donor (see Fig. S4). We did not find genes coding for the O_2-carrier (bacterio)hemerythrin, which has previously been suggested to be involved in O_2 scavenging or in shuttling O_2 directly to the PmoA enzyme complex (Chen *et al.*, 2012). Two types of aerobic respiratory chain complexes are encoded (Fig. S4): the proton-pumping type I NADH dehydrogenase (NDH-1, complex I; encoded by the ***nuoA-N*** operon) and the sodium-pumping NADH dehydrogenase (Na^+-NQR). The non-proton pumping type II NADH dehydrogenase (NDH-2; *ndh* and *ndh*A) was not detected. Genes coding for the terminal reductases of the cytochrome c oxidase complex (i.e. *cyo*E, *cox*CAB) and the cytochrome *bd* oxidase complex (also known as quinol reductase *bd* terminal reductase or high-affinity cytochrome *bd* ubiquinol oxidase, *cyd*AB; Fig. S4) were also detected. The denitrification pathway was incomplete: *nirK* and *norB* genes, involved in dissimilatory nitrate reduction, are present (Fig. 7, Supplementary File S1), but the dissimilatory nitrate reductase (*nar*G) and nitrous oxide reductase (*nosZ)* genes are absent.

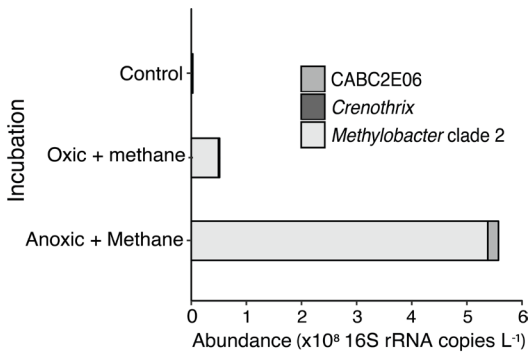

Fig. 6. The abundance of methanotrophic community members (as detected by 16S rRNA gene amplicon sequencing) in the winter incubation experiments performed with water from 12 m. Data are provided in Table S2. The OTU LL-pmoA-1 dominated all three experiments (Fig. S2).

Discussion

Both the high methane oxidation rates in the anoxic water column as well the result of the anoxic incubations suggest that AOM takes place in Lacamas Lake. In previous studies, freshwater methane oxidation under anoxic conditions has been observed to be performed by ANME (Eller *et al.*, 2005, Zigah *et al.*, 2015), by methane oxidizing bacteria working in close cooperation with photosynthetic oxygen producers (Oswald *et al.*, 2015), or by bacteria of the *Ca*. M. oxyfera, which are providing their own oxygen via a nitrite-reduction pathway (Ettwig *et al.*, 2010). None of these three mechanisms is likely to be responsible for methane oxidation in the hypolimnion of Lacamas Lake. No more than 0.2% of all 16S rRNA reads could be assigned to archaea, and none of the known ANME clades were detected. Although primer bias may decrease the number of reads assigned to archaea, the absence of ANME is not surprising, given the oxic/anoxic cycles in Lacamas Lake and the intolerance of ANME for oxygen. Although strict anaerobes could potentially survive in anoxic sediment layers during winter oxygenation, it is unlikely they are capable of rapidly occupying the anoxic niche when stratification occurs, especially considering their slow growth rates (ANME doubling times of 2-7 months; Nauhaus *et al.*, 2007; Scheller *et al.*, 2016). Methane oxidation fueled by photosynthesis in the hypolimnion would require deep light penetration, whereas Lacamas Lake secchi disk depth was <2 m at the time of sampling, making this option unlikely. Likewise, *Candidatus* M. oxyfera or other NC10-related 16S rRNA gene sequences were not detected in Lacamas Lake.

Methanotrophs such as *Methylomonas denitrificans*, *C. polyspora*, or *M. tundripaludum*, who couple methane oxidation to nitrite or nitrate reduction (Kits *et al.*, 2015a; 2015b; Oswald *et al.*, 2017; Rissanen *et al.*, 2018), are also potential candidates to perform methane oxidation in the anoxic water column. However, in our study, members of the *Methylobacter* clade 2 were identified as the dominant methanotrophs in the anoxic water column (12 – 17 m) during summer, in the summer water column incubations, at all depths of the oxic water column in winter, and in the anoxic winter incubations (Fig. 4C-D), as observed by the 16S rRNA gene (Fig. 3) and PmoA coding gene (Fig. 5) sequencing. This indicates that the *Methylobacter* clade 2 species detected in our study thrive not only under oxic conditions but also in anoxic environments, suggesting that this species is also capable of AOM like some other methanotrophs. The strongest evidence for this conclusion comes from the anoxic winter incubation experiment that resulted in a strong (39%) enrichment of a *Methylobacter* clade 2 species (Fig. 4).

Although low amounts of oxygen could have been present at the start of the anoxic incubation experiments, due to oxygen contamination during sampling or handling, we can rule this out as a driver of methane oxidation for several reasons. Firstly, the observed methane decrease over time was highly linear (R^2 of 0.999) and did not show an increased oxidation in the first 6 h, which would have been expected if oxygen contamination would have stimulated methane oxidation rates (Table S1). Secondly, the addition of oxygen to the summer incubation experiment with anoxic water from 12 m diminished methane oxidation (Fig. S1), showing that high oxygen concentrations inhibited methane oxidation, as was previously observed by Thottathil *et al.* (2019). Thirdly, De Brabandere *et al.* (2012) estimated the oxygen introduction by leakage from the oxygen-containing butyl caps of exetainers at ca. 300-400 nmol L^{-1}. Given the 2:1 stoichiometry of aerobic methane oxidation, oxygen contamination could thus only

have accounted for the first 0.15–0.2 mM oxidized in the exetainers, which is only 0.3% of the total oxidized methane. The stoppers used were double waded and should therefore give maximum protection against leakage. Oswald *et al.* (2016) estimated the maximum intrusion through butyl stoppers in serum bottles to be 13 nM day^{-1}. This could account for only 0.02% of the methane oxidation. Hence, although we cannot rule out the presence of traces of oxygen, the quantity of oxygen is simply not high enough to explain the amount of methane that is oxidized.

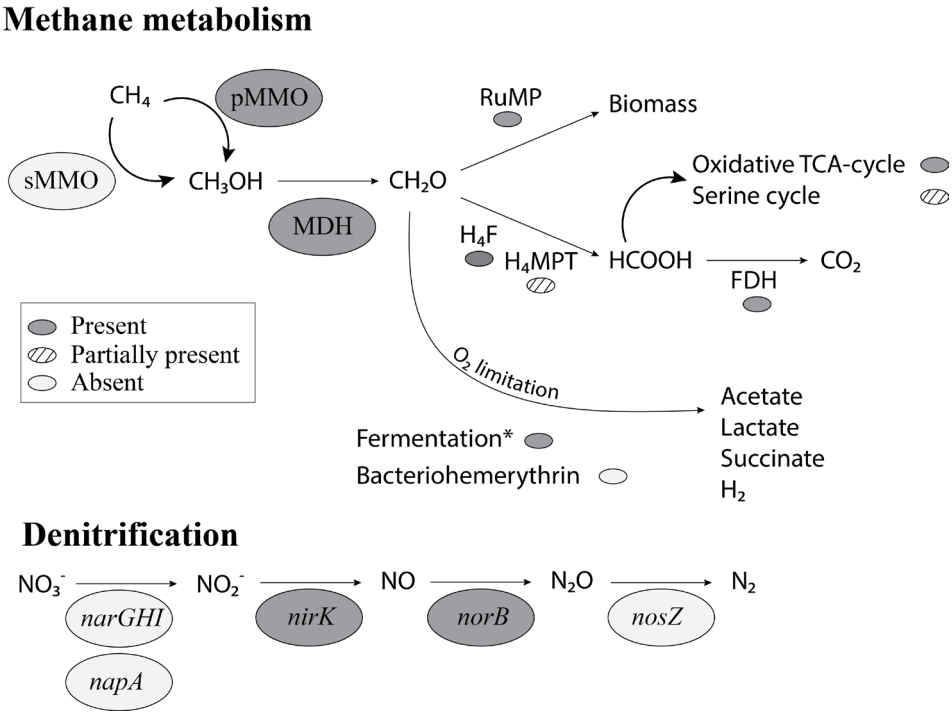

Fig. 7. Metabolic pathways of methane oxidation and denitrification in the predominant *Methylobacter* species present in Lacamas Lake as inferred from the presence of encoding genes in MAG bin-63. Enzymes/pathways indicated in dark grey were encoded by the genome, grey-streaked indicates the presence of an incomplete pathway. Light grey pathways were not detected. *The full fermentation pathway is shown in Fig. S4. FDH – formate dehydrogenase; H4F – methylene tetrahydrofolate pathway; H_4MPT – Tetrahydromethanopterin pathway; MDH – methanol dehydrogenase; pMMO – particulate methane monooxygenase; RuMP – ribulose monophosphate pathway; sMMO – soluble methane monooxygenase; TCA – tricarboxylic acid.

Several methanotrophs are known to contain genes encoding for parts of the nitrate reduction pathway, which has previously been shown to be coupled to methane oxidation under anoxic conditions (Smith *et al.*, 2018). Specifically, the genomes of some *Methylobacter* species encode a complete nitrate reduction pathway up to N_2O, possibly allowing them

to use nitrate as a terminal electron acceptor when oxygen is limiting (Smith *et al.*, 2018). However, other *Methylobacter* species only contain the *nirS*/*nirK* and *norB* genes, but lack the *narG* and *napA* genes for nitrate reduction, making them unable to perform complete denitrification (Svenning *et al.*, 2011; Smith *et al.*, 2018). *Methylobacter* species and closely related methanotrophs have previously been found to thrive in anoxic environments where methane oxidation could not be explained by the presence of known electron acceptors or pathways (Biderre-Petit *et al.*, 2011; Blees *et al.*, 2014; Martinez-Cruz *et al.*, 2017). The *Methylobacter* species detected in our study are not 100% identical to the known nitrate-reducing species *M. tundripaludum* (Figs. 3 and 5). The genome of the MAG bin-63, that reflects the abundant *Methylobacter* species in Lacamas Lake, lacked the nitrate reductase coding gene (*nar*G) involved in the dissimilatory reduction of nitrate (Fig. 7). This suggests that the dominant Lacamas Lake *Methylobacter* species cannot perform nitrate reduction itself, unless it utilizes reduction pathways that are up to this point unknown or incorrectly classified. If this species cannot perform nitrate reduction, it will need to reduce another electron acceptor to be able to perform methane oxidation. Potentially, it could use nitrite as an electron acceptor, as its genome contains the nitrite reductase gene, *nirK*, and the nitric-oxide reductase gene *norB*. Nitrate, but not nitrite, was provided to the experiments, but a non-methanotrophic organism could have converted the nitrate to nitrite before being used by the methanotrophs. Nitrate reduction was not measured in our experiments, so we can only speculate about these processes occurring. Nitrite reduction has been observed in *Methylomicrobium album* BG8 by Kits *et al.* (2015a), but not in any other methanotroph up to this point. No metabolic pathway involved in sulfate reduction could either be identified in the genome of the MAG bin-63, even though the addition of sulfate stimulated methane oxidation in the anoxic incubation experiments (Fig. 2).

The question of how this *Methylobacter* species can thrive under anoxic conditions (5-fold abundance and 4-fold oxidation rate increase with respect to oxic conditions, Fig. 2B; Fig. 6), therefore, remains fascinating but difficult to answer at this stage. The genome of MAG bin-63 included a complete RuMP pathway for C-1 assimilation from methane-derived formaldehyde, and a complete mixed-acid fermentation pathway to fumarate and acetate, indicating both high and low-oxygen adapted metabolism. The presence of the high-affinity cytochrome *bd* oxidase complex, the NADH-quinone oxidoreductase (nqr) and hydrogen dehydrogenase genes (Fig. S4) also support this hypothesis of low-oxygen adaptation. Fermentation-based methanotrophy has been detected before and it has been hypothesized that under low oxygen conditions, a metabolic switch to fermentation can be induced ((Morinaga *et al.*, 1979; Roslev and King, 1995; Kalyuzhnaya *et al.*, 2013; Gilman *et al.*, 2017), which may also occur in the *Methylobacter* species detected in Lacamas lake. Fermentation-based methanotrophy has, however, been shown to lead to low biomass production and methane turnover rate in a culture study of *Methylomicrobium alcaliphilum* (Kalyuzhnaya *et al.*, 2013), while biomass production by the *Methylobacter* in our experiments was exceptionally high, with doubling times of <10 h under anoxic conditions (Fig. 6). In addition, methane oxidation rates in Lacamas Lake's anoxic hypolimnion were higher than those reported in comparable lakes with a similar or lower methane concentration (Blees et al., 2014; Eller et al., 2005; Schubert et al., 2010). This raises considerable concerns whether this *Methylobacter* species can rely solely on a fermentation-based metabolism for methane oxidation.

An alternative explanation could be the existence of a metabolic syntrophy between the

methanotrophs converting methane into organic compounds (e.g. acetate, fumarate) and hydrogen, and microorganisms able to metabolize these excreted compounds (see Yu and Chistoserdova (2017) for a review). These partner organisms could stimulate methane oxidation by *Methylobacter* cells, and therefore the biomass production, by consumption of growth-limiting excreted compounds.

Here, we identify the potential syntrophic partner of the *Methylobacter* species by analyzing which microorganisms were high in relative abundance or increased in relative abundance together with the increase of the *Methylobacter* species. Sequences affiliated with the order Burkholderiales (Betaproteobacteria) occur abundantly in Lacamas Lake (up to 16.9 and 35.1% in the summer and winter water column, respectively; Table S5). Members of these groups have been described as being able to assimilate succinate, while using nitrate as an electron acceptor (Saito *et al.*, 2008). Bacteria of the family *Methylophilaceae* (Betaproteobacteria) also showed an increased abundance in the incubations with the highest methane oxidation rates (Fig. S5). They have often been detected in co-occurrence with methanotrophs, and have been shown to use reaction products of methanotrophy (Yu and Chistoserdova, 2017), coupling methanol oxidation to nitrate reduction (Kalyuzhnaya *et al.*, 2011). It is, however, unknown whether there is an advantage for the methanotrophs in this relationship. Furthermore, sequences closely related to the order Rhodocyclales were highly abundant in the anoxic summer water column and incubations, especially the genus *Sulfuritalea* (7.2–12.9%, Table S5). *Sulfuritalea hydrogenivorans* was isolated by Kojima and Fukui (2011) from the water column of a stratified lake and described as a facultative anaerobe, capable of oxidizing thiosulfate and hydrogen, using nitrate as an electron acceptor. Although we stress that the co-occurrence of these species cannot be used as a proof of a relationship and that the fermentation potential of the *Methylobacter* detected here is purely based on genome-inferred information, the co-occurrence of *Methylobacter* and Burkholderiales, *Methylophilaceae* and *Sulfuritalea* species is intriguing and would be a good target for further research, exploring whether the observed stimulation by nitrate in our incubation experiments could be indirect, via partner organisms. The stimulation of methane oxidation in incubation experiments with added sulfate could work similarly, although no potential partner organisms could be identified at this stage.

Conclusions

Methylobacter species have been found in many low-oxygen and anoxic zones in stratified lakes, similar to Lacamas Lake, but the electron acceptor used for methane oxidation remained unclear. Although the addition of nitrate and sulfate was found to stimulate methane oxidation in Lacamas Lake, the absence of a complete nitrate reduction pathway in the genome of the Lacamas lake *Methylobacter* species means the exact mechanism mediating this oxygen-limited methane oxidation remains unknown. No pathway involved in sulfate reduction could be identified either. Possibly, another member of the microbial community, capable of nitrate reduction, could provide the detected *Methylobacter* with nitrite, which could then be reduced to N_2O, coupling methane oxidation to nitrite reduction. Consortia of methanotrophs and partner organisms are well known from marine settings (i.e. sulfate-reducing bacteria and ANME; Boetius *et al.*, 2000), and have been suggested to also occur in lakes (Oshkin *et al.*, 2014; Hernandez *et al.*, 2015; Yu and Chistoserdova, 2017). The apparent lack of electron acceptors and genomic pathways that can explain methane oxidation by *Methylobacter* cells alone suggest that such a lacustrine consortium may exist, but clearly

more research is required to explore the involved organisms and metabolic pathways. Mixed-acid fermentation, as suggested for the detected *Methylobacter* species based on its genome, could be widespread in bacterial methanotrophs. The assumption that the key product of methane oxidation is always CO_2 might, therefore, need to be reconsidered, as fermentation products such as lactate, succinate and acetate could be a substantial sink for methane-derived carbon in oxygen-limited systems. Research on the genomic capacities for mixed-acid fermentation and the expression of these genes should be performed, as well as studies that focus on measuring the reduction of electron acceptors by methanotrophs and other possibly involved microorganisms, in order to find the link between electron acceptor reduction and methane oxidation rates.

Acknowledgements

The authors would like to thank Keith Birchfield, Sanne Vreugdenhil, and Maartje Brouwer for practical help in the laboratory and during fieldwork. We would also like to thank the Lacamas Shores Neighborhood Association for use of their facilities. We are grateful to the editor and reviewers for their comments, which greatly improved this paper. This research is supported by the Soehngen Institute of Anaerobic Microbiology (SIAM) Gravitation grant (024.002.002) to JSSD and LV of the Netherlands Ministry of Education, Culture and Science (OCW) and the Netherlands Organisation for Scientific Research (NWO).

Supplemental material

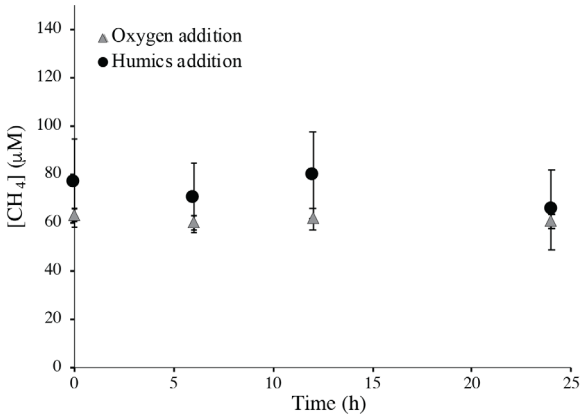

Fig. S1. Methane concentration over time in the incubation experiment with 12 m depth summer samples, with oxygen (grey triangles) or humic substance (black circles) added. No significant change in methane concentration over time was observed, the R^2 of the linear regression analysis was 0.04 for the oxygen addition experiment and 0.03 for the experiment with the addition of humic substances.

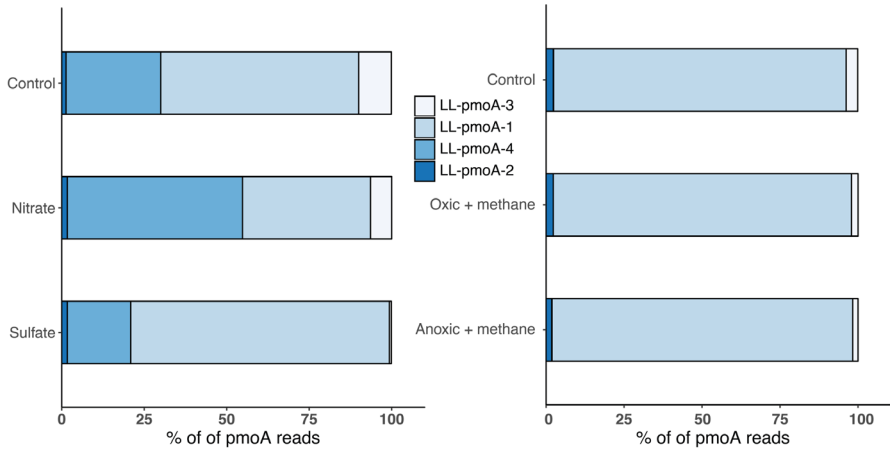

Fig. S2. PmoA distribution of incubation experiments in summer (A) and winter (B). Numbers are provided in Table S3.

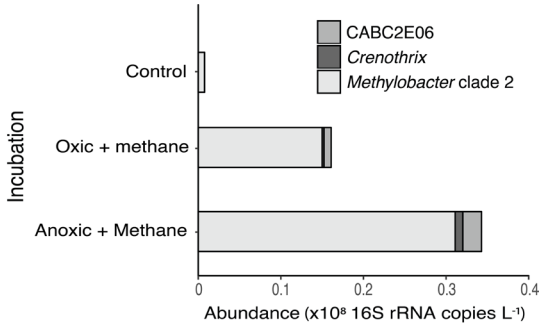

Fig. S3. The abundance of methanotrophic community members (as detected by 16S rRNA gene amplicon sequencing) in the winter incubation experiments performed with water from 17 m depth.

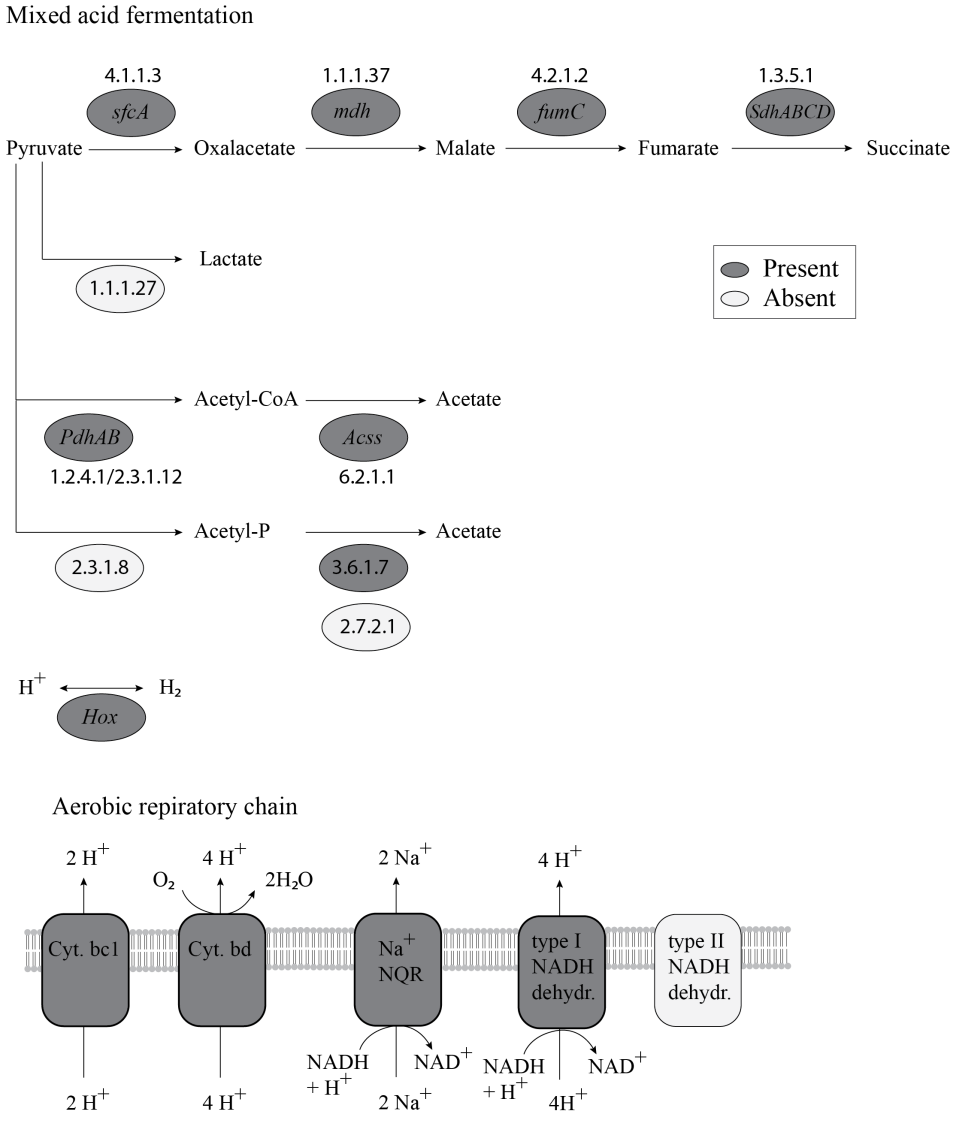

Fig. S4. Genome-inferred metabolic pathways of MAG bin-63. Pathways indicated in dark grey were detected, sequences of light grey pathways were lacking. Genes were indicated where possible; numbers refer to EC database numbers. For details, see Supplementary File S1.

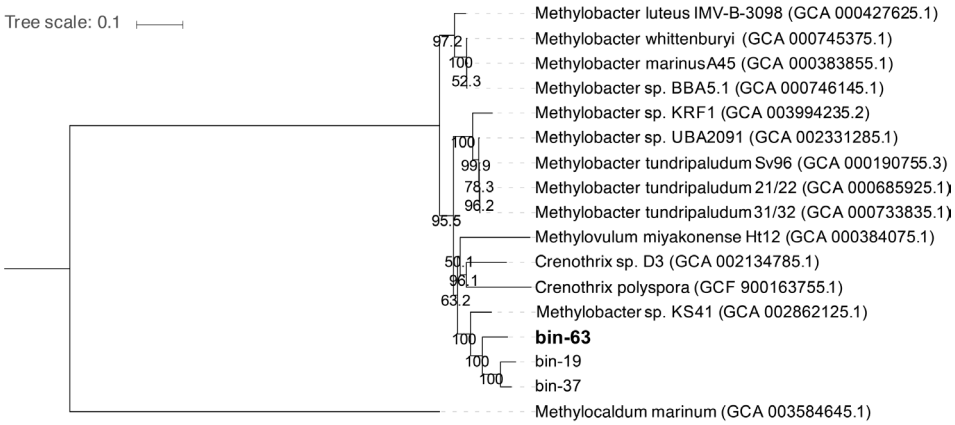

Fig. S5. Maximum likelihood phylogenetic tree based on 34 concatenated single-copy, protein-coding genes (following the method of Dombrowski et al., 2018) of the three highest average abundance MAGs (i.e. bin-63, bin-37, and bin-19) detected in the winter incubation experiment under anoxic conditions and amended with methane.

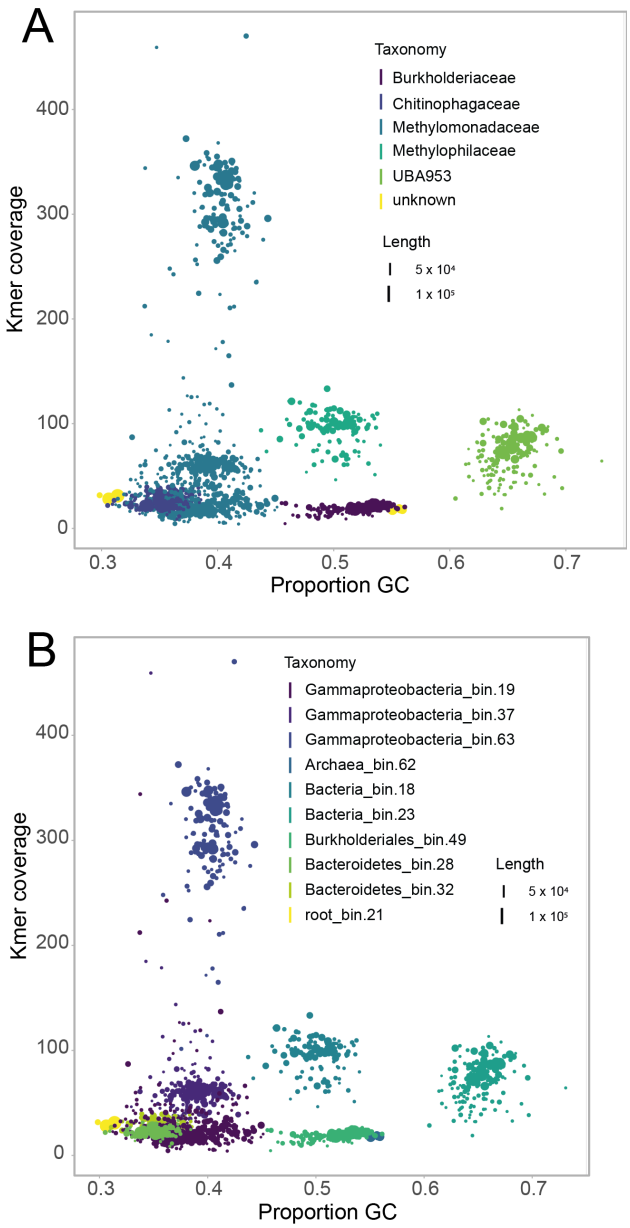

Fig. S6. GC coverage plots including the contigs of the 10 most abundant bins obtained in the sequenced sample with (A) the taxonomic classification of GTDB-Tk at the level of family, and (B) with the taxonomic classification of CheckM, indicating that the MAG bin-63, indicated in dark blue in panel B, was affiliated to the family Methylomonadaceae, indicated in teal in panel A.

Table S1. Methane oxidation rates (MOR) and additional information regarding the rate measurements. The R^2 given is the R^2 of the linear regression analysis used to determine the methane oxidation rate. The oxidizing equivalents surplus/deficiency indicates the mM of methane that could have been oxidized by the electron acceptor, after the amount that was oxidized within the 24 h incubation experiment was deducted.

	Depth (m)	MOR (mM/day)	t_0 [CH_4]	oxidized in 24 h (%)	R^2	[NO_3^-] or [SO_4^{2-}] (mM)	Potential CH_4 oxidation by [NO_3^-] or [SO_4^{2-}] (mm)[3]	Oxidizing equivalents surplus/deficiency (mM)[3]
Summer, natural conditions	3	-	2.7	-	0.01			
	5	-	2.2	-	0			
	7	18	28	63	0.96			
	9	7.3	102	7	0.2			
	12	9.2	107	9	0.25			
	15	46	286	16	0.42[2]			
	17	36	398	9	0.21[2]			
Summer, nitrate addition	5	0.4	0.7	57	0.8	116	73	72
	7	30	9.6	100[1]	0.65	146	92	62
	9	58	113	51	0.98	124	78	20
	12	72	158	46	0.71	74	47	-26
	15	64	156	41	0.9	146	92	28
Summer, sulfate addition	5	0.5	0.7	70	0.08	2230	2230	2229
	7	13	9	100[1]	0.84	2159	2159	2150
	9	52	117	44	0.96	2272	2272	2155
	12	40	91	44	0.76	2267	2267	2176
	15	74	158	47	0.92	2194	2194	2037
Winter, methane addition	3	-	176	-	0.01			
	7	-	134	-	0.01			
	12	-16.4	168	-10	0.17			
	17	7.7[4]	151	5	0.06			
Winter, anoxic + methane addition	12	20.6	194	11	0.22			
	17	36.5	256	14	0.17			
Winter, natural	17	0.03[4]	0.84	3	0.08			

[1]. the methane oxidation rate is based on the linear regression analysis, whilst the actual methane oxidation consumption in the incubation vials was lower due to methane limitation.

[2]. a subset of the datapoints was used (t_6, t_{12} and t_{24})

[3]. Using a 8:3 ratio of NO_3:CH_4 and a 1:1 ratio of SO_4:CH_4 (Segarra et al.)

[4]. Low R^2 of regression analysis

Table S2. Relative abundances (%) of known methanotrophs detected in the Lacamas Lake water column and incubation experiments (C denotes control) as determined by 16S rRNA gene amplicon sequencing. Any group with a percentage <0.1% is considered not significant and displayed as zero. Total reads obtained are indicated. Total 16S rRNA gene copies per liter were determined using quantitative PCR of the total prokaryotic community, with SD being the standard deviation of 3 experimental replicates. The taxonomic assignment of each of the mentioned methanotrophs is shown in Fig. 3.

	SUMMER										WINTER										
	Natural conditions (depth in m)							Incubations (12 m)			Natural conditions (depth in m)					Incubations (12 m)			Incubations (17 m)		
	3	5	7	9	12	15	17	C	NO_3^{2-}	SO_4^{2-}	3	5	12	15	17	C	CH_4/ oxic	CH_4/ anoxic	C	CH_4/ oxic	CH_4/ anoxic
CABC2E06	0	0.2	0.5	0.3	0.1	0.1	0.1	0.9	1	0.4	0	0	0	0	0	0	0.3	1	0	0.4	0.9
Crenotrix spp.	0	0	0.1	0.1	0	0	0	0.3	0.4	0.6	0	0.1	0	0	0.1	0	0.1	0.3	0	0.1	0.4
Methylobacter spp.	0	0.1	0.3	0.4	0.6	0.7	0.8	12	11	17	0.4	0.5	0.8	0.6	0.9	0.7	7	35	0.2	6.9	13
Methylomonas spp.	0	0.1	0.5	0.4	0.2	0.1	0.1	1.7	3.1	2.3	0	0	0	0.1	0	0	0	0	0	0	0
pLW-20	0	0.4	3.3	2.6	0.5	0.1	0	1.7	4	1.3	0	0	0	0.2	0	0	0.1	0.2	0	0	0.1
Unidentified *Methylococcaceae*	0	0.1	0.3	0.2	0.1	0	0	0.8	1.4	1.3	0	0	0	0	0	0	0	0	0	0.2	0.1
Reads per sample ($x10^6$)	1.7	1.4	1.9	1.8	0.9	1.5	1.7	1.5	1.8	1.5	8.8	1.7	1.4	2	1.6	1.7	1.6	1.3	1.4	1.3	1.5
Total 16S rRNA gene copies L^{-1} ($x10^8$)	4.1	5	4.6	5.4	5.5	6.8	3.1	10	3.2	3.3	2	3.4	2.8	3.1	3.6	7.1	4.8	11	1.6	2.2	2.4
SD	0.3	0.2	0.6	0.8	0.7	0.9	0.7	2.3	0.4	0.3	0.3	0.2	0.2	0.3	0.7	1.1	0.4	0.8	0.3	0.2	0.1

Table S3. *pmoA* relative abundance (%) in samples of the summer and winter water column and incubations (C denotes control). The tentative taxonomic assignment of the denovo sequences can be observed in Fig. 5.

	SUMMER										WINTER										
	Natural conditions (depth in m)							Incubations (12 m)			Natural conditions (depth in m)					Incubations (12 m)			Incubations (17 m)		
	3	5	7	9	12	15	17	C	NO_3^{2-}	SO_4^{2-}	3	5	12	15	17	C	CH_4/ oxic	CH_4/ anoxic	C	CH_4/ oxic	CH_4/ anoxic
LL-pmoA-1	12	0.6	0.2	0.6	16	85	93	60	39	78	94	96	96	97	96	-	97	97	94	96	96
LL-pmoA-2	0.3	0	0	0	0.3	1.5	1.5	1.3	1.7	1.7	1.7	1.9	1.7	1.8	1.8	-	1.7	2	2.3	2.3	1.8
LL-pmoA-3	78	43	9.9	4.9	3.8	0.6	0.8	9.9	6.4	0.6	3.4	1.7	1.7	1.5	1.9	-	1.6	0.7	3.7	2.1	1.7
LL-pmoA-4	9.9	56	90	95	80	13	4.2	29	53	19	0.8	0.4	0.5	0.2	0.1	-	0.1	0.1	0.1	0	0.1

Table S4. Characteristics of the MAGs affiliated to methanotrophs of the Methylococcales which are discussed in the text. Classification was inferred by GTDB-Tk. An unassigned species (i.e., s__) indicates that the query genome is either i) placed outside a named genus or ii) the ANI to the closest intra-genus reference genome with an AF >=0.65 is not within the species-specific ANI circumscription radius. Classification was performed by placement of the genome in the reference tree and by using the relative evolutionary divergence (RED). Red value indicates the relative evolutionary divergence for a query genome. aa_percent: indicates the percentage of the multiple sequence alignment spanned by the genome (i.e. percentage of columns with an amino acid).

bin id	Completeness (%)	Contamination (%)	Strain heterogeneity (%)	contigs	size (bp)	Average abundance	aa_percent	red_value	classification
bin.63	96	0.74	0	136	2225455	419	97	0.95023	d__Bacteria;p__Proteobacteria; c__Gammaproteobacteria;o__ Methylococcales; f__Methylomonadaceae;g__KS41
bin.37	92	5.3	14	282	2214630	77	87	0.951832	d__Bacteria;p__Proteobacteria; c__Gammaproteobacteria;o__ Methylococcales; f__Methylomonadaceae;g__KS41
bin.19	88	0.46	50	453	4678414	30	74	0.951132	d__Bacteria;p__Proteobacteria; c__Gammaproteobacteria;o__ Methylococcales; f__Methylomonadaceae;g__KS41

Table S5. Relative abundance (% of 16S rRNA gene reads) of *Sulfuritalea*, *Burkholderiales* and *Methylophilaceae* detected in Lacamas Lake by 16S rRNA gene amplicon sequencing (C denotes control).

	SUMMER										WINTER										
	Natural conditions (depth in m)							Incubations (12 m)			Natural conditions (depth in m)					Incubations (12 m)			Incubations (17 m)		
	3	5	7	9	12	15	17	C	NO_3^{2-}	SO_4^{2-}	3	5	12	15	17	C	CH_4/ oxic	CH_4/ anoxic	C	CH_4/ oxic	CH_4/ anoxic
Sulfuritalea (genus)	0.03	0.11	1.7	4.5	13	12	10	7.2	7.3	8.9	0.13	0.13	0.15	4.68	0.1	0.09	0.08	0.08	0.07	0.07	0.07
Burkholderiales (order)	4.5	7.1	14	15	17	11	8.6	12	8.7	11	28	23	35	22	28	19	17	8.5	19	15	10
Methylophilaceae (family)	0.85	1.4	2	1.3	1	0.64	0.69	3.7	5.2	3.7	0.72	0.7	1.2	1.1	1.5	0.94	2.6	6.8	1.4	3.1	3.1

Table S6. Experimental and sampling details. Samples for nutrient analysis were taken in duplicate (indicated with #), samples for methane oxidation rate linear regression analysis in quadriplicate (natural rate incubations indicated with +, amended incubations indicated with ^). For DNA analysis one filter per sampling moment and depth was taken (indicated with x).

		Nutrients						Microbial community		Incubations			
		Nitrate		Nitrite		Sulfate		DNA samples		Methane oxidation rate		Methane oxidizing community	
		0.2 µm filtered		0.2 µm filtered		Zn-Acetate (0.4 mg l)		0.3 µm filtered		24-hour incubations		72-hour incubations, then 0.2 µm filtered	
		Summer	Winter	Summer	Winter	Summer	Winter	Summer	Winter	Summer	Winter	Summer	Winter
Depth (m)	0												
	1												
	3	#	#	#	#	#	#		x	+	+		
	5	#		#		#		x	x	+			
	7	#	#	#	#	#	#	x		+	+		
	9	#		#		#		x		+			
	12	#	#	#	#	#	#	x	x	+, ^	+, ^	x, ^	x, ^
	15	#	#	#	#	#	#	x	x	+			
	17	#	#	#	#	#	#		x	+	+, ^		x, ^
	Inlet	#	#	#	#	#	#						

X. single sampling (for DNA purposes)
#. sampling in biological duplicate
+. sampling in biological quadruplicate

Table S7. List of 34 single-copy marker genes used for phylogenetic analysis of MAGs.

DNGNGWU00001
DNGNGWU00002
DNGNGWU00003
DNGNGWU00005
DNGNGWU00006
DNGNGWU00007
DNGNGWU00009
DNGNGWU00010
DNGNGWU00011
DNGNGWU00012
DNGNGWU00014
DNGNGWU00015
DNGNGWU00016
DNGNGWU00017
DNGNGWU00018
DNGNGWU00019
DNGNGWU00021
DNGNGWU00022
DNGNGWU00023
DNGNGWU00024
DNGNGWU00025
DNGNGWU00026
DNGNGWU00027
DNGNGWU00028
DNGNGWU00029
DNGNGWU00030
DNGNGWU00031
DNGNGWU00032
DNGNGWU00033
DNGNGWU00034
DNGNGWU00036
DNGNGWU00037
DNGNGWU00039
DNGNGWU00040

Table S8. Relative abundance of methanotroph OTUs as percentage of all reads in the sample (C denotes control). The taxonomic affiliation of the OTUs is shown in Fig. 3.

	SUMMER										WINTER										
	Natural conditions (depth in m)							Incubations (12 m)			Natural conditions (depth in m)					Incubations (12 m)			Incubations (17 m)		
	3	5	7	9	12	15	17	C	NO_3^{2-}	SO_4^{2-}	3	5	12	15	17	C	CH_4/ oxic	CH_4/ anoxic	C	CH_4/ oxic	CH_4/ anoxic
LL-16S-01	0	0	0.33	0.29	0	0	0	0.11	0.04	0.01	0	0	0	0	0	0	0	0	0	0	0
LL-16S-02	0	0.01	0	0.06	0	0	0	0.02	0.06	0	0	0	0	0	0	0	0	0	0	0	0.01
LL-16S-03	0	0	0.03	0.06	0	0	0	0	0.01	0.04	0	0	0	0	0	0	0	0	0	0	0
LL-16S-04	0	0	0.51	0.08	0	0	0	0	0	0.02	0	0	0	0	0	0	0	0	0	0	0
LL-16S-05	0	0.02	0.02	0.08	0.02	0	0	0.1	1	0.04	0	0	0	0	0	0	0	0	0	0	0
LL-16S-06	0	0.01	0.08	0.25	0	0	0	0.02	0.01	0.08	0	0	0	0	0	0	0	0	0	0	0.01
LL-16S-07	0	0	0	0.07	0	0	0	0.01	0.01	0.01	0	0	0	0	0	0	0	0	0.01	0.86	0.05
LL-16S-08	0	0	0	0	0	0	0	0.01	0.02	0.01	0	0	0	0	0	0	0	0	0	0	0
LL-16S-09	0	0	0	0	0	0	0	0.01	0.01	0.01	0	0	0	0	0	0	0	0	0	0	0.02
LL-16S-10	0	0	0	0	0	0	0	0	0	0	0	0	0	0	0	0	0	0	0	0.01	0.01
LL-16S-11	0	0.01	0.01	0.02	0	0	0	0.14	0.2	0.01	0	0	0	0	0	0	0	0	0	0	0
LL-16S-12	0	0.01	0	0	0	0	0	0.01	0.02	0	0	0	0	0	0	0	0	0	0	0.01	0.01
LL-16S-13	0	0	0	0	0	0	0.01	0.04	0.12	0.03	0	0	0	0	0	0	0.01	0.03	0	0	0
LL-16S-14	0	0	0	0	0	0	0	0	0	0	0	0	0	0	0	0	0	0	0	1.3	5
LL-16S-15	0	0	0	0	0	0	0	0	0	0	0	0	0	0	0	0	0	0	0	0	0
LL-16S-16	0.01	0	0.01	0.02	0.02	0.09	0.01	1.8	1.1	4.7	0.03	0.01	0.08	0.04	0.02	0.09	0.03	17	0	0	0
LL-16S-17	0	0	0	0	0.01	0.01	0.07	0.01	0.51	0.01	0	0.04	0	0.01	0.01	0	1.8	0.04	0	0	0
LL-16S-18	0	0	0	0	0	0	0	0.05	0.25	0.03	0	0	0	0	0	0	0	0	0	0	0
LL-16S-19	0	0	0	0	0	0	0	0	1.1	0.01	0	0	0	0	0	0	0.06	0.02	0	0	0

	SUMMER										WINTER										
	Natural conditions (depth in m)							Incubations (12 m)			Natural conditions (depth in m)					Incubations (12 m)			Incubations (17 m)		
	3	5	7	9	12	15	17	C	NO_3^{2-}	SO_4^{2-}	3	5	12	15	17	C	CH_4/ oxic	CH_4/ anoxic	C	CH_4/ oxic	CH_4/ anoxic
LL-16S-20	0	0	0	0	0	0	0	0.12	0.29	0.04	0	0	0.01	0	0	0	0	0.03	0	0	0
LL-16S-21	0	0	0	0	0	0.03	0	1.8	0.88	0.08	0.01	0.01	0	0	0	0	0	0.81	0	0	0
LL-16S-22	0	0	0	0	0	0	0	0.12	0.29	0.04	0	0	0.01	0	0	0	0	0.03	0	0	0
LL-16S-23	0	0	0	0	0.02	0	0.03	0.12	0.01	0.04	0	0	0.03	0.03	0.13	0.01	0.65	0.47	0	0.1	0.06
LL-16S-24	0	0	0	0	0	0	0.01	0.24	0.33	0.13	0	0	0	0	0	0	0.01	0.04	0.01	0.08	0.01
LL-16S-25	0	0	0	0	0	0	0	0	0	0	0	0	0	0	0	0	0	0	0.02	0	0.01

References

Altschul, S.F., Gish, W., Miller, W., Myers, E.W., and Lipman, D.J. (1990) Basic local alignment search tool. *J. Mol. Biol.* **215**: 403–410.

Andrews, S. (2010) FastQC: a quality control tool for high throughput sequence data. *http://www.bioinformatics.babraham.ac.uk/projects/fastqc/*.

Asbun, A., Besseling, M.A., Balzano, S., van Bleijswijk, J., Witte, H., Villanueva, L., Engelmann, J.C. (2019) Cascabel: a flexible, scalable and easy-to-use amplicon sequence data analysis pipeline. bioRxiv 809384; doi: https://doi.org/10.1101/809384

Aziz, R.K., Bartels, D., Best, A.A., Dejongh, M., Disz, T., Edwards, R.A., et al. (2008) The RAST Server : Rapid annotations using subsystems technology. *BMC Genomics* **9**: 75.

Bastviken, D., Tranvik, L.J., Downing, J.A., Crill, P.M., and Enrich-prast, A. (2011) Freshwater methane emissions offset the continental carbon sink. *Science* **331**: 50.

Besseling, M.A., Hopmans, E.C., Boschman, C.R., Sinninghe Damsté, J.S., and Villanueva, L. (2018) Benthic archaea as potential sources of tetraether membrane lipids in sediments across an oxygen minimum zone. *Biogeosciences* **15**: 4047–4064.

Biderre-Petit, C., Jézéquel, D., Dugat-Bony, E., Lopes, F., Kuever, J., Borrel, G., et al. (2011) Identification of microbial communities involved in the methane cycle of a freshwater meromictic lake. *FEMS Microbiol. Ecol.* **77**: 533–545.

Blees, J., Niemann, H., Wenk, C.B., Zopfi, J., Schubert, C.J., Kirf, M.K., et al. (2014) Micro-aerobic bacterial methane oxidation in the chemocline and anoxic water column of deep south-Alpine Lake Lugano (Switzerland). *Limnol. Oceanogr.* **59**: 311–324.

Boetius, A., Ravenschlag, K., Schubert, C.J., Rickert, D., Widdel, F., Gieseke, A., et al. (2000) A marine microbial consortium apparently mediating anaerobic oxidation of methane. **407**: 623–626.

Bolger, A.M., Lohse, M., and Usadel, B. (2014) Trimmomatic: A flexible trimmer for Illumina sequence data. *Bioinformatics* **30**: 2114–2120.

De Brabandere, L., Thamdrup, B., Revsbech, N.P., and Foadi, R. (2012) A critical assessment of the occurrence and extend of oxygen contamination during anaerobic incubations utilizing commercially available vials. *J. Microbiol. Meth.* **88**: 147–154.

Caporaso, J.G., Kuczynski, J., Stombaugh, J., Bittinger, K., Bushman, F.D., Costello, E.K., et al. (2010) QIIME allows analysis of high-throughput community sequencing data. **7**: 335–336.

Caporaso, J.G., Lauber, C.L., Walters, W.A., Berg-Lyons, D., Huntley, J., Fierer, N., et al. (2012) Ultra-high-throughput microbial community analysis on the Illumina HiSeq and MiSeq platforms. *ISME J.* **6**: 1621–1624.

Chen, K.H.C., Wu, H.H., Ke, S.F., Rao, Y.T., Tu, C.M., Chen, Y.P., et al. (2012) Bacteriohemerythrin bolsters the activity of the particulate methane monooxygenase (pMMO) in *Methylococcus capsulatus* (Bath). *J. Inorg. Biochem.* **111**: 10–17.

Costello, A.M. and Lidstrom, M.E. (1999) Molecular characterization of functional and phylogenetic genes from natural populations of methanotrophs in lake sediments. *Appl. Envir. Microbiol.* **65**: 5066–5074.

Darling, A.E., Jospin, G., Lowe, E., Matsen, F.A., Bik, H.M., and Eisen, J.A. (2014) PhyloSift: Phylogenetic analysis of genomes and metagenomes. *PeerJ*. **2**: e243.

Deemer, B.R., Harrison, J.A., Li, S., Beaulieu, J.J., Delsontro, T., Barros, N., et al. (2016) Greenhouse gas emissions from reservoir water surfaces: A new global synthesis. *BioScience* **66**: 949-964.

Deutzmann, J.S. and Schink, B. (2011) Anaerobic oxidation of methane in sediments of Lake Constance, an oligotrophic freshwater lake. *Appl. Environ. Microbiol.* **77**: 4429–4436.

Dombrowski, N., Teske, A.P., and Baker, B.J. (2018) Expansive microbial metabolic versatility and biodiversity in dynamic Guaymas Basin hydrothermal sediments. *Nat. Commun.* **9**: 4999.

Edgar, R.C. (2004) MUSCLE: Multiple sequence alignment with high accuracy and high throughput. *Nucleic Acids Res.* **32**: 1792–1797.

Edgar, R.C. (2010) Search and clustering orders of magnitude faster than BLAST. *Bioinformatics* **26**: 2460–2461.

Egger, M., Rasigraf, O., Sapart, C.J., Jilbert, T., Jetten, M.S.M., Röckmann, T., et al. (2014) Iron-mediated anaerobic oxidation of methane in brackish coastal sediments. *Environm. Sci. Technol.* **49**: 277-283.

Eller, G., Känel, L., Krüger, M., Ka, L., and Kru, M. (2005) Cooccurrence of aerobic and anaerobic methane oxidation in the water column of Lake Plußsee. *Appl. Environ. Microbiol.* **71**: 8925–8928.

Ettwig, K.F., Butler, M.K., Le Paslier, D., Pelletier, E., Mangenot, S., Kuypers, M.M.M., et al. (2010) Nitrite-driven anaerobic methane oxidation by oxygenic bacteria. *Nature* **464**: 543–548.

Ettwig, K.F., Zhu, B., Speth, D., Keltjens, J.T., Jetten, M.S.M., and Kartal, B. (2016) Archaea catalyze iron-dependent anaerobic oxidation of methane. *Proc. Nat. Acad. Sci. U.S.A.*, **113**: 12792-12796.

Gilman, A., Fu, Y., Hendershott, M., Chu, F., Puri, A.W., Smith, A.L., et al. (2017) Oxygen-limited metabolism in the methanotroph *Methylomicrobium buryatense* 5GB1C. *Peer J* **5**: e3945.

Guindon, S., Dufayard, J.F., Lefort, V., Anisimova, M., Hordijk, W., and Gascuel, O. (2010) New algorithms and methods to estimate maximum-likelihood phylogenies: Assessing the performance of PhyML 3.0. *Syst. Biol.* **59**: 307–321.

Gurevich, A., Saveliev, V., Vyahhi, N., and Tesler, G. (2013) QUAST: Quality assessment tool for genome assemblies. *Bioinformatics* **29**: 1072–1075.

Hernandez, M.E., Beck, D.A.C., Lidstrom, M.E., and Chistoserdova, L. (2015) Oxygen availability is a major factor in determining the composition of microbial communities involved in methane oxidation. *Peer J* **3**: e801.

Holmes, A.J., Costello, A., Lidstrom, M.E., and Murrell, J.C. (1995) Evidence that particulate methane monooxygenase and ammonia monooxygenase may be evolutionary related. *FEMS Microbiol. Lett.* **132**: 203–208.

Holtappels, M., Lavik, G., Jensen, M.M., and Kuypers, M. M. (2011). ^{15}N-labeling experiments to dissect the contributions of heterotrophic denitrification and anammox to nitrogen removal in the OMZ waters of the ocean. *Methods in Enzymology* **486**: 223-251

Kalyuzhnaya, M. G., Beck, D. A., Vorobev, A., Smalley, N., Kunkel, D. D., Lidstrom, M. E., & Chistoserdova, L. (2012). Novel methylotrophic isolates from lake sediment, description of Methylotenera versatilis sp. nov. and emended description of the genus Methylotenera. *International journal of systematic and evolutionary microbiology* **62**: 106-111.

Kalyuzhnaya, M.G., Yang, S., Rozova, O.N., Smalley, N.E., Clubb, J., Lamb, A., et al. (2013) Highly efficient methane biocatalysis revealed in a methanotrophic bacterium. *Nat. Commun.* **4**: 1–7.

Kang, D.D., Froula, J., Egan, R., and Wang, Z. (2015) MetaBAT, an efficient tool for accurately reconstructing single genomes from complex microbial communities. *Peer J* **3**: e1165.

Kits, K.D., Campbell, D.J., Rosana, A.R., and Stein, L.Y. (2015a) Diverse electron sources support denitrification under hypoxia in the obligate methanotroph *Methylomicrobium album* strain BG8. **6**: 1–11.

Kits, K.D., Klotz, M.G., and Stein, L.Y. (2015b) Methane oxidation coupled to nitrate reduction under hypoxia by the Gammaproteobacterium *Methylomonas denitrificans*, sp. nov. type strain FJG1. **17**: 3219–3232.

Knief, C. (2015) Diversity and habitat preferences of cultivated and uncultivated aerobic methanotrophic bacteria evaluated based on pmoA as molecular marker. *Front. Microbiol.* **6**: 1346.

Knittel, K. and Boetius, A. (2009) Anaerobic oxidation of methane: Progress with an unknown process. *Annu. Rev. Microbiol.* **63**: 311–334.

Kojima, H. and Fukui, M. (2011) *Sulfuritalea hydrogenivorans* gen. nov., sp. nov., a facultative autotroph isolated from a freshwater lake. *Int. J. Syst. Evol. Microbiol.* **61**: 1651–1655.

Ludwig, W., Strunk, O., Westram, R., Richter, L., Meier, H., Yadhukumar, et al. (2004) ARB: a software environment for sequence data. *Nucleic Acids Res.* **32**: 1363–71.

Marotta, H., Pinho, L., Gudasz, C., Bastviken, D., Tranvik, L.J., and Enrich-Prast, A. (2014) Greenhouse gas production in low-latitude lake sediments responds strongly to warming. *Nat. Clim. Chang.* **4**: 467–470.

Martinez-Cruz, K., Leewis, M.C., Herriott, I.C., Sepulveda-Jauregui, A., Anthony, K.W., Thalasso, F., and Leigh, M.B. (2017) Anaerobic oxidation of methane by aerobic methanotrophs in sub-Arctic lake sediments. *Sci. Total Environ.* **607–608**: 23–31.

Miller, C.S. (2013) Assembling full-length rRNA genes from short-read metagenomic sequence datasets using EMIRGE. In: *Methods in Enzymology*. (Vol. 531, pp. 333-352). Academic Press.

Morinaga, Y., Yamanaka, S., Yoshimura, M., Takinami, K., and Hirose, Y. (1979) Methane metabolism of the obligate methane-utilizing bacterium, *Methylomonas flagellata*, in methane-limited and oxygen-limited chemostat culture. *Agric. Biol. Chem.* **43**: 2453–2458.

Nauhaus, K., Albrecht, M., Elvert, M., Boetius, A., and Widdel, F. (2007) In vitro cell growth of marine archaeal-bacterial consortia during anaerobic oxidation of methane with sulfate. *Environ. Microbiol.* **9**: 187–196.

Nguyen, N.L., Yu, W.J., Gwak, J.H., Kim, S.J., Park, S.J., Herbold, C.W., et al. (2018) Genomic insights into the acid adaptation of novel methanotrophs enriched from acidic forest soils. *Front. Microbiol.* **9**: 1982.

Nurk S, Meleshko D, Korobeynikov A, P.P. (2017) metaSPAdes: A new versatile metagenomic assembler. *Genome Res.* **1**: 30–47.

Oshkin, I.Y., Beck, D.A., Lamb, A.E., Tchesnokova, V., Benuska, G., McTaggart, T.L., et al. (2014) Methane-fed microbial microcosms show differential community dynamics and pinpoint taxa involved in communal response. *ISME J.* **9**: 1–11.

Oswald, K., Graf, J.S., Littmann, S., Tienken, D., Brand, A., Wehrli, B., et al. (2017) *Crenothrix* are major methane consumers in stratified lakes. *ISME J.* **11**: 2124–2140.

Oswald, K., Milucka, J., Brand, A., Hach, P., Littmann, S., Wehrli, B., et al. (2016) Aerobic gammaproteobacterial methanotrophs mitigate methane emissions from oxic and anoxic lake waters. *Limnol. Oceanogr.* **61**: S101–S118.

Oswald, K., Milucka, J., Brand, A., Littmann, S., Wehrli, B., Kuypers, M.M.M., and Schubert, C.J. (2015) Light-dependent aerobic methane oxidation reduces methane emissions from seasonally stratified lakes. *PLoS One* **10**: e0132574.

Parks, D.H., Imelfort, M., Skennerton, C.T., Hugenholtz, P., and Tyson, G.W. (2015) CheckM : assessing the quality of microbial genomes recovered from isolates, single cells, and metagenomes. *Genome Res.* **25**: 1043–1055.

Quast, C., Pruesse, E., Yilmaz, P., Gerken, J., Schweer, T., Yarza, P., et al. (2013) The SILVA ribosomal RNA gene database project: improved data processing and web-based tools. *Nucleic Acids Res.* **41**: D590-6.

Raghoebarsing, A.A., Pol, A., van de Pas-Schoonen, K.T., Smolders, A.J., Ettwig, K.F., Rijpstra, W.I., et al. (2006) A microbial consortium couples anaerobic methane oxidation to denitrification. *Nature* **440**: 918–921.

Reeburgh, W.S. (2007) Oceanic methane biogeochemistry. *Chem. Rev.* **107**: 486–513.

Reed, D.C., Deemer, B.R., van Grinsven, S., and Harrison, J.A. (2017) Are elusive anaerobic pathways key methane sinks in eutrophic lakes and reservoirs? *Biogeochemistry* **134**: 29–39.

Rissanen, A.J., Saarenheimo, J., Tiirola, M., Peura, S., Aalto, S.L., Karvinen, A., and Nykänen, H. (2018) Gammaproteobacterial methanotrophs dominate methanotrophy in aerobic and anaerobic layers of boreal lake waters. *Aquat. Microb. Ecol.* **81**: 257–276.

Roslev, P. and King, G.M. (1995) Aerobic and anaerobic starvation metabolism in methanotrophic bacteria. *Appl. Environ. Microbiol.* **61**: 1563–1570.

Rudd, J.W., Furutani, A., Flett, R.J., & Hamilton, R.D. (1976). Factors controlling methane oxidation in shield lakes: The role of nitrogen fixation and oxygen concentration 1. Limnology and Oceanography, **21(3)**: 357-364.

Saito, T., Ishii, S., Otsuka, S., Nishiyama, M., and Senoo, K. (2008) Identification of novel betaproteobacteria in a succinate-assimilating population in denitrifying rice paddy soil by using stable isotope probing. *Microbes Environ.* **23**: 192–200.

Scheller, S., Yu, H., Chadwick, G.L., and Mcglynn, S.E. (2016) Artificial electron acceptors decouple archaeal methane oxidation from sulfate reduction. *Science* **351**: 1754–1756.

Schubert, C.J., Lucas, F.S., Durisch-Kaiser, E., Stierli, R., Diem, T., Scheidegger, O., et al. (2010) Oxidation and emission of methane in a monomictic lake (Rotsee, Switzerland). *Aquat. Sci.* **72**: 455–466.

Schubert, C.J., Vazquez, F., Lösekann-Behrens, T., Knittel, K., Tonolla, M., and Boetius, A. (2011) Evidence for anaerobic oxidation of methane in sediments of a freshwater system (Lago di Cadagno). *FEMS Microbiol. Ecol.* **76**: 26–38.

Seemann, T. (2014) Prokka: Rapid prokaryotic genome annotation. *Bioinformatics* **30**: 2068–2069.

Smith, G.J., Angle, J.C., Solden, L.M., Daly, R.A., Johnston, M.D., Borton, M.A., et al. (2018) Members of the genus *Methylobacter* are inferred to account for the majority of aerobic methane oxidation in oxic soils from a freshwater wetland. *MBio* **9**: 1–17.

Stoecker, K., Bendinger, B., Schöning, B., Nielsen, P.H., Nielsen, J.L., Baranyi, C., et al. (2006) Cohn's *Crenothrix* is a filamentous methane oxidizer with an unusual methane monooxygenase. *Proc. Natl. Acad. Sci.* **103**: 2363–2367.

Svenning, M.M., Hestnes, A.G., Wartiainen, I., Stein, L.Y., Klotz, M.G., Kalyuzhnaya, M.G., et al. (2011) Genome sequence of the arctic methanotroph *Methylobacter tundripaludum* SV96. *J. Bacteriol.* **193**: 6418–6419.

Tamura, K., Stecher, G., Peterson, D., Filipski, A., and Kumar, S. (2013) MEGA6: Molecular evolutionary genetics analysis version 6.0. *Mol. Biol. Evol.* **30**: 2725–2729.

Tavormina, P.L., Orphan, V.J., Kalyuzhnaya, M.G., Jetten, M.S.M., and Klotz, M.G. (2011) A novel family of functional operons encoding methane/ammonia monooxygenase-related proteins in gammaproteobacterial methanotrophs. *Environ. Microbiol. Rep.* **3**: 91–100.

Thottathil, S.D., Reis, P.C.J., and Prairie, Y.T. (2019) Methane oxidation kinetics in northern freshwater lakes. *Biogeochemistry* **143**: 105-116.

Valenzuela, E.I., Avendaño, K.A., Balagurusamy, N., Arriaga, S., Nieto-Delgado, C., Thalasso, F., and Cervantes, F.J. (2019) Electron shuttling mediated by humic substances fuels anaerobic methane oxidation and carbon burial in wetland sediments. *Sci. Total Environ.* **650**: 2674–2684.

Vigliotta, G., Nutricati, E., Carata, E., Tredici, S.M., De Stefano, M., Pontieri, P., et al. (2007) *Clonothrix fusca* Roze 1896, a filamentous, sheathed, methanotrophic -proteobacterium. *Appl. Environ. Microbiol.* **73**: 3556–3565.

Villada, J.C., Duran, M.F., & Lee, P.K. (2019). The unique coding sequence of pmoCAB operon from type Ia methanotrophs simultaneously optimizes transcription and translation. bioRxiv, 543546.

Yu, Z. and Chistoserdova, L. (2017) Communal metabolism of methane and the rare earth element switch. *J. Bacteriol.* **199**: e00328-17.

Yuan, C., Lei, J., Cole, J., and Sun, Y. (2015) Reconstructing 16S rRNA genes in metagenomic data. *Bioinformatics* **31**: i35-i43.

Zhang, J., Kobert, K., Flouri, T., and Stamatakis, A. (2014) PEAR: A fast and accurate Illumina Paired-End reAd mergeR. *Bioinformatics* **30**: 614–620.

Zigah, P.K., Oswald, K., Brand, A., Dinkel, C., Wehrli, B., and Schubert, C.J. (2015) Methane oxidation pathways and associated methanotrophic communities in the water column of a tropical lake. **60**: 553-572.

Chapter 4. Impact of electron acceptor availability on methane-influenced microorganisms in an enrichment culture obtained from a stratified lake

Sigrid van Grinsven
Jaap S. Sinninghe Damsté
John Harrison
& Laura Villanueva

Published in Frontiers in Microbiology, 2020

Abstract

Methanotrophs are of major importance in limiting methane emissions from lakes. They are known to preferably inhabit the oxycline of stratified water columns, often assumed due to an intolerance to atmospheric oxygen concentrations, but little is known on the response of methanotrophs to different oxygen concentrations, as well as their preference for different electron acceptors. In this study, we enriched a methanotroph of the *Methylobacter* genus from the oxycline and the anoxic water column of a stratified lake, that was also present in the oxic water column in winter. We tested the response of this *Methylobacter*-dominated enrichment culture to different electron acceptors, i.e. oxygen, nitrate, sulfate and humic substances, and found that in contrast to earlier results with water column incubations, oxygen was the preferred electron acceptor, leading to methane oxidation rates of 45 - 72 pmol cell^{-1} day^{-1}.
Despite the general assumption of methanotrophs preferring microaerobic conditions, methane oxidation was most efficient under high oxygen concentrations (>600 µM). Low (<30 µM) oxygen concentrations still supported methane oxidation, but no methane oxidation was observed with trace oxygen concentrations (<9 µM) or under anoxic conditions. Remarkably, the presence of nitrate stimulated methane oxidation rates under oxic conditions, raising the methane oxidation rates by 50% when compared to oxic incubations with ammonium. Under anoxic conditions no net methane consumption was observed, however, methanotroph abundances were 2-3 times higher in incubations with nitrate and sulfate compared to anoxic incubations with ammonium as N-source. Metagenomic sequencing revealed the absence of a complete denitrification pathway in the dominant methanotroph *Methylobacter*, but the most abundant methylotroph *Methylotenera* seemed capable of denitrification, which can possibly play a role in the enhanced methane oxidation rates under nitrate-rich conditions.

Introduction

Methane is the second-most important greenhouse gas on earth and a direct reduction in methane emissions is needed to keep global temperatures below the goal of 1.5 °C above pre-industrial level (Rogelj *et al.*, 2018). Methanotrophy, the microbial conversion of methane to carbon dioxide, is a key process in limiting methane emissions from aquatic systems. Segarra et al. (2015) estimated the decrease in freshwater wetland emissions by methane oxidation to be up to 50 %, while Martinez-Cruz et al. (2018) estimated up to 34% of produced methane in lake sediments is consumed by methanotrophy. In marine systems, anaerobic oxidation of methane (AOM) is estimated to reduce methane emissions by 90 % (Knittel and Boetius, 2009). A consortium of anaerobic methane oxidizing archaea (ANME) and sulfate reducing bacteria using sulfate as the electron acceptor for methane oxidation is responsible for this process (Boetius *et al.*, 2000). In the water column of freshwater systems, these archaea are rarely detected, likely due to their zero tolerance to oxygen. Many anoxic lakes and reservoirs experience regular or irregular intrusions of oxygen that make these systems less suitable habitats for ANME. Methane oxidizing bacteria (MOB) are often detected in freshwater systems, at the oxic-anoxic interface and more rarely, in the anoxic water column (e.g. Rudd and Hamilton 1975; Harrits and Hanson 1980; Oswald et al. 2016; Milucka et al. 2015; Michaud et al. 2017; Blees et al. 2014; Biderre-Petit et al. 2011). Although most methanotrophs require oxygen to oxidize methane, MOB are often assumed to prefer low-oxygen conditions over oxygen saturation. Several studies suggest an inhibitory effect of atmospheric oxygen concentrations on the methane oxidation rate (Rudd and Hamilton, 1975; Van Bodegom *et al.*, 2001; Danilova *et al.*, 2016; Thottathil *et al.*, 2019). A few species of MOB have been described that could potentially use electron acceptors other than oxygen, such as nitrite (Ettwig *et al.*, 2010) and nitrate (Kits *et al.*, 2015; Oswald *et al.*, 2017; Rissanen *et al.*, 2018). Sulfate has also been suggested as an electron acceptor in freshwater sediments but not in the water column (Schubert *et al.*, 2011). Organic matter and humic substances, which are shown to be able to function as both an electron donor and acceptor (Lovley *et al.*, 1996; Klüpfel *et al.*, 2014; Valenzuela *et al.*, 2019), have been suggested to play a role in AOM in lakes (Saxton *et al.*, 2016; Reed *et al.*, 2017), but have so far only been shown to impact aquatic AOM performed by ANME in marine (Scheller *et al.*, 2016) and tropical wetland systems (Valenzuela et al. 2017, 2019).
Several studies (Murase and Frenzel, 2007; Jones and Grey, 2011; Sanseverino *et al.*, 2012) have shown that methane-derived carbon is an important contributor to aquatic food webs on different scales. Many microbes cannot use methane and therefore depend on the conversion of methane-derived carbon by methanotrophs. Generally, methane-derived carbon is assumed to end up in methanotroph biomass or CO_2, the main reaction product of methane oxidation. However, under oxygen-limited conditions, MOB have been shown to excrete metabolites such as methanol, formaldehyde, formate, acetate and succinate (Xin *et al.*, 2004, 2007; Kalyuzhnaya *et al.*, 2013; Gilman *et al.*, 2017), that can be used by other members of the microbial community.
This study aims to expand the knowledge of how oxygen and other potential terminal electron acceptors affect methanotrophs, especially *Methylobacter*, which occur naturally in oxic, microoxic and anoxic zones of stratified lake water columns. Previously, we showed that *Methylobacter* sp. is an important methanotroph in the seasonally stratified Lake Lacamas and water column incubation experiments revealed that it is capable of methane oxidation

under a variety of conditions (van Grinsven *et al.*, 2020). Here we describe the establishment of an enrichment culture dominated by *Methylobacter*, and used it to evaluate the effects of the concentration of the potential electron acceptor (oxygen, nitrate, sulfate and humic substances) on methane oxidation rates and microbial community structure using 16S rRNA gene amplicon sequencing. Furthermore, the metabolic potential of selected microbial groups stimulated in the enrichment cultures was also determined by a metagenomic sequencing approach.

Material and methods

Sample collection

Suspended particulate matter samples were collected on April 9, 2018 from the center of Lacamas Lake, WA, USA (45.62N, 122.43W). Lacamas Lake is a seasonally stratified, hypereutrophic system with an average depth of 7.8 m and maximum depth of 19.8 m, which is on the Environmental Protection Agency list of impaired and threatened waters. It is monomictic, with stratification occurring yearly in May and a turnover mixing period from October to December. During sampling, the lake was not stratified, as determined using a Hydrolab DS5X sonde (Hach, Loveland, US) with sensors for conductivity, temperature, dissolved oxygen, and pH. At the moment of sampling, the oxygen concentration was >350 µM throughout the water column, the temperature 4 - 8 °C and the methane concentration <1 µM. Water was collected from 12 m depth using a VanDorn sampler, stored in carboys, and transported back to the lab, where it was filtered within 96 h over 47 mm 0.7 µm pore size glass fiber filters. Filters were stored in non-filtered lake water from 12 m depth, and kept at 4 °C until shipment and further processing.

Cultivation

The suspended particulate matter that was collected on the filters was scraped off and transferred under oxic conditions to 20 mL nitrate mineral salts (NMS) medium (Whittenbury *et al.*, 1970), in a 120 ml acid-washed and autoclaved glass pressure bottle with butyl rubber stopper. A flow scheme is shown in Fig. S1. Methane (1 ml, 99.99% pure) was added and the bottle was stored at 15 °C in the dark. Every two weeks, the pressure bottle was opened under oxic conditions, and two ml of cell-containing medium was transferred to 18 ml fresh sterile NMS medium in a sterile 120 ml glass pressure bottle with butyl stopper, after which 1 ml methane was added again. These steps were repeated every two weeks. After 8 weeks, the resulting enrichment culture was studied using Catalyzed reporter deposition Fluorescence In Situ Hybridization (CARD-FISH) with probes MLB482 (targeting *Methylobacter*; Gulledge *et al.*, 2001) and Creno445 (targeting *Crenothrix*; Oswald *et al.*, 2017), following the protocol as described on https://www.arb-silva.de/fish-probes/fish-protocols. The medium was filtered over a 10 µm mesh glass fiber filter (Whatmann) to separate cell clusters from single cells, as illustrated in Fig. S1. The cell material that remained on the filter was scraped off and transferred to a sterile 120 ml bottle with NMS media. The steps described above were repeated for this enrichment culture. The amount of biomass was increased by replicating the subculture in eight 500 - 1000 ml glass bottles. After eight weeks, cells were harvested by centrifugation at 2800 x *g* for 5 min. The supernatant was discarded and all biomass of the

enrichment cultures was combined to create one uniform concentrated enrichment culture in NMS medium. Cell density was not measured. A 20 ml aliquot was used for DNA analysis.

Incubation experiments with the enrichment culture

Two sets of incubation experiments were performed using the methanotroph enrichment culture. A first set of experiments was aimed at the response of *Methylobacter* to the electron acceptors nitrate (in the presence and absence of oxygen), sulfate and humic substances and is referred to as the "electron acceptor experiments". The second set of experiments, referred to as the "O_2-concentration experiment" was set-up to study the response of *Methylobacter* sp. to different oxygen concentrations. An overview of the experimental setup of these two experiments is provided in Table S1.

All experiments were performed in triplicate. "Electron acceptor experiments" were performed in 260 ml acid-washed and autoclaved glass bottles with butyl rubber stoppers with a total volume of 210 ml media. "O_2-concentration experiments" were performed in 120 ml bottles containing 70 ml media. The media of the "anoxic incubation" bottles and all bottles of the "O_2-concentration experiment" were prepared using boiled ultrapure water, to minimize the initial oxygen concentration of the media. Each incubation bottle was inoculated with the same amount of concentrated enrichment culture. All media in the anoxic bottles was bubbled with nitrogen for 20 min to remove residual oxygen, after which the bottles were closed, crimp sealed, and the headspace was flushed and exchanged with N_2 gas using a GRInstruments (Wijk bij Duurstede, the Netherlands) automatic gas exchanger. Abiotic controls were set up identically to the bottles for the anoxic experiments, but were not inoculated with the concentrated enrichment culture. This resulted in a lower liquid volume and, therefore, in a methane concentration ±120 µM lower than in the anoxic incubations.

All bottles were supplemented with 2.6 ml 100% methane (Sigma-Aldrich), shaken vigorously for 1 min to establish equilibrium between the gas and water phase, and the methane concentration in the gas phase was subsequently measured by gas chromatography with flame ionization detection (GC-FID, Thermo Scientific Focus GC). The bottles were subsequently incubated at 15 °C in the dark. Bottles were shaken at sampling moments.

Electron acceptor incubation experiments

"Electron acceptor incubations" lasted three days for the oxic experiments, and 33 days for anoxic incubation experiments. Incubation experiments with nitrate (i.e. oxic and anoxic nitrate incubations) were performed with the same NMS medium that was used for cultivation, as described above, containing nitrate as only nitrogen source (Whittenbury *et al.*, 1970). Control, sulfate-supplemented and humic-supplemented incubations of the "electron acceptor experiments" were performed with an AMS medium, containing ammonium rather than nitrate as nitrogen source (1 g l^{-1} KNO_3 was replaced with 0.5 g l^{-1} NH_4Cl, as described by (Whittenbury *et al.*, 1970). As the enrichment culture used for inoculation was in NMS media, relatively small amounts of nitrate were introduced in the control, sulfate-supplemented and humic-supplemented incubations experiments. Anoxic nitrate-supplemented bottles of the "electron acceptor experiment" were amended with 0.3 g additional KNO_3 (in addition to the KNO_3 that was present in the NMS media). To the sulfate-supplemented bottles, 0.35 g Na_2SO_4 was added (target concentration 0.012 M). The humic substances-supplemented bottles contained 1 g of commercially available humic acids mixture (Sigma-Aldrich).

Methane concentrations in the headspace were measured by extracting 50 µl gas using a gas-tight syringe, daily during the first four days and irregularly after this initial phase. All methane analyses using a GC-FID were performed in triplicate. Methane oxidation rates were determined using linear regression analysis (Microsoft Excel version 16.16.10).
Upon termination of the experiment, all bottles were sampled for DNA by filtering the contents of the individual bottles over individual 47 mm 0.2 µm pore size polycarbonate filters. All samples were stored at -80 °C until DNA was extracted by using the RNeasy Powersoil Total RNA extraction + DNA elution kits. DNA extracts were kept at -80 °C until further processing.

O_2-concentration experiments
All experiments were performed with the NMS medium, and the same concentrated culture used to inoculate the "electron acceptor experiments", although 3 weeks were in between the start of the "electron acceptor experiments" and "O_2-concentration experiments". All bottles of the "O_2-concentration experiments" were setup as anoxic bottles, and left for 2 days after setup, after which bottles were randomly divided into 4 groups, of which 3 received air injections. Bottles for the anoxic experiment received no injection, 'trace oxygen' bottles received 20 µl air ([O_2] 7.5-9 µM), 'microoxic' bottles received 160 µl air ([O_2] 23-30 µM), and 'saturated oxygen' bottles received 5000 µl air ([O_2] ±600 µM). The methane concentration in all bottles was measured on day 3 and 5, after which the "saturated oxygen" incubations were terminated. The "microoxic" and "trace oxygen" bottes received another air injection on day 6 and day 13, identical to the volume of the first injections. On day 14, all incubations were terminated. DNA was sampled following the same procedure as described above, but extraction was done with the RNeasy Powersoil DNA extraction kit, after which the DNA extracts were kept at -80 °C until further processing.

16S rRNA gene analysis
The general 16S rRNA archaeal and bacteria primer pair 515F and 806RB targeting the V4 region (Caporaso *et al.*, 2012) was used for the 16S rRNA gene amplicon sequencing and analysis, as described in Besseling *et al.*, (2018) with a melting temperature of 56°C. PCR products were gel purified using the QIAquick Gel-Purification kit (Qiagen), pooled and diluted. Sequencing was performed by the Utrecht Sequencing Facility (Utrecht, the Netherlands), using an Illumina MiSeq sequencing platform (Caporaso *et al.*, 2010). The 16S rRNA gene amplicon sequences were analyzed by the Cascabel pipeline (Asbun *et al.*, 2019) including quality assessment by FastQC (Andrews *et al.*, 2015), assembly of the paired-end reads with Pear (Zhang *et al.*, 2014), library demultiplexing, OTU clustering and representative sequence selection ('longest' method) by diverse Qiime scripts (Caporaso *et al.*, 2010). The OTU clustering algorithm was uclust (Edgar, 2010) with an identity threshold of 97% and assign taxonomy with BLAST (Altschul *et al.*, 1990) by using the Silva 128 release as reference database (https://www.arb-silva.de/;Quast *et al.*, 2013). To compare the *Methylobacter* OTUs, we focused on OTUs with relative abundances >0.4% of the total 16S rRNA gene reads.
16S rRNA gene copies were quantified using quantitative PCR (qPCR) with the same primer pair as used for amplicon sequencing (515F, 806RB). The qPCR reaction mixture (25 µl) contained 1 U of Pico Maxx high fidelity DNA polymerase (Stratagene, Agilent Technologies, Santa Clara, CA) 2.5 µl of 10x Pico Maxx PCR buffer, 2.5 µl 2.5 mM of each dNTP, 0.5 µl BSA (20 mg ml^{-1}), 0.02 pmol $µl^{-1}$ of primers, 10,000 times diluted SYBR Green® (Invitrogen) (optimized

concentration), 0.5 µl of $MgCl_2$ (50 mM) and ultrapure sterile water. The cycling conditions for the qPCR reaction were the following: initial denaturation 98 °C for 30 s, 45 cycles of 98 °C for 10 s, 56 °C for 20 s, followed by a plate read, 72 °C for 30 s, and 80 °C for 25 s. Specificity of the reaction was tested with a gradient melting temperature assay from 55 °C to 95 °C with 0.5 °C increments of 5 s. The qPCR reactions were performed in triplicate with standard curves encompassing a range from 10^3 to 10^7 molecules μl^{-1}. qPCR efficiency for the 16S rRNA gene quantification was 103.7% with R^2=0.980. For quantification of microbial groups, we make the simplifying assumption that all microorganisms of the microbial community in Lacamas Lake contained a single 16S rRNA gene copy in their genome.

Representative sequences were extracted from the dataset and compared with closely related sequences by performing a phylogenetic analysis by using the maximum likelihood method and the General Time Reversible model in MEGA6 (Tamura *et al.*, 2013). Additionally, the phylogenetic placement of the MAG LL-enrich-bin26 (Table S2) attributed to the *Methylobacter* genus was further assessed and compared to the MAG bin-63 of the *Methylobacter* clade 2 reported in van Grinsven et al. (2019) by using Phylosift (v. 1.0.1, Darling et al. (2014)) based on 34 marker genes as described in van Grinsven et al., 2019. The 16S rRNA amplicon reads (raw data) have been deposited in the NCBI Sequence Read Archive (SRA) under BioProject number PRJNA598329, BioSamples SAMN13712582-SAMN13712612.

Metagenome analysis

The sample that was selected for metagenomic sequencing originated from the 10 µm filtrate, (Fig. S1). DNA was extracted as described above and used to prepare a TruSeq DNA nano library which was further sequenced with Illumina MiSeq 2×300 bp generating over 46 million 2×300 bp paired-end reads. Data was analyzed with an in-house pipeline as described in van Grinsven et al. (2019). The binning of MAGs was performed with DAS Tool with penalty for duplicate marker genes and megabin penalty of 0.3. Quality of the metagenome-assembled genomes (MAGs) was assessed using CheckM v1.0.7 running the lineage-specific workflow (Parks *et al.*, 2015). MAGs were annotated with Prokka v1.12 (Seemann, 2014) and by the Rapid annotation using subsystem technology (RAST) pipeline v2.0 (Aziz *et al.*, 2008). The annotation of key metabolic pathways was refined manually. In order to classify the MAGs according to their relative abundance in the sequenced sample, MetaBAT was run again by using the abundance estimation (total average depth, average abundance or also called average coverage of each contig included in the bin) generated by MetaSPAdes and checked again with CheckM as included in Table S2. The completeness and redundancy of the MAG bins was assessed by the DAS_Tool Package (Sieber *et al.*, 2018). The taxonomic classification of the MAGs of interest was determined by using GTDB-Tk (v0.3.2; http://gtdb.ecogenomic.org) (Table S2). The metagenome of the sample specified in Table S3 is available in NCBI under BioProject number PRJNA598329, BioSample SAMN13712974. The sequence raw data of the MAGs LL-enrich-bin-26, and bin-28 are deposited in NCBI under BioSample numbers SAMN13735002 and SAMN13735003, respectively.

Results

The most abundant methanotroph of Lacamas Lake, a seasonally stratified lake, is a *Methylobacter* species; it was detected in the oxic water column in winter, and in the microoxic oxycline and the anoxic hypolimnion in the summer (van Grinsven *et al.*, 2020). In order to be able to further study the response of this methanotroph to different concentrations of oxygen and other electron acceptors, an enrichment culture was established.

Enrichment culture microbial community

The enrichment culture was dominated by gene sequences attributed to *Methylobacter* clade 2 (43 %; Fig. 1;Smith *et al.*, 2018)), accompanied by 2.8 % of *Methylomonas* sp. and 0.1 % other methanotrophs, all part of the order Methylococcales (Table 1). The *Methylobacter* OTUs with the highest relative abundances were LLE-16S-2, 7, 8, 10 and 12 (Table S4). These OTUs form a phylogenetic subcluster of closely related sequences (i.e. 96-99% similarity; Supplementary File 1) in the *Methylobacter* clade 2 cluster (i.e. the Lacamas Lake OTU cluster; Fig. 1B) together with the detected sequences in the Lacamas Lake water column (i.e. LL-16S-number). The most closely related cultured species was *Methylobacter tundripaludum* (Fig. 1A).

Apart from *Methylobacter* sp., also bacteria of the genus *Methylotenera* were highly abundant in the enrichment culture. They represent 21% of the total 16S rRNA gene copies (Table 1). Detected OTUs classified as *Methylotenera* clustered with two uncultured bacterium clones; the most closely related cultured species was *Methylotenera versatilis* (Fig. 2). Bacteria of the genus *Flavobacterium* were also relatively abundant in the enrichment culture (5.5 %; Table 2), as well as members of the order *Burkholderiales* (8.3 %; Table 2).

Metabolic potential of the main microbial components of the enrichment culture

In order to characterize the metabolic potential of the main microbial components of the enrichment culture, we performed metagenomic sequencing of a sample derived from the 10 µm filtrate (see Fig. S1). *Methylobacter* sp. were less abundant than in the enrichment (i.e. 22 vs 43% the total 16S rRNA gene reads). However, the distribution of the OTUs attributed to *Methylobacter* spp. in this sequenced sample was similar to that reported in the enrichment culture (Table S4). High relative abundances of *Methylotenera* (i.e. 24%) and *Methylomonas* (17%) were also evident (Table S3).

Metagenome sequencing resulted in three most abundant MAG bins affiliated to the methanotrophs *Methylobacter* sp. (i.e. LLE-enrich-bin26), *Methylomonas* sp. (i.e. LLE-enrich-bin27), and to the methylotroph *Methylotenera* sp. (i.e. LLE-enrich-bin28) (Table S2). Here, we focus on the metabolic characterization of the MAG bins affiliated to *Methylobacter* and *Methylotenera* due to their higher relative abundance in the enrichment culture (Table 1), specifically of the genetic potential of the nitrogen and methane and carbon metabolism. The MAG bin LLE-enrich-26 is taxonomically classified as a *Methylobacter* sp and harbors all the genes encoding for the particulate methane monooxygenase (pMMO; see Supplementary File 2) allowing for the conversion from methane to methanol, while the *Methylotenera* MAG LLE-enrich-bin28 lacks this gene (Supplementary File 3; Fig. 3). The genes required for the further conversion from methanol to CO_2 are present in both MAGs (see Fig. 3).

Table 1. Relative abundance of 16S rRNA gene reads (% of total) attributed to methylotrophs, and 16S rRNA copies per L^{-1} in the sample as determined using quantitative PCR.

	Culture			"Electron acceptor experiment"					"O_2-concentration experiment"			
	Starting lake water	Enrichment culture	Control, oxic	Nitrate, oxic	Control, anoxic	Nitrate, anoxic	Sulfate, anoxic	Humics, anoxic	Saturated	Micro-oxic	Trace	Anoxic
Methylobacter spp. (%)	0.6	43	44	38	11	25	19	1.6	23	21	19	20
Methylomonas spp. (%)	0.2	2.8	4.6	6.6	0.4	4.8	1.2	0.3	1.4	1.9	2	1.9
Other Methylo-coccales (%)	0.02	0.1	0.5	0.5	0.3	0.5	0.4	0.2	0.2	0.3	0.3	0.2
Methylotenera spp. (%)	1	21	15	22	13	17	14	14	12	11	13	11
Total 16S rRNA copies per L^{-1}, x 10^7	n.d.	n.d.	1.8	1.5	2.5	1.8	1.8	1.3	1.9	2.1	1.5	1.6
Methanotroph cells per L^{-1} [a], x 10^6	n.d.	n.d.	4.3	3.3	1.5	2.6	1.9	0.1	2.3	2.4	1.6	1.7

[a] Calculated with assuming 2 copies of the 16s rRNA gene per *Methylobacter* cell, 3 copies per *Methylomonas* cell, and 1 copy per 'other Methylococcales' cell.
n.d. not determined

Table 2. Relative abundance of 16S rRNA gene reads (% of total) of other microbial groups discussed in the manuscript.

	Culture			"Electron acceptor experiment"					"O_2-concentration experiment"			
	Starting lake water	Enrichment culture	Control oxic	Nitrate oxic	Control anoxic	Nitrate anoxic	Sulfate anoxic	Humics anoxic	Saturated	Micro-oxic	Trace	Anoxic
Brevundimonas	0.1	0.5	0.6	0.5	15	3.2	10	1.3	2.2	3.2	3.1	3.5
Burkholderiaceae	15	8.3	12	6	11	11	10	30	9.5	10	10	10
Flavobacterium	1.5	5.5	4	5.4	18	10	16	16	12	14	16	14
Pseudomonas	0.2	0.1	0.3	0.2	3	2	1.3	5.9	0.5	1.1	1	0.9
Rhodocyclaceae	0.8	0.2	0.4	0.4	1.9	0.9	1.9	2.1	0.9	1.8	1.8	1.8
Sulfuritalea	0.4	0.2	0.2	0.2	1.0[a]	0.5	1.3	0.9	0.2	0.5	0.5	0.6

[a] High standard deviation between triplicate incubations of 0.45%

Regarding the nitrogen metabolism pathways, both the *Methylobacter* and *Methylotenera* LLE-enrich-bin26 and 28 MAGs harbor the genes encoding for nitrate transporters, assimilatory nitrate reductase (*Nas*), nitrite reductase (*NirBD*) to ammonia, and to nitric oxide (*NirK*), as well as the gene coding for the nitric oxide reductase (*NorBC*) to nitrous oxide (N_2O), but not the genes coding for the nitrous oxide reductase (*NorZ*) to dinitrogen gas (Fig. 3).

Methane consumption and change in microbial community composition in incubation experiments with different electron acceptors

Two sets of incubation experiments were performed using the methanotroph enrichment culture obtained. A first set of experiments was aimed at the response of *Methylobacter* sp. to the electron acceptors nitrate (in the presence and absence of oxygen), sulfate and humic substances. In all oxic experiments, methane was consumed rapidly (Fig. 4). The experiments were terminated within 2–3 days in anticipation of methane depletion. The net methane consumption rate of the incubation with nitrate was higher than the control incubation with ammonium (310 and 200 µmol L^{-1} day^{-1}, respectively). We estimated that the total number of methanotrophic bacteria in the oxic incubations was $3.3 \times 10^6 - 4.3 \times 10^6$ cells per L^{-1} (Table 1).

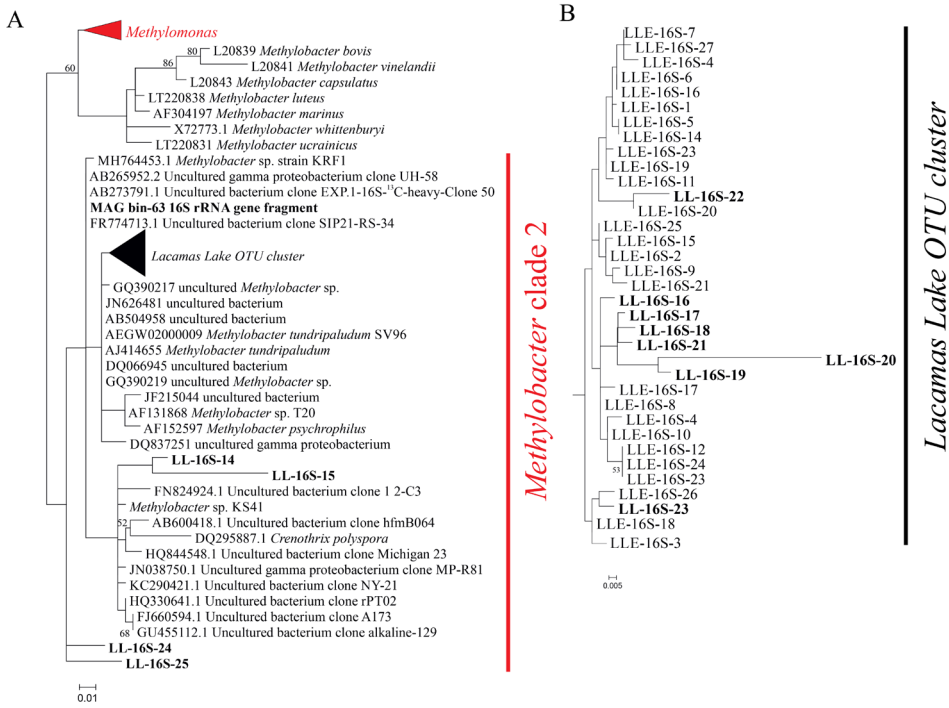

Fig. 1. A) Phylogenetic 16S rRNA gene tree in which the representative sequences of the methanotrophic groups detected in the 16S rRNA gene amplicon sequencing analysis *(i.e Methylomonas* and *Methylobacter)* of the incubation experiments are indicated in red. B) Zoom in on the Lake Lacamas *Methylobacter* cluster as defined in the text. LL-16S-number sequences in bold represent OTU sequences previously detected in Lacamas Lake water column and water column incubations as described in van Grinsven et al. (2019). LLE-

16S-number sequences correspond to the *Methylobacter* OTU sequences detected in this study and are listed in Table S4. The MAG bin-63 16S rRNA gene sequence corresponds to the 16S rRNA sequence of the most abundant MAG bin in a water column incubation experiment sample which taxonomically assigned to *Methylobacter*, as described in van Grinsven et al. (2019).The phylogenetic analysis was restricted to the sequence fragment (approximately 290 bp) obtained with the 16S rRNA amplicon sequencing analysis. Maximum likelihood estimation was performed using the General Time Reversible model.

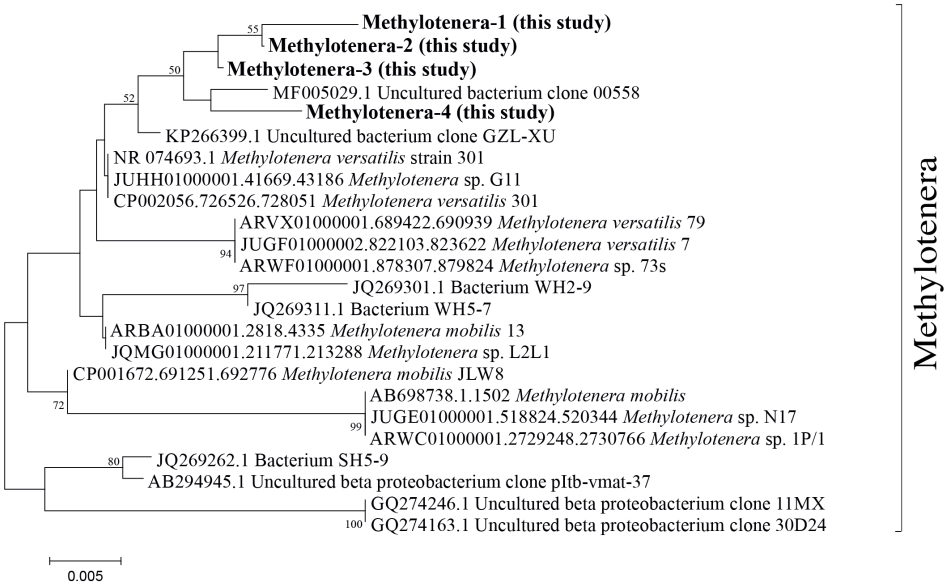

Fig. 2. Phylogenetic 16S rRNA gene tree with representative sequences of the OTUs classified as *Methylotenera* indicated in bold. The phylogenetic analysis was restricted to the sequence fragment (approximately 290 bp) obtained with the 16S rRNA amplicon sequencing analysis. Maximum likelihood estimation was performed using the General Time Reversible model.

The methane turnover rate per cell is, therefore, estimated to be 45 and 72 pmol cell^{-1} day^{-1} for the control and nitrate-amended oxic incubations. No net methane consumption could be detected under anoxic conditions, even with the addition of the alternative electron acceptors, nitrate, sulfate, or humic substances (Fig. 4). Nitrate concentration measurements showed no clear difference between nitrate concentrations at the start and the end of the experiment (Fig. S2), mainly due to large variations between the samples and the high starting concentrations. The relative abundance of *Methylobacter* sp. was significantly higher ($p < 0.05$; Table S5) in the two oxic incubations of the "electron acceptor experiment" when compared to the anoxic incubations. The *Methylobacter* abundance in the oxic incubations (43 % and 38 % for control and nitrate-supplemented, respectively; Table 1) was not significantly different due to substantial variation between replicates. The addition of different electron acceptors in the anoxic incubations changed the microbial community (Table 1 and 3). The addition of nitrate or sulfate resulted into a significantly ($p < 0.05$; Table S5) higher *Methylobacter* abundance (25 and

18 %, respectively; Table 1) compared to the anoxic control (11 %; Table 1). *Methylobacter* OTUs LLE-16S-2 and 7 were the most abundant in the oxic incubations, similarly to the enrichment culture (Table S4). LLE-16S-12, which was highly abundant in the enrichment culture, became less dominant in the incubations. Similar to the oxic incubations, LLE-16S-2 and 7 were the most abundant *Methylobacter* OTUs in the anoxic control and nitrate incubations, with in addition a relatively high abundance of LLE-16S-9 (Table S4). Sequences closely related to *Methylotenera* (Fig. 2) remained relatively abundant in all incubation experiments (14 – 29 %; Table 1). Bacteria of the genera *Flavobacterium*, *Brevundimonas* and *Pseudomonas* had a higher relative abundance in anoxic than in oxic incubations, both with and without nitrate, although *Brevundimonas* was more abundant in anoxic incubations without nitrate (Table 2). *Brevundimonas* comprised 15 % and 3 % of the total microbial abundance in anoxic control and nitrate-supplemented incubations, respectively. The genus *Sulfuritalea* was more abundant in the anoxic sulfate incubations (1.3 %) than in nitrate incubations (0.5 %; Table 2). The microbial community composition of the incubation with added humic substances was completely different compared to the other anoxic incubations (Table 1 and 3), with a remarkably high relative abundance of bacteria of the order *Burkholderiales* and the family *Comamonadaccea* (31 % and 16%, respectively). The relative abundance of total archaeal 16S rRNA gene sequences was below 0.5 % in all incubations.

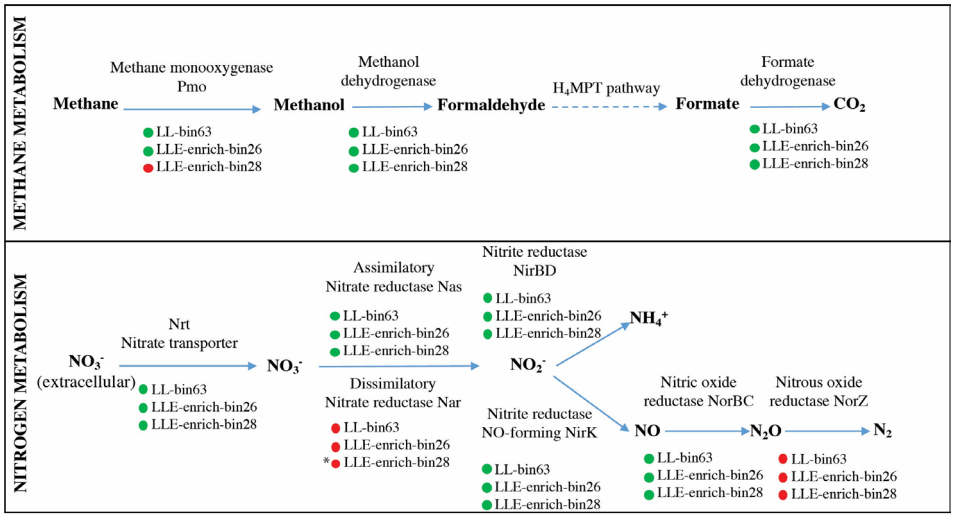

Fig. 3. Description of the genes present in the *Methylobacter* LLE-enrich-bin26 and *Methylotenera* LLE-enrich-bin28 regarding their methane and nitrogen metabolic pathways, and comparison with the *Methylobacter* MAG LL-bin63 previously obtained from incubations with Lacamas Lake water samples (van Grinsven et al., 2019). Green and red circles indicate presence/absence of the coding gene. * *Methylotenera* LLE-enrich-bin28 may have the potential to perform dissimilatory nitrate reduction in the absence of the *Nar* gene, as explained in the text.

Microbial community composition and methane consumption in incubation experiments with different oxygen concentrations

A second set of incubations experiments performed with the *Methylobacter* sp. enrichment culture was aimed at the response of *Methylobacter* sp. to different oxygen conditions. We incubated the enrichment culture under saturated ([O_2] >600 µM), microoxic ([O_2] 23–30 µM), trace oxygen ([O_2] 7.5–9 µM) and anoxic conditions.

Methane consumption rates were two orders of magnitude higher under oxygen saturation condition than under microoxic conditions (520 and 6.4 µM day^{-1} respectively). Under trace oxygen and anoxic conditions, no methane consumption was observed (Fig. 4B). Based on the measured concentrations of methane and estimated concentrations of oxygen in the vials, a ratio of methane and oxygen consumption was calculated. The oxygen concentration in the saturated oxygen incubations (±640 mM) was, assuming methanotrophy was the only process consuming oxygen, present in surplus, and thus sufficient for a 2:1 molar ratio of oxygen:methane usage. In the microoxic incubation bottles, between 6 and 8 µmol of methane was consumed over the whole duration of the experiment. The amount of oxygen present in the microoxic incubations was estimated, based on oxygen measurements and injected air volume, to be maximum 7.1 µmol, allowing for a maximum ratio of 1:1 in the oxygen:methane usage.

The relative abundance of 16S rRNA gene sequences attributed to *Methylobacter* was highest in the incubation under saturated oxygen conditions (23 %; Table 1), but the absolute abundance of all methanotrophs (including *Methylotenera*, *Methylomonas*, *Methylotenera* or other Methylococcales) was not significantly different between the oxic, microoxic, trace and anoxic experiments ($1.6-2.3 \times 10^6$ cells L^{-1}; Table 1). Overall, the communities of the microoxic, suboxic and anoxic incubations were similar, whereas the community under saturated oxygen conditions was significantly different, with lower relative abundances of all non-methanotrophic species as listed in Table 2.

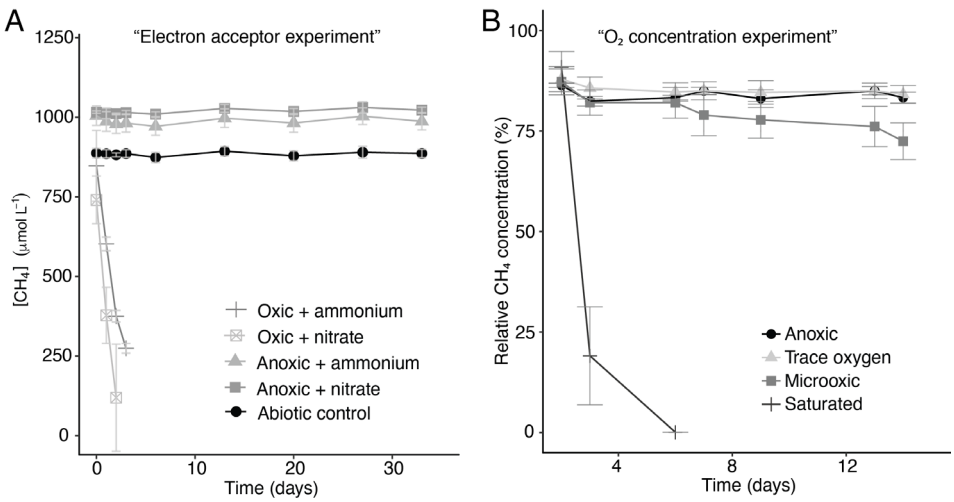

Fig. 4. Methane concentration over time during the incubation experiments with different electron acceptors (A) and methane concentration in incubation experiments with different oxygen

concentrations normalized to the concentration at t_0 (t_0 = 100%) (B). Error bars represent the standard error of triplicate incubations. The methane concentration over time of the incubations to which sulfate and humic substances were added is not shown but was very similar to the ammonium and nitrate-supplemented anoxic incubations.

Discussion

Lacamas Lake, the source of the material used for our enrichment culture, contained uncultured *Methylobacter* species thriving in the oxic and anoxic water column as well as in the microoxic oxycline (van Grinsven *et al.*, 2019). Incubations with water column samples revealed that these bacteria oxidized large amounts of methane (72 μM day^{-1}) under anoxic conditions in the stratified summer water column, stimulated by the addition of both nitrate and sulfate (van Grinsven *et al.*, 2019), but were also naturally present in the oxic, methane-depleted winter water column. Phylogenetic analysis showed that the *Methylobacter* species of the Lacamas Lake summer and winter water column and incubations grouped closely together with the *Methylobacter* species that dominated the enrichment culture (i.e. 96-99% similarity; Fig. 1). *Methylobacter* and related methanotrophs have been previously detected in lakes, mostly under microoxic conditions (± 60 M, Rudd and Hamilton, 1975; Harrits and Hanson, 1980; Oswald *et al.*, 2016; Michaud *et al.*, 2017), but also in anoxic environments, such as sediments or anoxic lake waters (Biderre-Petit *et al.*, 2011; Milucka *et al.*, 2015; Martinez-Cruz *et al.*, 2017). Although most bacteria falling in the *Methylobacter* group are known as aerobic methanotrophs, it has recently been suggested that specific species contain the genomic potential to perform anaerobic methane oxidation, or methane oxidation under strong oxygen limitation, by coupling methane oxidation to nitrate reduction (Svenning *et al.*, 2011; Smith *et al.*, 2018) or by using a fermentation pathway (van Grinsven *et al.*, 2019). Knowledge on the effect of other electron acceptors (i.e. sulfate, humic substance) on *Methylobacter* is, however, lacking, and often the biochemical pathways involved in methanotrophy under anoxic conditions remain unclear (Biderre-Petit *et al.*, 2011; Blees *et al.*, 2014; Martinez-Cruz *et al.*, 2017; Reed *et al.*, 2017). Despite the increase in methane oxidation rates (from 9 to 72 mM day^{-1}) that was observed in anoxic Lacamas Lake incubations with the addition of nitrate, the genome of the dominant *Methylobacter* species did not encode all the genes required to perform denitrification, and its mechanisms for anaerobic methane oxidation therefore remained unclear (van Grinsven *et al.*, 2019).

In the current study, we aimed to determine the preference of the *Methylobacter* species, and other methanotrophs present in Lacamas Lake, for oxygen concentrations and electron acceptors other than oxygen, such as nitrate, by means of laboratory incubations with an enrichment culture.

Methylobacter in water column and enrichment culture incubations

The *Methylobacter* OTU sequences detected in the enrichment culture obtained from Lacamas Lake were closely related to the sequences previously detected both in Lacamas Lake water column and incubation studies with lake water samples, as was confirmed by the 16S rRNA gene phylogeny (Fig. 1). In addition, the *Methylobacter* MAG bin obtained from the enrichment culture (i.e. LLE-enrich-bin26) was also closely related to the *Methylobacter* MAG previously

obtained in an incubation with Lacamas Lake water (i.e. LL-bin63; van Grinsven et al., 2019, see Fig. S3). Therefore, we conclude that the *Methylobacter* species obtained in the enrichment culture in this study is representative of those existing in Lacamas Lake and can thus be used to draw conclusions on their electron acceptor and oxygen preferences, which can be extrapolated to the conditions in the original system. Both the two *Methylobacter* MAGs coincided in their genetic potential to oxidize methane, perform mixed-acid fermentation from pyruvate to succinate and H_2 (Fig. S4), as well as in harboring an incomplete denitrification pathway (Fig. 3). Several methanotrophs contain parts of the denitrification pathway, but only few species have been shown to couple methane oxidation to denitrification (Smith *et al.*, 2018). Based on its genetic potential, the *Methylobacter* species present in our incubation experiments could be capable of dissimilatory nitrite reduction, but as no nitrite was provided in the incubations experiments, we don't expect this pathway to be relevant for methane oxidation.

Methylotenera-Methylobacter co-occurrence

Bacteria of the genus *Methylotenera*, which were highly abundant in our enrichment culture incubations (11 – 22%), have often been detected in co-occurrence with methanotrophs, and have been shown to use reaction products of methanotrophy (Yu and Chistoserdova, 2017), coupling methanol oxidation to nitrate reduction (Kalyuzhnaya *et al.*, 2011). Their relative abundance increased not only in the enrichment culture, but also in water column incubations with high methane oxidation rates (van Grinsven *et al.*, 2019), and an interaction between *Methylobacter* and *Methylotenera* is, therefore, not unlikely. The *Methylotenera* LLE-enrich-bin28 MAG has the genomic potential to oxidize methanol (Fig. 3), but lacks the *pmoA* gene necessary for the oxidation of methane. Its denitrification pathway seems incomplete, as the gene encoding for dissimilatory reduction of nitrate to nitrite (*Nap*/*Nar* gene) was missing. A mutant phenotype study on *Methylotenera* mobilis, however, demonstrated that the single subunit nitrate reductase (*Nap*), Mmol_1648, appears to be involved in both the assimilatory and dissimilatory denitrification pathways (Mustakhimov *et al.*, 2013). The nitrate reductase (*Nas*) detected in our *Methylotenera* LLE-enrich-bin28 MAG was homologous to the nitrate reductase (*Nap*) of *M. mobilis*. The *Methylotenera* species detected in our incubations may therefore also be able to perform denitrification, similarly to the *Methylotenera* species that have been described in literature before (*M. mobilis* and *Methylotenera versatilis*, Lapidus *et al.*, 2011; Mustakhimov *et al.*, 2013).

Role of nitrate and ammonium in methane oxidation

The methane oxidation rate of the oxic incubation experiments was higher than observed previously in environmental studies (Eller *et al.*, 2005; Schubert *et al.*, 2010; Blees *et al.*, 2014), but a proper comparison between an enrichment culture and environmental studies is difficult to make. The methane oxidation rate in the oxic incubations with nitrate was significantly higher than in the ammonium control incubations (311 µmol L^{-1} day^{-1} and 195 µmol L^{-1} day^{-1}, respectively), despite the fact that the methanotroph abundance was higher in the oxic control (8.6 x10^6 copies per L^{-1} in control, 6.7 x10^6 copies per L^{-1} in nitrate-amended incubations). Ammonium (NH_4^+), which was added to the control experiment as nitrogen source, can lower methanotrophic activity due to the structural similarity between CH_4 and NH_4^+, causing competitive inhibition (Bédard and Knowles, 1989). The affinity of the methane monooxygenase enzyme for CH_4 is however 600-1300-fold higher than the affinity

for NH_4^+, so we expect this effect to be of little influence. Generally, ammonium stimulates methanotroph growth and protein synthesis by providing bioavailable nitrogen (Bodelier *et al.*, 2000), although recent research in soils found a decrease in methane oxidation rates after ammonium addition (Walkiewicz *et al.*, 2018). Nitrate has also been suggested in earlier studies to inhibit methane oxidation under oxic conditions (Geng *et al.*, 2017; Walkiewicz and Brzezińska, 2019), although the observed effect in those studies could have been due to high salt concentrations, not specifically nitrate (Dunfield and Knowles, 1995) or due to conversion of nitrate to nitrite (Roco *et al.*, 2016), which is known to be an inhibitor of methane oxidation (Dunfield and Knowles, 1995; Hutsch, 1998).

As we consider ammonium inhibition unlikely, we assume a stimulating effect of nitrate on the oxic methane oxidation rate. As discussed above, the dominant *Methylobacter* species in both the enrichment cultures as well as the water column lacks the genes for a complete denitrification pathway. A complete assimilatory nitrate reduction pathway was present, and nitrate can thus be used for protein synthesis, enhancing growth. Another possibility would however be an interaction with *Methylotenera*, which is likely capable of denitrification. *Methylotenera* could function as a syntrophic partner for *Methylobacter*, as has been observed in several methane oxidizing bacteria and archaea (Boetius *et al.*, 2000; Milucka *et al.*, 2015; Krause *et al.*, 2017). Whether such a partnership indeed exists in our incubation experiments, requires more research.

Methylobacter sp. under oxygen limitation

Surprisingly, in contrast to the water column incubation studies, in which methane oxidation by *Methylobacter* was highest under oxygen-limiting conditions (van Grinsven et al. 2019), methane oxidation in incubations with the enrichment culture was highest under oxygen saturated conditions (Fig. 4B). Methane oxidation under low-oxygen conditions (microoxic, ($[O_2]$ 23–30 µM) occurred, but was much less efficient than methanotrophy under oxygen saturation conditions. The oxygen concentration in the closed bottles was measured only at the start of the incubations, and the concentrations may thus have changed over the course of the experiments. Air was, however, injected into the microoxic and trace oxygen incubation bottles on day 2, 6 and 13, in order to prevent oxygen depletion. Despite being aerobes, methanotrophs are generally assumed to be (partially) inhibited by oxygen concentrations >60 µM or at least stimulated by low oxygen conditions (Rudd and Hamilton, 1975; Van Bodegom *et al.*, 2001; Danilova *et al.*, 2016; Walkiewicz *et al.*, 2018; Thottathil *et al.*, 2019; Walkiewicz and Brzezińska, 2019), resulting in a low methane oxidation efficiency at high oxygen concentrations. A recent study by Thottathil *et al.* (2019) stated that methane oxidation rates are only at 20% of their maximum value at oxygen saturation, and that the fact that this oxygen inhibition is generally not considered for global models, may offset the total methane oxidation potential calculations greatly, expressing the need for additional studies on the response of methanotrophs to different oxygen concentrations. Our data reveal that this general assumption about oxygen inhibition of methanotrophy is not correct for the *Methylobacter* species present in this lake system.

The methane oxidation detected in the microoxic conditions may depend partially on a fermentative pathway, as was also suggested for methanotrophs in the Lacamas Lake water column (van Grinsven *et al.*, 2019), with an energy yield too low for cell growth but supporting only cell maintenance. It, however, remains unclear why the *Methylobacter* cells in the trace oxygen and anoxic incubations, that possibly went into a dormant state, remain almost as

abundant as the *Methylobacter* cells in the oxic and microoxic experiment, whilst no methane oxidation and thus no energy production seemed to take place in the first two. Similarly, methanotrophs remained a substantial part of the community in the anoxic electron acceptor incubations, despite no detectable methane oxidation, with higher *Methylobacter* abundances in nitrate and sulfate-amended incubations, compared to the control (19 and 25 %; 4.3×10^6 and 3.3×10^6 methanotroph cells per L^{-1}, in nitrate and sulfate incubations respectively, while only 11 %; 2.6×10^6 methanotroph cells per L^{-1}, in anoxic control). The used DNA method cannot distinguish between dead, dormant or active cells, but the strong contrast between the nitrate and sulfate incubations, and the incubations with humic substances, in which a major reduction in *Methylobacter* relative abundance to 1.6 % and a decrease in methanotroph abundance to 1×10^5 cells per L^{-1} (Table 1) was observed, suggest a difference between the treatments exists. Methanotrophs were shown to have an efficient survival mechanism under starvation in anoxic conditions, compared to starvation under oxic conditions (Roslev and King, 1995), increasing their change of survival under stress conditions.

Methane oxidation occurred directly after oxygen injection into oxic and microoxic bottles (Fig. 4), despite the fact that the cultures were under anoxic conditions for several days before the start of the experiment. It is unknown whether the cells were in a dormant state under anoxic conditions, but these results show no recovery time was needed, therefore implying a fast adaptation mechanism. This ability to rapidly adapt to anoxic or oxic conditions could be a strategy of methanotrophs living in dynamic environments, such as seasonally stratified water columns, allowing them to rapidly adapt to the changing conditions of their niche.

Fermentation-based methane oxidation, which could potentially be performed by *Methylobacter* under trace oxygen conditions, has been shown to occur under extremely low methane oxidation and growth rates (1.75 nmol min^{-1} per mg $protein^{-1}$; Kalyuzhnaya *et al.*, 2013). Rates like these were below the detection limit of our methods, opening the possibility of low-rate methane oxidation in the trace oxygen incubations.

Methane oxidation under anoxic conditions

No methane oxidation was observed under anoxic conditions in the *Methylobacter* enrichment culture obtained in this study, despite *Methylobacter* being present and active under anoxic conditions in the incubations performed with water column samples (van Grinsven *et al.*, 2019). Possibly, the anaerobic methane oxidation rates were too low to detect by our methods. Rates in anoxic lake waters have been reported to be in the range of 0.1 – 2.5 µM day^{-1} (Blees *et al.*, 2014; Oswald *et al.*, 2016). If comparable rates would occur in our anoxic incubations, the result would be a total decrease in methane of 3.2 – 80 µM over the full 32-day period, which would be difficult to detect given the large fluctuation between our measurements. The measured methane oxidation rates in the Lacamas Lake water anoxic water column were however much higher (up to 45 µM day^{-1}, van Grinsven *et al.*, 2019). Simultaneous methane production, counteracting the decrease in the concentration of methane caused by oxidation, could also have masked methane consumption. Methane production in anoxic systems is commonly observed, both in environmental and culture studies (Reeburgh, 2007; Conrad *et al.*, 2011; Grasset *et al.*, 2018), and could be fueled by reaction products of methane oxidation by *Methylobacter*, such as acetate or methanol (Oremland and Polcin, 1982). We did however not detect commonly known methane producers such as methanogenic archaea by the 16S rRNA gene diversity analysis.

Possibly, non-methanotrophic members of the microbial community, that are present in the natural community of the Lacamas Lake water column, are essential in mediating methane oxidation under anoxic conditions. These microbes may not have been selected in the oxic enrichment process used in this study. In this regard, Oswald *et al.*, (2015) showed that methanotrophs in the anoxic hypolimnion of Lake Rotsee were dependent on phototrophic microorganisms for the production of oxygen, to mediate their methane oxidation pathway. This pathway was not relevant in our incubations, which were performed in the dark, but a similar collaboration between a non-methanotrophic species and *Methylobacter* species may be essential in mediating methane oxidation under anoxic conditions. A possible candidate could be bacteria of the genus *Sulfuritalea*, that were abundant in the water column incubations in which anoxic methane oxidation was observed (van Grinsven *et al.*, 2020), but which were only present in low relative abundance in the enrichment culture and the incubation experiments of the current study (Table 2). They could be potentially involved as a partner in anoxic methane oxidation due to their capabilities of nitrate reduction (Kojima and Fukui, 2011). In contrast, bacteria of the order *Burkholderiales* were abundant in both the water column incubations and the enrichment culture incubations, although they were most abundant in the enrichment incubations with humic substances, which actually contained the lowest abundance of methanotrophs (Table 1 and 3). Another possibility could be the composition of the medium. The enrichment culture incubation experiments were performed on a rich media, including common trace metals and a vitamin solution. Certain compounds may however been present in the lake water, that were missing in the medium. Lanthanides, part of the rare earth elements, have been shown to affect *Methylobacter* (Krause *et al.*, 2017) and were not added to the enrichment medium. Possibly, compounds like these were lacking in the enrichment incubation experiments and limited anaerobic methane oxidation.

Conclusions

Studies have found methanotrophs at a wide range of locations and environmental conditions. Despite these observations, little is known about the drivers of the spatial distribution that is observed, while recent research stressed the importance of a correct representation of the non-linear response of methane oxidation rates to oxygen concentrations (Thottathil *et al.*, 2019). The effect of nitrogen and oxygen concentrations on methanotrophs was shown to differ strongly between similar environments, likely due to the different organic carbon content (Walkiewicz and Brzezińska, 2019), indicating the relationships between methane oxidation rates, methanotroph abundance, nitrogen source and oxygen concentration are complicated and more work is needed to understand these relationships. Our study shows that *Methylobacter*, a methanotroph often assumed to thrive under low oxygen conditions, preferred high-oxygen conditions over a microoxic environment under laboratory conditions. When comparing this data with an environmental study with the same *Methylobacter* species, we however see that the oxygen response of this species is dependent on factors we do not yet fully understand, potentially involving interactions with other non-methanotrophic microorganisms present in the same system. More research is therefore needed to reveal the pathways and microorganisms involved in the aerobic and anaerobic methane oxidation by this *Methylobacter* species.

Acknowledgements

We sincerely thank Keith Birchfield for sample collection and taking care of the sample transport to the Netherlands. We thank Maartje Brouwer and Sanne Vreugdenhil for help with qPCR analysis, Alejandro Abdala and Julia Engelmann for support with the bioinformatics analyses, and Jan van Ooijen of the NIOZ nutrient lab. Darci Rush is appreciated for her help in proofreading this manuscript. This research is supported by the Soehngen Institute of Anaerobic Microbiology (SIAM) Gravitation grant (024.002.002) to JSSD and LV of the Netherlands Ministry of Education, Culture and Science (OCW) and the Netherlands Organisation for Scientific Research (NWO).

Supplemental material

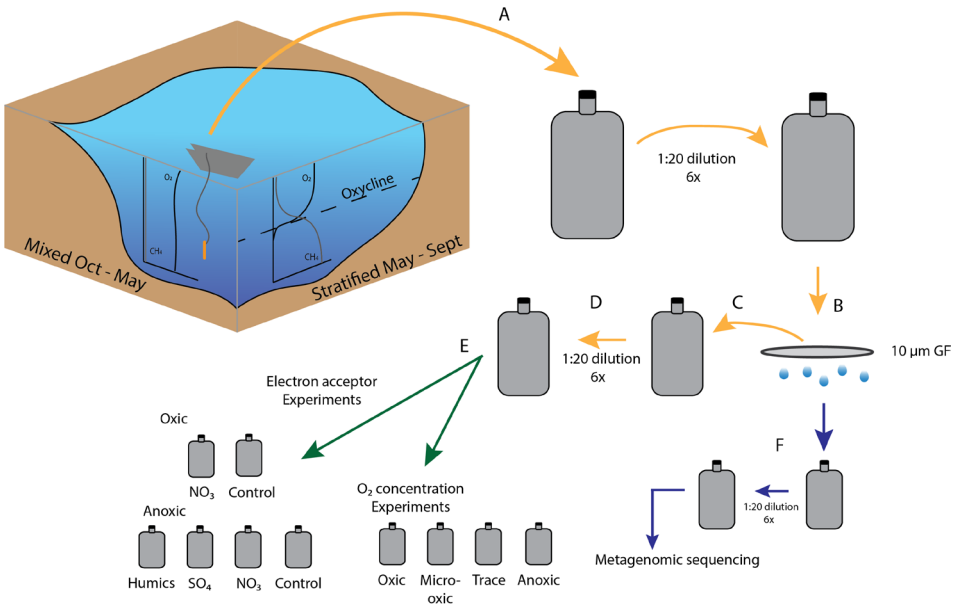

Fig. S1 Overview of experimental methods. The lake graphic represents Lacamas Lake, with on the left side the mixed winter water column, homogeneously low in methane and rich in oxygen, and on the right side the stratified summer water column, with a methane-rich oxygen-depleted deeper water layer and a methane-poor and oxygen-rich top water layer. Samples for this study were collected in the mixed winter water column, transferred onto nitrate mineral salts (NMS) media (A) and received methane. The enrichment culture was subcultured six times, by transferring culture to fresh media rich in methane in a 1:20 dilution, before using size separation (B) to increase the *Methylobacter* relative abundance. The particulate matter that remained on the 10 µm filter was scraped off and suspended in fresh media (C). The resulting cultures were again subcultured six times (D), and afterwards combined and concentrated to create one concentrated culture that was used to set up incubation experiments (E). A sample for metagenomic sequencing was obtained via subculturing of the filtrate (F). This metagenomic sequencing sample is described in Table S3. For more details, see the Experimental setup section.

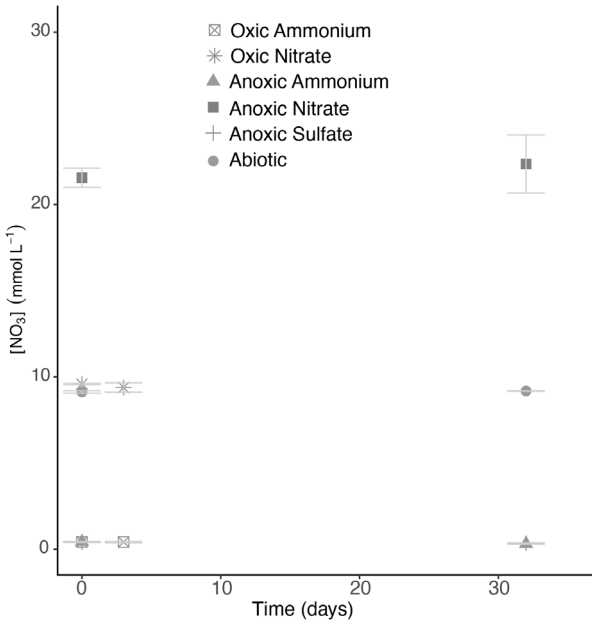

Fig. S2. Nitrate concentration at the start and end of the electron acceptor incubation experiments. Error bars represent the standard error over triplicate incubations.

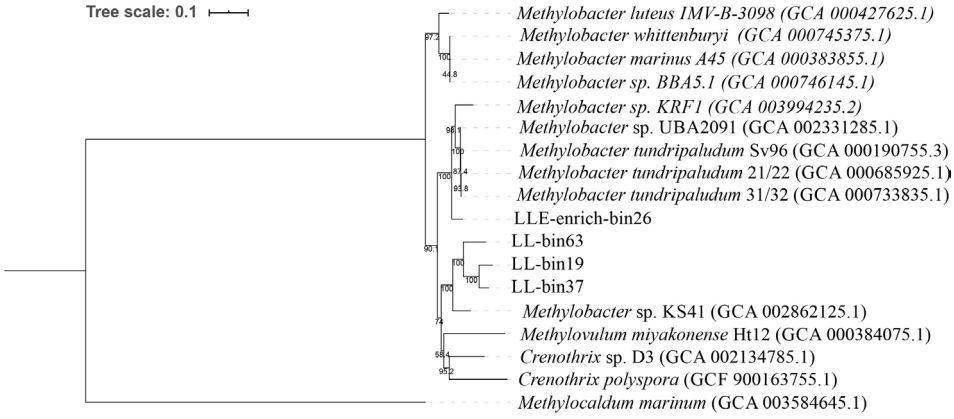

Fig. S3. Maximum likelihood phylogenetic tree based on 34 concatenated single-copy, protein-coding genes (following the method of Dombrowski et al., 2018) of the MAG bin LLE-enrich-bin26 and the MAGs as described in van Grinsven et al. (2019) (i.e. bin-63, bin-37, and bin-19).

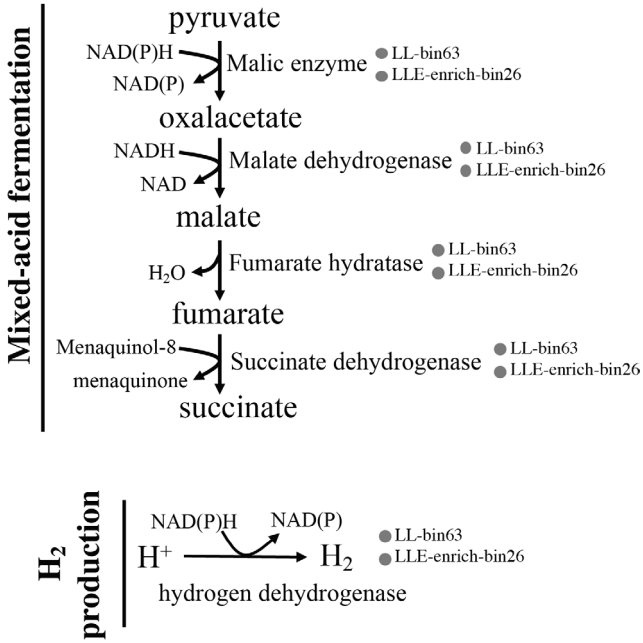

Fig. S4. Predicted pathway for mixed-acid fermentation from pyruvate to succinate and H2 production in the *Methylobacter* LL-bin63 and *Methylobacter* LLE-enrich-bin26 (Circles indicate all coding genes were present in both bins).

Table S1. Overview of the media (AMS – ammonium mineral salts, NMS – nitrate mineral salts) used in the incubation experiments, and of the additions of methane, additional nitrate, sulfate or humic substances to the incubation experiments.

	"Electron acceptor experiment"				"O_2-concentration experiment"			
	Control	Nitrate	Sulfate	Humics	Saturated	Micro-oxic	Trace	Anoxic
AMS media	x		x	x				
NMS media		x			x	x	x	x
CH_4	x	x	x	x	x	x	x	x
Additional NO_3^-		x						
Na_2SO_4			x					
Humic substances				x				

Table S2. Characteristics of the most abundant MAGs detected in the sample derived from the 10 µm filtrate (Fig. S1), which contained a high diversity in methanotrophs (i.e. 22% *Methylobacter* and 17% *Methylomonas*) and a high relative abundance of *Methylotenera* (i.e. 24%) based on 16S rRNA gene amplicon sequencing. Avg = average. Classification was inferred by GTDB-Tk as indicated in the material and methods.

Bin	Contigs	Bases	Avg Abundance	Completeness	Redundancy	GTDBTK Tax
LL-enrich-bin26	415	4213939	615.934	96.08	35.29	d__Bacteria;p__Proteobacteria;c__Gammaproteobacteria;o__Methylococcales;f__Methylomonadaceae;g__Methylobacter_A;s__
LL-enrich-bin27	436	4488068	583.699	66.67	13.73	d__Bacteria;p__Proteobacteria;c__Gammaproteobacteria;o__Methylococcales;f__Methylomonadaceae;g__Methylomonas;s__
LL-enrich-bin28	547	3908447	365.183	98.04	7.89	d__Bacteria;p__Proteobacteria;c__Gammaproteobacteria;o__Burkholderiales;f__Methylophilaceae;g__Methylotenera

Table S3. Composition of the sample that was used for metagenome sequencing.

	Metagenome sample
Methylobacter spp.	22
Methylomonas spp.	17
Other Methylococcales	0.3
Methylotenera spp.	24
Total 16S rRNA copies per L^{-1}	8.1 x10^5
Methanotroph 16S rRNA copies per L^{-1}	3.2 x10^5

Table S4. Relative abundance (%) of *Methylobacter* OTUs (>0.4% in at least one of the samples) in respect to the total 16S rRNA gene reads in the amplicon sequencing analysis for each incubation and for the enrichment sample used for the metagenomic sequencing.

		"Electron acceptor experiment"							"O_2-concentration experiment"				Enrich-ment
	Starting sample	Enrichment culture	Control, oxic	Nitrate, oxic	Control, anoxic	Nitrate, anoxic	Sulfate, anoxic	Humics, anoxic	Satu-rated	Micro-oxic	Trace	Anoxic	Metagenome
LLE-16S-1	0.0	0.1	1.6	0.3	0.0	0.1	0.1	0.0	0.3	0.1	0.3	0.1	0.8
LLE-16S-2	0.0	0.7	1.3	1.1	1.0	0.2	0.2	0.0	0.8	0.3	1.1	0.1	0.0
LLE-16S-3	0.0	0.0	0.6	0.0	0.0	0.4	0.2	0.0	0.2	0.0	0.0	0.3	0.0
LLE-16S-4	0.0	0.3	1.0	0.2	0.0	0.3	0.1	0.0	0.1	0.1	0.0	0.1	0.6
LLE-16S-5	0.0	0.3	0.8	0.3	0.0	0.2	0.2	0.0	0.1	0.1	0.2	0.2	0.4
LLE-16S-6	0.0	0.7	0.7	0.1	0.0	0.2	0.0	0.0	0.1	0.1	0.0	0.2	0.1
LLE-16S-7	0.0	10	0.5	1.4	0.0	0.9	0.2	0.0	0.2	0.2	0.5	0.6	1.3
LLE-16S-8	0.0	0.7	0.5	0.1	0.2	0.4	0.5	0.0	0.2	0.5	0.4	0.4	0.0
LLE-16S-9	0.0	0.3	0.3	0.1	0.5	0.5	0.3	0.0	0.1	0.3	0.0	0.5	0.0
LLE-16S-10	0.0	0.7	0.6	0.2	0.0	0.2	0.1	0.0	0.2	0.1	0.1	0.3	0.2
LLE-16S-11	0.0	0.1	1.2	0.3	0.0	0.1	0.1	0.0	0.1	0.0	0.0	0.1	0.0
LLE-16S-12	0.0	5.0	0.6	1.1	0.0	0.6	0.3	0.0	0.3	0.2	0.3	0.5	0.9
LLE-16S-13	0.0	0.3	0.5	0.5	0.0	0.1	0.1	0.0	0.1	0.1	0.1	0.1	0.1
LLE-16S-14	0.0	0.0	0.6	0.6	0.0	0.2	0.1	0.0	0.1	0.1	0.2	0.1	0.5
LLE-16S-15	0.0	0.1	0.3	0.1	0.1	0.2	0.3	0.0	0.2	0.3	0.1	0.7	0.0
LLE-16S-16	0.0	0.0	0.5	0.1	0.0	0.2	0.2	0.0	0.2	0.2	0.1	0.3	0.2
LLE-16S-17	0.0	0.2	0.2	0.0	0.1	0.2	0.1	0.0	0.4	0.2	0.2	0.5	0.0
LLE-16S-18	0.0	0.1	0.3	0.7	0.1	0.1	0.0	0.0	0.4	0.2	0.2	0.4	0.0
LLE-16S-19	0.0	0.1	0.5	1.1	0.0	0.4	0.2	0.0	0.3	0.2	0.0	0.5	0.3
LLE-16S-20	0.0	0.1	0.1	0.4	0.0	0.1	0.0	0.0	0.0	0.0	0.0	0.1	0.0
LLE-16S-21	0.0	0.4	0.1	0.3	0.1	0.1	0.4	0.0	0.0	0.1	0.1	0.2	0.0
LLE-16S-22	0.0	0.4	0.5	0.8	0.0	0.2	0.1	0.0	0.0	0.1	0.1	0.1	0.2
LLE-16S-23	0.0	0.0	0.5	1.4	0.0	0.0	0.0	0.0	0.0	0.4	0.3	0.3	0.3
LLE-16S-24	0.0	0.1	0.2	0.4	0.0	0.3	0.1	0.0	0.1	0.1	0.1	0.1	0.2
LLE-16S-25	0.0	0.0	0.1	0.4	0.1	0.2	0.1	0.0	0.0	0.6	0.2	0.4	0.0
LLE-16S-26	0.0	0.0	0.1	0.5	0.0	0.0	0.0	0.0	0.1	0.0	0.0	0.1	0.0
LLE-16S-27	0.0	0.0	0.0	0.5	0.0	0.0	0.0	0.0	0.1	0.0	0.0	0.0	0.0

Table S5. P-value of t-tests between *Methylobacter* relative abundances of the three replicates per incubation type, indicating whether the difference in relative abundance between sample categories was statistically significant.

Methylobacter	Oxic control	Oxic nitrate	Anoxic control	Anoxic nitrate	Anoxic sulfate
Oxic control		0.13	2.2E-05	0.002	0.0002
Oxic nitrate			0.001	0.02	0.004
Anoxic control				0.01	0.02
Anoxic nitrate					0.08
Anoxic sulfate					

References

Altschul, S.F., Gish, W., Miller, W., Myers, E.W., and Lipman, D.J. (1990) Basic local alignment search tool. *J. Mol. Biol.* **215**: 403–410.

Andrews, S., Krueger, F., Seconds-Pichon, A., Biggins, F., and Wingett, S. (2015) FastQC. A quality control tool for high throughput sequence data. Babraham Bioinformatics. *Babraham Inst.* **1**: 1.

Asbun, A.A., Besseling, M.A., Balzano, S., van Bleijswijk, J., Witte, H., Villanueva, L., and Engelmann, J.C. (2019) Cascabel: a flexible , scalable and easy-to-use amplicon sequence data analysis pipeline. *BioRxiv* **809384**:.

Aziz, R.K., Bartels, D., Best, A., DeJongh, M., Disz, T., Edwards, R.A., et al. (2008) The RAST Server: Rapid annotations using subsystems technology. *BMC Genomics* **9**: 1–15.

Bédard, C. and Knowles, R. (1989) Physiology, biochemistry, and specific inhibitors of CH4, NH4+, and CO oxidation by methanotrophs and nitrifiers. *Microbiol. Rev.* **53**: 68–84.

Besseling, M.A., Hopmans, E.C., Christine Boschman, R., Sinninghe Damsté, J.S., and Villanueva, L. (2018) Benthic archaea as potential sources of tetraether membrane lipids in sediments across an oxygen minimum zone. *Biogeosciences* **15**: 4047–4064.

Biderre-Petit, C., Jézéquel, D., Dugat-Bony, E., Lopes, F., Kuever, J., Borrel, G., et al. (2011) Identification of microbial communities involved in the methane cycle of a freshwater meromictic lake. *FEMS Microbiol. Ecol.* **77**: 533–545.

Blees, J., Niemann, H., Wenk, C.B., Zopfi, J., Schubert, C.J., Kirf, M.K., et al. (2014) Micro-aerobic bacterial methane oxidation in the chemocline and anoxic water column of deep south-Alpine Lake Lugano (Switzerland). *Limnol. Oceanogr.* **59**: 311–324.

Van Bodegom, P., Stams, F., Mollema, L., Boeke, S., and Leffelaar, P. (2001) Methane Oxidation and the Competition for Oxygen in the Rice Rhizosphere. *Appl. Environ. Microbiol.* **67**: 3586–3597.

Bodelier, P.L.E., Roslev, P., Henckel, T., and Frenzel, P. (2000) Stimulation by ammonium-based fertilizers of methane oxidation in soil around rice roots. *Nature* **403**: 421.

Boetius, A., Ravenschlag, K., Schubert, C.J., Rickert, D., Widdel, F., Gieseke, A., et al. (2000) A marine microbial consortium apparently mediating anaerobic oxidation of methane. *Nature* **407**: 623–626.

Caporaso, J.G., Kuczynski, J., Stombaugh, J., Bittinger, K., Bushman, F.D., Costello, E.K., et al. (2010) QIIME allows analysis of high-throughput community sequencing data. *Nat. Methods* **7**: 335–336.

Caporaso, J.G., Lauber, C.L., Walters, W.A., Berg-Lyons, D., Huntley, J., Fierer, N., et al. (2012) Ultra-high-throughput microbial community analysis on the Illumina HiSeq and MiSeq platforms. *ISME J.* **6**: 1621–1624.

Conrad, R., Noll, M., Claus, P., Klose, M., Bastos, W.R., and Enrich-Prast, A. (2011) Stable carbon isotope discrimination and microbiology of methane formation in tropical anoxic lake sediments. *Biogeosciences* **8**: 795–814.

Danilova, O. V., Suzina, N.E., Van De Kamp, J., Svenning, M.M., Bodrossy, L., and Dedysh, S.N. (2016) A new cell morphotype among methane oxidizers: A spiral-shaped obligately microaerophilic methanotroph from northern low-oxygen environments. *ISME J.* **10**: 2734–2743.

Darling, A.E., Jospin, G., Lowe, E., Matsen, F.A., Bik, H.M., and Eisen, J.A. (2014) PhyloSift: Phylogenetic analysis of genomes and metagenomes. *PeerJ* **2**: e243.

Dunfield, P. and Knowles, R. (1995) Kinetics of inhibition of methane oxidation by nitrate, nitrite, and ammonium in a humisol. *Appl. Environ. Microbiol.* **61**: 3129–3135.

Edgar, R.C. (2010) Search and clustering orders of magnitude faster than BLAST. *Bioinformatics* **26**: 2460–2461.

Eller, G., Känel, L., Krüger, M., Ka, L., and Kru, M. (2005) Cooccurrence of Aerobic and Anaerobic Methane Oxidation in the Water Column of Lake Plußsee. *Appl. Environ. Microbiol.* **71**: 8925–8928.

Ettwig, K.F., Butler, M.K., Le Paslier, D., Pelletier, E., Mangenot, S., Kuypers, M.M.M., et al. (2010) Nitrite-driven anaerobic methane oxidation by oxygenic bacteria. *Nature* **464**: 543–548.

Geng, J., Cheng, S., Fang, H., Yu, Guirui, Li, X., Si, G., et al. (2017) Soil nitrate accumulation explains the nonlinear responses of soil CO2 and CH4 fluxes to nitrogen addition in a temperate needle-broadleaved mixed forest. *Ecol. Indic.* **79**: 28–36.

Gilman, A., Fu, Y., Hendershott, M., Chu, F., Puri, A.W., Smith, A.L., et al. (2017) Oxygen-limited metabolism in the methanotroph Methylomicrobium buryatense 5GB1C. *Peer J* **5**: e3945.

Grasset, C., Mendonça, R., Villamor Saucedo, G., Bastviken, D., Roland, F., and Sobek, S. (2018) Large but variable methane production in anoxic freshwater sediment upon addition of allochthonous and autochthonous organic matter. *Limnol. Oceanogr.* **63**: 1488–1501.

van Grinsven, S., Asbun, A.A., Julia, C., Harrison, J., and Villanueva, L. (2020) Methane oxidation in anoxic lake water stimulated by nitrate and sulfate addition. *Environ. Microbiol.* **22**: 766–782.

Gulledge, J., Ahmad, A., Steudler, P.A., Pomerantz, W.J., and Cavanaugh, C.M. (2001) Family- and Genus-Level 16S rRNA-Targeted Oligonucleotide Probes for Ecological Studies of Methanotrophic Bacteria. *Appl. Environ. Microbiol.* **67.10**: 4726–4733.

Harrits, S.M. and Hanson, R.S. (1980) Stratification of aerobic methane-oxidizing organisms in Lake Mendota, Madison, Wisconsin. *Limnol. Oceanogr.* **25**: 412–421.

Hutsch, B.W. (1998) Methane oxidation in arable soil as inhibited by ammonium, nitrite, and organic manure with respect to soil pH. In, *Biology and Fertility of Soils*.

Jones, R.I. and Grey, J. (2011) Biogenic methane in freshwater food webs. *Freshw. Biol.* **56**: 213–229.

Kalyuzhnaya, M.G., Beck, D.A.C., Vorobev, A., Smalley, N., Kunkel, D.D., Lidstrom, M.E., and Chistoserdova, L. (2011) Novel methylotrophic isolates from lake sediment, description of Methylotenera versatilis sp. nov. and emended description of the genus Methylotenera. *Int. J. Syst. Evol. Microbiol.* **62**: 106–111.

Kalyuzhnaya, M.G., Yang, S., Rozova, O.N., Smalley, N.E., Clubb, J., Lamb, A., et al. (2013) Highly efficient methane biocatalysis revealed in a methanotrophic bacterium. *Nat. Commun.* **4**: 1–7.

Kits, K.D., Klotz, M.G., and Stein, L.Y. (2015) Methane oxidation coupled to nitrate reduction under hypoxia by the Gammaproteobacterium Methylomonas denitrificans, sp. nov. type strain FJG1. *Environ. Microbiol.* **17**: 3219–3232.

Klüpfel, L., Piepenbrock, A., Kappler, A., and Sander, M. (2014) Humic substances as fully regenerable electron acceptors in recurrently anoxic environments. *Nat. Geosci.* **7**: 195–200.

Knittel, K. and Boetius, A. (2009) Anaerobic Oxidation of Methane: Progress with an Unknown Process. *Annu. Rev. Microbiol.* **63**: 311–334.

Kojima, H. and Fukui, M. (2011) Sulfuritalea hydrogenivorans gen. nov., sp. nov., a facultative autotroph isolated from a freshwater lake. *Int. J. Syst. Evol. Microbiol.* **61**: 1651–1655.

Krause, S.M.B., Johnson, T., Karunaratne, Y.S., Fu, Y., Beck, D.A.C., Chistoserdova, L., and Lidstrom, M.E. (2017) Lanthanide-dependent cross-feeding of methane-derived carbon is linked by microbial community interactions. *Proc. Natl. Acad. Sci. U. S. A.* **114**: 358–363.

Lapidus, A., Clum, A., LaButti, K., Kaluzhnaya, M.G., Lim, S., Beck, D.A.C., et al. (2011) Genomes of three methylotrophs from a single niche reveal the genetic and metabolic divergence of the methylophilaceae. *J. Bacteriol.* **193**: 3757–3764.

Lovley, D.R., Coates, J.D., BluntHarris, E.L., Phillips, E.J.P., and Woodward, J.C. (1996) Humic substances as electron acceptors for microbial respiration. *Nature* **382**: 445–448.

Martinez-Cruz, K., Leewis, M.C., Herriott, I.C., Sepulveda-Jauregui, A., Anthony, K.W., Thalasso, F., and Leigh, M.B. (2017) Anaerobic oxidation of methane by aerobic methanotrophs in sub-Arctic lake sediments. *Sci. Total Environ.* **607–608**: 23–31.

Martinez-Cruz, K., Sepulveda-Jauregui, A., Casper, P., Anthony, K.W., Smemo, K.A., and Thalasso, F. (2018) Ubiquitous and significant anaerobic oxidation of methane in freshwater lake sediments. *Water Res.* **144**: 332–340.

Michaud, A.B., Dore, J.E., Achberger, A.M., Christner, B.C., Mitchell, A.C., Skidmore, M.L., et al. (2017) Microbial oxidation as a methane sink beneath the West Antarctic Ice Sheet. *Nat. Geosci.* **10**: 582–586.

Milucka, J., Kirf, M., Lu, L., Krupke, A., Lam, P., Littmann, S., et al. (2015) Methane oxidation coupled to oxygenic photosynthesis in anoxic waters. *ISME J.* **9**: 1991–2002.

Murase, J. and Frenzel, P. (2007) A methane-driven microbial food web in a wetland rice soil. *Environ. Microbiol.* **9**: 3025–3034.

Mustakhimov, I., Kalyuzhnaya, M.G., Lidstrom, M.E., and Chistoserdova, L. (2013) Insights into denitrification in Methylotenera mobilis from denitrification pathway and methanol metabolism mutants. *J. Bacteriol.* **195**: 2207–2211.

Oremland, R.S. and Polcin, S. (1982) Methanogenesis and sulfate reduction: competitive and noncompetitive substrates in estuarine sediments. *Appl. Environ. Microbiol.* **44**: 1270–1276.

Oswald, K., Graf, J.S., Littmann, S., Tienken, D., Brand, A., Wehrli, B., et al. (2017) Crenothrix are major methane consumers in stratified lakes. *ISME J.* **11**: 2124–2140.

Oswald, K., Milucka, J., Brand, A., Hach, P., Littmann, S., Wehrli, B., et al. (2016) Aerobic gammaproteobacterial methanotrophs mitigate methane emissions from oxic and anoxic lake waters. *Limnol. Oceanogr.* **61**: S101–S118.

Oswald, K., Milucka, J., Brand, A., Littmann, S., Wehrli, B., Kuypers, M.M.M., and Schubert, C.J. (2015) Light-dependent aerobic methane oxidation reduces methane emissions from seasonally stratified lakes. *PLoS One* **10**: e0132574.

Parks, D.H., Imelfort, M., Skennerton, C.T., Hugenholtz, P., and Tyson, G.W. (2015) CheckM: Assessing the quality of microbial genomes recovered from isolates, single cells, and metagenomes. *Genome Res.* **25**: 1043–1055.

Quast, C., Pruesse, E., Yilmaz, P., Gerken, J., Schweer, T., Yarza, P., et al. (2013) The SILVA ribosomal RNA gene database project: improved data processing and web-based tools. *Nucleic Acids Res.* **41**: D590-6.

Reeburgh, W.S. (2007) Oceanic methane biogeochemistry. *Chem. Rev.* **107**: 486–513.

Reed, D.C., Deemer, B.R., van Grinsven, S., and Harrison, J.A. (2017) Are elusive anaerobic pathways key methane sinks in eutrophic lakes and reservoirs? *Biogeochemistry* **134**: 29–39.

Rissanen, A.J., Saarenheimo, J., Tiirola, M., Peura, S., Aalto, S.L., Karvinen, A., and Nykänen, H. (2018) Gammaproteobacterial methanotrophs dominate methanotrophy in aerobic and anaerobic layers of boreal lake waters. *Aquat. Microb. Ecol.* **81**: 257–276.

Roco, C.A., Bergaust, L.L., Shapleigh, J.P., and Yavitt, J.B. (2016) Reduction of nitrate to nitrite by microbes under oxic conditions. *Soil Biol. Biochem.* **100**: 1–8.

Rogelj, J., Shindell, D., Jiang, K., Fifita, S., Forster, P., Ginzburg, V., et al. (2018) Mitigation Pathways Compatible With 1.5°C in the Context of Sustainable Development. *Glob. Warm. 1.5°C. An IPCC Spec. Rep. […]* 2.

Roslev, P. and King, G.M. (1995) Aerobic and anaerobic starvation metabolism in methanotrophic bacteria. *Appl. Environ. Microbiol.* **61**: 1563–1570.

Rudd, J.W.M. and Hamilton, R.D. (1975) Factors controlling rates of methane oxidation and the distribution of the methane oxidizers in a small stratified lake. *Arch. Hydrobiol* **75**: 522–538.

Sanseverino, A.M., Bastviken, D., Sundh, I., Pickova, J., and Enrich-Prast, A. (2012) Methane carbon supports aquatic food webs to the fish level. *PLoS One* **7**: e42723.

Saxton, M.A., Samarkin, V.A., Schutte, C.A., Bowles, M.W., Madigan, M.T., Cadieux, S.B., et al. (2016) Biogeochemical and 16S rRNA gene sequence evidence supports a novel mode of anaerobic methanotrophy in permanently ice-covered Lake Fryxell, Antarctica. *Limnol. Oceanogr.* **61**: S119–S130.

Scheller, S., Yu, H., Chadwick, G.L., and Mcglynn, S.E. (2016) Artificial electron acceptors decouple archaeal methane oxidation from sulfate reduction. *Science.* **351**: 703–707.

Schubert, C.J., Lucas, F.S., Durisch-Kaiser, E., Stierli, R., Diem, T., Scheidegger, O., et al. (2010) Oxidation and emission of methane in a monomictic lake (Rotsee, Switzerland). *Aquat. Sci.* **72**: 455–466.

Schubert, C.J., Vazquez, F., Loesekann-Behrens, T., Knittel, K., Tonolla, M., and Boetius, A. (2011) Evidence for anaerobic oxidation of methane in sediments of a freshwater system (Lago di Cadagno). *FEMS Microbiol. Ecol.* **76**: 26–38.

Seemann, T. (2014) Prokka : rapid prokaryotic genome annotation. **30**: 2068–2069.

Segarra, Schubotz, F., Samarkin, V., Yoshinaga, M.Y., Hinrichs, K., and Joye, S.B. (2015) High rates of anaerobic methane oxidation in freshwater wetlands reduce potential atmospheric methane emissions. *Nat. Commun.* **6**: 1–8.

Sieber, C.M.K., Probst, A.J., Sharrar, A., Thomas, B.C., Hess, M., Tringe, S.G., and Banfield, J.F. (2018) Recovery of genomes from metagenomes via a dereplication, aggregation and scoring strategy. *Nat. Microbiol.* **3**: 836–843.

Smith, G.J., Angle, J.C., Solden, L.M., Daly, R.A., Johnston, M.D., Borton, M.A., et al. (2018) Members of the Genus Methylobacter Are Inferred To Account for the Majority of Aerobic Methane Oxidation in Oxic Soils from a Freshwater Wetland. *MBio* **9**: 1–17.

Svenning, M.M., Hestnes, A.G., Wartiainen, I., Stein, L.Y., Klotz, M.G., Kalyuzhnaya, M.G., et al. (2011) Genome Sequence of the Arctic Methanotroph Methylobacter tundripaludum SV96. *J. Bacteriol.* **193**: 6418–6419.

Tamura, K., Stecher, G., Peterson, D., Filipski, A., and Kumar, S. (2013) MEGA6: Molecular evolutionary genetics analysis version 6.0. *Mol. Biol. Evol.* **30**: 2725–2729.

Thottathil, S.D., Reis, P.C.J., and Prairie, Y.T. (2019) Methane oxidation kinetics in northern freshwater lakes. *Biogeochemistry* **143**: 105–116.

Valenzuela, E.I., Avendaño, K.A., Balagurusamy, N., Arriaga, S., Nieto-Delgado, C., Thalasso, F., and Cervantes, F.J. (2019) Electron shuttling mediated by humic substances fuels anaerobic methane oxidation and carbon burial in wetland sediments. *Sci. Total Environ.* **650**: 2674–2684.

Valenzuela, E.I., Prieto-davó, A., López-lozano, N.E., García-gonzález, A.S., López, M.G., and Cervantes, J. (2017) Anaerobic Methane Oxidation Driven by Microbial Reduction of Natural Organic Matter in a Tropical Wetland. *Appl. Environ. Microbiol.* **83**: 1–15.

Walkiewicz, A. and Brzezińska, M. (2019) Interactive effects of nitrate and oxygen on methane oxidation in three different soils. *Soil Biol. Biochem.* **133**: 116–118.

Walkiewicz, A., Brzezińska, M., and Bieganowski, A. (2018) Methanotrophs are favored under hypoxia in ammonium-fertilized soils. *Biol. Fertil. Soils* **54**: 861–870.

Whittenbury, R., Phillips, K.C., and Wilkinson, J.F. (1970) Enrichment, Isolation and Some Properties of Methane-utilizing Bacteria. *J. Gen. Microbiol.* **61**: 205–218.

Xin, J.Y., Cui, J.R., Niu, J.Z., Hua, S.F., Xia, C.G., Li, S. Ben, and Zhu, L.M. (2004) Production of methanol from methane by methanotrophic bacteria. *Biocatal. Biotransf.* **22**: 225–229.

Xin, J.Y., Zhang, Y.X., Zhang, S., Xia, C.G., and Li, S. Ben (2007) Methanol production from CO2 by resting cells of the methanotrophic bacterium Methylosinus trichosporium IMV 3011. *J. Basic Microbiol.* **47**: 426–435.

Yu, Z. and Chistoserdova, L. (2017) Communal Metabolism of Methane and the Rare Earth Element Switch. *J. Bacteriol.* **199**: e00328-17.

Zhang, J., Kobert, K., Flouri, T., and Stamatakis, A. (2014) PEAR: A fast and accurate Illumina Paired-End reAd mergeR. *Bioinformatics* **30**: 614–620.

Chapter 5. Nitrate enables the transfer of methane-derived carbon from the methanotroph *Methylobacter* sp. to the methylotroph *Methylotenera* sp. in eutrophic lake water

Sigrid van Grinsven
Jaap S. Sinninghe Damsté
John Harrison
Lubos Polerecky
& Laura Villanueva

Submitted to Limnology & Oceanography

Abstract

Eutrophic lakes are major contributors to global aquatic methane emissions. Methanotrophy, performed by methane oxidizing bacteria, results in the production of biomass, fermentation products and/or CO_2, making methane-derived carbon available to non-methanotrophic organisms. Methanotrophs can co-occur with methylotrophs which are expected to consume methane-derived carbon. However, it is unknown if this interaction requires cell-to-cell contact, whether physicochemical factors affect this interaction, and what role this interaction may play in ecosystems and biogeochemical cycling in lakes. Here, we performed incubations of an enrichment culture obtained from a eutrophic lake with ^{13}C-labeled methane, revealing the transfer of methane-derived carbon from the methanotroph *Methylobacter* to a methylotroph of the genus *Methylotenera*. CARD-FISH and NanoSIMS analyses showed that these microorganisms occur both in mixed clusters and as single cells, and that their interaction does not require physical cell contact. In addition, the carbon transfer between the partners is dependent on the presence of nitrate, which is potentially used by *Methylotenera* sp. and in turn may affect the methane oxidation rate of *Methylobacter* sp. This interaction, and its dependence on nitrate, may have important implications for the carbon cycle in eutrophic lakes worldwide.

Introduction

Methane, a greenhouse gas with a warming potential 34 times greater than CO_2 (Forster *et al.*, 2007), is emitted to the atmosphere by numerous sources, both anthropogenic and natural, among which aquatic systems such as wetlands, lakes and reservoirs contribute about 16–23% to global methane emissions (Conrad 2009; Bastviken et al. 2011; Saunois et al. 2016; DelSontro et al. 2018). Methane production in aquatic systems occurs naturally, but its emission rates can be strongly influenced by human impacts such as eutrophication and warming (Yvon-Durocher *et al.*, 2014; Deemer *et al.*, 2016). Methane consumption by microbes (i.e. methanotrophy) is performed by either archaea or bacteria occupying distinct ecological niches, consuming a substantial portion of the produced methane (Bastviken *et al.*, 2008). Methane oxidizing bacteria (MOB) are mostly aerobes, with few species capable of methane oxidation under anoxic conditions, by using nitrite, nitrate, sulfate and possibly humic substances as electron acceptors (Ettwig *et al.*, 2010; Schubert *et al.*, 2011; Kits *et al.*, 2015; Saxton *et al.*, 2016; Oswald *et al.*, 2017; Reed *et al.*, 2017; Valenzuela *et al.*, 2019).

Methane oxidation is a key process in the carbon cycle of shallow, eutrophic lakes. The majority of aquatic organisms, both bacteria and species of higher trophic levels, are unable to use methane directly. They are therefore dependent on the conversion of methane into other carbon compounds by MOB, which can be a major component of the carbon budget of lake water columns, comparable to the contribution of phytoplankton primary production (Taipale *et al.*, 2011). Methane oxidation by MOB proceeds mostly to carbon dioxide (Murrell, 2010), although recent studies have shown that MOB can perform mixed-acid fermentation in anoxic environments resulting in excretion of other reaction products such as acetate, succinate and H_2 (Kalyuzhnaya *et al.*, 2013; van Grinsven *et al.*, 2020a). It has also been shown that intermediates of the methane oxidation reaction, such as methanol and formaldehyde, can be excreted into the ecosystem (Xin *et al.*, 2007; Tavormina *et al.*, 2017) and further used as a carbon source by non-methanotrophic microorganisms, with important implications for higher trophic levels (Jones *et al.*, 1999; Murase and Frenzel, 2007; Jones and Grey, 2011; Sanseverino *et al.*, 2012; He *et al.*, 2015). The release of methanol, however, leads to an energy deficiency in the methanotrophic cell, as the conversion of methane to methanol is energy consuming. Energy is only gained at further steps in the methane metabolism (Xin *et al.*, 2004, 2007). It is, therefore, unclear whether there is a gain for the methanotrophs in the excretion of methanol.

Methylotrophs (i.e. microbes consuming single-carbon compounds) of the genera *Methylophilus* and *Methylotenera* have been shown to co-occur with methanotrophs and suggested to consume methanol derived from the methanotroph (Oshkin *et al.*, 2014). A study by Krause *et al.* (2017) with synthetic co-cultures, established with isolates from lake sediment, suggested a cross-feeding mechanism in which the methylotroph induces a change in gene expression of the methanotroph, resulting in release of methanol for its growth. However, it is unknown (i) whether there is a gain for the methanotroph, either through a transfer of vitamins or direct interspecies electron transfer (DIET) as previously suggested (Yu and Chistoserdova, 2017), and (ii) if this interaction requires a physical contact between the partners. Besides, the effect of the physicochemical environmental conditions on this presumed partnership has not yet been determined.

In this study, we further investigated the transfer of methane-derived carbon in an enrichment culture, obtained from the water column of a eutrophic lake, which was dominated by the methanotroph *Methylobacter* sp. and a non-methanotrophic methylotroph of the genus *Methylotenera*. Stable isotope probing (SIP) and Nanoscale Secondary Ion Mass Spectrometry (NanoSIMS) confirmed the transfer of carbon between the partners, and demonstrated that physical contact between the partners is not essential. Up to now, studies have focused on artificial, non-complex communities, or soil/sediment systems. Here, we introduce the first visualization of the co-occurrence, and possible partnership, of *Methylobacter* and *Methylotenera* species in a water column enrichment. Temperate zone lakes, such as the source of the enrichment culture used in this study, are experiencing intense eutrophication, resulting in an increase in nitrate loads and in situ concentrations (Moore *et al.*, 2003). Both the genera *Methylobacter* and *Methylotenera* have been associated with denitrification before (Mustakhimov *et al.*, 2013; Smith *et al.*, 2018), but whether nitrate affects their interaction has never been assessed. Our results suggest a link between the nitrogen and carbon cycle, via a stimulating effect of nitrate on methane oxidation rates and transfer, which could in turn affect the trophic transfer of methane-derived carbon in lake systems, with implications for the wider community and carbon balance of temperate eutrophic lakes.

Material and methods

Sample collection, enrichment and incubation experiments

Enrichment cultures were established as described in van Grinsven et al. (2020b). Briefly, suspended particulate matter from the oxic water column of Lacamas Lake (WA, USA) was collected by filtration through a 0.7 mm pore size glass fiber GF/F filter, transferred to nitrate mineral salts (NMS) medium (Whittenbury *et al.*, 1970), and supplied with methane (99.99% purity). After 12 weeks at 15°C, during which the culture was transferred 6 times, the larger cell clusters were separated from the smaller clusters and single cells by filtration over a 10 mm filter, after which both fractions were resuspended in NMS media and treated similarly to the earlier subcultures. After 8 weeks, the cells of each culture (named "Particle culture" and "Filtrate culture") were harvested by centrifugation (2800 x g for 5 min, 15°C) and used as inoculum for incubation experiments. A sample of each inoculum was stored for DNA-analysis.

Incubation experiments were supplied with 100% ^{13}C-labeled methane (Sigma-Aldrich), in the absence and presence of nitrate as described for the "particle culture" in van Grinsven et al. (2020b). The procedure for the "filtrate culture" was identical. Briefly, incubation experiments with nitrate were performed with oxic NMS medium, which was also used for cultivation as described above, containing nitrate as the only nitrogen source (Whittenbury et al. 1970). Ammonium incubations were performed with an oxic AMS medium, containing ammonium rather than nitrate as nitrogen source (1 g l^{-1} KNO_3 was replaced with 0.5 g l^{-1} NH_4Cl, as described by Whittenbury et al., 1970). All incubation experiments were performed in triplicate in 260 ml acid-washed and autoclaved glass pressure bottles with butyl stoppers, containing 200 ml media and 2.6 ml 100% ^{13}C-labeled methane (10% v/v methane, Sigma-Aldrich) in the air headspace, at atmospheric pressure. All incubations were performed at 15 °C in the dark, lasting 2-3 days. Daily measurements of the headspace methane concentration

of oxic incubations ("particle" and "filtrate" culture) were performed via gas chromatography with a flame ionization detector (GC-FID), as described in van Grinsven et al. (2020b). At termination, samples were taken for visual analysis of both cultures, as described below, and, for the incubations with the "particle culture", for determination of the NH_4^+, NO_3^- and NO_2^- concentrations by Continuous Flow Analyses, performed on a QuAAtro Segmented Flow Analyzer (Seal Analytical). All incubation experiments were then terminated by filtering onto polycarbonate filters (47 mm diameter, 0.2 mm pore size; Millipore). Filters were stored at -80 °C until DNA extraction using the RNeasy Powersoil Total RNA extraction + DNA elution kit. DNA extracts were stored at -20 °C until further processing.

Sample preparation for DNA-SIP analysis

Samples from the "particle culture" incubation experiments were used for DNA-SIP analysis. Fraction separation was performed by CsCl density gradient centrifugation of the total DNA, as described in detail by Suominen *et al.* (2019), following the protocol of Dunford and Neufeld (2010). Briefly, 4 µg of total DNA was added to a CsCl solution, obtaining a final density of 1.725 g ml^{-1}, which was put in 5.1 ml QuickSeal Polyallomer tubes (Beckman Coulter, Brea, CA). The samples were centrifuged for 60 h at 44,000 rpm (177,000 x *g*) at 20°C using a Vti 65.2 rotor (Beckmann Coulter, Brea, CA). The CsCl solution, containing the DNA, was then divided into 12 equal fractions, and the gradient formation was checked by measuring the density of a 10 µl sub-sample of each fraction with a digital refractometer (AR2000 Reichert Technologies, Buffalo, NY). To precipitate the collected DNA, 2 volumes of PEG solution were added (30% PEG6000, 1.6 M NaCl) together with 20 µg of polyacrylamide as a carrier, followed by incubating at room temperature for 2 h and pelleting the DNA by centrifugation at 13,000 x *g* for 30 min at 4°C. Pellets were washed with 70% ethanol, air-dried and resuspended in PCR-grade water.

16S rRNA gene amplification, data processing and quantification

Total DNA and DNA that was obtained after the DNA-SIP procedure was used for PCR amplification by using the general 16S rRNA archaeal and bacteria primer pair 515F and 806RB targeting the V4 region (Table S1; Caporaso *et al.*, 2012) as described in van Grinsven et al. (2020b). Briefly, after amplification, the PCR products were gel-purified using the QIAquick Gel-Purification kit (Qiagen) and pooled and diluted. Sequencing was performed by the Utrecht Sequencing Facility (Utrecht, the Netherlands), using an Illumina MiSeq sequencing platform. The Cascabel pipeline was used for the analysis of the 16S rRNA gene amplicon sequences (Asbun *et al.*, 2019). This included quality assessment by FastQC (Andrews *et al.*, 2015), assembly of the paired-end reads with Pear (Zhang *et al.*, 2014), and assignment of taxonomy (including pick representative set of sequences with 'longest' method) with blast using the Silva 128 release as reference database (https://www.arb-silva.de/). The 16S rRNA amplicon reads (raw data) have been deposited in the NCBI Sequence Read Archive (SRA) under BioProject ID PRJNA603000.

16S rRNA gene copies were quantified using quantitative PCR (qPCR) with the same primer pair as used for amplicon sequencing (515F, 806RB) on a Rotor-Gene 6000 (Corbett Research, Sydney). The qPCR reaction mixture (25 µL) contained 0.5 U of Phusion High-Fidelity DNA Polymerase (Thermo Scientific), 1x Phusion HF Buffer, 0.2 µM of each dNTP, 20µg of BSA, 0.6 pmol $µL^{-1}$ of both primers, 0.5x EvaGreen dye (0.625 µM) in aqueous solution (Biotium,

Hayward) and AccuGENE Molecular Biology Water (Lonza, Basel). The cycling conditions for the qPCR reaction were as follow: initial denaturation 98 C for 30 s, 45 cycles of 98 °C for 10 s, 50 °C for 20 s, followed by fluorescence data acquisition, 72 °C for 30 s, and 80 °C for 25 s. Specificity of the reaction was tested with a gradient melting temperature assay, from 55 °C to 95 °C with 0.5 °C increments of 5 s apiece. The qPCR reactions were performed in duplicate with standard curves encompassing a range from 10^1 to 10^7 molecules μL^{-1}. qPCR efficiency for the 16S rRNA gene quantification was 100% with $R^2 = 0.996$.
The 16S rRNA gene sequencing and the qPCR data of the DNA-SIP experiment were combined with the measured density of each DNA-SIP fraction to calculate the average density of specific species (*Methylobacter*, *Methylotenera* and *Flavobacterium*) per treatment (ammonium or nitrate amended incubations, only for the 'particle culture').

CARD-FISH and imaging
Cells for catalyzed reporter deposition fluorescence in situ hybridization (CARD-FISH) analysis were collected at the end of incubation experiment (i.e. for both the "particle" and "filtrate" cultures) by transferring 10 ml of medium to a 50 mL tube. Formaldehyde was added to a final concentration of 4% and the tubes were left overnight at 4°C to fixate the cells. The formaldehyde-fixed cells of the ammonium- and nitrate-supplemented incubation experiments were deposited onto gold-coated polycarbonate filters, other samples were deposited on non-coated polycarbonate filters (both 0.45 mm pore size). Cell density was checked with SybrGreen staining after which filters were used for CARD-FISH. In short, cells were embedded in low-melting point agarose before being permeabilized using lysozyme (10 g L^{-1}) for 1 h at 37 °C. Probes (50 ng μL^{-1}) were mixed with hybridization buffer in a 1:200 ratio. Filters were incubated with hybridization mix for 18 h at 35 °C. Probe details are shown in Table S1. Probe sequences for *Methylobacter* and *Methylotenera* were validated to fit the specific species in our samples using the 16S rRNA sequences that were obtained by Illumina MiSeq sequencing (described above). Dyes Alexa 488 and Alexa 555 were used in the amplification step. The complete protocol can be found at https://www.arb-silva.de/fish-probes/fish-protocols.
After CARD-FISH staining, filters were viewed and imaged using an Axioplan microscope with fluorescence filters L09 (BP 450/490 nm, FT 510 nm, LP 520 nm) and Cy3 (BP 535/50 nm, FT 620/25 nm, LP 565 nm). Images of cells that were used in this publication were taken with either the Axioplan microscope or using a Nikon Eclipse Ti microscope with an ET-mCherry filter at the Utrecht University Biology Imaging Centre.

NanoSIMS data collection and processing
Analysis by Nanoscale Secondary Ion Mass Spectrometry (NanoSIMS) was performed with the NanoSIMS 50L instrument (Cameca, Gennevilliers, France) operated at Utrecht University, using the same filters as treated and imaged for CARD-FISH. First, areas on the filter containing target cells were located by fluorescence microscopy (see above) and marked using photo-ablation. This helped their localization in the NanoSIMS instrument. Each area of interest (squares of 20-40 mm in size) was first pre-sputtered until secondary ion yields stabilized. Afterwards, the area was rasterred multiple times (typically 20-80 planes) with a Cs^+ primary ion beam (1-2 pA, dwell time of 1 ms/pixel) while detecting the secondary ions $^{12}C^{14}N^-$ and $^{13}C^{14}N^-$ with separate electron multiplier detectors. NanoSIMS data was processed

with the Look@NanoSIMS software (Polerecky *et al.*, 2012). After alignment of individual planes, regions of interest (ROIs) corresponding to individual cells were drawn manually based on the $^{12}C^{14}N$ ion counts, which represent biomass. Subsequently, the cellular ^{13}C atom fraction was evaluated from the total ion counts of $^{13}C^{14}N$ and $^{12}C^{14}N$ accumulated over the ROI pixels as $x(^{13}C) = {}^{13}C^{14}N/({}^{13}C^{14}N+{}^{12}C^{14}N)$. ROI classification as *Methylobacter*, *Methylotenera* and 'others' was done based on the overlay of the NanoSIMS and fluorescence (CARD-FISH) images. A sample of the culture not grown on $^{13}CH_4$ was used as a control sample (Fig. S3). Due to the low number of imaged cells, no statistical analysis was performed on NanoSIMS data.

Results

The experimental procedures that lead to two enrichment cultures used for this study have been described previously (van Grinsven et al., 2020a, b). Shortly, the first enrichment culture ("particle culture") was dominated by 16S rRNA gene sequences affiliated to the methanotroph *Methylobacter* sp. (43%) and to the methanol-oxidizing methylotroph *Methylotenera* sp. (21%; Fig. S1), and was obtained from the mixed winter water column of the eutrophic Lacamas Lake (van Grinsven et al., 2020b). This culture was used to perform incubation studies under oxic/anoxic conditions with the addition of ammonium or nitrate as nitrogen source as previously reported, showing methane oxidation occurred under oxic, but not under anoxic conditions (van Grinsven et al., 2020b; Fig. S1, Table S2). The aerobic methane oxidation rate was enhanced by the presence of nitrate (van Grinsven et al., 2020b). The *Methylobacter* sp. 16S rRNA gene sequences from the enrichment culture, as well as from natural waters, field and laboratory incubation experiments (van Grinsven et al., 2020a,b), formed a subcluster of closely related sequences (i.e. 96-99% similarity) within the *Methylobacter* sp. clade 2 cluster (described in Smith *et al.*, 2018). Besides this *Methylobacter* sp.-dominated enrichment culture, a second enrichment culture was obtained with similar relative abundances of *Methylotenera* sp. and total methanotrophs, but rather than a domination of *Methylobacter* sp., the methanotrophic community consisted of both *Methylobacter* and *Methylomonas* spp. ("particle culture"; Fig. S1; Table S2).

^{13}C-label incorporation analysis by DNA-SIP

The "particle enrichment culture" (containing 43% *Methylobacter* sp. and 21% *Methylotenera* sp., Fig. S1) was used for incubation experiments with ^{13}C-labeled methane to be able to follow the incorporation of methane-derived carbon into the DNA of the microbial community by using DNA-SIP. In both the incubation experiments with ammonium and nitrate, ^{13}C-methane was the only external carbon source, as no CO_2 was added and the experiments were performed in the dark to exclude phototrophic CO_2 fixation and oxygen production. ^{13}C-enrichment of the cells will increase the molecular weight of the DNA, causing the DNA to end up in higher density fractions than unlabeled DNA. A high average density, and thus ^{13}C-enrichment, was observed for both the *Methylobacter* and *Methylotenera* genera, compared to DNA belonging to the unlabeled *Flavobacterium* genus (Fig. 1). *Flavobacterium* comprised 6–8% of the total 16S rRNA gene reads in the various incubations. *Methylotenera* sp. was ^{13}C-enriched in the incubation with nitrate, but only to a minor extent in the incubation with ammonium (Fig. 1). In contrast, *Methylobacter* sp. was ^{13}C-enriched in the incubation experiments with nitrate and

ammonium, although the average density of the *Methylobacter* DNA fractions (i.e. the ^{13}C-label incorporation) was higher in the incubation with nitrate than with ammonium (Fig. 1).

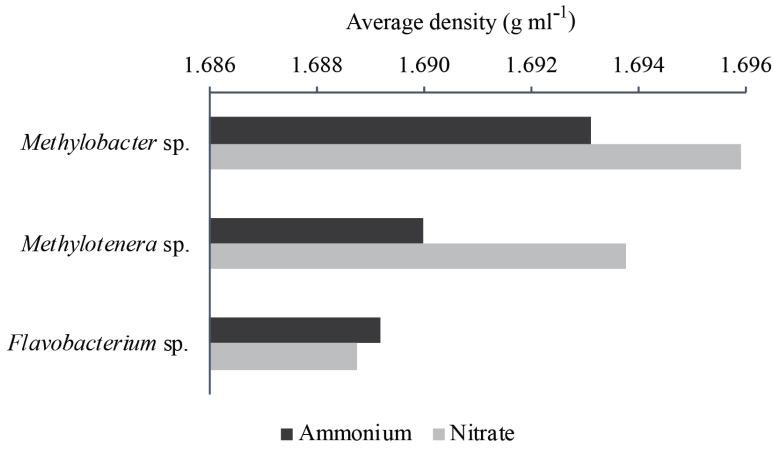

Fig. 1. Average density (in g ml^{-1}) of *Methylobacter* sp., *Methylotenera* sp. and *Flavobacterium* sp. DNA fractions as observed in the DNA-SIP analysis of the incubation experiments with the "particle enrichment culture" amended with ammonium and nitrate. ^{13}C-labeling of the DNA results in a higher average density, as is observed in *Methylobacter* sp. in both the ammonium and nitrate incubations, and in *Methylotenera* sp. in the nitrate incubation. *Flavobacterium* sp. is a non-methylotrophic genus that was abundant in both the ammonium and nitrate incubations (5–8% of total 16S rRNA reads, van Grinsven et al., 2020b), which serves as a reference.

Visualization of Methylobacter and Methylotenera cells

Microbial cells were identified using CARD-FISH with probes Mlb482 (targeting *Methylobacter*) and MET1216 (targeting the family *Methylophilaceae*, which, in our incubation experiments, was dominated by the genus *Methylotenera*, with <3% of *Methylophilaceae* 16S rRNA reads belonging to non-*Methylotenera* genera). Both *Methylobacter* and *Methylophilaceae* (from here on called *Methylotenera*) cells were abundant in the incubations with ammonium and nitrate, of both the "particle" and "filtrate" cultures, with *Methylobacter* cells more abundant than *Methylotenera* cells, based on visual assessment. Based on the positive CARD-FISH imaging with the Mlb482 probe, *Methylobacter* cells were rod-shaped, 2–3 mm in length and found in large and small clusters, in pairs, or as single cells (Fig. 2). Some clusters were sheet-like, with a single layer of cells (Fig. 2D), whereas other clusters were stacked in several layers and visible as piles of cells in the microscope images (Fig. 2C). MET1216-*Methylotenera*-stained cells were more variable in shape and size than the *Methylobacter* cells, and appeared in rod and cocci shapes, 1-3 µm in length. Combined clusters of *Methylobacter* and *Methylotenera* seemed to be dominated by *Methylobacter* cells, with a lower abundance of *Methylotenera* cells spread throughout the cluster (Fig. 2B, 5C). *Methylotenera* cells were also found as single cells (Fig. 2A), or in clusters containing only *Methylotenera* cells (Fig. 3G).

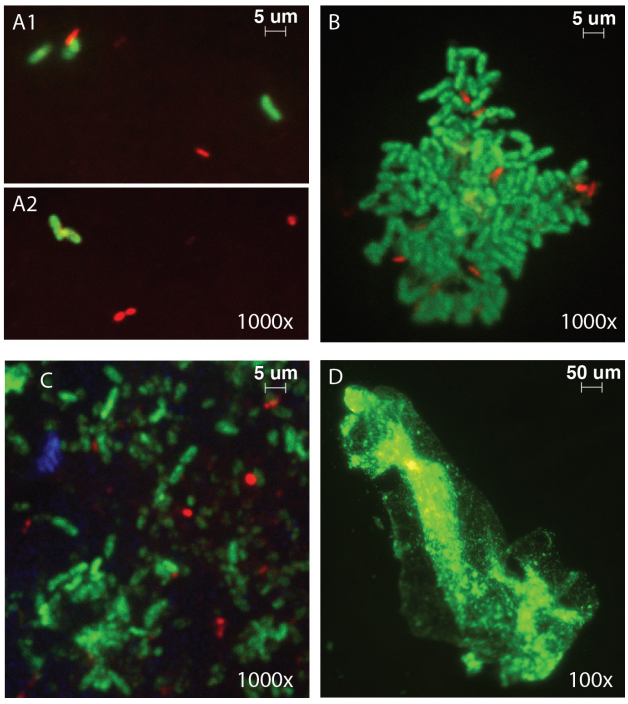

Fig. 2. Representative images revealing CARD-FISH stained cells in the incubation experiments: A; cells in pairs, B; single-layer cluster, C; Multi-layer cluster, D; sheet-like cluster. *Methylobacter* sp. is shown in green and *Methylotenera* sp. in red in panels A, B and C. The sample used for panel D was not stained for *Methylotenera* sp. cells and thus only *Methylobacter* sp. cells are visible (in green). Panel A1 and A2 show two separate images of the same incubation and microscope slide. The microscope magnification that was used is shown in the bottom-right corner of images.

^{13}C-label incorporation analysis by NanoSIMS

Microbial assimilation of the ^{13}C-labeled carbon in the incubations with ammonium and nitrate, of both the "particle" and "filtrate" cultures, was also evaluated using NanoSIMS, showing ^{13}C incorporation in cells of both *Methylobacter* and *Methylotenera* spp. (Fig. 3). No difference was observed in label incorporation between the two enrichment cultures ("particle culture" and "filtrate culture"; Fig. S2). In contrast, natural abundance of ^{13}C (atom fraction 0.0105) was observed in *Methylobacter* and *Methylotenera* cells grown with non-labeled methane, as well as in microbial community members not belonging to the *Methylobacter* and *Methylotenera* genera (i.e. cells that did not get fluorescently labeled by CARD-FISH) that were present in the labeled-methane incubations (Fig. S3). The degree of ^{13}C incorporation in *Methylobacter* and *Methylotenera* ranged widely among individual cells (^{13}C atom fractions ranging between 0.01–0.5). In addition, for both genera unlabeled cells were detected in the labeled-methane incubations, often in close proximity to highly ^{13}C-labeled cells (Fig. 3). ^{13}C-labeled cells were detected in both ammonium and nitrate-supplemented incubations and also in *Methylotenera* cells that were not in close proximity to *Methylobacter* cells (Fig. 3G-I).

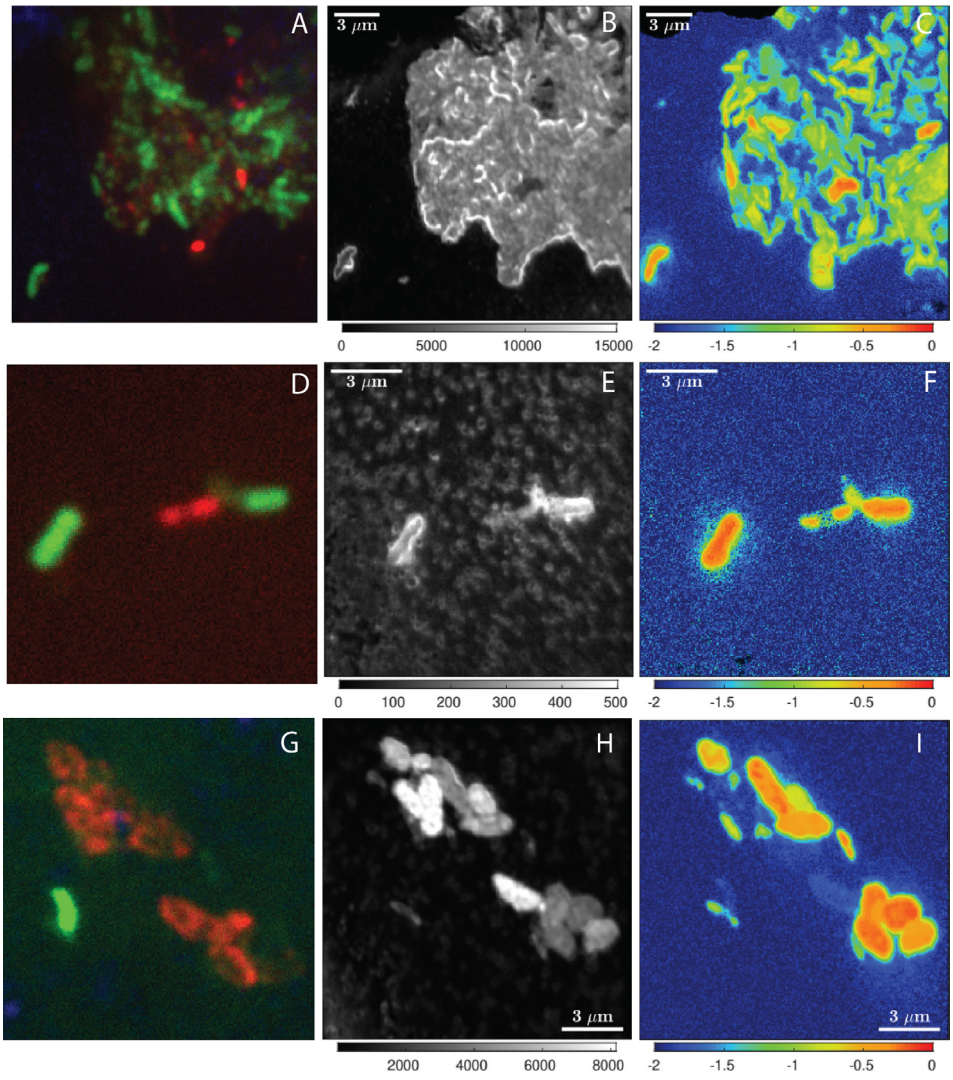

Fig. 3. A large (A-C) and two small (D-F and G-I) cell clusters, consisting of *Methylobacter* sp. and *Methylotenera* sp. cells, detected in the incubation with nitrate. Panels A, D and G show CARD-FISH images with green cells representing *Methylobacter* sp. cells (Mlb482 probe) and red cells representing *Methylotenera* sp. cells (MET1216 probe). Panels B, E and H show images of $^{12}C^{14}N$ ion counts, representing biomass distribution on the filter. Panels C, F and I show the corresponding images of ^{13}C atom fraction (calculated as $^{13}C^{14}N/(^{12}C^{14}N+^{13}C^{14}N)$), and shown in a log-scale for improved visibility), revealing the presence of methane-derived ^{13}C in both *Methylobacter* and *Methylotenera* cells. An overview of the $^{13}C^{14}N/(^{12}C^{14}N+^{13}C^{14}N)$ values of regions of interest is shown in Fig. S2.

Discussion

Methane-derived carbon is an important carbon source for many ecosystems (Murase and Frenzel, 2007; Jones and Grey, 2011; Sanseverino *et al.*, 2012), and methanotrophs such as *Methylobacter* sp. can play a key role in the food web of aquatic systems, facilitating the transfer of methane-derived carbon up to higher trophic levels. Earlier experiments in Lacamas Lake showed high methane turnover rates (70 μM day^{-1} in water column incubations, 420 μM day^{-1} in enrichment culture experiments; van Grinsven *et al.*, 2020a, b). The microbial community of the enrichment cultures obtained was dominated by *Methylobacter* and *Methylotenera* species (van Grinsven et al. 2020a, b; Fig. S1). Methanotrophs of the genus *Methylobacter* are commonly found in lakes, wetlands, marine systems, soils and rice paddies (Bowman *et al.*, 1994; Smith *et al.*, 1997; Wartiainen *et al.*, 2006; Khmelenina *et al.*, 2010; Wei *et al.*, 2016b). Members of the *Methylotenera* genus are known for their capability to oxidize methanol, using oxygen or nitrate as an electron acceptor (Kalyuzhnaya *et al.*, 2006; Mustakhimov *et al.*, 2013). The co-occurrence of methanotrophs and non-methanotrophic methylotrophs in Lacamas Lake is not unprecedented; it has been detected in lake systems before and has been suggested to involve a partnership based on the exchange of carbon compounds (Oshkin *et al.*, 2014; Hernandez *et al.*, 2015; Wei *et al.*, 2016a). However, the mechanism behind the relationship between the organisms remains under debate. Most earlier studies were performed on artificial communities or co-cultures, although several studies on Lake Washington sediment microcosms suggested that a methylotroph–methanotroph partnership could be of large importance in determining the response to changes in methane concentration in lake sediments (Beck *et al.*, 2011; Oshkin *et al.*, 2014; Hernandez *et al.*, 2015). A co-occurrence of *Methylobacter* and methylotrophs and ^{13}C-labeled methane uptake by both species were also shown in Arctic sediments and soils, but the cause of the ^{13}C-labeling of the methylotroph was not further investigated (Martineau *et al.*, 2010; He *et al.*, 2012).

To the best of our knowledge, this study is the first one that provides direct evidence and visualization of methane-derived carbon incorporation in both species and, thus, a potential partnership of bacteria belonging to the families *Methylococcaceae* and *Methylophilaceae* in the water column of a lake. This partnership has been suggested to be affected by the amount of methanol generated from methane, released by the methanotroph, which was recently shown to be affected by lanthanides (Krause *et al.*, 2017). Earlier studies have addressed the effect of oxygen on the co-occurrence of methanotrophs and non-methanotrophic methylotroph (Oshkin *et al.*, 2014; Hernandez *et al.*, 2015), but no other electron acceptors have been examined, nor were physical effects like aggregate formation evaluated. Here, we examined the effect of both chemical and physical factors on the methanotroph-methylotroph partnership, specifically on the interaction between *Methylobacter-Methylotenera*.

The *Methylobacter* species that dominated the enrichment culture and the water column of Lacamas Lake, in both summer and winter, was shown to belong to the *Methylobacter* clade 2, with *Methylobacter tundripaludum* as the most closely related cultured relative (>96% identical, van Grinsven *et al.*, 2020a). The *Methylotenera* sp. present in the enrichment culture are closely related to species isolated from Lake Washington sediments (Kalyuzhnaya *et al.*, 2006, 2011), as was determined by van Grinsven et al. (2020b). The co-occurrence of the two species was found in the water column of Lacamas Lake, in water column incubations, and in enrichment cultures obtained from the Lacamas Lake water column (R^2 = 0.7 for correlation

between *Methylobacter* and *Methylotenera* spp. relative abundance), and also in sediment and arctic lake samples (He *et al.*, 2012; Oshkin *et al.*, 2014; de Jong *et al.*, 2018; Fig. 4). This and the relative high abundance of these species suggests that this interaction may be relevant for the carbon transfer in lake food webs.

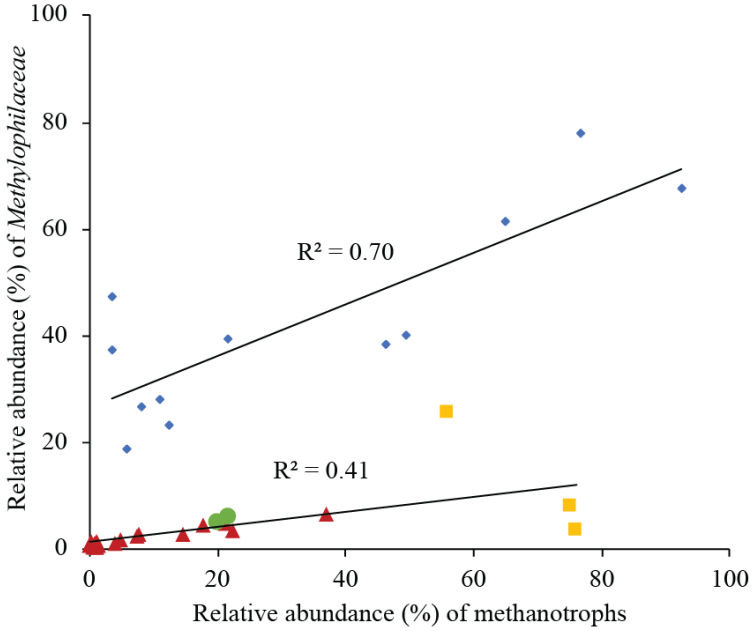

Fig. 4. Methanotroph and *Methylophilacea* (which includes the genus *Methylotenera*) relative abundance in the water column and incubations of Lacamas lake, the source of the enrichment culture used in this study, as observed by van Grinsven et al. (2020a) (red triangles), in sediment incubation experiments by Oshkin et al. (2014) (blue diamonds), Arctic sediment enrichment cultures by de Jong et al. (2018) (green circles), and Arctic water column enrichment cultures by He et al. (2012) (yellow squares). The trendlines show the linear regression of the Oshkin et al. (2014) data (blue diamonds; upper trendline), and the combined linear regression of the de Jong et al. (2018), He et al. (2012) and van Grinsven et al. (2019) data (lower trendline).

Carbon transfer from Methylobacter to Methylotenera cells

The presence of ^{13}C-labeled 16S rRNA genes sequences belonging to the non-methanotrophic *Methylotenera* sp. in our oxic incubations supplemented with nitrate (Fig. 1) revealed the incorporation of methane-derived carbon into *Methylotenera* sp. Its genome did not contain the gene required for the first step of methane oxidation, *pmoA* (van Grinsven et al., 2020b). This is consistent with their absence in any of the other published genomes of *Methylotenera* species (*M. mobilis* and *M. versatilis*; Kalyuzhnaya *et al.*, 2006, 2008, 2011; Lapidus *et al.*, 2011). Therefore, a direct usage of the labeled methane by the *Methylotenera* sp. is highly unlikely. Labeled CO_2 or biomass, produced by methanotrophs, could potentially lead to indirect labeling of community members (i.e. scrambling), including *Methylotenera* sp. As many organisms can fix CO_2, autotrophic ^{13}C-CO_2 assimilation would be expected to result in a low

signal among several autotrophic groups among the microbial community. In contrast, we observe no labeling in non-methylotrophs (i.e. *Flavobacterium* sp.; Fig. 1), and a highly elevated labeling in *Methylotenera* species. We, therefore, expect *Methylotenera* sp. to use other highly labeled carbon substrates, that cannot be used by the majority of the community, rather than labeled CO_2. Labeled biomass degradation, and consumption of the degradation products, could have also resulted in labeling of non-methanotrophs, but the incubation experiments lasted only 2–3 days, therefore we expect labeled biomass degradation to be a minor component of labeled carbon cycling in the incubation setup.

The co-occurrence of *Methylobacter* and *Methylotenera* spp. in natural environments has been studied in sediments, soils and landfills, but not in the water column of lakes (Martineau *et al.*, 2010; He *et al.*, 2012; Beck *et al.*, 2013; Hernandez *et al.*, 2015; Wei *et al.*, 2016b). Based on these previous studies, and on the genes of the carbon metabolism detected in the genome of the *Methylotenera* sp. present in our experiments (no *pmoA* gene detected, complete methanol oxidation pathway to CO_2; van Grinsven *et al.*, 2020b), we expect methanol to be the methane-derived component that is assimilated by *Methylotenera* sp. The production of methanol, by conversion of methane to methanol, is the first step in the methane oxidation process by methane oxidizing bacteria such as *Methylobacter* sp. (Fig. 5). Typically, methanol continues to be oxidized to formaldehyde, and the carbon is then assimilated or released as CO_2 (Fig. 5). Excretion of methanol by methanotrophs has been observed before, and was described as a mismatch between processes in the cell, producing more methanol than can be consumed, resulting in a release of methanol outside the cell (Tavormina *et al.*, 2017). The release of methanol has been shown to lead to an energy deficiency in the methanotroph (Xin *et al.*, 2004, 2007), resulting in a decreased methane oxidation rate. Previous studies have reported high free methanol concentrations in methanotroph cultures (up to 100 M, Xin *et al.*, 2004, 2007; Tavormina *et al.*, 2017) that seem to inhibit further methanol production by the methanotrophic cells. In that sense, the consumption of free methanol by *Methyloterena* sp. could stimulate activity of the methanotrophs, by removing the surplus of inhibitory methanol from the media. Although carbon transfer from methanotrophs to methylotrophs is generally suggested to be based on methanol exchange (Oshkin *et al.*, 2014; Wei *et al.*, 2016a), another study has also shown formaldehyde excretion and accumulation in the medium by methanotrophs under high oxygen concentrations (Costa *et al.*, 2001), up to formaldehyde concentrations that inhibited the methanotrophs. As the oxygen concentration in our incubation experiments was high, it is also possible that formaldehyde was excreted by the *Methylobacter* sp. The removal of formaldehyde by the *Methylotenera* sp. would then enhance the methane oxidation rate by reducing the concentration of formaldehyde to subtoxic levels.

Spatial analysis of the Methylobacter–Methylotenera interaction

The NanoSIMS data of our study confirms our DNA-SIP data that methane-derived carbon is assimilated by *Methylobacter* sp. as well as *Methylophilaceae* (according to 16S rRNA sequencing >97% assigned to *Methylotenera* spp.) cells, and that no other community members got ^{13}C-labeled. In addition, the combination of CARD-FISH and NanoSIMS analyses was used to visualize the co-occurrence of *Methylobacter* and *Methylotenera* spp. for the first time. This data showed (^{13}C-labeled) *Methylobacter* and *Methylotenera* spp. in close vicinity (Fig 2B, C; Fig. 3A–C), as well as physically separated (Fig. 2A; Fig. 3D–I), revealing that the interaction between the methanotroph *Methylobacter* sp. and the methylotroph *Methylotenera* sp. is apparently

independent of direct physical interaction of the two partners. We cannot exclude the possibility that the cell-distribution has changed due to the deposition and fixation process, but our data, which show a large number of single cells and clusters of only *Methylotenera* sp. cells (e.g. Figs. 2A and 2D), lead us to the assume that these distributions reflect the distributions in the enrichment culture.

The exchanged methane-derived carbon products could be dissolved in the medium, and reach the methylotrophs via diffusion. However, this would imply that these carbon-products are available 'free-for-all', which raises the question why specifically *Methylotenera* sp. can profit from these carbon-excretions, and not other methylotrophs. If the methane-derived carbon products are indeed released into the water column, and are thus freely accessible to other organisms, this could also have implications for the methane cycle from the production side, as these compounds could then be used for methylotrophic methanogenesis (Lovley and Klug, 1983; Narrowe *et al.*, 2019). The lack of physical contact between *Methylobacter* sp. and *Methylotenera* sp. makes DIET, which has been shown to be important in the relationship between anaerobic methane oxidizing archaea and their syntrophic partners (Wegener *et al.*, 2015; Krukenberg *et al.*, 2018) and has also been suggested to happen between *Methylobacter* sp. and *Methylotenera* sp. (Yu and Chistoserdova, 2017), unlikely. The lack of cell-to-cell contact between part of the *Methylobacter* and *Methylotenera* cells, and the expectation that nanowires do not occur over these distances and in these species, invalidate this possibility for the interaction between *Methylobacter* and *Methylotenera* cells.

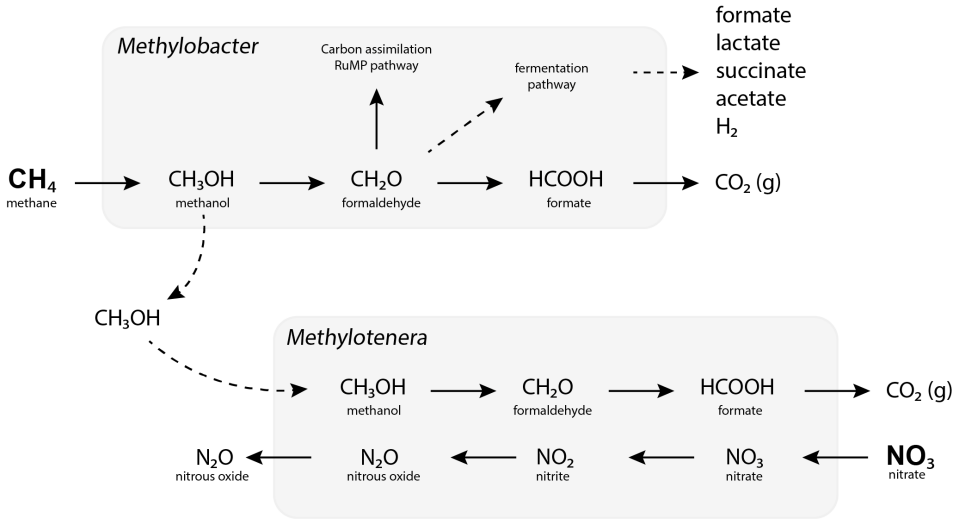

Fig. 5. Schematic representation of the relevant pathways in the methanotroph *Methylobacter* sp. and in the methylotroph *Methylotenera* sp. Although energetically unfavorable for the methanotrophs, methane-derived carbon is expected to partially 'leak' from the methanotroph after the conversion to methanol, to be used by the methylotroph *Methylotenera* sp. The methanol that does not leave the methanotroph cell is converted to formaldehyde, which is then partially used for carbon assimilation via the RuMP pathway and partially leaves the cell as CO_2, or in the case of oxygen limitation, formaldehyde can enter a fermentative pathway, eventually leaving the cell as mixed-acid fermentation products. Methanol is oxidized in *Methylotenera* sp., possibly coupled to the reduction of nitrate.

Effect of nitrate on the Methylobacter-Methylotenera interaction

Collectively, the results of this study show, in line with the results of van Grinsven et al. (2020b), that nitrate stimulates methane oxidation by the methanotroph *Methylobacter* and that, under oxic conditions with nitrate, but not or very limited in the presence of ammonium, products of methane oxidation by *Methylobacter* sp. are incorporated into the non-methanotrophic *Methylotenera* cells. Similarly, in water column incubations enhanced methane oxidation rates were observed after the addition of nitrate (van Grinsven *et al.*, 2020). The nitrate concentration in the water column of eutrophic Lacamas Lake has been shown to vary strongly over the year (0.2–75 µM; Deemer *et al.*, 2011; van Grinsven *et al.*, 2019), and the effect of nitrate on methane oxidation rates and carbon transfer may thus have important implications in the lake ecosystem. Ammonium can cause competitive inhibition of methane oxidation due to its structural similarity to methane (Bédard and Knowles, 1989), although the much higher affinity of the methane monooxygenase enzyme for methane (600–1300-fold higher) likely limits this effect. Earlier studies have found both increases and decreases in the methane oxidation rate after ammonium addition (Bodelier *et al.*, 2000; Walkiewicz *et al.*, 2018), as well as for nitrate addition (Geng *et al.*, 2017; Walkiewicz and Brzezińska, 2019). The nitrate inhibitory effect may be indirect, due to the conversion of nitrate to nitrite (Roco *et al.*, 2016), which is known as an inhibitor of methane oxidation (Dunfield and Knowles, 1995; Hütsch, 1998). As high methane oxidation rates in both our ammonium and nitrate-amended incubations were observed, inhibition does not seem to be an important factor. Nitrate has been shown before to be used by methanotrophs for denitrification, which can be coupled to methane oxidation when oxygen is limiting (Smith *et al.*, 2018). However, the genome of the *Methylobacter* sp. present in our incubations lacks the *nar* gene required to perform the dissimilatory conversion of nitrate to nitrite, as previously reported in van Grinsven *et al.* (2020a). We did detect, however, the *norBC* and *nirK* genes, encoding for part of the denitrification pathway, from nitrite to nitrous oxide, as well as the *nas* gene, encoding for nitrate to nitrite conversion in the assimilatory nitrate reduction pathway (van Grinsven *et al.*, 2020a). Given the high seasonal nitrate inflow in eutrophic systems such as Lacamas Lake, the observed stimulation of *Methylobacter* sp. by the addition of nitrate could give these methanotrophs an advantage in occupying their niche. Possibly, the enhanced methane oxidation rates are related to the enhanced methane-derived carbon-assimilation by *Methylotenera* sp. Only in the presence of nitrate, *Methylotenera* sp. assimilates significant amounts of methane-derived carbon. In the incubations with ammonium, DNA of *Methylotenera* sp. was labeled to only a small degree, despite its high relative abundance in those incubations (15.3%). In order to determine whether this could provide an explanation of the enhanced methane oxidation rates by nitrate addition, we explore what may cause the different behavior of *Methylotenera* sp. in the incubations with ammonium and nitrate. One explanation could simply be enhanced activity of *Methylobacter* sp. in the nitrate incubations, causing a higher substrate availability to *Methylotenera* sp. We, however, consider this unlikely as the major driver since the methane oxidation rate in the incubation experiments, and thus the production of methane-derived reaction products, was 2–4 times higher than in water column incubations, where we also observe a co-occurrence of *Methylobacter* sp. and *Methylotenera* sp. (van Grinsven *et al.*, 2020a). There could, however, be factors that affect the release of reaction intermediate by *Methylobacter* cells, which is generally considered an unfavorable process for the *Methylobacter* sp. itself. Factors that are known to affect the methanol release by methanotrophic bacteria are the concentrations of lanthanides (Krause *et al.*, 2017) and CO_2 (Xin *et al.*, 2004) in the medium. We are, however, the first to suggest

an effect of nitrate on the excretion of reaction intermediates. Another possibility is that not the excretion (by *Methylobacter* sp.) is dependent on the presence of nitrate, but the uptake of reaction products by *Methylotenera* sp. Several studies have discussed whether nitrate is required for methanol oxidation by *Methylotenera* sp. and although an increase in relative abundance of *Methylotenera* sp. was observed in incubations with nitrate (Beck *et al.*, 2013), none have shown the effect of nitrate on the methane-derived ^{13}C-label incorporation. Mustakhimov *et al.* (2013) have shown in oxic conditions the operation of an active denitrification pathway in *M. mobilis*, but it was not essential. Genome analysis of the *Methylotenera* sp. present in our incubations revealed the presence of the genes encoding for nitrate transporters, assimilatory nitrate reductase (Nas), nitrite reductase (NirBD) to ammonia, and to nitric oxide (NirK), as well as the gene coding for the nitric oxide reductase (NorBC) to nitrous oxide (N_2O) (van Grinsven et al., 2020b). A study by Mustakhimov *et al.* (2013) studying the phenotype of mutants of *M. mobilis* in genes predicted to encode functions of the denitrification pathway, demonstrated that the single subunit nitrate reductase (Nap; Mmol_1648) appears to be involved in both the assimilatory and dissimilatory denitrification pathways. Here, we confirmed that the assimilatory nitrate reductase Nas of the *Methylotenera* sp. genome reported in our incubations was homologous to the nitrate reductase Nap of *M. mobilis*, therefore suggesting that the *Methylotenera* sp. detected in our incubations is also able to perform denitrification (Fig. 5).

Wastewater treatment studies have explored the potential use of aerobic methane oxidation-coupled denitrification for efficient removal of both methane and nitrate from waste (Modin *et al.*, 2008; Zhu *et al.*, 2016). More research is needed to determine whether the *Methylobacter–Methylotenera* interaction that is found in this study, would be suitable for such an industrial application.

Conclusions

Overall, cross-feeding on methane-derived carbon seems to be an important driver for the relationship between *Methylobacter* sp. and *Methylotenera* sp., and a possible gain for the *Methylobacter* species would be the removal of toxic compounds that inhibit methanotrophy. As no physical contact seems to be required for the *Methylobacter-Methylotenera* interaction, an exchange of electrons between the two species seems unlikely, as well as any other direct exchange of compounds. Released compounds are more likely to be freely available in the medium. Earlier research has shown that *Methylotenera* sp. can actively affect the methanol dehydrogenase gene expression in *Methylobacter* sp. (Krause *et al.*, 2017), and our research suggests that nitrate is an important factor in this interaction. More research on the pathways, mechanisms and potential beneficial effects for *Methylobacter* sp. is, however, required.

The observed nitrate-dependence of methane-derived carbon incorporation into *Methylotenera* sp. is novel and may be relevant for culture and ecosystems studies, although nitrate concentrations in environmental systems are generally much lower than in these enrichment cultures (up to 75 mM in the Lacamas Lake water column). Nevertheless, the *Methylobacter–Methylotenera* interaction could play a role in linking the carbon and nitrogen cycles of methane-rich lakes, with implications for the transfer of methane-derived carbon through the trophic levels of lake food webs.

Acknowledgements

We thank Keith Birchfield for sample collection, Michiel Kienhuis (Utrecht University NanoSIMS facility) for NanoSIMS analysis, Ilya Grigoriev (Utrecht University Biology Imaging Centre) for help with fluorescence microscopy and photo-ablation, Alejandro Abdala Asbun for help with bioinformatic analyses, and Saara Suominen, Sanne Vreugdenhil and Maartje Brouwer for help with DNA-SIP analyses. We also thank Cornelia Welte for helpful comments on an earlier draft of this manuscript. This work was supported by the Soehngen Institute of Anaerobic Microbiology (SIAM) Gravitation grant (024.002.002) of the Netherlands Ministry of Education, Culture and Science (OCW) and the Netherlands Organisation for Scientific Research (NWO) to JSSD and LV. The NanoSIMS facility at Utrecht University was financed through a large infrastructure grant (175.010.2009.011) by NWO.

Supplemental material

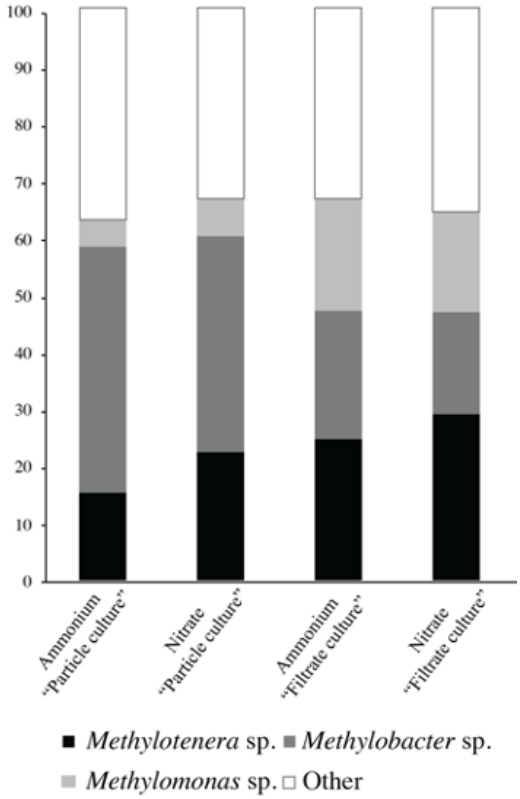

Fig. S1. Relative abundances (in % of the total 16S rRNA sequencing reads) of *Methylobacter*, *Methylomonas* and *Methylotenera* spp. at the end of the incubation experiments. Fig. adapted from van Grinsven et al. (2020b).

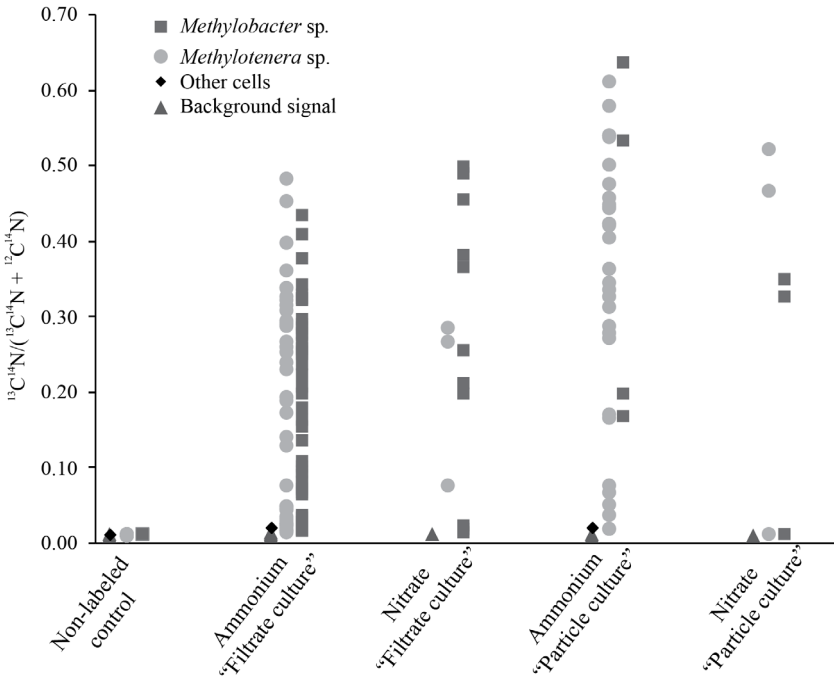

Fig. S2. Average ($^{13}C^{14}N/(^{13}C^{14}N+^{12}C^{14}N)$) atom fractions of NanoSIMS ROIs in the ammonium and nitrate treatment of both the 'particle culture' and 'filtrate culture'.

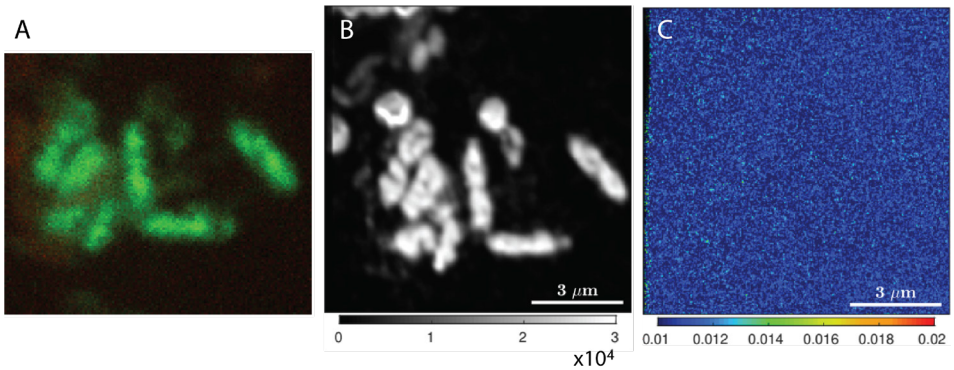

Fig. S3. CARD-FISH and NanoSIMS images of a control enrichment culture, grown without labeled methane. A; CARD-FISH images with green cells representing *Methylobacter* (Mlb482 probe). B; NanoSIMS $^{12}C^{14}N$ signal, representing biomass, C; NanoSIMS ^{13}C atom fraction ($^{13}C^{14}N/(^{12}C^{14}N + {}^{13}C^{14}N)$).

Table S1. Probe and primer sequences that were used for DNA amplification and CARD-FISH hybridization. For the CARD-FISH probes, the % formamide in the hybridization buffer is displayed.

Name	Sequence 5' - 3'	Formamide % [a]	Target	Reference
515F	GTGYCAGCMGCCGCGGTAA	-	General 16S rRNA bacteria and archaea	Caporaso *et al.*, 2012
806RB	GGACTACNVGGGTWTCTAAT	-	General 16S rRNA bacteria and archaea	Apprill *et al.*, 2015
MLB482	GGTGCTTCTTCTAAAGGTAATGT	35%	*Methylobacter*	Gulledge *et al.*, 2001
MET1216	TTACGTGTGAAGCCCTGGC	35%	*Methylophilales*	Own data and Ginige *et al.* (2004)

* if applicable

Table S2. Relative abundance of 16S rRNA operational taxonomic units, as detected in the incubation experiment samples used for NanoSIMS and DNA-SIP analysis. Adapted from van Grinsven et al. (2020b) ("Particle culture" data included in van Grinsven et al. 2020b).

	Ammonium		Nitrate	
	"Particle culture"	"Filtrate culture"	"Particle culture"	"Filtrate culture"
LLE-16S-1	1.6	0.8	0.3	0.1
LLE-16S-2	1.3	0.0	1.1	0.0
LLE-16S-3	0.6	0.0	0.0	0.0
LLE-16S-4	1.0	0.6	0.2	0.6
LLE-16S-5	0.8	0.4	0.3	0.3
LLE-16S-6	0.7	0.1	0.1	0.1
LLE-16S-7	0.5	1.3	1.4	1.0
LLE-16S-8	0.5	0.0	0.1	0.0
LLE-16S-9	0.3	0.0	0.1	0.0
LLE-16S-10	0.6	0.2	0.2	0.4
LLE-16S-11	1.2	0.0	0.3	1.0
LLE-16S-12	0.6	0.9	1.1	1.1
LLE-16S-13	0.5	0.1	0.5	0.3
LLE-16S-14	0.6	0.5	0.6	0.2
LLE-16S-15	0.3	0.0	0.1	0.0
LLE-16S-16	0.5	0.2	0.1	0.4
LLE-16S-17	0.2	0.0	0.0	0.0
LLE-16S-18	0.3	0.0	0.7	0.0
LLE-16S-19	0.5	0.3	1.1	0.0
LLE-16S-20	0.1	0.0	0.4	0.1
LLE-16S-21	0.1	0.0	0.3	0.1
LLE-16S-22	0.5	0.2	0.8	0.2
LLE-16S-23	0.5	0.3	1.4	0.0
LLE-16S-24	0.2	0.2	0.4	0.0
LLE-16S-25	0.1	0.0	0.4	0.0
LLE-16S-26	0.1	0.0	0.5	0.0
LLE-16S-27	0.0	0.0	0.5	0.0
LLE-16S-28	0.1	0.0	0.0	0.0

References

Andrews, S., Krueger, F., Seconds-Pichon, A., Biggins, F., and Wingett, S. (2015) FastQC. A quality control tool for high throughput sequence data. Babraham Bioinformatics. *Babraham Inst.* **1**: 1.

Asbun, A.A., Besseling, M.A., Balzano, S., van Bleijswijk, J., Witte, H., Villanueva, L., and Engelmann, J.C. (2019) Cascabel: a flexible , scalable and easy-to-use amplicon sequence data analysis pipeline. *BioRxiv* **809384**:.

Bastviken, D., Cole, J.J., Pace, M.L., and van de Bogert, M.C. (2008) Fates of methane from different lake habitats: Connecting whole-lake budgets and CH4 emissions. *J. Geophys. Res. Biogeosciences* **113**: 1–13.

Bastviken, D., Tranvik, L.J., Downing, J.A., Crill, P.M., and Enrich-Prast, A. (2011) Freshwater Methane Emissions Offset the Continental Carbon Sink. *Science (80-.).* **331**: 50.

Beck, D.A.C., Hendrickson, E.L., Vorobev, A., Wang, T., Lim, S., Kalyuzhnaya, M.G., et al. (2011) An integrated proteomics/transcriptomics approach points to oxygen as the main electron sink for methanol metabolism in Methylotenera mobilis. *J. Bacteriol.* **193**: 4758–4765.

Beck, D.A.C., Kalyuzhnaya, M.G., Malfatti, S., Tringe, S.G., Glavina del Rio, T., Ivanova, N., et al. (2013) A metagenomic insight into freshwater methane-utilizing communities and evidence for cooperation between the Methylococcaceae and the Methylophilaceae. *Peer J* **1**: e23.

Bédard, C. and Knowles, R. (1989) Physiology, biochemistry, and specific inhibitors of CH4, NH4+, and CO oxidation by methanotrophs and nitrifiers. *Microbiol. Rev.* **53**: 68–84.

Bodelier, P.L.E., Roslev, P., Henckel, T., and Frenzel, P. (2000) Stimulation by ammonium-based fertilizers of methane oxidation in soil around rice roots. *Nature* **403**: 421.

Bowman, J.P., Sly, L.I., Nichols, P.D., and Hayward, A.C. (1994) Revised taxonomy of the methanotrophs: Description of Methylobacter gen. nov., Emendation of Methylococcus, validation of Methylosinus and Methylocystis species, and a proposal that the family Methylococcaceae includes only the group I methanotrophs. *Int. J. Syst. Bacteriol.* **44**: 375–375.

Caporaso, J.G., Lauber, C.L., Walters, W.A., Berg-Lyons, D., Huntley, J., Fierer, N., et al. (2012) Ultra-high-throughput microbial community analysis on the Illumina HiSeq and MiSeq platforms. *ISME J.* **6**: 1621–1624.

Conrad, R. (2009) The global methane cycle: Recent advances in understanding the microbial processes involved. *Environ. Microbiol. Rep.* **1**: 285–292.

Costa, C., Vecherskaya, M., Dijkema, C., and Stams, A.J.M. (2001) The effect of oxygen on methanol oxidation by an obligate methanotrophic bacterium studied by in vivo 13C nuclear magnetic resonance spectroscopy. *J. Ind. Microbiol. Biotechnol.* **26**: 9–14.

Deemer, B.R., Harrison, J. a., and Whitling, E.W. (2011) Microbial dinitrogen and nitrous oxide production in a small eutrophic reservoir: An in situ approach to quantifying hypolimnetic process rates. *Limnol. Oceanogr.* **56**: 1189–1199.

Deemer, B.R., Harrison, J.A., Li, S., Beaulieu, J.J., Delsontro, T., Barros, N., et al. (2016) Greenhouse Gas Emissions from Reservoir Water Surfaces: A New Global Synthesis. *Bioscience* **66**: 949–964.

DelSontro, T., Beaulieu, J.J., and Downing, J.A. (2018) Greenhouse gas emissions from lakes and impoundments: Upscaling in the face of global change. *Limnol. Oceanogr. Lett.* **3**: 64–75.

Dunfield, P. and Knowles, R. (1995) Kinetics of inhibition of methane oxidation by nitrate, nitrite, and ammonium in a humisol. *Appl. Environ. Microbiol.* **61**: 3129–3135.

Dunford, E.A. and Neufeld, J.D. (2010) DNA stable-isotope probing (DNA-SIP). *J. Vis. Exp.* **42**: e2027.

Ettwig, K.F., Butler, M.K., Le Paslier, D., Pelletier, E., Mangenot, S., Kuypers, M.M.M., et al. (2010) Nitrite-driven anaerobic methane oxidation by oxygenic bacteria. *Nature* **464**: 543–548.

Geng, J., Cheng, S., Fang, H., Yu, Guirui, Li, X., Si, G., et al. (2017) Soil nitrate accumulation explains the nonlinear responses of soil CO2 and CH4 fluxes to nitrogen addition in a temperate needle-broadleaved mixed forest. *Ecol. Indic.* **79**: 28–36.

van Grinsven, S., Asbun, A.A., Julia, C., Harrison, J., and Villanueva, L. (2020a) Methane oxidation in anoxic lake water stimulated by nitrate and sulfate addition. *Environ. Microbiol.* **22**: 766–782.

van Grinsven, S., Sinninghe Damsté, J.S., Harrison, J. and, Villanueva, L. (2020b) Impact of electron acceptor availability on methane-influenced microorganisms in an enrichment culture obtained from a stratified lake. *Front. Microbiol.*, in press.

He, R., Wooller, M.J., Pohlman, J.W., Quensen, J., Tiedje, J.M., and Leigh, M.B. (2012) Diversity of active aerobic methanotrophs along depth profiles of arctic and subarctic lake water column and sediments. *ISME J.* **6**: 1937–1948.

He, R., Wooller, M.J., Pohlman, J.W., Tiedje, J.M., and Leigh, M.B. (2015) Methane-derived carbon flow through microbial communities in arctic lake sediments. *Environ. Microbiol.* **17**: 3233–3250.

Hernandez, M.E., Beck, D.A.C., Lidstrom, M.E., and Chistoserdova, L. (2015) Oxygen availability is a major factor in determining the composition of microbial communities involved in methane oxidation. *PeerJ* **3**: e801.

Hütsch, B.W. (1998) Methane oxidation in arable soil as inhibited by ammonium, nitrite, and organic manure with respect to soil pH. *Biol. Fertil. Soils* **28**: 27–35.

Jones, R.I. and Grey, J. (2011) Biogenic methane in freshwater food webs. *Freshw. Biol.* **56**: 213–229.

Jones, R.I., Grey, J., Sleep, D., and Arvola, L. (1999) Stable Isotope Analysis of Zooplankton Carbon Nutrition in Humic Lakes. *Oikos* 97–104.

de Jong, A.E.E., in 't Zandt, M.H., Meisel, O.H., Jetten, M.S.M., Dean, J.F., Rasigraf, O., and Welte, C.U. (2018) Increases in temperature and nutrient availability positively affect methane-cycling microorganisms in Arctic thermokarst lake sediments. *Environ. Microbiol.* **20**: 4314–4327.

Kalyuzhnaya, M.G., Beck, D.A.C., Vorobev, A., Smalley, N., Kunkel, D.D., Lidstrom, M.E., and Chistoserdova, L. (2011) Novel methylotrophic isolates from lake sediment, description of Methylotenera versatilis sp. nov. and emended description of the genus Methylotenera. *Int. J. Syst. Evol. Microbiol.* **62**: 106–111.

Kalyuzhnaya, M.G., Bowerman, S., Lara, J.C., Lidstrom, M.E., and Chistoserdova, L. (2006) Methylotenera mobilis gen. nov., sp. nov., an obligately methelamine-utilizing bacterium within the family Methylophilaceae. *Int. J. Syst. Evol. Microbiol.* **56.12**: 2819–2823.

Kalyuzhnaya, M.G., Lapidus, A., Ivanova, N., Copeland, A.C., McHardy, A.C., Szeto, E., et al. (2008) High-resolution metagenomics targets specific functional types in complex microbial communities. *Nat. Biotechnol.* **26**: 1029–1034.

Kalyuzhnaya, M.G., Yang, S., Rozova, O.N., Smalley, N.E., Clubb, J., Lamb, A., et al. (2013) Highly efficient methane biocatalysis revealed in a methanotrophic bacterium. *Nat. Commun.* **4**: 1–7.

Khmelenina, V.N., Shchukin, V.N., Reshetnikov, A.S., Mustakhimov, I.I., Suzina, N.E., Eshinimaev, B.T., and Trotsenko, Y.A. (2010) Structural and functional features of methanotrophs from hypersaline and alkaline lakes. *Microbiology* **79**: 472–482.

Kits, K.D., Klotz, M.G., and Stein, L.Y. (2015) Methane oxidation coupled to nitrate reduction under hypoxia by the Gammaproteobacterium Methylomonas denitrificans, sp. nov. type strain FJG1. *Environ. Microbiol.* **17**: 3219–3232.

Krause, S.M.B., Johnson, T., Karunaratne, Y.S., Fu, Y., Beck, D.A.C., Chistoserdova, L., and Lidstrom, M.E. (2017) Lanthanide-dependent cross-feeding of methane-derived carbon is linked by microbial community interactions. *Proc. Natl. Acad. Sci. U. S. A.* **114**: 358–363.

Krukenberg, V., Riedel, D., Gruber-Vodicka, H.R., Buttigieg, P.L., Tegetmeyer, H.E., Boetius, A., and Wegener, G. (2018) Gene expression and ultrastructure of meso- and thermophilic methanotrophic consortia. *Environ. Microbiol.* **20**: 1651–1666.

Lapidus, A., Clum, A., LaButti, K., Kaluzhnaya, M.G., Lim, S., Beck, D.A.C., et al. (2011) Genomes of three methylotrophs from a single niche reveal the genetic and metabolic divergence of the methylophilaceae. *J. Bacteriol.* **193**: 3757–3764.

Lovley, D.R. and Klug, M.J. (1983) Methanogenesis from methanol and methylamines and acetogenesis from hydrogen and carbon dioxide in the sediments of a eutrophic lake. *Appl. Environ. Microbiol.* **45**: 1310–1315.

Martineau, C., Whyte, L.G., and Greer, C.W. (2010) Stable isotope probing analysis of the diversity and activity of methanotrophic bacteria in soils from the Canadian high Arctic. *Appl. Environ. Microbiol.* **76**: 5773–5784.

Modin, O., Fukushi, K., Nakajima, F., and Yamamoto, K. (2008) A membrane biofilm reactor achieves aerobic methane oxidation coupled to denitrification (AME-D) with high efficiency. *Water Sci. Technol.* **58**: 83–87.

Moore, J.W., Schindler, D.E., Scheuerell, M.D., Smith, D., and Frodge, J. (2003) Lake eutrophication at the urban fringe, Seattle region, USA. *Ambio* **32**: 13–18.

Murase, J. and Frenzel, P. (2007) A methane-driven microbial food web in a wetland rice soil. *Environ. Microbiol.* **9**: 3025–3034.

Murrell, J.C. (2010) The Aerobic Methane Oxidizing Bacteria (Methanotrophs). In, *Handbook of Hydrocarbon and Lipid Microbiology.*, pp. 1953–1966.

Mustakhimov, I., Kalyuzhnaya, M.G., Lidstrom, M.E., and Chistoserdova, L. (2013) Insights into denitrification in Methylotenera mobilis from denitrification pathway and methanol metabolism mutants. *J. Bacteriol.* **195**: 2207–2211.

Narrowe, A.B., Borton, M.A., Hoyt, D.W., Smith, G.J., Daly, R.A., Angle, J.C., et al. (2019) Uncovering the Diversity and Activity of Methylotrophic Methanogens in Freshwater Wetland Soils. *mSystems* **4**: 1–15.

Oshkin, I.Y., Beck, D.A., Lamb, A.E., Tchesnokova, V., Benuska, G., McTaggart, T.L., et al. (2014) Methane-fed microbial microcosms show differential community dynamics and pinpoint taxa involved in communal response. *ISME J.* **9**: 1–11.

Oswald, K., Graf, J.S., Littmann, S., Tienken, D., Brand, A., Wehrli, B., et al. (2017) Crenothrix are major methane consumers in stratified lakes. *ISME J.* **11**: 2124–2140.

Polerecky, L., Adam, B., Milucka, J., Musat, N., Vagner, T., and Kuypers, M.M.M. (2012) Look@NanoSIMS - a tool for the analysis of nanoSIMS data in environmental microbiology. *Environ. Microbiol.* **14**: 1009–1023.

Reed, D.C., Deemer, B.R., van Grinsven, S., and Harrison, J.A. (2017) Are elusive anaerobic pathways key methane sinks in eutrophic lakes and reservoirs? *Biogeochemistry* **134**: 29–39.

Roco, C.A., Bergaust, L.L., Shapleigh, J.P., and Yavitt, J.B. (2016) Reduction of nitrate to nitrite by microbes under oxic conditions. *Soil Biol. Biochem.* **100**: 1–8.

Sanseverino, A.M., Bastviken, D., Sundh, I., Pickova, J., and Enrich-Prast, A. (2012) Methane carbon supports aquatic food webs to the fish level. *PLoS One* **7**: e42723.

Saunois, M., Bousquet, P., Poulter, B., Peregon, A., Ciais, P., Canadell, J.G., et al. (2016) The global methane budget 2000 – 2012. *Earth Syst. Sci. Data* **8**: 697–751.

Saxton, M.A., Samarkin, V.A., Schutte, C.A., Bowles, M.W., Madigan, M.T., Cadieux, S.B., et al. (2016) Biogeochemical and 16S rRNA gene sequence evidence supports a novel mode of anaerobic methanotrophy in permanently ice-covered Lake Fryxell, Antarctica. *Limnol. Oceanogr.* **61**: S119–S130.

Schubert, C.J., Vazquez, F., Loesekann-Behrens, T., Knittel, K., Tonolla, M., and Boetius, A. (2011) Evidence for anaerobic oxidation of methane in sediments of a freshwater system (Lago di Cadagno). *FEMS Microbiol. Ecol.* **76**: 26–38.

Smith, G.J., Angle, J.C., Solden, L.M., Daly, R.A., Johnston, M.D., Borton, M.A., et al. (2018) Members of the Genus Methylobacter Are Inferred To Account for the Majority of Aerobic Methane Oxidation in Oxic Soils from a Freshwater Wetland. *MBio* **9**: 1–17.

Smith, K.S., Costello, A.M., and Lidstrom, M.E. (1997) Methane and trichloroethylene oxidation by an estuarine methanotroph, Methylobacter sp. strain BB5.1. *Appl. Environ. Microbiol.* **63**: 4617–4620.

Suominen, S., Dombrowski, N., Sinninghe Damsté, J.S., and Villanueva, L. (2020) A diverse uncultivated microbial community is responsible for organic matter degradation in the Black Sea sulphidic zone. *Environ. Microbiol.*

Taipale, S., Kankaala, P., Hahn, M., Jones, R., and Tiirola, M. (2011) Methane-oxidizing and photoautotrophic bacteria are major producers in a humic lake with a large anoxic hypolimnion. *Aquat. Microb. Ecol.* **64**: 81–95.

Tavormina, P.L., Kellermann, M.Y., Antony, C.P., Tocheva, E.I., Dalleska, N.F., Jensen, A.J., et al. (2017) Starvation and recovery in the deep-sea methanotroph Methyloprofundus sedimenti. *Mol. Microbiol.* **103.2**: 242–252.

Valenzuela, E.I., Avendaño, K.A., Balagurusamy, N., Arriaga, S., Nieto-Delgado, C., Thalasso, F., and Cervantes, F.J. (2019) Electron shuttling mediated by humic substances fuels anaerobic methane oxidation and carbon burial in wetland sediments. *Sci. Total Environ.* **650**: 2674–2684.

Walkiewicz, A. and Brzezińska, M. (2019) Interactive effects of nitrate and oxygen on methane oxidation in three different soils. *Soil Biol. Biochem.* **133**: 116–118.

Walkiewicz, A., Brzezińska, M., and Bieganowski, A. (2018) Methanotrophs are favored under hypoxia in ammonium-fertilized soils. *Biol. Fertil. Soils* **54**: 861–870.

Wartiainen, I., Hestnes, A.G., McDonald, I.R., and Svenning, M.M. (2006) Methylobacter tundripaludum sp. nov., a methane-oxidizing bacterium from Arctic wetland soil on the Svalbard islands, Norway (78° N). *Int. J. Syst. Evol. Microbiol.* **56.1**: 109–113.

Wegener, G., Krukenberg, V., Riedel, D., Tegetmeyer, H.E., and Boetius, A. (2015) Intercellular wiring enables electron transfer between methanotrophic archaea and bacteria. *Nature* **526**: 587–590.

Wei, X.M., He, R., Chen, M., Su, Y., and Ma, R.C. (2016a) Conversion of methane-derived carbon and microbial community in enrichment cultures in response to O2-availability. *Environ. Sci. Pollut. Res.* **23**: 7517–7528.

Wei, M., Qiu, Q., Qian, Y., Cheng, L., and Guo, A. (2016b) Methane oxidation and response of Methylobacter/Methylosarcina methanotrophs in flooded rice soil amended with urea. *Appl. Soil Ecol.* **101**: 174–184.

Whittenbury, R., Phillips, K.C., and Wilkinson, J.F. (1970) Enrichment, Isolation and Some Properties of Methane-utilizing Bacteria. *J. Gen. Microbiol.* **61**: 205–218.

Xin, J.Y., Cui, J.R., Niu, J.Z., Hua, S.F., Xia, C.G., Li, S. Ben, and Zhu, L.M. (2004) Production of methanol from methane by methanotrophic bacteria. *Biocatal. Biotransf.* **22**: 225–229.

Xin, J.Y., Zhang, Y.X., Zhang, S., Xia, C.G., and Li, S. Ben (2007) Methanol production from CO2 by resting cells of the methanotrophic bacterium Methylosinus trichosporium IMV 3011. *J. Basic Microbiol.* **47**: 426–435.

Yu, Z. and Chistoserdova, L. (2017) Communal Metabolism of Methane and the Rare Earth Element Switch. *J. Bacteriol.* **199**: e00328-17.

Yvon-Durocher, G., Allen, A.P., Bastviken, D., Conrad, R., Gudasz, C., St-Pierre, A., et al. (2014) Methane fluxes show consistent temperature dependence across microbial to ecosystem scales. *Nature* **507**: 488–91.

Zhang, J., Kobert, K., Flouri, T., and Stamatakis, A. (2014) PEAR: A fast and accurate Illumina Paired-End reAd mergeR. *Bioinformatics* **30**: 614–620.

Zhu, J., Wang, Q., Yuan, M., Tan, G.A., Sun, F., Wang, C., et al. (2016) Microbiology and potential applications of aerobic methane oxidation coupled to denitrifacation (AME-D) process : A review. *Water Res.* **90**: 203–215.

Chapter 6. Assessing the effect of humic substances and Fe(III) as potential electron acceptors for anaerobic methane oxidation in a marine anoxic system

Sigrid van Grinsven
Jaap S. Sinninghe Damsté
& Laura Villanueva

Abstract

Marine anaerobic methane oxidation (AOM) is generally assumed to be coupled to sulfate reduction, via a consortium of anaerobic methane oxidizing archaea (ANME) and sulfate reducing bacteria (SRB). ANME-1 are, however, often found as single cells, or only loosely aggregated with SRB, suggesting they perform a form of AOM independent of sulfate reduction. Oxidized metals and humic substances have been suggested as potential electron acceptors for ANME, but up to now, AOM linked to reduction of these compounds has only been shown for the ANME-2 and ANME-3 clades. Here, we explore the effect of different electron acceptors on anaerobic methane oxidation rates in incubations with anoxic Black Sea water containing ANME-1b. Incubation experiments with ^{13}C-methane and addition of the humic acids analogue anthraquinone-disulfonate (AQDS) showed a stimulating effect of AQDS on methane oxidation. Fe^{3+} enhanced the ANME-1b abundance, but did not substantially increase methane oxidation. Sodium molybdate, which was added as an inhibitor of sulfate reduction, surprisingly enhanced methane oxidation, possibly related to the dominant abundance of *Sulfurospirillum* in those incubations. Our data suggests the potential involvement of ANME-1b in AQDS-enhanced anaerobic methane oxidation, possibly via electron shuttling to AQDS or via interaction with other members of the microbial community.

Introduction

Methane is a potent greenhouse gas (warming potential 34 times greater than CO_2 (Forster *et al.*, 2007) and its atmospheric concentrations is rapidly increasing (Stocker *et al.*, 2013). There is a large and continuous production of methane in anaerobic marine sediments by methanogenic archaea. However, most of this methane is converted into carbon dioxide by oxidation, when methane is still in the sediment. It is estimated that marine anaerobic methane oxidizers consume 70-300 Tg CH_4 $year^{-1}$, reducing the atmospheric methane budget by 10-60% (Reeburgh, 2007; Conrad, 2009). The methane that is not oxidized in the sediments, gets released into the water column, via diffusion or bubbling. From there, it can be emitted to the atmosphere. Methane oxidation in the water column can also (partially) consume this methane and thus forms an additional filter to prevent methane emission from marine systems.

To be thermodynamically favorable, anaerobic methane oxidation needs to be coupled to the reduction of another compound. In marine settings, this compound is generally sulfate, and anaerobic methane oxidation is typically performed by a consortium of anaerobic methane oxidizing archaea (ANME) and sulfate reducing bacteria (SRB) (Boetius *et al.*, 2000). Methane oxidation coupled to sulfate reduction yields a Gibbs free energy yield of only –17 kJ mol^{-1}, which is near the minimum requirement for life, possibly being one of the factors explaining the slow growth rates of anaerobic marine methane oxidizers (doubling times 2-7 months; (Nauhaus *et al.*, 2007; Orphan *et al.*, 2009). Theoretically, methane oxidation coupled to the reduction of other compounds, such as Fe^{3+}, nitrate or nitrite, has a substantially higher energy yield (Segarra *et al.*, 2013). Metal-oxide dependent AOM by ANME has been detected in enrichment cultures (Ettwig *et al.*, 2016), but despite the thermodynamic advantages, observations of AOM not coupled to sulfate reduction in natural situations have been scarce. Egger et al. (2014) demonstrated iron oxide-mediated AOM was likely to occur in sediments of the Bothnian Sea (North-East Baltic), but the microorganisms involved were not identified. Scheller et al. (2016) showed that ANME were capable of performing methane oxidation with Fe^{3+} and 9,10-anthraquinone-2,6-disulfonate (AQDS), which was used as a humic acid analogue. Iron-mediated AOM, catalyzed by humic substances, was also detected by Valenzuela et al. (2019). Bai et al. (2019) also showed nitrate-reducing ANME were capable of using AQDS as an electron acceptor.

ANME oxidize methane via a reversed methanogenesis pathway (e.g. Hinrichs et al. 1999; Hallam et al. 2004). Three clades of ANME including several subclasses are recognized, all related to different groups of methanogens, namely ANME-1, ANME-2 and ANME-3 (Hinrichs *et al.*, 1999; Orphan *et al.*, 2001; Knittel *et al.*, 2005; Niemann *et al.*, 2006). All clades are regularly found in syntrophy with sulfate reducing bacteria (SRB), but whereas ANME-2 and ANME-3 are generally found in aggregates together with SRB cells, ANME-1 are often observed as single cells or loose aggregates (Cui *et al.*, 2015). The mechanism behind the ANME–SRB syntrophy is still under debate. A relationship based on the exchange of reaction products has been proposed (Valentine and Reeburgh, 2000; Moran *et al.*, 2008; Milucka *et al.*, 2012; Cui *et al.*, 2015), but other studies also suggested direct interspecies electron transfer (McGlynn *et al.*, 2015; Wegener *et al.*, 2015). ANME has been shown to be capable of forming intracellular wiring, creating a cell-to-cell connection that could allow a direct shuttling of electrons (Meyerdierks *et al.*, 2010; McGlynn *et al.*, 2015; Wegener *et al.*, 2015; Krukenberg *et al.*, 2018).

In this regard, the electron shuttling to abiotic particles such as oxidized metals or AQDS has only been observed in ANME of the clade ANME-2 (Scheller *et al.*, 2016; Bai *et al.*, 2019).
The Black Sea is rich in methane due to the release from numerous cold seeps, and despite active methane oxidation in the sediments, water column methane concentrations below the chemocline are ca. 10-15 mM (Reeburgh et al. 1991; Schubert et al. 2006a). ANME-1 have been detected in the Black Sea water column before (Durisch-Kaiser et al. 2005; Wakeham et al. 2003; Sollai et al. 2019; Schubert et al. 2006a). The ^{13}C-depleted stable carbon isotopic composition of a- and monocyclic biphytanes derived of the characteristic membrane lipids of ANME-1 revealed that these archaea actively consume methane in the water column (Wakeham et al. 2003). ANME have been suggested to play a major role in decreasing water column methane concentrations (Schubert et al. 2006b). Although ANME-1 have often been observed in environments low in sulfate, and without a syntrophic SRB partner, their methane oxidation pathway independent of sulfate reduction remains unknown (Yanagawa *et al.*, 2011). Previous studies have suggested a decoupling between AOM and sulfate reduction in the Black Sea water column, as no substantial stable carbon isotope depletion of SRB phospholipid fatty acid could be detected (Wakeham *et al.*, 2003). As AOM coupled to the reduction of alternative electron acceptors, such as humic substances or Fe^{3+}, has a much higher (theoretical) energy gain than sulfate-mediated AOM, the availability of these electron acceptors could theoretically make AOM more thermodynamically favorable for ANME-1b (Segarra *et al.*, 2013).
To explore the metabolic versatility of ANME, we studied the ANME-1b subgroup present in the anoxic water column of the Black Sea. We collected suspended particulate matter (SPM) from the water column, which was used for incubation studies with $^{13}CH_4$, exploring the response of the microbial community to AQDS and Fe^{3+} in the presence of sodium molybdate (an inhibitor of sulfate reduction). The $^{13}CO_2$ concentration was followed over time as a measure for methane oxidation. The microbial diversity at the end of the incubation experiments was analyzed by 16S rRNA gene sequencing to assess changes in the community composition under different conditions.

Material and methods

Sample collection
Sampling was performed during cruise 64PE444 on R/V *Pelagia* in August 2018 at station 42° 53.8' N 30° 40.7' E. The conditions in the water column at the moment of sampling are shown in Fig. S1. Water samples were taken using a conductivity-temperature-density (CTD) system equipped with Niskin sampling bottles. Samples for nutrient analysis were collected directly after CTD recovery. A constant N_2 flow during CTD sampling was used to retain anoxic conditions. N_2 flushed pressure bottles (1 L) were filled with water collected at 1000 m depth by piercing the butyl stoppers with a needle.
Water column SPM from a depth of 1,000 m was collected onto GF75 pore size 0.3 mm glass fiber filters (Advantec, Dublin, US) using a McLane WTS-LV in situ pump (McLane, East Falmouth), completed with a special filter head for anoxic sampling. Pumps were left in the water column to filter for 6 h. After pump recovery, the filter heads were transported to an anoxic glovebag, which was flushed with N_2 three times before the overlying anoxic water

was removed from the filters. Filters were then transferred to 1 L glass bottles filled with anoxic water collected from 1,000 m, closed and stored in the dark at 4-10°C for 60 days until incubations were set up in the laboratory. Another filter was directly stored at -80°C for analysis of the in situ microbial community. Water column samples for nutrient and DNA analysis were collected as described in Sollai et al. (2019) and Suominen et al. (2020).

Incubations with suspended particulate matter

To set up the incubation experiments, water column SPM was retrieved by scraping off the top layer of the glass fiber filters under anoxic conditions inside an anaerobic glove bag (Sigma) under N_2 atmosphere, and subsequently resuspended in 1 L of anoxic artificial seawater (commercially available mixture of sea salts, Sigma Aldrich, containing 28 mM SO_4^{2-} but no sulfide)) in incubation bottles of 1.2 L. Due to the used method, fibers of the filter were also present in the incubation bottles. ^{15}N-ammonium chloride (0.016 g) was also added for stable isotope activity measurements, but in the end ^{15}N incorporation was not measured. The medium was boiled and flushed with N_2 to remove oxygen and 10 ml $^{13}CH_4$ (99% labelled; Sigma-Aldrich) was added resulting in a methane concentration of 500 mM. Depending on the type of incubation, 4.1 g sodium molybdate (Sigma-Aldrich), 0.03 g iron(III) citrate (Sigma-Aldrich), or 1.65 g anthraquinone-2,7-disulfonic acid disodium salt (AQDS, TCI Chemicals) or a combination of these (Table S1) was added to the medium. Autoclaved artificial seawater was used as an abiotic control to assess abiotic variations and instrument variability of the measured parameters. All bottles were incubated in the dark at 10°C for 58 days. Every 14 days, the bottles were shaken and headspace gas was withdrawn for analysis. At the termination of the incubations, 10 ml of the medium was collected for nutrient analysis, stored at -20°C until analysis, and processed as previously described (Sollai *et al.*, 2019). The remaining medium was filtered over 0.3 m GF75 filters (Advantec, Dublin, US) for DNA analysis and was stored at -80°C.

$^{13}CO_2$ analysis

^{13}C-labeled carbon dioxide concentrations in the headspace of the incubation bottles were measured using a gas chromatograph (GC) equipped with a mass spectrometer (MS) (Agilent, 7890B GC with 5975C MSD) in analytical triplicates. To study and compare the relatively small production or consumption of these compounds in the different incubation experiments (with slightly different starting concentrations), the data of each individual incubation bottle was normalized on the starting value (t_0) as 100%.

DNA extraction and analysis

DNA was extracted from the filters using the PowerSoil DNA extraction kit (MoBio Laboratories, Carlsbad, CA, USA) and stored at -80°C until further analysis. The general 16S rRNA archaeal and bacteria primer pair 515F and 806RB targeting the V4 region (Caporaso *et al.*, 2012) was used for the 16S rRNA gene amplicon sequencing and analysis, as described in Besseling et al. (2018). PCR products were gel purified using the QIAquick Gel-Purification kit (Qiagen), pooled and diluted. Sequencing was performed by the Utrecht Sequencing Facility (Utrecht, the Netherlands), using an Illumina MiSeq sequencing platform. Analysis of the 16S rRNA gene amplicon sequences was performed with the Cascabel pipeline (Asbun *et al.*, 2019), including quality assessment by FastQC (Andrews *et al.*, 2015), assembly of the paired-

end reads with Pear (Zhang *et al.*, 2014), and assign taxonomy (including pick representative set of sequences with 'longest' method) with blast by using the Silva 128 release as reference database (https://www.arb-silva.de/). For analysis purposes, only species with a relative abundance greater than 0.001 were assumed significant. For tables and figures, results of duplicate bottles of the same treatment were averaged. The 16S rRNA amplicon reads (raw data) have been deposited in the NCBI Sequence Read Archive (SRA) under BioProject ID PRJNA605700.

Quantitative PCR 16S rRNA gene

16S rRNA gene copies were quantified using quantitative PCR (qPCR) with the same primer pair as used for amplicon sequencing (515F, 806RB) on a Rotor-Gene 6000 (Corbett Research, Sydney). The qPCR reaction mixture (25 µL) contained 0.5 U of Phusion High-Fidelity DNA Polymerase (Thermo Scientific), 1x Phusion HF Buffer, 0.2 µM of each dNTP, 20 µg of BSA, 0.6 pmol μL^{-1} of both primers, 0.5x EvaGreen dye (0.625 µM) in aqueous solution (Biotium, Hayward) and AccuGENE Molecular Biology Water (Lonza, Basel). The cycling conditions for the qPCR reaction were as follow: initial denaturation 98°C for 30 s, 45 cycles of 98°C for 10 s, 50°C for 20 s, followed by fluorescence data acquisition, 72°C for 30 s, and 80°C for 25 s. Specificity of the reaction was tested with a gradient melting temperature assay, from 55°C to 95°C with 0.5°C increments of 5 s apiece. The qPCR reactions were performed in duplicate with standard curves encompassing a range from 10^1 to 10^7 molecules μL^{-1}. qPCR efficiency for the 16S rRNA gene quantification was 100% with $R^2 = 0.996$. For quantification of microbial groups, we assumed all microorganisms of the microbial community contained a single 16S rRNA copy in their genome, which has been confirmed by genome analysis for the ANME-1 group (Meyerdierks *et al.*, 2010).

Results

The microbial community of the deep Black Sea water column was studied during incubation experiments, specifically focused at the response to additions of different electron acceptors and their effect on anaerobic methane oxidation. The methanotrophic activity in the incubations was assessed by the addition of ^{13}C-labeled methane, followed by the analysis of $^{13}CO_2$ concentrations over time.

Water column physicochemical conditions and in situ microbial community

The Black Sea water column is over 2,000 m deep and permanently stratified, with, at our station, an oxycline around 75 m depth (Fig. S1). Water was sampled at 1,000 m depth. The sulfate concentration at this depth was 17 mM and the nitrite concentration 21 nM (Fig. S1). Diversity estimates based on 16S rRNA gene amplicon sequencing at 1,000 m depth showed that the archaeal abundance was 2×10^5 copies per L (i.e. 1.5% of the total 16S rRNA reads; Fig. 1). 21% of the archaeal 16S rRNA reads was classified as ANME-1b (0.3% of the total 16S rRNA reads; Table 1 and S2; Fig. 2), corresponding to 4×10^4 copies per L^{-1}. No known methanotrophs other than ANME-1b were detected in the library of 16S rRNA reads from 1,000 m depth (average 190,000 reads per sample; Table S2). The abundance of methanogenic archaea (defined as 16S rRNA gene reads assigned to the Methanomicrobia, Methanococci,

Methanobacteria, Methanomassiliicoccales and Methanofastidiosales, but excluding ANME) amounted 4 x 10^3 copies per L^{-1} (2% of the archaeal 16S rRNA gene reads; Table 1 and S2; Fig. 1 and 2). 16S rRNA gene reads attributed to bacteria were closely related to Cloacimonadia (2 x 10^6 copies per L, 19% of total 16S rRNA reads), Dehalococcoidia (9 x 10^5 copies per L, 7.7%), Deltaproteobacteria (1 x 10^6 copies per L, 9.8%, of which 5 x 10^5 copies per L falling into SEEP-SRB cluster and 6 x 10^5 copies per L to *Desulfatiglans* spp.), plus many other, less abundant groups (36% 'other bacteria'; Fig. 1).

Abiotic and control incubations

$^{13}CO_2$ concentrations in the abiotic incubations (artificial seawater with added $^{13}CH_4$) and control (artificial seawater with added $^{13}CH_4$ and microbial matter from the SPM) remained constant over the course of the experiment after a small initial decrease (Fig. 3). The ANME-1b abundance in the control incubations was 2 x10^4 copies per L^{-1}, corresponding to 1.4% of the archaeal 16S rRNA gene reads. No other ANME clades were detected. Reads assigned to methanogenic archaea made up 1 x 10^5 copies per L^{-1} (6.6% of the archaeal 16S rRNA gene reads; Table 1; Fig. 2), Bathyarchaeia 8 x 10^5 copies per L^{-1} (40% of the archaeal 16S rRNA gene reads; Fig. 2). The bacterial community was similar to that of the water column at 1,000 m depth (Fig. 1 and S2), except for a higher relative abundance of Campylobacteria (1 x 10^7 copies per L^{-1}, 16% of total 16S rRNA reads; Fig. 1) and Gammaproteobacteria (9 x 10^6 copies per L^{-1}, 12%; Fig. 1). The genus *Sulfurimonas*, belonging to the Campylobacteria, comprised 5 x 10^6 copies per L^{-1}, corresponding to 7% of the 16S rRNA reads, the genus *Sulfurospirillum* (Campylobacteria) 5 x 10^6 copies per L^{-1} (6%; Table S2), *Desulfatiglans* (Deltaproteobacteria) 2 x 10^6 copies per L^{-1} (3%), *Fusibacter* (Clostridia) 1 x 10^6 copies per L^{-1} (2%) and SEEP-SRB (Deltaproteobacteria) 4 x 10^5 copies per L^{-1} (1%; Table 1 and S2). Each of these bacterial groups, except for SEEP-SRB, was more abundant in the control incubations than in the water column (Table 1; Fig. S2).

Incubations with sodium molybdate

Sodium molybdate was used as inhibitor of sulfate reduction in a subset of the incubation experiments, both with and without the addition of alternative electron acceptors (overview available in Table S1). In the incubation with only sodium molybdate, an increase of 65% in the $^{13}CO_2$ concentration was observed from day 0 to day 30, after which the concentration slightly decreased (Figs. 3 and S3). The abundance of ANME-1b was 6 x 10^4 copies per L^{-1} in the molybdate incubation, which corresponded to a relative abundance of 1% of the archaeal 16S rRNA gene reads (Table 1; Fig. 2). The abundance of methanogenic archaea increased substantially to 1.5 x 10^6 copies per L^{-1} (27% of the archaeal 16S rRNA reads; Table 1; Fig. 2). Archaea of the Bathyarchaeia were relatively abundant compared to other archaea (3 x 10^6 copies per L^{-1}, 52% of archaeal 16S rRNA reads; Fig. 1). The total 16S rRNA gene reads were strongly dominated by reads attributed to Campylobacteria (5 x 10^7 copies per L^{-1}, 31%), specifically of the genus *Sulfurospirillum* (5 x 10^7 copies per L^{-1}, 27%; Table 1 and S2).

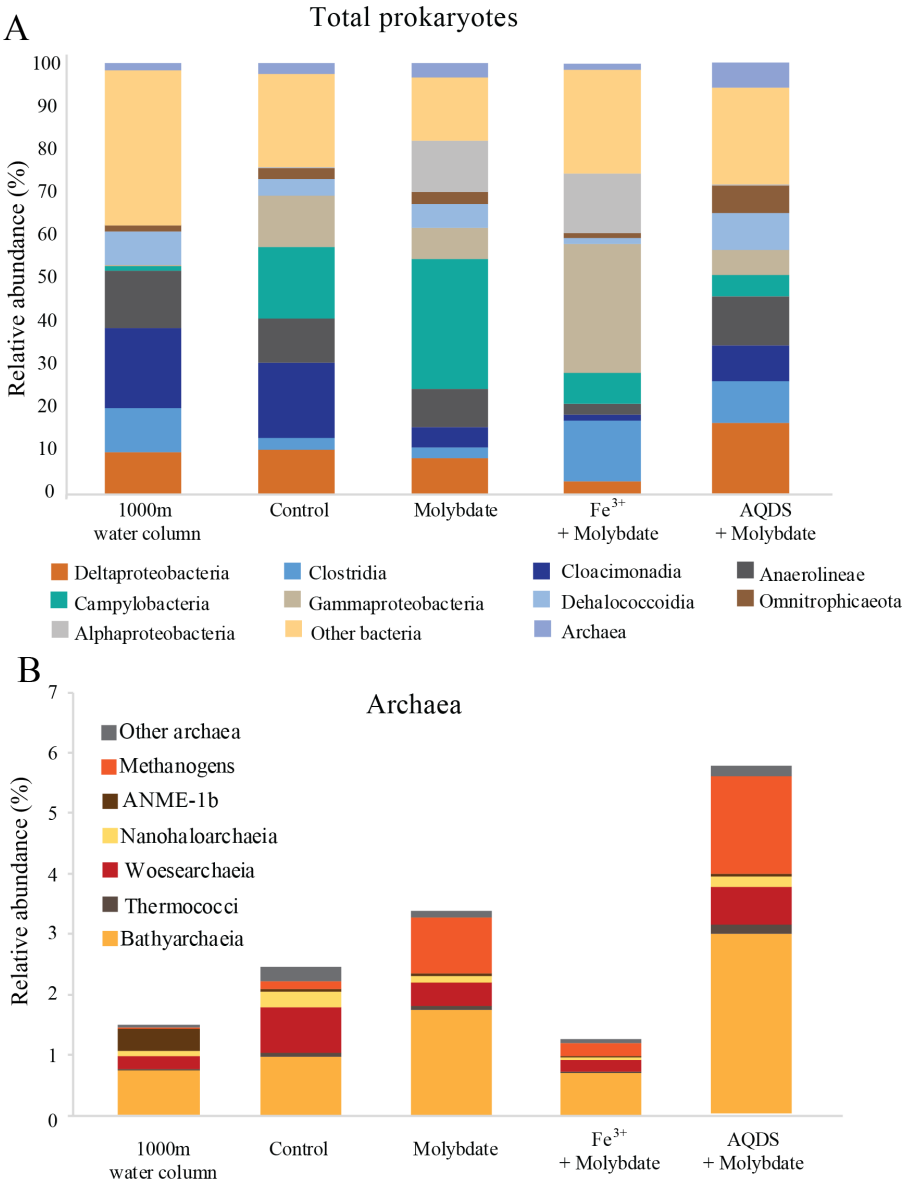

Fig. 1. Total prokaryotic (A) and archaeal (B) diversity in Black Seas water from 1,000 m depth and at the end of the various incubation experiments, expressed as percentage of total 16S rRNA gene reads. Methanogens defined here as all species belonging to the Methanomicrobia, Methanococci, Methanobacteria, Methanomassiliicoccales and Methanofastidiosales, excluding any ANME.

Members of the Deltaproteobacteria *Desulfatiglans* comprised 1 x 10^7 copies per L^{-1} (7%; Table 1 and S2), the *Sulfurimonas* 4 x 10^6 copies per L^{-1} (2%) and SEEP-SRB 9 x 10^5 copies per L^{-1} in the incubations with molybdate only (1%; Table 1 and S2).

Incubations with sodium molybdate and soluble Fe^{3+} complexes

The $^{13}CO_2$ concentration in the Fe^{3+} amended incubations showed a slight increase during the experiment (on average 5%; Fig. 3, Fig. S3) although the difference with the starting concentration was small. The abundance of ANME-1b was 1 x 10^5 copies per L^{-1} (1.3% of the archaeal reads; Table 1; Fig. 2). The abundance of methanogenic archaea was 2 x 10^6 copies per L^{-1} (17% of the archaeal 16S rRNA gene reads; Table 1; Fig. 2), the abundance of Bathyarchaeia was 5 x 10^6 copies per L^{-1} (56% of the archaeal reads; Fig. 2). Gammaproteobacteria dominated the Fe^{3+}-amended incubations (2 x 10^8 copies per L^{-1}, 30% of total 16S rRNA reads, dominated by Vibrionales; Fig. 1). The abundance of *Sulfurospirillum* was 4 x 10^7 copies per L^{-1} (5%, Table 1 and S2), the abundances of *Desulfatiglans*, *Fusibacter* and *Sulfurimonas* were 1–2 x 10^7 copies per L^{-1} for all three genera (2% of the 16S rRNA gene reads; Table 1 and S2).

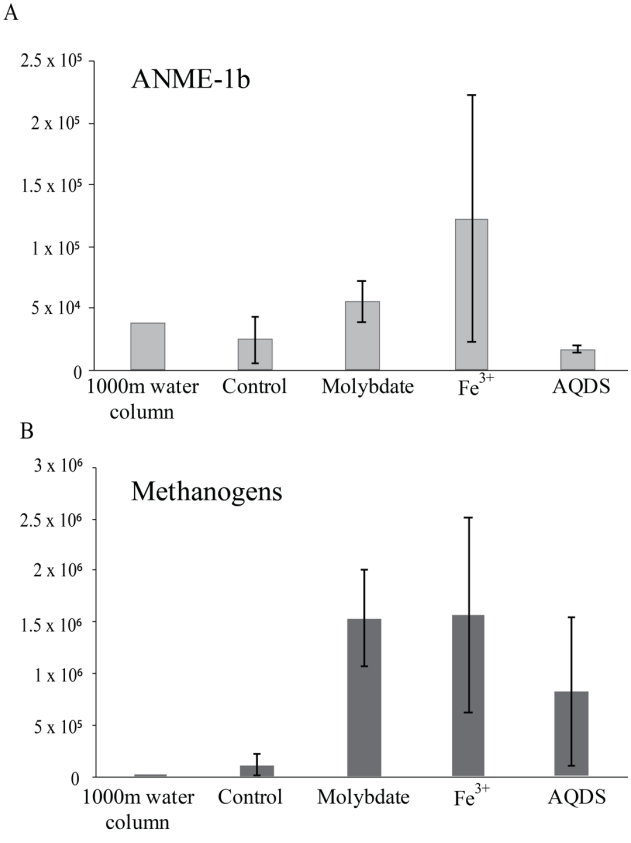

Fig. 2. Abundance of ANME-1b (A) and methanogens (B; defined here as all species belonging to the Methanomicrobia, Methanococci, Methanobacteria, Methanomassiliicoccales and Methanofastidiosales, excluding any ANME) in natural Black Sea water from 1,000 m depth and at the end of the various incubation experiments, in 16S rRNA gene copies L^{-1}. T-tests showed the differences between the treatments were not statistically significant. Values for duplicate bottles are averaged, except for the 1000 m sample, for which only one sample was used. Notice the different scale on the y-axis.

Incubations with sodium molybdate and AQDS

The addition of AQDS to the incubations resulted in an increase of 38% in $^{13}CO_2$ concentrations over the course of the experiment (Fig. 3; Fig. S3). The abundance of ANME-1b at the end of the incubation was 2 x 10^4 copies per L^{-1} (1% of archaeal 16S rRNA reads; Table 1; Fig. 2). The abundance of methanogenic archaea was 8 x 10^5 copies per L^{-1} (30% of archaeal reads; Table 1; Fig. 2). The Bathyarchaeia made up just over half of the archaeal 16S rRNA reads (1 x 10^6 copies per L^{-1}, 52%; Fig. 1). The 16S rRNA gene reads of bacteria were assigned to several major groups, each making up 5–18% of the community, with the Deltaproteobacteria being the most abundant (18%; Fig. 1). The Deltaproteobacteria were dominated by the genus *Desulfatiglans* (6 x 10^6 copies per L^{-1}, 13% of 16S rRNA reads; Table 1 and S2). The abundance of the genus *Fusibacter* was 3 x 10^6 copies per L^{-1} (7%; Table 1 and S2). The abundance of the SEEP-SRB cluster was 8 x 10^5 copies per L^{-1} (representing 2% of 16S rRNA reads; Table 1 and S2). *Sulfurimonas*, *Sulfurospirillum* and *Sulfurovum* abundances were 2 x 10^6, 3 x 10^5 and 2 x 10^5 copies per L^{-1}, respectively (representing 3, 0.6 and 0.4% of 16S rRNA reads, respectively; Table 1 and S2).

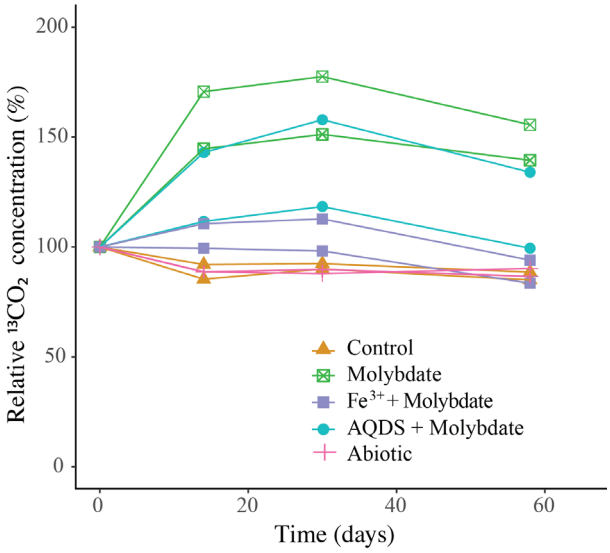

Fig. 3. Change over time of $^{13}CO_2$ in the incubation experiments, normalized to the concentration at t_0 (t_0 = 100%). The duplicate incubation bottles of each experiment are both shown individually. Actual concentrations are shown in Fig. S3.

Discussion

Most commonly, marine AOM is coupled to sulfate reduction via a syntrophic relationship between ANME and SRB, based on the exchange of electrons or reaction intermediates (Boetius *et al.*, 2000). In the past decade, several alternative electron acceptors for marine methane oxidation were proposed to be used by ANME, such as nitrate (Haroon *et al.*, 2013), iron and manganese (Beal et al., 2009), and humic substances (Sivan et al. 2011; Segarra et al. 2013; Scheller et al. 2016). ANME-1 are often found in the vicinity of SRB, but unlike ANME-2, they are found to be only loosely associated, not tightly aggregated (Reitner *et al.*, 2005; Gründger *et al.*, 2019), which raises the question if ANME-1 performs anaerobic methane oxidation

independent of SRB and sulfate reduction. Here, we addressed this question by performing incubation experiments with alternative electron acceptors, using suspended particulate matter collected from the anoxic Black Sea water column which is naturally relatively rich in sulfate (17 mM, Fig. S1) and where ANME-1b is present in the deep waters (4×10^4 ANME-1b 16S rRNA gene copies per L^{-1} at 1,000 m; Fig. 2; Table 1). No other organisms known to perform methane oxidation were detected at 1,000 m depth. Therefore, we assume that AOM at this depth in the water column and in our incubation experiments is performed by ANME-1b, allowing us to test the electron donor preferences of ANME-1b in an incubation setup.

Table 1. Abundance (16S rRNA copies per L^{-1}) of major species in the incubation experiments and the Black Sea water column.

Treatment	Total 16S rRNA copies ml^{-1}	Archaea		Bacteria					
		ANME-1b	Methanogens[1]	*Desulfatiglans*	*Fusibacter*	SEEP-SRB	*Sulfurimonas*	*Sulfurospirillum*	*Sulfurovum*
1000m water column	1.2×10^7	3.8×10^4	4.0×10^3	5.6×10^5	8.4×10^3	4.5×10^5	5.9×10^4	2.0×10^4	1.7×10^4
Control	7.8×10^7	2.4×10^4	1.2×10^5	2.1×10^6	1.2×10^6	4.4×10^5	5.4×10^6	4.6×10^6	2.6×10^6
Molybdate	1.7×10^8	5.5×10^4	1.5×10^6	1.1×10^7	3.1×10^6	9.1×10^5	4.1×10^6	4.5×10^7	4.0×10^5
Fe^{3+}	7.6×10^8	1.2×10^5	1.6×10^6	1.2×10^7	1.5×10^7	1.4×10^6	1.5×10^7	3.5×10^7	3.5×10^6
AQDS	4.7×10^7	1.7×10^4	8.2×10^5	6.1×10^6	3.2×10^6	8.2×10^5	1.6×10^6	2.6×10^5	1.8×10^5

1. namely here Methanomicrobia, Methanococci, Methanobacteria, Methanomassiliicoccales and Methanofastidiosales, but excluding all ANME groups

Enhanced methane oxidation by ANME-1b in molybdate and in AQDS incubations

In the control incubations, which contained the same sulfate-containing artificial seawater, SPM and $^{13}CH_4$ as the other experiments, no increase in the $^{13}CO_2$ concentration over time was observed. Possibly, methane oxidation did not occur, or at too low rates to observe over the 60-day experiment. Methane oxidation rates by ANME in the Black Sea were previously reported to be 0.5–7 nmol L^{-1} day^{-1} at 1,000 m (Wakeham *et al.*, 2003). The highest $^{13}CO_2$ production rates observed in our experiments were much lower than would be expected at those methane oxidation rates (Fig. S3). Potentially, the change in conditions from the water column to the incubation bottles affected the activity and methane turnover rate of ANME-1b. A change in pressure is known to affect both ANME and SRB abundance and activity (Cassarini et al., 2019). Another possibility would be that $^{13}CO_2$ is produced by ANME-1b but is simultaneously consumed by methanogens, SRB or other microbial groups, and therefore no increase is detectable in the gas headspace. As we did not measure ^{13}C incorporation in the biomass, we cannot fully determine the faith of the labeled substrate.

The addition of only molybdate, and of molybdate plus AQDS, increased methane oxidation as seen by the detected increase of $^{13}CO_2$ (Fig. 3). As we assume sulfate reduction was inhibited by the addition of sodium molybdate (Wilson and Bandurski, 1958), it seemed surprising that methane oxidation could occur in the incubations with the addition of molybdate only and no alternative electron acceptor such as humic substances or Fe^{3+}. Even if the inhibition

of sulfate reduction was incomplete, and some sulfate reduction-coupled AOM would still have occurred, the methane oxidation rate in the molybdate-only experiments would not be expected to be higher than in the control incubations, that also contain sulfate and methane, but no inhibiting molybdate. We therefore consider it unlikely that sulfate-mediated AOM was responsible for the observed $^{13}CO_2$ production, in both the molybdate only and the molybdate + AQDS incubation. More likely, an alternative form of AOM occurred when sulfate-mediated AOM was inhibited, possibly leading to more favorable energetic conditions for ANME ($\Delta G^{o'}$ sulfate-mediated AOM -17 kJ mol^{-1}, $\Delta G^{o'}$ AQDS-mediated AOM -41 kJ mol^{-1}; Scheller et al. 2016). Although we consider it likely that AQDS was involved in AOM in the AQDS incubations, the question arises what was the role of molybdate, and whether it was molybdate rather than AQDS causing the enhanced $^{13}CO_2$ production that was observed in those incubations, given the high $^{13}CO_2$ production in the molybdate only incubation. However, if it was purely the molybdate that caused the increase in methane oxidation rates in both the molybdate and in the AQDS incubations, the incubations with Fe^{3+} (containing molybdate) would have also been expected to show increased $^{13}CO_2$ production, which was not the case (Fig. 3). No substantial $^{13}CO_2$ production was observed in the Fe^{3+} incubations, despite the relatively high abundance of ANME-1b compared to the AQDS incubations (Fig. 2). The ANME-1b in the Fe^{3+} incubations may have been inactive, or involved in methanogenesis rather than in methanotrophic pathways (Lloyd et al. 2011; Bertram et al. 2013; Kevorkian et al. 2020). Possibly, the total 16S rRNA gene copies in the AQDS amended incubations, and thus also the ANME-1b abundance, was underestimated due to an inhibitory effect of humic substances on qPCR reactions, which is widely recognized (Albers *et al.*, 2013; Sidstedt *et al.*, 2015) and could complicate the comparison between incubations with and without humic substances.

Potential role of sulfur cycling organisms

Several different sulfur processes have been linked to marine AOM, i.e. the reduction of sulfate (Boetius *et al.*, 2000), zero-equivalent sulfur (Milucka *et al.*, 2012) or polysulfides (Vigneron *et al.*, 2019). To explore the role of sulfur cycling in our incubation experiments, we studied the organisms that were present and are known to be involved in sulfur cycling. The only sulfur compounds that were added to the incubation experiments were sulfate, as part of the artificial seawater salts mixture, organic sulfur-containing microbial biomass of the SPM, and possibly small amounts of sulfur compounds that were present in the natural water column and that were transferred with the SPM that was used as the inoculum. We chose to add sulfate to all experiments, including those with molybdate, Fe^{3+} and AQDS, to retain similar conditions in all experiments, varying only the molybdate and alternative electron acceptor availability. Several microbial groups that are known to be involved in the sulfur cycle were abundant in the incubations. SRB were assumed to be inhibited by the addition of molybdate to all but the control incubations, but as we did not measure sulfate consumption or sulfide production within the incubation experiments, it was not possible to determine whether sulfate reduction was completely inhibited.

The genera *Sulfurimonas*, *Sulfurospirillum* and *Sulfurovum* increased drastically in abundance in the control incubations when compared to the water column (Table 1 and S2; Fig. S2). This change could potentially be attributed to a bottle effect, in which the incubation conditions favor specific bacterial groups. These microorganisms have all been described to use sulfur (elemental S or polysulfides), thiosulfate or sulfite as electron acceptor, and, for some

strains, also as electron donor (Straub and Schink, 2004; Nakagawa *et al.*, 2005; Mino *et al.*, 2014; Goris and Diekert, 2016). *Sulfurimonas*, and likely also *Sulfurovum and Sulfurospirillum*, are capable of oxidizing sulfide to produce sulfate as an end product and elemental sulfur and polysulfide as intermediate products (Goris *et al.*, 2014; Han and Perner, 2015; Ross *et al.*, 2016). The ability to autotrophically fix CO_2 is likely widely present in different *Sulfurimonas*, *Sulfurospirillum* and *Sulfurovum* species (Mino *et al.*, 2014; Han and Perner, 2015). *Sulfurovum* and some *Sulfurimonas* strains are also capable of oxidizing sulfide and of using H_2 as an electron donor (Takai *et al.*, 2006; Mino *et al.*, 2014). It is unclear which compounds were cycled in our incubation experiments, and which effect the addition of molybdate had on these processes. In the control incubation, where no inhibitor of sulfate reduction was present, we expect active sulfate reduction and sulfur cycling to occur. As the named species are capable of CO_2 fixation, they may have decreased the $^{13}CO_2$ concentration in the control experiments, possibly diminishing the increase in headspace $^{13}CO_2$ that was expected to occur and that was taken as a measure of methane oxidation.

In the incubation with only molybdate, *Sulfurospirillum* sp. dominated the community (5×10^7 copies per L^{-1}, 27% of 16S rRNA reads; Table 1 and S2). As this was the main distinguishing factor between the molybdate and the other incubations, it could potentially be related to the enhanced AOM that was observed in these incubations (Fig. 3). Recent research has suggested partner-independent AOM coupled to polysulfide reduction as a novel pathway of methane oxidation by ANME-1 (Vigneron *et al.*, 2019), and potentially, *Sulfurospirillum* could produce these polysulfides. The production of polysulfides, however, requires the oxidation of sulfide, which was not added to our incubation experiments. It could be produced by the sulfur cycling organisms present (*Sulfurimonas*, *Sulfurospirillum*, *Sulfurovum*, SEEP-SRB) but it is unclear whether this could occur in the presence of molybdate, and why then specifically *Sulfurospirillum* became highly abundant in the molybdate incubations. In the AQDS incubations, *Sulfurospirillum* abundance was two orders of magnitude lower than in the molybdate only incubation (3×10^5 copies per L^{-1}, 0.6%; Table 1 and S2). In the Fe^{3+} amended incubation, the *Sulfurospirillum* abundance (4×10^7 copies per L^{-1}; Table 1) was comparable to the molybdate incubation, although the relative abundance was much lower (5%; Table S2).

Bacteria of the genera *Desulfatiglans* and *Fusibacter* became relatively more abundant in the incubations with AQDS (*Desulfatiglans* 13% of the 16S rRNA gene reads AQDS incubations, versus 3% in control incubations; *Fusibacter* 7% in AQDS incubations, vs. 2% in control incubations; Table S2), although this is not reflected in the absolute abundances (Table 1). *Desulfatiglans* sp. and *Fusibacter* sp. are known as strict anaerobes that can reduce sulfate, thiosulfate or sulfur, while oxidizing carbohydrates or other organic electron donors, such as AQDS (Ravot *et al.*, 1999; Suzuki *et al.*, 2014; Fadhlaoui *et al.*, 2015). Recently, *Desulfatiglans* sp. have been found to cooccur with ANME-1 and SEEP-SRB in estuarine sediments (Kevorkian *et al.*, 2020). It is, however, unknown whether the sulfur compound reduction by *Desulfatiglans* sp. and *Fusibacter* sp. here could be coupled to AOM, and which sulfur compound they use here, as sulfate reduction is expected to be inhibited by the molybdate that was present in the incubations with AQDS.

Potential methanogenesis by methanogens, ANME and Bathyarchaeota

The abundance of methanogens in the molybdate and Fe^{3+} incubations was 10-fold higher than in control incubations (Table 1; Fig. 2). Possibly, part of the produced CO_2 in the

incubations is converted back to CH_4 by these methanogens, which would mean that the net produced $^{13}CO_2$ is higher than was measured. It remains unclear what caused this increase in the methanogenic abundance.
Besides, ANME-1b has been shown to also be capable of methanogenesis, specifically under high H_2 concentrations (Kevorkian *et al.*, 2020). Although we did not measure H_2 in our incubations, H_2 may have built up as the consumption of H_2 by SRB was likely inhibited by molybdate. Therefore, it is possible that ANME-1b switched to a methanogenic metabolism, producing methane rather than consuming it. In the molybdate and AQDS + molybdate incubations, a decrease in the $^{13}CO_2$ concentration is observed after day 30 (Fig. 3 and S2). Possibly, this could be linked to such a metabolic switch.
The phylum Bathyarchaeota (i.e. the former Miscellaneous Crenarchaeotal Group) increased in abundance in all incubations supplemented with molybdate (i.e. from 8×10^5 copies per L^{-1} in the control to 3×10^6, 5×10^6 and 1×10^6 copies per L^{-1} in molybdate only, Fe^{3+} and AQDS, respectively; Fig. 1). The increase in the relative abundance of Bathyarchaeota is highest in the incubations with molybdate only and with AQDS (Fig. 1). The Bathyarchaeota are known to be metabolically diverse, with subgroups potentially capable of methanogenesis (Evans *et al.*, 2015), although organisms performing organic matter degradation and dissimilatory nitrogen and sulfur reduction are also present within this phylum (Webster *et al.*, 2010; Lloyd *et al.*, 2013; Seyler *et al.*, 2014; Zhang *et al.*, 2016; Zhou *et al.*, 2018). The co-occurrence of Bathyarchaeota and ANME-1b in methane cold seeps has been suggested to be based on an indirect trophic relationship rather than a direct interaction (Niu *et al.*, 2017) and the cause of the increase of the abundance of this phylum in our molybdate, Fe^{3+} and AQDS amended incubations remains unclear.

Conclusions

Overall, we show that both molybdate and AQDS can stimulate methane oxidation in incubations with material from the Black Sea water column, containing ANME-1b. Enhanced methane oxidation by AQDS has been shown for ANME-2 in marine sediments (Scheller *et al.*, 2016) and also Valenzuela et al. (2017) observed an increase in $^{13}CO_2$ production in sediment incubations with AQDS, but only when sulfate reduction was not inhibited and with barely detectable ANME-1 and ANME-3 abundances, making it difficult to assess which organisms were involved. To our knowledge, this is the first study showing that additions of molybdate, and of molybdate plus AQDS, are stimulating methane oxidation in incubations with water column SPM. We also believe this is the first study that suggests that ANME-1b is involved in an AQDS-stimulated AOM pathway. The mechanism behind the stimulating effects of molybdate and AQDS remain unclear. More research, including detailed measurements of the sulfur compounds in solution and gene expression analysis is needed to reveal whether ANME-1b is indeed involved in AQDS-dependent AOM, whether sulfur compounds and a partner organism are involved, and what could be the role of this process in marine environments.

Acknowledgements

The authors thank the captain and crew of the R/V Pelagia, Dina Castillo Boukhchtaber and Saara Suominen for help with sampling. Marianne Baas, Marcel van der Meer, Maartje Brouwer and Sanne Vreugdenhil are thanked for help with laboratory procedures. This research is supported by the Soehngen Institute of Anaerobic Microbiology (SIAM) Gravitation grant (024.002.002) to JSSD and LV of the Netherlands Ministry of Education, Culture and Science (OCW) and the Netherlands Organisation for Scientific Research (NWO).

Supplemental material

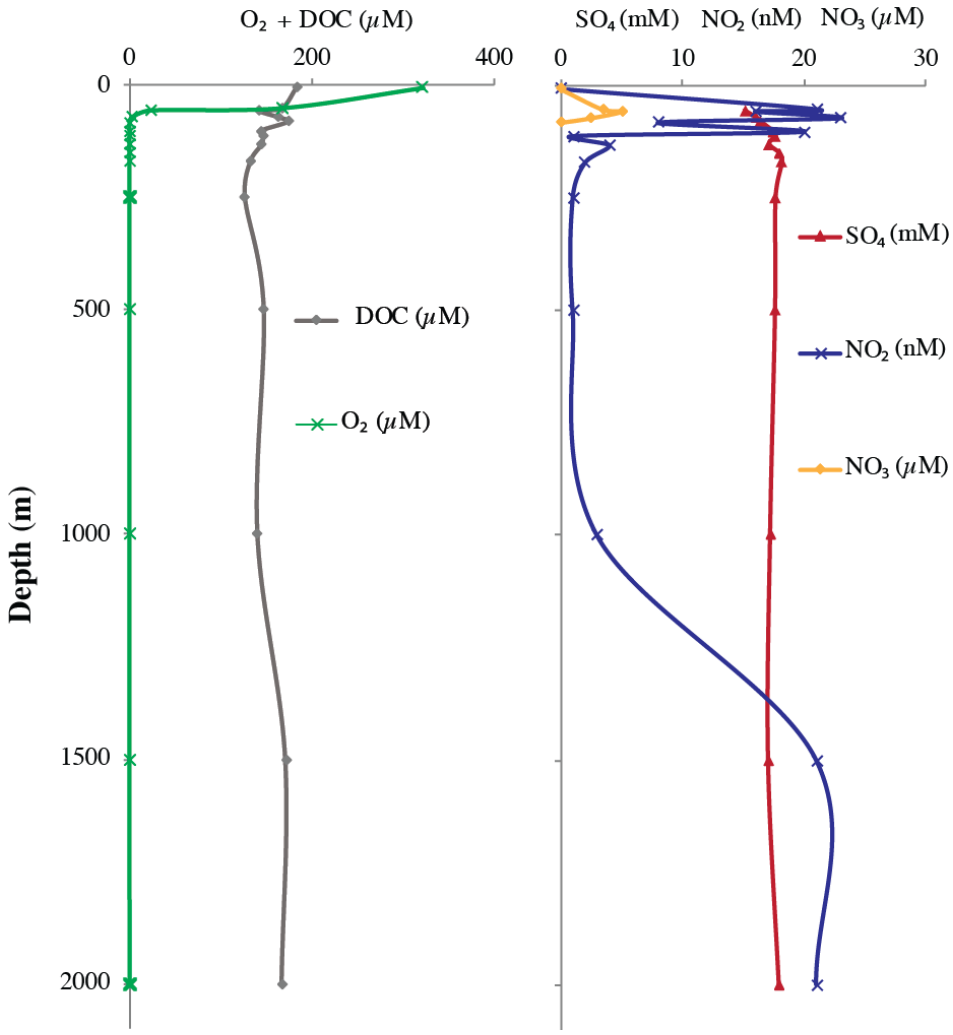

Fig. S1. Environmental conditions in the Black Sea water column at the time of sampling.

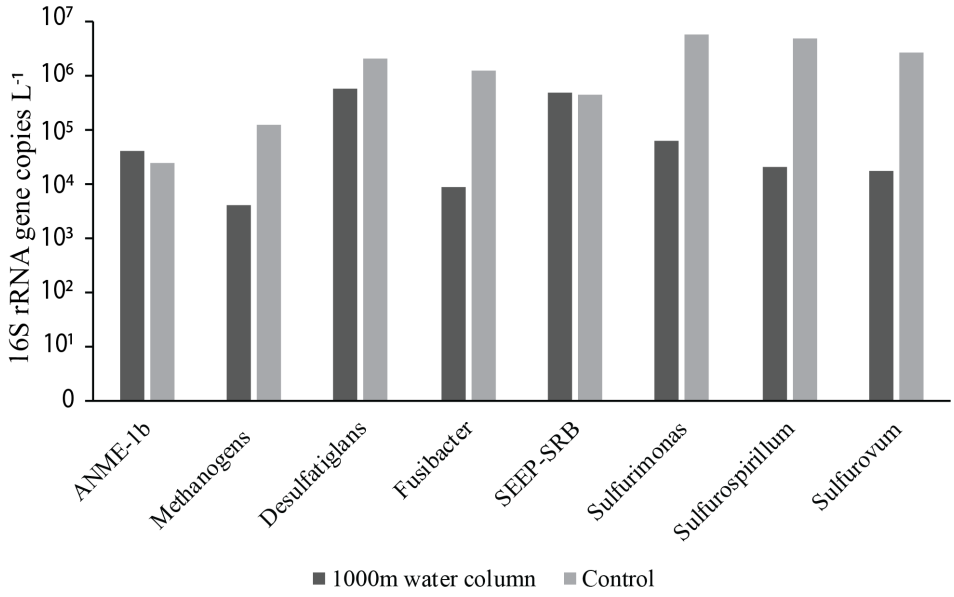

Fig. S2. Abundance of major groups in the Black Sea water column (1,000m depth) and the control incubation experiment, in 16S rRNA copies per L^{-1}.

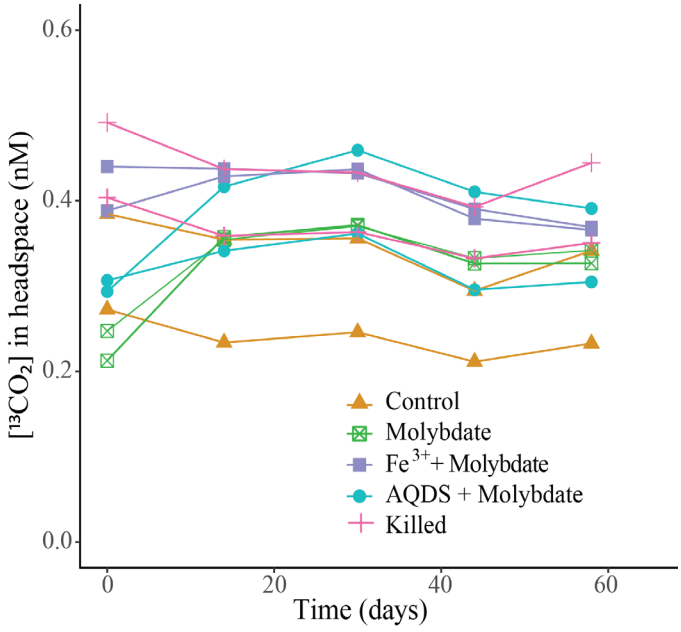

Fig. S3. $^{13}CO_2$ concentration in the headspace of the incubations with different electron acceptors.

Table S1. Overview of the incubation experiments.

	Artificial seawater[1]	$^{13}CH_4$	$^{15}NH_4$	Sodium Molybdate	Fe^{3+} citrate	AQDS
Abiotic control	x	x				
Control	x	x	x			
Molybdate	x	x	x	x		
Fe^{3+} + molybdate	x	x	x	x	x	
AQDS + molybdate	x	x	x	x		x

1. Commercially available sea salts mixture (Sigma Aldrich)

Table S2. Total number of 16S rRNA reads per incubation, and the relative abundance (as % of the total 16S rRNA gene reads) of major species in the incubation experiments and the Black Sea water column. Values for duplicate bottles are averaged.

Treatment	Total 16S reads per experiment	Archaea		Bacteria					
		ANME-1b	Methanogens[1]	*Desulfatiglans*	*Fusibacter*	SEEP-SRB	*Sulfurimonas*	*Sulfurospirillum*	*Sulfurovum*
1000m water column	2.3×10^5	0.3	0.03	4.7	0.07	3.8	0.50	0.17	0.14
Control	2.1×10^5	0.03	0.15	2.6	1.5	0.56	6.9	5.9	3.3
Molybdate	2.4×10^5	0.03	0.92	6.8	1.8	0.54	2.4	27	0.2
Iron-oxides	1.7×10^5	0.02	0.22	1.6	1.9	0.19	1.9	4.6	0.5
AQDS	9.8×10^4	0.04	1.8	13	6.9	1.8	3.4	0.6	0.4

1. namely here Methanomicrobia, Methanococci, Methanobacteria, Methanomassiliicoccales and Methanofastidiosales, but excluding all ANME groups

References

Albers, C.N., Jensen, A., Bælum, J., and Jacobsen, C.S. (2013) Inhibition of DNA Polymerases Used in Q-PCR by Structurally Different Soil-Derived Humic Substances. *Geomicrobiol. J.* **30**: 675–681.

Andrews, S., Krueger, F., Seconds-Pichon, A., Biggins, F., and Wingett, S. (2015) FastQC. A quality control tool for high throughput sequence data. Babraham Bioinformatics. *Babraham Inst.* **1**: 1.

Asbun, A.A., Besseling, M.A., Balzano, S., van Bleijswijk, J., Witte, H., Villanueva, L., and Engelmann, J.C. (2019) Cascabel: a flexible , scalable and easy-to-use amplicon sequence data analysis pipeline. *BioRxiv* **809384**:.

Bai, Y., Wang, X., Wu, J., Lu, Y., Fu, L., Zhang, F., et al. (2019) Humic substances as electron acceptors for anaerobic oxidation of methane driven by ANME-2d. *Water Res.* **164**: 114935.

Beal, E.J., House, C.H., and Orphan, V.J. (2009) Manganese- and iron-dependent marine methane oxidation. *Science* **325**: 184–187.

Bertram, S., Blumenberg, M., Michaelis, W., Siegert, M., Krüger, M., and Seifert, R. (2013) Methanogenic capabilities of ANME-archaea deduced from 13C-labelling approaches. *Environ. Microbiol.* **15**: 2384–2393.

Besseling, M.A., Hopmans, E.C., Christine Boschman, R., Sinninghe Damsté, J.S., and Villanueva, L. (2018) Benthic archaea as potential sources of tetraether membrane lipids in sediments across an oxygen minimum zone. *Biogeosciences* **15**: 4047–4064.

Boetius, A., Ravenschlag, K., Schubert, C.J., Rickert, D., Widdel, F., Gieseke, A., et al. (2000) A marine microbial consortium apparently mediating anaerobic oxidation of methane. *Nature* **407**: 623–626.

Caporaso, J.G., Lauber, C.L., Walters, W.A., Berg-Lyons, D., Huntley, J., Fierer, N., et al. (2012) Ultra-high-throughput microbial community analysis on the Illumina HiSeq and MiSeq platforms. *ISME J.* **6**: 1621–1624.

Cassarini, C., Zhang, Y., and Lens, P.N.L. (2019) Pressure Selects Dominant Anaerobic Methanotrophic Phylotype and Sulfate Reducing Bacteria in Coastal Marine Lake Grevelingen Sediment. *Front. Environ. Sci.* **6**: 162.

Conrad, R. (2009) The global methane cycle: Recent advances in understanding the microbial processes involved. *Environ. Microbiol. Rep.* **1**: 285–292.

Cui, M., Ma, A., Qi, H., Zhuang, X., and Zhuang, G. (2015) Anaerobic oxidation of methane: An "active" microbial process. *Microbiologyopen* **4**: 1–11.

Durisch-Kaiser, E., Klauser, L., Wehrli, B., and Schubert, C. (2005) Evidence of intense archaeal and bacterial methanotrophic activity in the Black Sea water column. *Appl. Environ. Microbiol.* **71**: 8099–8106.

Egger, M., Rasigraf, O., Sapart, C.J., Jilbert, T., Jetten, M.S.M., Röckmann, T., et al. (2014) Iron-mediated anaerobic oxidation of methane in brackish coastal sediments. *Environ. Sci. Technol.* **49**: 277–283.

Ettwig, K.F., Zhu, B., Speth, D., Keltjens, J.T., Jetten, M.S.M., and Kartal, B. (2016) Archaea catalyze iron-dependent anaerobic oxidation of methane. *Proc. Natl. Acad. Sci. U. S. A.* **113**: 12792–12796.

Evans, P.N., Parks, D.H., Chadwick, G.L., Robbins, S.J., Orphan, V.J., Golding, S.D., and Tyson, G.W. (2015) Methane metabolism in the archaeal phylum Bathyarchaeota revealed by genome-centric metagenomics. *Science.* **350**: 434–438.

Fadhlaoui, K., Hania, W. Ben, Postec, A., Fauque, G., Hamdi, M., Ollivier, B., and Fardeau, M.L. (2015) Fusibacter fontis sp. Nov., a sulfur-reducing, anaerobic bacterium isolated from a mesothermic Tunisian spring. *Int. J. Syst. Evol. Microbiol.* **65**: 3501–3506.

Forster, P., Ramaswamy, V., Artaxo, P., Berntsen, T., Betts, R., Fahey, D.W., et al. (2007) Changes in Atmospheric Constituents and in Radiative Forcing In: Climate Change 2007: The Physical Science Basis. Contribution of Working Group I to the Fourth Assessment Report of the Intergovernmental Panel on Climate Change , Cambridge University Press Cambridge University Press.

Goris, T. and Diekert, G. (2016) The genus Sulfurospirillum. In, *Organohalide-Respiring Bacteria*., pp. 209–234.

Goris, T., Schubert, T., Gadkari, J., Wubet, T., Tarkka, M., Buscot, F., et al. (2014) Insights into organohalide respiration and the versatile catabolism of Sulfurospirillum multivorans gained from comparative genomics and physiological studies. *Environ. Microbiol.* **16**: 3562–3580.

Gründger, F., Carrier, V., Svenning, M.M., Panieri, G., Vonnahme, T.R., Klasek, S., and Niemann, H. (2019) Methane-fuelled biofilms predominantly composed of methanotrophic ANME-1 in Arctic gas hydrate-related sediments. *Sci. Rep.* **9**: 9725.

Hallam, S.J., Putnam, N., Preston, C.M., Detter, J.C., Rokhsar, D., Richardson, P.M., and DeLong, E.F. (2004) Reverse methanogenesis: testing the hypothesis with environmental genomics. *Science.* **305**: 1457–1462.

Han, Y. and Perner, M. (2015) The globally widespread genus Sulfurimonas: Versatile energy metabolisms and adaptations to redox clines. *Front. Microbiol.* **6**: 1–17.

Haroon, M.F., Hu, S., Shi, Y., Imelfort, M., Keller, J., Hugenholtz, P., et al. (2013) Anaerobic oxidation of methane coupled to nitrate reduction in a novel archaeal lineage. *Nature* **500**: 567–70.

Hinrichs, K.U., Hayes, J.M., Sylva, S.P., Brewert, P.G., and DeLong, E.F. (1999) Methane-consuming archaebacteria in marine sediments. *Nature* **398**: 802–805.

Kevorkian, R., Callahan, S., Winstead, R., and Lloyd, K.G. (2020) ANME-1 archaea drive methane accumulation and removal in estuarine sediments. *BioRxiv Prepr.*

Knittel, K., Losekann, T., Boetius, A., Kort, R., and Amann, R. (2005) Diversity and distribution of methantrophic acrhaea at cold seeps. *Appl. Environ. Microbiol.* **71**: 467–479.

Krukenberg, V., Riedel, D., Gruber-Vodicka, H.R., Buttigieg, P.L., Tegetmeyer, H.E., Boetius, A., and Wegener, G. (2018) Gene expression and ultrastructure of meso- and thermophilic methanotrophic consortia. *Environ. Microbiol.* **20**: 1651–1666.

Lloyd, K.G., Alperin, M.J., and Teske, A. (2011) Environmental evidence for net methane production and oxidation in putative ANaerobic MEthanotrophic (ANME) archaea. *Environ. Microbiol.* **13**: 2548–2564.

Lloyd, K.G., Schreiber, L., Petersen, D.G., Kjeldsen, K.U., Lever, M.A., Steen, A.D., et al. (2013) Predominant archaea in marine sediments degrade detrital proteins. *Nature* **496**: 215–218.

McGlynn, S.E., Chadwick, G.L., Kempes, C.P., and Orphan, V.J. (2015) Single cell activity reveals direct electron transfer in methanotrophic consortia. *Nature* **526**: 531–535.

Meyerdierks, A., Kube, M., Kostadinov, I., Teeling, H., Glöckner, F.O., Reinhardt, R., and Amann, R. (2010) Metagenome and mRNA expression analyses of anaerobic methanotrophic archaea of the ANME-1 group. *Environ. Microbiol.* **12**: 422–439.

Milucka, J., Ferdelman, T.G., Polerecky, L., Franzke, D., Wegener, G., Schmid, M., et al. (2012) Zero-valent sulphur is a key intermediate in marine methane oxidation. *Nature* **491**: 541–546.

Mino, S., Kudo, H., Arai, T., Sawabe, T., Takai, K., and Nakagawa, S. (2014) Sulfurovum aggregans sp. nov., A hydrogenoxidizing, Thiosulfate-reducing chemolithoautotroph within the Epsilonproteobacteria isolated from a deep-sea hydrothermal vent chimney, And an emended description of the genus Sulfurovum. *Int. J. Syst. Evol. Microbiol.* **64**: 3195–3201.

Moran, J.J., Beal, E.J., Vrentas, J.M., Orphan, V.J., Freeman, K.H., and House, C.H. (2008) Methyl sulfides as intermediates in the anaerobic oxidation of methane. *Environ. Microbiol.* **10**: 162–173.

Nakagawa, S., Takai, K., Inagaki, F., Hirayama, H., Nunoura, T., Horikoshi, K., and Sako, Y. (2005) Distribution, phylogenetic diversity and physiological characteristics of epsilon-Proteobacteria in a deep-sea hydrothermal field. *Environ. Microbiol.* **7**: 1619–1632.

Nauhaus, K., Albrecht, M., Elvert, M., Boetius, A., and Widdel, F. (2007) In vitro cell growth of marine archaeal-bacterial consortia during anaerobic oxidation of methane with sulfate. *Environ. Microbiol.* **9**: 187–196.

Niemann, H., Lösekann, T., De Beer, D., Elvert, M., Nadalig, T., Knittel, K., et al. (2006) Novel microbial communities of the Haakon Mosby mud volcano and their role as a methane sink. *Nature* **443**: 854–858.

Niu, M., Fan, X., Zhuang, G., Liang, Q., and Wang, F. (2017) Methane-metabolizing microbial communities in sediments of the Haima cold seep area, northwest slope of the South China Sea. *FEMS Microbiol. Ecol.* **93**: 1–13.

Orphan, V.J., House, C.H., and Hinrichs, K. (2001) Methane-consuming archaea revealed by directly coupled isotopic and phylogenetic analysis. *Science.* **293**: 484–488.

Orphan, V.J., Turk, K.A., Green, A.M., and House, C.H. (2009) Patterns of 15N assimilation and growth of methanotrophic ANME-2 archaea and sulfate-reducing bacteria within structured syntrophic consortia revealed by FISH-SIMS. *Environ. Microbiol.* **11**: 1777–1791.

Ravot, G., Magot, M., Fardeau, M.L., Patel, B.K.C., Thomas, P., Garcia, J.L., and Ollivier, B. (1999) Fusibacter paucivorans gen. nov., sp. nov., an anaerobic, thiosulfate- reducing bacterium from an oil-producing well. *Int. J. Syst. Bacteriol.* **49**: 1141–1147.

Reeburgh, W.S. (2007) Oceanic methane biogeochemistry. *Chem. Rev.* **107**: 486–513.

Reeburgh, W.S., Ward, B.B., Whalen, S.C., Sandbeck, K.A., Kilpatrickt, K.A., and Kerkhof, L.J. (1991) Black Sea methane geochemistry. *Deep Sea Res. Part A. Oceanogr. Res. Pap.* **38**: S1189–S1210.

Reitner, J., Peckmann, J., Reimer, A., Schumann, G., and Thiel, V. (2005) Methane-derived carbonate build-ups and associated microbial communities at cold seeps on the lower Crimean shelf (Black Sea). *Facies* **51**: 66–79.

Ross, D.E., Norman, R.., Marshall, C.W., and May, H.D. (2016) Comparative genomic analysis of sulfurospirillum cavolei MES reconstructed from the metagenome of an electrosynthetic microbiome. *PLoS One* **11**: e0151214.

Scheller, S., Yu, H., Chadwick, G.L., and Mcglynn, S.E. (2016) Artificial electron acceptors decouple archaeal methane oxidation from sulfate reduction. *Science.* **351**: 703–707.

Schubert, C.J., Coolen, M.J.L., Neretin, L.N., Schippers, A., Abbas, B., Durisch-Kaiser, E., et al. (2006a) Aerobic and anaerobic methanotrophs in the Black Sea water column. *Environ. Microbiol.* **8**: 1844–1856.

Schubert, C.J., Durisch-Kaiser, E., Holzner, C.P., Klauser, L., Wehrli, B., Schmale, O., et al. (2006b) Methanotrophic microbial communities associated with bubble plumes above gas seeps in the Black Sea. *Geochemistry, Geophys. Geosystems* **7**.

Segarra, K.E.A., Comerford, C., Slaughter, J., and Joye, S.B. (2013) Impact of electron acceptor availability on the anaerobic oxidation of methane in coastal freshwater and brackish wetland sediments. *Geochim. Cosmochim. Acta* **115**: 15–30.

Seyler, L.M., McGuinness, L.M., and Kerkhof, L.J. (2014) Crenarchaeal heterotrophy in salt marsh sediments. *ISME J.* **8**: 1534–1543.

Sidstedt, M., Jansson, L., Nilsson, E., Noppa, L., Forsman, M., Rådström, P., and Hedman, J. (2015) Humic substances cause fluorescence inhibition in real-time polymerase chain reaction. *Anal. Biochem.* **487**: 30–37.

Sivan, O., Adler, M., Pearson, A., Gelman, F., Bar-Or, I., John, S.G., and Eckert, W. (2011) Geochemical evidence for iron-mediated anaerobic oxidation of methane. *Limnol. Oceanogr.* **56**: 1536–1544.

Sollai, M., Villanueva, L., Hopmans, E.C., Reichart, G.J., and Sinninghe Damsté, J.S. (2019) A combined lipidomic and 16S rRNA gene amplicon sequencing approach reveals archaeal sources of intact polar lipids in the stratified Black Sea water column. *Geobiology* **17**: 91–109.

Stocker, T.F., D. Qin, G.-K., Plattner, M., Tignor, S., K. Allen, J., Boschung, A., et al. (2013) IPCC, 2013: Summary for policymakers. In: Climate Change 2013: The physical science basis. Contribution of working group I to the fifth assessment report of the Intergovernmental panel on climate change. *Cambridge Univ. Press. Cambridge, United Kingdom*.

Straub, K.L. and Schink, B. (2004) Ferrihydrite-Dependent Growth of Sulfurospirillum deleyianum through Electron Transfer via Sulfur Cycling. *Society* **70**: 5744–5749.

Suominen, S., Dombrowski, N., Sinninghe Damsté, J.S., and Villanueva, L. (2020) A diverse uncultivated microbial community is responsible for organic matter degradation in the Black Sea sulphidic zone. *Environ. Microbiol.*

Suzuki, D., Li, Z., Cui, X., Zhang, C., and Katayama, A. (2014) Reclassification of Desulfobacterium anilini as Desulfatiglans anilini comb. nov. within Desulfatiglans gen. nov., And description of a 4-chlorophenol-degrading sulfate-reducing bacterium, Desulfatiglans parachlorophenolica sp. nov. *Int. J. Syst. Evol. Microbiol.* **64**: 3081–3086.

Takai, K., Suzuki, M., Nakagawa, S., Miyazaki, M., Suzuki, Y., Inagaki, F., and Horikoshi, K. (2006) Sulfurimonas paralvinellae sp. nov., a novel mesophilic, hydrogen- and sulfur-oxidizing chemolithoautotroph within the Epsilonproteo-bacteria isolated from a deep-sea hydrothermal vent polychaete nest, reclassification of Thiomicrospira denitrificans as S. *Int. J. Syst. Evol. Microbiol.* **56**: 1725–1733.

Valentine, D.L. and Reeburgh, W.S. (2000) New perspectives on anaerobic methane oxidation. *Env. Microbiol* **2**: 477–484.

Valenzuela, E.I., Avendaño, K.A., Balagurusamy, N., Arriaga, S., Nieto-Delgado, C., Thalasso, F., and Cervantes, F.J. (2019) Electron shuttling mediated by humic substances fuels anaerobic methane oxidation and carbon burial in wetland sediments. *Sci. Total Environ.* **650**: 2674–2684.

Valenzuela, E.I., Prieto-davó, A., López-lozano, N.E., García-gonzález, A.S., López, M.G., and Cervantes, J. (2017) Anaerobic Methane Oxidation Driven by Microbial Reduction of Natural Organic Matter in a Tropical Wetland. *Appl. Environ. Microbiol.* **83**: 1–15.

Vigneron, A., Alsop, E.B., Cruaud, P., Philibert, G., King, B., and Baksmaty, L. (2019) Contrasting Pathways for Anaerobic Methane Oxidation in Gulf of Mexico Cold Seep Sediments. *Appl. Environ. Sci.* **4**: e00091-18.

Wakeham, S.G., Lewis, C.M., Hopmans, E.C., Schouten, S., and Sinninghe Damsté, J.S. (2003) Archaea mediate anaerobic oxidation of methane in deep euxinic waters of the Black Sea. *Geochim. Cosmochim. Acta* **67**: 1359–1374.

Webster, G., Rinna, J., Roussel, E.G., Fry, J.C., Weightman, A.J., and Parkes, R.J. (2010) Prokaryotic functional diversity in different biogeochemical depth zones in tidal sediments of the Severn Estuary, UK, revealed by stable-isotope probing. *FEMS Microbiol. Ecol.* **72**: 179–197.

Wegener, G., Krukenberg, V., Riedel, D., Tegetmeyer, H.E., and Boetius, A. (2015) Intercellular wiring enables electron transfer between methanotrophic archaea and bacteria. *Nature* **526**: 587–590.

Wilson, L.G. and Bandurski, R.S. (1958) Enzymatic reactions involving sulfate, sulfite, selenate, and molybdate. *J. Biol. Chem.* **233**: 975–981.

Yanagawa, K., Sunamura, M., Lever, M.A., Morono, Y., Hiruta, A., Ishizaki, O., et al. (2011) Niche separation of methanotrophic archaea (ANME-1 and -2) in methane-seep sediments of the Eastern Japan Sea offshore Joetsu. *Geomicrobiol. J.* **28**: 118–129.

Zhang, J., Kobert, K., Flouri, T., and Stamatakis, A. (2014) PEAR: A fast and accurate Illumina Paired-End reAd mergeR. *Bioinformatics* **30**: 614–620.

Zhang, W., Ding, W., Yang, B., Tian, R., Gu, S., Luo, H., and Qian, P.Y. (2016) Genomic and transcriptomic evidence for carbohydrate consumption among microorganisms in a cold seep brine pool. *Front. Microbiol.* **7**: 1825.

Zhou, Z., Pan, J., Wang, F., Gu, J.D., and Li, M. (2018) Bathyarchaeota: Globally distributed metabolic generalists in anoxic environments. *FEMS Microbiol. Rev.* **42**: 639–655.

Summary - Samenvatting

Summary

Methane is a potent greenhouse gas and one of the major contributors to global warming. Although a large part of the methane emission comes from natural sources, it is also heavily affected by human interference. Aquatic systems, both marine and freshwater, contribute to methane emissions, as methane is produced in anoxic sediments. The aquatic methane production can be enhanced by processes such as eutrophication and warming. Methane consumption, which can decrease methane emissions, can take place in both oxic and anoxic environments, and is performed by methane oxidizing archaea or bacteria, called methanotrophs. As methane consumption proceeds via a redox reaction – methane oxidation coupled to the reduction of another compound – the availability of suitable electron acceptors has a large impact on the methane removal rates. When considering relevant electron acceptors for methane oxidation, it is, however, important to know which methanotrophs are present in the system, and which electron acceptors they are capable of using.

Based on their predominant presence in (micro)oxic natural systems, methane oxidizing bacteria are generally considered aerobes, with a preference for low-oxygen environments. Methane oxidizing archaea, in contrast, are strict anaerobes and generally require a microbial partner to perform methane oxidation. Although the majority of environments where methanotrophs are found support these assumptions, a more diverse picture emerged over the last decade. Methane oxidizing bacteria have been found to use specific pathways to be able to live in the anoxic zones of aquatic systems, via collaboration with phototrophs or via reduction of nitrite, producing oxygen in their cells for an intra-aerobic pathway. Methane oxidizing archaea have been seen to shuttle electrons to metals or humic substances, excluding the need for a biological partner. This thesis focusses on further exploring these recently discovered capabilities and electron acceptor preferences of both methane oxidizing bacteria and archaea.

To study methane oxidizing bacteria, the eutrophic, temperate zone Lacamas Lake (WA, US) was chosen as a study system. Lacamas Lake is steadily stratified in summer and uniformly mixed during winter, resulting in strongly changing redox conditions over de seasons and, in summer, over depth. This natural variation in conditions was used to study the preference of methanotrophs in de natural water column, as well as in incubation experiments amended with different electron acceptors. These experiments showed high methane oxidation rates in the anoxic water column, with a *Methylobacter* species as the dominant methanotrophic bacterium. Modelling exercises suggested that in summer, the in situ concentrations of the electron acceptors oxygen, nitrate and sulfate were too low to explain the observed methane oxidation rates, suggesting that a novel methane oxidation pathway or electron acceptor could be involved. Experiments in which nitrate and sulfate were added to the lake water showed enhanced methane oxidation rates. These electron acceptors are known to be involved in methane oxidation, although sulfate is primarily known as electron acceptor of marine methane oxidation. Incubation experiments with the addition of humic substances or oxygen showed decreased rates, suggesting these electron acceptors are not involved in methane oxidation in Lacamas Lake. Specific methanotrophic bacteria have been shown previously to contain the genes encoding for a denitrification pathway, allowing them to couple methane oxidation to nitrate reduction. Although the stimulating effect of nitrate on the methane oxidation rate would suggest such a coupling in Lacamas Lake, not all genes required for a

complete denitrification pathway were detected in the genome of the *Methylobacter* species that was present in Lacamas Lake. This suggested the involvement of a partner organism, capable of performing a reduction reaction that can be coupled to methane oxidation, possibly exchanging compounds with the methanotroph.

In order to further study methane oxidation by the Lacamas Lake *Methylobacter* species, an enrichment culture was established. The enrichment culture was dominated by a *Methylobacter* species, but also contained a non-methane consuming methylotroph *Methylotenera* species in high relative abundance. A correlation between the abundance of *Methylobacter* and *Methylotenera* species was also found in the Lacamas Lake water column and in incubation experiments. The enrichment culture was used to examine the response of the *Methylobacter* sp. to different concentrations of oxygen, as well as the presence of the potential electron acceptors nitrate, sulfate and humic substances. Whereas the *Methylobacter* species preferred anoxic conditions in the water column incubations, the enrichment culture was not able to perform methane oxidation under anoxic or trace-oxygen conditions. Methane oxidation under both micro-oxic and saturated oxygen conditions was observed, with a stimulating effect of nitrate on the oxic methane oxidation rates.

To further explore the potential interaction of *Methylobacter* and a partner, stable isotope probing, using ^{13}C-labelled methane, was used to follow the flow of methane-derived carbon. It was discovered that the methylotroph *Methylotenera* received carbon compounds from the *Methylobacter* species. Similar carbon transfer has been previously suggested to be based on the leakage of methanol by *Methylobacter*, which is in turn oxidized by *Methylotenera*. It, however, remained unclear why *Methylobacter* would release large proportions of methanol, as it results in a loss of energy for the *Methylobacter* cells. However, the experiments described in this thesis revealed that the incorporation of methane-derived carbon into *Methylotenera* only occurred in the presence of nitrate. Furthermore, the genome of the *Methylotenera* species in the enrichment culture encodes the proteins for a complete denitrification pathway. Possibly, *Methylotenera* was performing nitrate reduction and could enhance methane oxidation by *Methylobacter*, explaining the enhanced oxic methane oxidation rates that were observed in the incubations with nitrate, both in the summer water column and enrichment culture experiments. More research is, however, needed to further elucidate the relationship between the two microorganisms and its implications for the natural water column.

Methane oxidizing bacteria are of major importance in limiting methane emissions from freshwater systems. On a global scale, anaerobic methane oxidizing archaea (ANME) are responsible for the majority of the aquatic methane oxidation, especially in marine systems. The electron acceptor preference of ANME in the Black Sea water column was studied. The Black Sea is the largest anoxic basin in the world, and its deep water column is rich in methane. The methanotroph species that is present in the Black Sea anoxic water column, ANME-1b, is known to often occur without a sulfate-reducing partner, in contrast to other types of ANME. The metabolic diversity of ANME-1b was studied in incubation experiments with ^{13}C-methane and several alternative electron acceptors. Fe^{3+} and anthraquinone-2,6-disulfonate (AQDS) were added to anoxic incubations with water column suspended particulate matter in the presence of sodium molybdate, a sulfate reduction inhibitor. The addition of AQDS results in an increase in $^{13}CO_2$ production, which indicates that ANME-1b is stimulated by the presence of AQDS. By evaluating the wider microbial community, we were able to suggest the potential involvement of several sulfur-cycling species in the methane oxidation process, although the

interaction between the ANME and sulfur cycling bacteria, as well as the processes involved, need to be further investigated in order to elucidate their potential role.

The results of this thesis show that a wide range of electron acceptors need to be considered when the methane oxidation potential in environmental systems is studied. Methane oxidizing bacteria and archaea use a completely different metabolic pathway to oxidize methane. Some of the electron acceptors they could potentially use are similar, such as humic substances and nitrite/nitrate, but this thesis shows that the response to similar electron acceptors differs between methane oxidizing bacteria and ANME, and even between different species of methane oxidizing bacteria. It, therefore, remains difficult to classify 'universal' electron acceptors for anaerobic methane oxidation. The non-methanotrophic partner organisms potentially involved in methane oxidation also show a large variety between marine and freshwater systems. Overall, this thesis shows that methane oxidation is a complex process with many parameters influencing the oxidation rates and microbial players involved. Although the results describe several pathways that could be relevant for environmental systems, more research is required to translate the laboratory experiments to in situ conditions.

Samenvatting

Methaan is een broeikasgas dat een belangrijke bijdrage levert aan het mondiale broeikaseffect. Een groot deel van de wereldwijde methaanemissies komt van natuurlijke bronnen maar wordt ook sterk beïnvloed door menselijk handelen. Zowel mariene als zoetwater ecosystemen dragen bij aan de methaanemissies doordat methaan kan vrijkomen vanuit zuurstofloze sedimenten waar methaan geproduceerd wordt door archaea. De methaanproductie kan worden beïnvloed door antropogene effecten als eutrofiëring en opwarming. Methaanconsumptie kan de emissie van methaan uit meren en zeeën verlagen. Het kan plaatsvinden onder zowel zuurstofrijke als zuurstofloze omstandigheden, uitgevoerd door methaan-consumerende archaea of bacteriën, tezamen methanotrofen genoemd. Methaanconsumptie is een redoxreactie, bestaande uit de oxidatie van methaan die gekoppeld is aan een reductie-reactie, waarbij de beschikbaarheid van elektronenacceptoren in grote mate de afbraaksnelheid van methaan bepaalt. Om te achterhalen welke elektronenacceptoren relevant zijn voor methaanoxidatie in een systeem is het belangrijk om te weten welke methanotrofen aanwezig zijn en welke elektronenacceptoren zij in staat zijn te gebruiken.

Methaanoxiderende bacteriën worden over het algemeen gerekend tot de aerobe organismen, hoewel ze een voorkeur kennen voor zuurstofarme systemen. Methaanoxiderende archaea zijn strikt anaeroob en leven over het algemeen in symbiose met een partner micro-organisme. Hoewel de meerderheid van de systemen waarin deze bacteriën en archaea worden aangetroffen bovenstaande stellingen bevestigen, zijn er in het afgelopen decennium diverse soorten methanotrofen ontdekt die een ook onder andere omstandigheden gedijen. Specifieke soorten methaanoxiderende bacteriën zijn in staat gebleken te overleven in zuurstofloze omgevingen: ze werken samen met fototrofe organismen, of reduceren zelf nitriet om zo zuurstof binnen hun cel te produceren voor de oxidatie van methaan. Methaanoxiderende archaea blijken elektronen naar metalen of organische stoffen te kunnen transporteren, en daarmee symbiose met een biologische partner onnodig te maken. Dit proefschrift verkent de mogelijkheden en voorkeuren van methaanoxiderende bacteriën en archaea om diverse elektronenacceptoren te gebruiken.

Het eutrofe Lacamas Lake, een meer gelegen in de gematigde klimaatzone, wordt in dit proefschrift bestudeerd als studieobject voor methaanoxiderende bacteriën. Lacamas Lake is gedurende de zomer gestratificeerd, met een zuurstofrijk epilimnion en een zuurstofloos hypolimnion, en in de winter volledig gemengd; zomer en winter worden dus gekenmerkt door sterk veranderde redoxomstandigheden. De stratificatie in de zomer leidt tot wisselende omstandigheden op verschillende diepten in het meer. Deze variaties zijn gebruikt om de voorkeuren van de methanotrofen in de waterkolom te bestuderen. Incubatie-experimenten toonden aan dat de snelheid van methaanoxidatie in het zuurstofloze water hoog was en voornamelijk door aan *Methylobacter* gerelateerde methanotrofen uitgevoerd werd. Modelering van de methaanoxidatie liet zien dat de concentraties van verschillende elektronenacceptoren in de zomer te laag zijn om de geobserveerde methaanoxidatie te kunnen verklaren. Een mogelijke verklaring zou een onbekend methaanoxidatiemechanisme kunnen zijn, hoewel experimenten met toegevoegd nitraat en sulfaat een stimulerend effect op de methaanoxidatie lieten zien. Deze stoffen zijn bekend als elektronenacceptoren van methaanoxidatie, hoewel sulfaat voornamelijk bekend is als elektronenacceptor in marine

systemen. Het toevoegen van organische stoffen en zuurstof aan Lacamas Lake incubatie-experimenten remde de methaanoxidatiereactie, hetgeen suggereert dat deze stoffen niet betrokken zijn bij methaanoxidatie in dit meer. Eerder is aangetoond dat specifieke methanotrofe bacteriën genen bezitten die denitrificatie, waarschijnlijk gekoppeld aan methaanoxidatie, mogelijk maken. Deze genen zijn echter niet aanwezig in het genoom van de *Methylobacter* bacterie in Lacamas Lake. Het is daarom aannemelijk dat een ander micro-organisme optreedt als partner van *Methylobacter*, waarbij deze partner een reductiereactie uitvoert die gekoppeld kan worden aan methaanoxidatie, waarbij mogelijkerwijs stoffen worden uitgewisseld tussen de twee organismen.
Methaanoxidatie door de *Methylobacter* bacterie werd vervolgens bestudeerd met behulp van een verkregen verrijkingscultuur die gedomineerd werd door de *Methylobacter* bacterie, maar ook een relatief hoog aandeel aan *Methylotenera* cellen bevatte. *Methylotenera* is een methylotroof die niet in staat is methaan te consumeren. Ook in het meer zelf en in de eerder uitgevoerde incubatie-experimenten leek een verband te bestaan tussen de abundantie van *Methylobacter* en *Methylotenera* cellen. De verrijkingscultuur werd gebruikt om het effect van de zuurstofconcentraties en aanwezigheid van de potentiële elektronenacceptoren, nitraat, sulfaat en humusstoffen, te testen. Hoewel de *Methylobacter* bacterie in het meer een voorkeur vertoonde voor zuurstofloze condities, werd in de experimenten met de verrijkingscultuur geen methaanoxidatie gemeten onder zuurstofloze en zeer zuurstofarme omstandigheden. Methaanoxidatie kon wel worden vastgesteld in experimenten met kleine hoeveelheden zuurstof en onder zuurstofverzadigde omstandigheden, waarbij de aanwezigheid van nitraat de aerobe methaanoxidatie versnelde. Om de mogelijke interactie tussen de *Methylobacter* soort en eventuele partnerorganismes te onderzoeken werd ^{13}C-gelabeld methaan gebruikt. Dit maakte het mogelijk koolstof afkomstig van ^{13}C-methaan te volgen in de verrijkingscultuur. Dit liet zien dat de methylotroof *Methylotenera* koolstof ontving van de *Methylobacter* bacterie, een vergelijkbaar resultaat met eerdere onderzoeken, die als verklaring een lekkage van methanol uit *Methylobacter* cellen gaven. Dit gelekte methanol zou gebruikt worden door de *Methylotenera* cellen maar de reden voor het optreden van dit proces bleef onduidelijk. De experimenten met de verrijkingscultuur laten zien dat het inbouwen van methaan-afgeleid koolstof in *Methylotenera* cellen alleen gebeurt wanneer nitraat aanwezig is. Het genoom van de *Methylotenera* bacterie codeert bovendien een compleet denitrificatie proces. *Methylotenera* zou dus potentieel nitraat kunnen reduceren en daarbij methaanoxidatie kunnen stimuleren, wat een verklaring zou kunnen bieden voor de gevonden stijging in methaanoxidatie door *Methylobacter* in de aanwezigheid van nitraat. Meer onderzoek is nodig om de relatie tussen de twee organismen verder te ontrafelen.
Methaanoxidatie in het mariene milieu vindt ook vaak plaats onder anoxische condities, maar in tegenstelling tot zoetwatermeren zijn het hier archaea (anaerobic methane oxidizing archaea, ANME) die een belangrijke rol spelen. De voorkeur voor verschillende elektronenacceptoren van methaanoxiderende archaea aanwezig in de waterkolom van de Zwarte Zee werd onderzocht. De Zwarte Zee is 's werelds grootste en diepste zuurstofloze waterbekken. Het anoxische water beneden de ca. 100 m is rijk aan methaan. De methanotroof aanwezig in de waterkolom van de Zwarte Zee is van het ANME-1b type en staat erom bekend vaak voor te komen zonder een sulfaat-reducerende partner, in tegenstelling tot andere typen ANME. De metabolische diversiteit van ANME-1b werd bestudeerd aan de hand van incubatie-experimenten met biologisch materiaal verkregen uit de waterkolom waaraan ^{13}C-methaan,

Fe^{3+}, anthraquinoon-2,6-disulfonaat (AQDS) en/of natriummolybdaat werden toegevoegd. Toevoeging van AQDS veroorzaakte een toename in $^{13}CO_2$ productie, hetgeen geïnterpreteerd wordt als een stimulerend effect op ANME-1b. Een analyse van de algemene microbiële samenstelling leidde tot de identificatie van diverse gebruikers van zwavelhoudende stoffen. Deze bacteriën zijn mogelijk betrokken bij het methaanoxidatie-proces, hoewel de interactie tussen de methanotrofen en deze bacteriën en de processen die hierin een rol spelen verder onderzocht dienen te worden om hier meer duidelijkheid over te verschaffen.

De resultaten beschreven in dit proefschrift tonen aan dat diverse elektronenacceptoren relevant kunnen zijn voor methaanoxidatie in aquatische systemen. Methaanoxiderende bacteriën en archaea gebruiken totaal verschillende metabolische routes om methaan te oxideren. Sommige elektronenacceptoren die zij zouden kunnen gebruiken zijn wel vergelijkbaar, zoals humusstoffen en nitriet/nitraat, maar dit proefschrift laat zien dat ook deze elektronenacceptoren niet hetzelfde effect hebben op methaanoxiderende bacteriën en archaea, en zelfs niet op verschillende soorten methaanoxiderende bacteriën. Het blijft daarom lastig om 'universele' elektronenacceptoren voor anaerobe methaanoxidatie aan te wijzen. De niet-methanotrofe partnerorganismen die potentieel betrokken zijn bij methaanoxidatie verschillen ook tussen marine en zoetwater systemen. Methaanoxidatie is dus een complex proces, waar veel parameters van invloed op zijn. De resultaten laten ook zien dat diverse niet-methanotrofen een belangrijke rol kunnen vervullen in het proces van methaanoxidatie. Voorzichtigheid is geboden bij het vertalen van laboratoriumstudies naar natuurlijke systemen en aanvullend onderzoek naar het methaanoxidatieproces, door middel van in situ experimenten, is daarom wenselijk.

Synthesis

Synthesis

Oxygen concentration and methane oxidation
The research included in this thesis shows that the role of oxygen in methane oxidation by methane oxidizing bacteria is complex, and no general rules seem to hold. Whereas several studies have shown that methanotrophic bacteria are inhibited by atmospheric concentrations of oxygen, our enrichment culture, established with Lake Lacamas suspended particulate matter, show the highest methane removal rates at oxygen saturation conditions, by a methanotroph species that is mostly found in anoxic conditions in the natural environment. In incubations with water column samples, however, a strong preference for anoxic conditions over oxic conditions was observed. This inconsistency between the enrichment culture and the water column incubations may be due to differences in the microbial community composition or the (micro)nutrient availability in the two situations. For future research, it would be interesting to perform incubations with the enrichment culture in autoclaved lake water rather than in the defined medium used for the enrichments, to test whether (micro)nutrient availability was of influence. Regardless of the cause or mechanisms behind the oxygen inconsistency, however, these results show that many factors and processes are affecting the methanotroph and its interaction with oxygen.

Nitrate and methane oxidation
In eutrophic systems such as Lacamas Lake, nitrate inputs are high, mostly due to agricultural or urban run-off in the watershed. Despite the high input, analysis of the Lacamas Lake water column indicated that the nitrate concentration in the hypolimnion is low, probably due to high nitrate consumption rates. It is important to realize that eutrophic lakes are not necessarily rich in nitrate throughout the water column: quick scavengers may profit more from the nitrate input than others. This rapid turnover of compounds makes it difficult to access their availability in the water column: the fact that we cannot measure high concentrations of nitrate, does not mean it is not available or consumed in high rates, given the continuous input through the inflowing stream. To assess the nitrate availability, the internal nitrogen cycle would have to be studied, for example via isotope-tracer experiments. Such detailed studies of the nitrogen cycle go beyond the scope of this thesis, but would be essential if one would want to assess the nitrate availability and ultimately the effect of this pool on the methanotrophic community and interacting species.
A high nitrate inflow may cause algal blooms, and subsequent anoxia in the water column, a phenomenon often observed in eutrophic lakes such as Lacamas Lake. Although the nitrate input could favor methane production in this way, the results included in this thesis indicate that nitrate can also enhance methane oxidation, both in oxic and anoxic conditions. Although the overall effects of high nutrient loads on aquatic systems are definitely undesirable, it is of key importance to further evaluate the potential enhancing effect of nitrate inputs on the methane oxidation rates.

Denitrification metabolic potential of methanotrophs
A difficulty in assessing the link between methane and nitrate cycling is the current lack of studies on the genes involved in the denitrification pathway of methanotrophs and methylotrophs, as well as studies on pure culture to assess their metabolism. More

fundamental research is needed to determine whether specific species are capable of performing denitrification. With the knowledge now available, the study included in chapter 3 of this thesis concluded that the *Methylobacter* species detected in Lacamas Lake do not contain a complete denitrification pathway. It is possible though that the assimilatory nitrate reduction gene that was detected in the genome of the Lacamas Lake *Methylobacter* species (*Nas* gene), and that is considered to be unrelated to the dissimilatory nitrate reduction pathway, may be involved in the dissimilatory pathway, similar to what has been observed in *Methylotenera* (Mustakhimov et al., 2013, described in Chapter 5). If this would indeed be the case, it could largely shift the interpretation of the denitrification potential of many methanotrophs, as this specific gene is the missing component of the denitrification pathway in many methanotroph genomes (Smith *et al.*, 2018). More research is, however, needed to confirm or deny this hypothesis. Another option to determine whether specific species are capable of denitrification could be to use labeled nitrogen compounds, such as ^{15}N, to assess the faith of different nitrogen compounds in incubation studies.

The effect of denitrification-methane oxidation on greenhouse gas emissions

If denitrification would indeed be coupled to methane oxidation in lakes, another question arises: Which reaction products will result from a coupled methane oxidation-denitrification reaction, and what are its implications for lake greenhouse gas emissions? Methane oxidation transforms CH_4 into CO_2, a much less potent greenhouse gas. The reaction product of denitrification can however be N_2O (or N_2, but the genes to convert N_2O to N_2 are not commonly observed in methanotrophs), which is a greenhouse gas too. The removal of methane could thus, in case it is coupled to denitrification, lead to the emission of other greenhouse gases. To assess whether these emissions are environmentally relevant, a collaboration between modelers, biogeochemists and microbiologists would be required.

Relevance for the wider microbial community

Although this thesis has its focus on bacterial and archaeal methanotrophs, it also shows there is an important role for the wider microbial community in the methane oxidation process. In the studies of this thesis performed in the Lacamas Lake system, this relates to the potential involvement of nitrate reducers and of methylotrophs, while the experiments conducted in the Black Sea water column suggest that sulfur-cycling organisms other than the traditional SRB could potentially play an important role in facilitating methane oxidation. Overall, these studies show that studying the wider microbial community is essential to assess the processes involved in environmental methane oxidation. The addition of different electron acceptors affects the microbial community, resulting in a change in the biogeochemical processes that might affect methane oxidation rates. To map the microbial community and the interaction between the members, ecological network modelling could be used. Another way would be to use markers, such as isotopically labeled compounds, to trace the involvement of certain microbial partners in specific processes. The importance of the microbial community also highlights the importance of environmental studies, besides the batch culture studies that are performed with MOB and ANME by previous studies.

Further research

Although the studies included in this thesis have been able to identify and characterize methanotrophs in both freshwater and marine environments, several questions still remain. In the case of the methane oxidizing archaea (ANME), the extremely slow growth and methane turnover rates in the Black Sea experiments made it difficult to produce statistically significant datasets. Such slow growth is common in anoxic environments, and to be able to properly assess such organisms, long-term studies would be advantageous. Another option would be to use more sensitive methods, for example ^{14}C-methane labeling rather than ^{13}C-methane labeling, to be able to detect low methane oxidation rates.

In the case of the freshwater methane oxidation studies conducted in Lacamas Lake, it would have been extremely helpful to not only analyze microbial abundance and diversity by 16S rRNA gene amplicon analysis, but to also determine the microbial activity, for example using transcriptomic approaches. Such data could be used to determine which microbial members and genes are involved in methane oxidation under oxygen stress and in the presence of nitrate and sulfate.

Acknowledgements - Dankwoord

Acknowledgements - Dankwoord

Five years ago, I walked into the NIOZ without any knowledge of anaerobic microbiology. The NIOZ had a very old molecular lab, no anaerobic lab, and it had been a long time since anyone cared for measuring methane. While I was struggling to get my microbiology knowledge up from high school level to proper PhD level, the NIOZ microbiology division upgraded greatly. Nowadays, the NIOZ has great facilities, several people are working on methane, and I can (almost) call myself a doctor in anaerobic microbiology.
The person I have to thank most for that is of course Laura Villanueva. For getting the NIOZ labs into shape, but even way more for keeping me on track. Laura, thank you so much for having faith in me, stimulating me to learn, but also allowing me to make mistakes. Your door was always open if I had a question, but at the same time you gave me a lot of space to develop myself as a researcher in the direction I preferred. Due to your supervision I could get the most out of myself. You were enthusiastic about my many many crazy plans, but also told me to be careful to not run out of time.
Jaap, we did not get to work together as much as we had planned or hoped. Nevertheless, I greatly value your input and your critical comments that made my manuscripts and thesis much better.

Saara, we started at the same time in the SIAM program and shared a lot of victories but also insecurities. You were available when I needed someone to aerate my frustrations to, but also ready to help me back up with a positive note.
Erinke, jij was de stille support op de achtergrond. Hoeveel waarde dat had besefte ik eigenlijk pas toen je naar Oxford verhuisde en afspreken ineens niet meer zo makkelijk was. Maar ik ben ervan overtuigd dat we -los van elkaar of samen- de hele wereld over kunnen verhuizen en nog steeds een hechte band houden.

Sophie, I'll never forget the little notes you sometimes put on my desk. Especially 'You need breaks too!' and the bottle of gin. You are a great friend, in good and in bad times.
Laura Schreuder, ik ben zo blij dat we samen nog in Alkmaar hebben kunnen wonen! Heerlijk koffiedrinken, eerst zonder en daarna met Boaz. Het heeft me de eenzame tijd van het schrijven door gesleept.
Nathalie, ik vind het zo bijzonder hoe onze wegen al meer dan 20 jaar blijven kruisen, hoe we elkaar steeds weer terugvinden. Bedankt voor alle steuntjes in de rug!
Mama, papa, Theo, Maartje, Stijn, Jur, Jisk, Dennis: jullie onvoorwaardelijke steun is iets bijzonders, een veilige haven waar ik niet zonder kan.
Dinja, Marijn, Merlijn, Lotte en Lieuwe, bedankt voor het bieden van een luisterend oor wanneer nodig, maar vooral voor alle afleiding van de thesis-stress, opvallend vaak in de vorm van bier ;)

John, the opportunity you gave me to work in your lab was the basis of my scientific career. It was at your lab that I learned how much I like science, and that was mainly because you gave me a chance to be creative and independent. Our continued collaboration during my PhD was very productive and helpful. Thank you for everything, also to everyone else in your lab!

Keith, of course I thank you for sending me Lacamas materials and helping me sampling. But above all the practical help, you were mainly a great help to keep the spirits high. You are always cheerful, never complaining. We've always shared our love and hate of the PNW – loving the landscapes and the people, hating the long and grey winters. Perhaps one day we'll meet again – in a nice & sunny, outdoorsy place please!

Dan, I still find it crazy coincidence how you found the ad for this PhD position, and told me to take a look at it, while I wasn't even looking for a job yet and we were also thousands of km away from Texel. Thanks!!

Peter & Irene, bedankt voor de leuke discussies en natuurlijk voor het beschikbaar stellen van jullie huisje in Berlijn: het was de perfecte plek voor ontspanning en inspanning, en heeft zeker bijgedragen aan het tot stand komen van deze thesis.
Darci and Dina, you were the perfect office mates! We had a lot of fun (Darci, I still love maize) and lots of talks (Dina, take holidays!).
Diana and Alejandro, you are the kindest people I know.
Zeynep and Charlie, thanks for cat therapy and loads of fun.
Maartje en Sanne, you made endless DNA extractions much more fun, and you've helped me so much.
All the other NIOZ colleagues: thanks for coffee breaks, kale tours, help in the lab, science talks and fun times.
SIAM PhD's, thank you for making me feel a bit less lost in the world of science. Laura Valk, samen naar ISME was super, ik ben onder de indruk van jouw doorzettingsvermogen en ik wens je het allerbeste, in Denemarken en daarna.
Victorie vrijwilligers, jullie waren mijn andere wereld, die waarin niemand echt wist wat ik nou eigenlijk voor ingewikkelds deed de hele dag. En dat was heel fijn. Proost, en bedankt!
In het bijzonder Thijs, je liet me welkom voelen in Alkmaar, en natuurlijk bedankt voor de fantastische broodjes-grappen.

En tenslotte natuurlijk Han, mijn rots in de branding. *I can shine, even in the darkness, but I crave the light that you bring*. Jij geeft alles wat extra glans, in de afgelopen jaren en in de avonturen die bezig zijn en komen gaan.

About the author

Sigrid van Grinsven was born on May 10, 1991 in Zevenaar, The Netherlands. In 2009, she graduated from secondary school (VWO) at the Bisschop Bekkers College in Eindhoven, after which she studied Soil, Water, Atmosphere at Wageningen University, including a 6 months Erasmus exchange program at the Czech University of Life Sciences, Prague. Her bachelor's thesis, performed at the Aquatic Ecology group of Wageningen University, was on the role of nitrogen and phosphate in Dutch streams. After obtaining her bachelor's degree in 2012, she enrolled in a full-time board year at the Wageningen University students sports center, in the role of secretary. In 2013, she started the master's program Earth, Life and Climate at Utrecht University, with a specialization in biogeochemistry. In 2014, she completed a 6-month research internship at the Washington State University Vancouver, under the supervision of Dr. John Harrison. Her master's thesis research was performed at Utrecht University, and included fieldwork at Lake Taihu in China as well as NanoSIMS analysis at the Utrecht facility, supervised by Dr. Lubos Polerecky. Directly after obtaining her Master's degree in August 2015, she started a PhD project at the Royal Netherlands Institute of Sea Research under the supervision of Dr. Laura Villanueva and Prof. Dr. Jaap Sinninghe Damsté, which included several research cruises and a continued collaboration with the Washington State University.